University of Cape Town
Department of Chemical Engineering
Minerals to Metals Research Group

Assessing the Distribution, Composition and Potential Human Health Implications of Metal-Bearing Particulate Matter in the Saldanha Bay Municipality

Submitted to the Department of Chemical Engineering, University of Cape Town for the fulfilment of the degree:

Master of Science in Engineering in Chemical Engineering

Researcher: Laylaa Ebrahim

Supervisor: Assoc. Prof. Jennifer Lee Broadhurst

Co-Supervisor: Dr. Johanna von Holdt

October 2023

SYNOPSIS

Whilst mining contributes to both local and national economies, it can also have a significant impact on the surrounding environment. An example of one of the impacts is air pollution through the emission of particulate matter (PM). PM can have a range of different diameters, however PM that has an aerodynamic equivalent diameter of less than 2.5 and 10 microns, also known as $PM_{2.5}$ and PM_{10}, respectively, is of particular concern as it is known to reduce the quality of air and can cause adverse health effects on surrounding communities. PM from mining-related operations such as the transportation, stockpiling and handling of metal ores can result in mine dust significantly impacting communities far away from the mine itself. It is this challenge that is explored in this study, with the focus on the Saldanha Bay Municipality situated within the West Coast District of South Africa.

There are many industries that handle different types of metal ores in the Saldanha Bay Municipality. Additionally, the Saldanha Bay Municipality is also home to the Port of Saldanha, which is known as South Africa's deepest port and accommodates large ore-carriers. The bulk commodities that are exported from the port are transported through the municipality to the port by means of railway lines. However, this form of transport is a contributing factor to the dispersion of dust from the ore, due to the use of open-top carts that transport the ore. Additionally, there are other activities of concern that could result in PM emissions and include the stockpiling of the ores as well as the loading of the ores onto the bulk carriers. The result of these activities has driven members of the surrounding communities to question the quality of the air in the municipality, largely resulting from the discolouration of infrastructure from the red iron ore dust.

This study set out to determine the concentrations and composition of ambient PM in the municipality, and to conduct a preliminary assessment of the potential sources and health implications of these dust emissions. The first part of this study involved a desktop investigation to identify potential emission sources and suitable measurement sites, based on current industrial activities, weather patterns and existing air quality data and monitoring programmes within the municipality. The second part of the study included field measurements of ambient PM concentrations at selected sites, and the collection, and analysis of physical PM samples for mineral and elemental composition. The different types of equipment that were installed included low-cost particulate sensors, gravimetric samplers, dust fallout buckets, and Big Spring Number Eights (BSNEs). The PM concentration data that were obtained from the particulate sensors were processed in R and analysed in real-time, aggregated to 1-hour and 24-hour averages, the latter two according to legislation set out by the National Ambient Air Quality Standards (NAAQS). The PM samples that were collected from the gravimetric samples, dust fallout buckets and BSNEs were analysed to determine the mineral and elemental composition. Finally, the results from the initial desktop study and fieldwork were used to assess potential point sources of PM emissions, as well as the potential health implications associated with PM exposure and the minerals and elements found in the physical PM samples collected.

The results from this study have indicated that whilst there were no exceedances of both $PM_{2.5}$ and PM_{10} daily concentrations according to the NAAQS, there were exceedances according to the WHO guidelines. It was also found that some of these exceedances were random spikes in the data, due to a possible fault within the sensor itself. Both $PM_{2.5}$ and PM_{10} concentrations were also plotted as a function of wind speed and direction, in the form of pollution roses and polar plots, which ultimately assisted in the identification of potential sources of emission within the municipality. The results from the dust fallout bucket indicated that the dust fall rate for each sample collected was higher than the acceptable rate outlined by South African legislation. The dust sub-sample comprised predominantly of quartz, calcite, and hematite, whilst the salt sub-sample was predominantly sodium chloride. The combined BSNE sample is representative of the air in the Saldanha area. This sample was predominantly comprised of quartz, feldspar, and hematite. The QEMSCAN analysis of the combined BSNE sample also provided the mass% of minerals across the different size fraction between <5 - <250 µm. It was also found that 65.9% of the particles were found in the <5 µm size fraction, which indicates that there is a possibility that some of those particles are respirable. Most of the filter papers were analysed quantitatively and indicated that minerals such as sodium chloride, quartz, hematite, calcium carbonate, titanium dioxide and manganese oxide were present. Two filter papers from the ARA N-FRM sampler indicated the presence of elements such as iron, magnesium, and potassium, to mention a few, while also indicating the presence of several elements in trace quantities. The analysis of the salt sub-sample and the filter papers indicated the presence of potentially toxic elements such as uranium, lead, and arsenic, although present in trace amounts.

The potential sources of emission identified by analysis of the pollution roses, polar plots and the physical PM samples include the Transnet Iron Ore Terminal, the MPT (non-listed company 3), Tronox Namakwa Sands, the Tabakbaai Quarry, Pendula VDM, Afrimat Aggregates, Afrimat Quarry and the non-listed companies 1A, 1B and 2. With regards to potential health implications, according to literature, it was found that PM exposure can result in both respiratory as well as cardiovascular diseases, which are the two major causes of mortality on a global scale. Other potential health implications that have been highlighted according to minerals/elements found in the results include lung disease and cancer, kidney damage, amongst others.

It is recommended that future studies investigate installing a different low-cost particulate sensor alongside the PurpleAir Particulate Sensor for comparison of PM concentrations. Future studies are also recommended to install the PurpleAir Particulate Sensors at different study sites for the same amount of time, to allow for a fair comparison of PM concentrations. It is also recommended that the PurpleAir Particulate Sensors be installed for complete seasons, to provide a more holistic view on the exceedances that occur. It is also recommended that future studies investigate the use of a PI-SWERL with collected ore samples exported from the port, which could provide a robust index of the potential dust emissions. Future studies should consider using this study's PM observational concentration data in an atmospheric dispersion model as input and validation of such to simulate best- and

worst-case scenarios of PM emissions. From this, it is proposed that the empirical data is made use of for future laboratory and field studies. Furthermore, the observational and simulated PM data should be compared for the validation of the model.

PLAGIARISM DECLARATION

I know that plagiarism is wrong. Plagiarism is to use another's work and pretend that it is my own.

I have used the UCT Harvard Referencing System for citation and referencing. In this report, all contributions to, and quotations from, the work(s) of other people have been cited and referenced.

This report is my own work. I have not allowed and will not allow anyone to copy my work.

Full name	Peoplesoft ID	Date	Signature
Laylaa Ebrahim	1500376	10/10/2023	Signed by candidate

ACKNOWLEDGMENTS

I wish to convey my gratitude to all listed below, whose invaluable support helped to make this study possible.

- To my Lord, I am deeply grateful to you for providing me with the strength and the ability to carry out and complete my study.
- I extend my heartfelt gratitude to both Associate Prof. Jennifer Lee Broadhurst and Dr. Johanna von Holt for their unwavering guidance and support over the last four years. The mentorship and commitment that you both have shown in nurturing my development as an academic are immeasurable. I am thankful for the wealth of skills and knowledge that you both have imparted to me. I appreciate all that you have both done for me.
- I would like to thank the NRF for sponsoring this study.
- I would also like to acknowledge the Mine Dust Network and the GCRF for allowing me to be a part of their groups.
- To everyone in the Saldanha Bay Municipality who have helped me in this study. Rene Toesie, Andre Wicht, Garrett van Schalkwyk, Wendy Bezuidenhout and Bruce de Beer at the West Coast Mall, Elmi Dixon and Valenceo Scheepers. I will always appreciate the help that you all provided me with.
- To my amazing husband, Rayhaan, I want to express my deepest gratitude for the unconditional love, steadfast support and constant encouragement that you have provided me with during my master's journey. For the last year and 10 months, you have made significant sacrifices and shouldered additional responsibilities to ease my path towards completing my master's degree. Thank you for always being by my side, I could not have done it without you.
- To my dear parents (Mummy, Papa, Mom, and Dad), my siblings (Muhammad, Mahdiyyah, Ammaarah and Razeen) and my best friends (Imaad, Farhana and Saarah), I extend my heartfelt appreciation for your steadfast support, love and encouragement, without which, I would not have been able to complete this study.
- To my incredible friends, CK, Ireland and Sage. I want to express my deep gratitude for being my pillars of strength and for consistently being by my side. I value that you all have always been there for me and for the help you all provided during difficult times. I am immensely thankful for each one of you.
- To my managers, Pierre, Henriette and Miché, and my GDP friends, I extend my sincere appreciation for your continuous support and encouragement. Your unwavering belief in me has been a driving force behind my ability to successfully complete this study.

Table of Contents

List of Figures

List of Tables

ACRONYMS

ADZ	Aquaculture Development Zone
AEL	Atmospheric Emission License
AQA	Air Quality Act
AQM	Air Quality Monitoring
AQO	Air Quality Officer
BSNE	Big Spring Number Eight
CSV	Comma-separated values
EA	Environmental Authorisation
EIA	Environmental Impact Assessment
EPA	Environmental Protection Agency
FRM	Federal Reference Method
GDP	Gross Domestic Product
ICP-AES	Inductively Coupled Plasma – Atomic Emission Spectroscopy
ICP-MS	Inductively Coupled Plasma – Mass Spectroscopy
IDZ	Industrial Development Zone
LPM	Litres per minute
Micron	micrometre (µm)
MPT	Multi-Purpose Terminal
NAAQS	National Ambient Air Quality Standards
NEM: AQA	National Environment Management: Air Quality Act
NOAA	National Oceanic and Atmospheric Administration
PM	Particulate Matter
$PM_{2.5}$	Particulate matter with an equivalent aerodynamic diameter of 2.5 µm
PM_{10}	Particulate matter with an equivalent aerodynamic diameter of 10 µm
QEMSCAN	Quantitative Evaluation of Minerals by Scanning Electron Microscopy
RH	Relative Humidity
SAAELIP	South African Atmospheric Emission Licensing and Inventory Portal

SD	Secure Digital
SEM-EDX	Scanning Electron Microscopy – Energy Dispersive X-ray
tpa	tonnes per annum
TSP	Total Suspended Particles
US EPA	United States Environmental Protection Agency
WHO	World Health Organization
XRD	X-ray Diffraction Analysis
XRF	X-ray Fluorescence

CHAPTER 1: INTRODUCTION

The mining value chain in South Africa is reported to be the bedrock of the county's history and is an economic anchor to communities across South Africa (Cassim, Goodman & Rajagopal, 2019). Although the mining industry plays a crucial role in supporting human advancement and global economy, it can also have a substantial impact on the surrounding environment (Marimuthu et al., 2021). Excessive reliance on natural resources often results in their unsustainable exploitation, which subsequently has negative environmental impacts such as the release of harmful gases into the atmosphere and other climatic concerns (Marimuthu et al., 2021). One of these impacts that is of concern is air pollution through the emission of particulate matter (PM). PM that has an aerodynamic equivalent diameter of less than 2.5 and 10 microns, also known as $PM_{2.5}$ and PM_{10} are known to cause adverse effects on human health (United States Environmental Protection Agency, 2022a). Although mine dust is usually associated with mining operations and large volume waste impoundments, other activities such as the transportation, stockpiling and handling of ores can result in mine dust impacting communities situated far away from the mine itself. It is this challenge that is explored in this study with a focus on the Saldanha Bay Municipality situated within the West Coast District of South Africa.

This chapter introduces this study, carried out in the Saldanha Bay Municipality. The background of this study is presented, with a focus on the challenge that is faced in the municipality with regards to air pollution. The problem statement, scope as well as the limitations faced in this study are also presented. Finally, the structure of the dissertation is outlined in this chapter.

1.1. Background of Study

South Africa is known as one of the most naturally resource-rich nations in the world (Antin, 2013). The mining industry of South Africa has, historically, always been at the core of the country's economic development and has played a crucial role in the attraction of foreign investment and the creation of global enterprises (Antin, 2013).

In South Africa, mining and its associated activities are known to contribute to both the local and national economies, with the advantage of access to the three main ports that enable the export of bulk commodities. South Africa has seven coastal ports: Richards Bay, Durban, East London, Ngqura, Port Elizabeth, Cape Town and Saldanha. The three South African ports that carry out bulk mineral operations are the Ports of Richards Bay, Port Elizabeth and Saldanha. According to Transnet (n.d.), these three ports are known to be important hubs of logistical transportation for essential mineral consignments. Mueller et al. (2011) have reported that in areas where ports are located, many sources of air pollution can be found. These sources include industries, ship traffic, as well as the combustion of fuels by port-related vehicles (Mueller et al., 2011; Zhou et al., 2020). Healy et al. (2009) have reported that the main pollutants contributing to air pollution at shipping terminals include particulate matter (PM),

nitrogen as well as sulphur oxides. Kumar and Kumar (2017) have reported that the burden of air pollution associated from the exploration and exploitation stages at the mine extends to mining activities such as transportation and handling of metal ores at stock yards. Furthermore, the exposure to certain pollutants through air pollution can potentially result in various adverse health effects, with the World Health Organisation (WHO) reporting that approximately 4.2 million premature deaths worldwide were caused by exposure to ambient air pollution in 2019 (World Health Organisation, 2022).

A National Infrastructure Plan was adopted in 2012 by the South African Government (South African Government, n.d.). This plan was adopted to address the major challenges that the country faces today, which include challenges such as poverty and unemployment. Therefore, the Cabinet established a committee known as the Presidential Infrastructure Coordinating Committee (PICC) to develop, integrate and implement the National Infrastructure Plan (South African Government, n.d.). The PICC was also responsible for the development of 18 strategic integrated projects (SIPs) (South African Government, n.d.). This study was carried out within the Saldanha Bay Municipality, in which the Port of Saldanha is located. It is South Africa's deepest port and is regarded as important for both economic growth along the West Coast and national growth as it has been listed as SIP 5: Saldanha-Northern Cape development corridor (SLR Consulting, 2018; South African Government, n.d.). The SIP 5 includes the expansion of both the railway line that transports the metal ores to Saldanha as well as the port, where the ore is exported from by ship. Other incentives include expanding the back-of-port industrial capacity, which include an Industrial Development Zone (IDZ) as well as to build relationships for oil and gas trade along the West Coast of Africa (South African Government, n.d.).

Feasibility studies for the export of iron ore commenced in 1969 and the construction of the port started in 1973. In September 1976, the first ship load of iron ore was exported from the port. However, by this time, the Saldanha Bay harbour was recognised as an international port, with the ability to accommodate large ore-carriers (Anchor Environmental, 2017). Approximately 6 years later, diversification of the terminal was introduced to include the handling and export of other bulk commodities, including copper, lead, and zinc concentrates. According to Transnet (2013), almost 20 years later, steel, heavy minerals and manganese ores were also incorporated into the handling and exports.

The commodities exported from the port are transported to the port by use of railway lines. This form of transport could potentially be considered as a contributing factor to the dispersion of dust from the ore, due to the use of open-top carts that are used to transport the metal ores through the municipality to the port. Furthermore, once the ore has arrived at the port, the ore is stockpiled, handled, and loaded onto the ore carriers for export (PD Naidoo & Associates & SRK Consulting Engineers and Scientists, n.d.). According to a report by the World Health Organisation (1999), it is at this stage when large amounts of dust is produced.

The port is situated 6.9 km, 19.6 km, and 21.3 km to Saldanha, Langebaan and Vredenburg, respectively. These areas consist of communities who have subsequently raised their concerns regarding the impacts of air pollution from the port's activities. These issues include

the dust emissions from the transport of the ores through these communities via the railway line, the handling and open stockpiling of the ores, as well as the effect of poor air quality on human health (WSP, 2018). According to WSP (2018), there is a great sense of distrust between members of the community and the port, as it has been highlighted that the port carries out their own dust fall monitoring, instead of employing an independent third party. Although the municipality does carry out its own monitoring, there have been gaps in the PM monitoring data, due to air quality monitoring (AQM) stations being out of operation. It was also highlighted by several members of the community that they believe they suffer from respiratory complications, and yet, there has not been any further action taken to research if a link exists between the respiratory complications and the emissions from the port. Furthermore, there has also been financial implications on home and business owners to maintain their homes and buildings, due to the red/pink stain from the iron ore dust (WSP, 2018). The other concern that the community has, is the impact that the emissions from the port have on the tourism, fishing, and aquaculture industries, which are known to play a significant economic role in the municipality (WSP, 2018).

1.2. Problem Statement

The presence of the Port of Saldanha has resulted in the transportation of different types of metal ores for export through the Saldanha Bay Municipality. The metal ores are transported in uncovered wagons, stockpiled in open yards until export, and then loaded onto large ore-carriers. These activities result in considerable emissions of PM into the atmosphere. Although there are two air quality monitoring stations performing continuous $PM_{2.5}$ and PM_{10} monitoring, one in Saldanha and the other in Vredenburg, as well as seven dust fallout bucket sites, quantitative analysis of PM emissions and their compositions have been limited to date. Subsequently, it has been difficult to identify and assess the possible sources of emission and the potential impacts on the health and well-being of the surrounding communities.

1.3. Study Scope and Objectives

The overarching aim of this study was to assess the particulate matter (PM) concentration and composition in the Saldanha Bay Municipality, and based on these results, to assess the potential sources and potential health implications of these emissions. To achieve this aim, the following research questions were posed:

i. What are the concentration profiles of PM at the key study sites within the region?
ii. What are the chemical and physical characteristics of the collected PM samples?
iii. Based on the results from (i) and (ii), what are the potential sources of emission that contribute to PM contamination in the Saldanha Bay municipality?
iv. Based on the results from (i) and (ii), what are the potential health implications?

This study consisted of three phases, designed to address these research questions Phase one of this study involved working closely with the Air Quality Officer (AQO) at the Saldanha

Bay Municipality to determine the potential receptor and study sites for installation of the PM monitoring and sampling equipment. With the help of the AQO and the active participation by members of the community, a total of seven study sites were chosen. This included the two existing Air Quality Monitoring (AQM) stations that are used by the municipality.

Phase two included the fieldwork and laboratory analysis of this study. The fieldwork study included sampling of PM that was carried out using low-cost particulate sensors (PurpleAir Particulate sensors) and gravimetric samplers at the selected study sites. Other air quality equipment such as dust fallout buckets and Big Spring Number Eights (BSNEs) were also used at two study sites. $PM_{2.5}$ and PM_{10} concentrations obtained from the particulate sensors were analysed in RStudio using R and compared to both the standards outlined by South African legislation and guidelines set by the World Health Organisation (WHO). Furthermore, using the PM data obtained and meteorological data from a local weather station, pollution roses and polar plots were constructed to assist in identifying the potential sources of emission as well as analysing seasonal variations of PM as a function of wind direction. Physical PM samples from the gravimetric samplers, dust fallout buckets and BSNEs were analysed for both elemental and mineralogical composition using different analytical techniques.

The third and final phase consisted of the processing and interpretation of the primary data with a view to understand the nature and patterns of PM pollution and the potential sources and health risks associated with these emissions. It should, however, be noted that this study does not entail a detailed health risk assessment. Similarly, dispersion modelling does not form part of the scope of this study. It is envisaged that the results from this study can be used to inform such studies by providing information on the potential components of concern and their possible sources.

It should be noted that the first two key research questions are addressed based directly on the results derived through Phases 1 and 2 of this study. Key research questions iii and iv are interpretive questions and will be addressed through linkages between literature and the results in Phase 3.

1.4. Limitations of the study

One of the limitations of this study included travel restrictions to the Saldanha Bay Municipality in 2020 and 2021 due to the COVID19 pandemic, which resulted in samples left in the field, sometimes for a longer period than initially planned. Loadshedding, with no access to a power back-up, was another limitation of this study, as some of the sampling equipment depended on electricity to operate. The duration of continuous PM and sample monitoring was also limited, due to access to study sites as well as loadshedding that was experienced in the municipality. Another limitation of this study included the combination of the four dust fallout bucket samples into one. This was because the individual masses collected were not sufficient to be analysed, therefore, it was necessary to combine the four samples into one to be analysed. Lastly, like the dust fallout bucket samples, another limitation was the combination

of the samples collected from the BSNEs. The samples collected at two study sites were combined into one, for the same reason the dust fallout bucket samples were combined.

1.5. Structure of Dissertation

This dissertation is structured as follows:

- Chapter 1 introduces the study by providing background. The problem statement, scope of the study and limitations of the study are also outlined in this chapter.
- Chapter 2 reviews the relevant literature pertaining to this study.
- Chapter 3 provides the methods used in this study, which consist of the three phases. Phase one involves the monitoring and sampling receptor and study site selection and descriptions. Phase two includes the fieldwork and laboratory analysis, and phase three provides the data analysis and interpretation of the PM data and the physical PM samples obtained.
- Chapter 4 provides the PM results obtained from the particulate sensors. It also provides the results of the physical PM samples that were analysed using analytical techniques.
- Chapter 5 summarises and synthesises the results presented in Chapter 4, with specific reference to the four key research questions.
- Chapter 6 concludes this study. Furthermore, recommendations are also made for future research and development studies.

CHAPTER 2: LITERATURE REVIEW

This chapter outlines the importance of South African shipping terminals as well as the pollution that occurs in and around these terminals, with the focus on particulate matter (PM), particularly regarding metal ore exports. The effects of PM on both human health and the environment are presented. Furthermore, management, monitoring and mitigation measures of PM are also critically analysed. The Saldanha Bay case study is introduced in terms of areas of concern and current monitoring methods. The aims and objectives of this study are included, as well as a summary of Chapter 2.

2.1. The Importance of South African Shipping Terminals

Maritime transportation is solely responsible for seaborne trade to take place on a global level and has since become the backbone of the global economy being responsible for approximately 90% of global trade (Wan et al., 2021). The United Nations Conference on Trade and Development (2013) has reported that developing countries have been contributing increasing shares and growth to trade and the world GDP, and in addition have also been increasing their contribution to maritime trade. Statistics have also indicated that in 2011, 60% of world maritime trade originated in developing countries, with 57% of this trade delivered within their territories. Therefore, as a result, it has been reported that developing countries, such as South Africa, are emerging as major exporters on a global level (United Nations Conference on Trade and Development, 2013).

South Africa has eight coastal ports: Richards Bay, Durban, East London, Ngqura, Port Elizabeth, Mossel Bay, Cape Town and Saldanha. Some of the ports in the country can handle large Crude Carriers as well as ultra-large container ships. The three ports that carry out bulk mineral operations are the Ports of Richards Bay, Port Elizabeth and Saldanha. These three ports are known to be important hubs of logistical transportation for essential mineral consignments (Transnet, 2021). All eight Ports mentioned above are operated by Transnet and are shown in Figure 1 below.

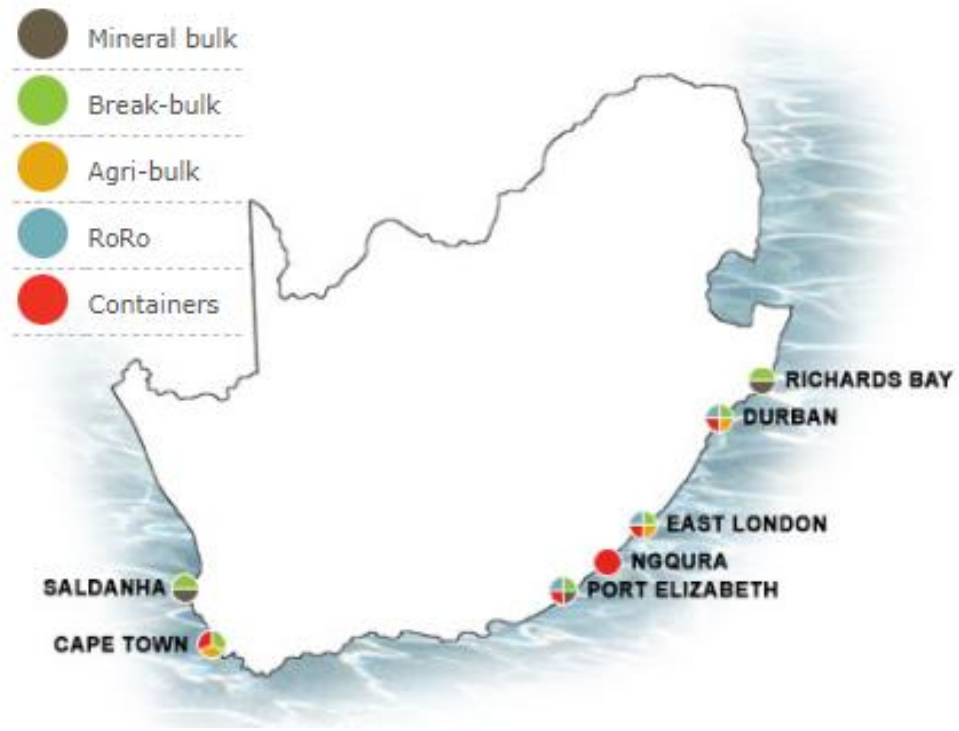

Figure 1: Transnet's seven main Shipping Terminals in South Africa (Transnet, 2021)

2.2. Air Pollution at Bulk Commodity Shipping Terminals

Shipping terminals are major hubs for economic activities; however, they are also one of the main sources of environmental pollution in coastal areas (Bailey & Solomon, 2004). Bailey and Solomon (2004) predicted that due to the increase in global trade, the economic activity at ports would increase and continue in the future. This prediction was confirmed in a study by Ballini and Bozzo (2015), who have reported that indeed there has been an increase in international shipping, which has consequently resulted in the increase of environmental impact by air pollution, despite the governance in place to curb this increase. Healy et al. (2009) have reported that the main pollutants emitted by shipping terminals include particulate matter (PM), nitrogen oxides as well as sulphur oxides.

Mining is known to play a significant role in economic development in a region and country. In addition to this, there exists the burden of air pollution associated from the exploration and exploitations stages at the mine to the transportation and handling of the ores at stock yards (Kumar & Kumar, 2017). Tian, Liang and Li (2019) have reported that developing countries face a challenge due to the lack of management as well as preventative measures with regards to the release of heavy metals into the atmosphere during mining and mining-related activities. A similar situation is one that is experienced in the present-day in Saldanha Bay in South Africa, where the metal ores, iron ore in particular, are transported in open-top carts by rail, from the mines to the Transnet Terminal in Saldanha Bay (Figure 2) (PD Naidoo & Associates & SRK Consulting Engineers and Scientists, n.d.).

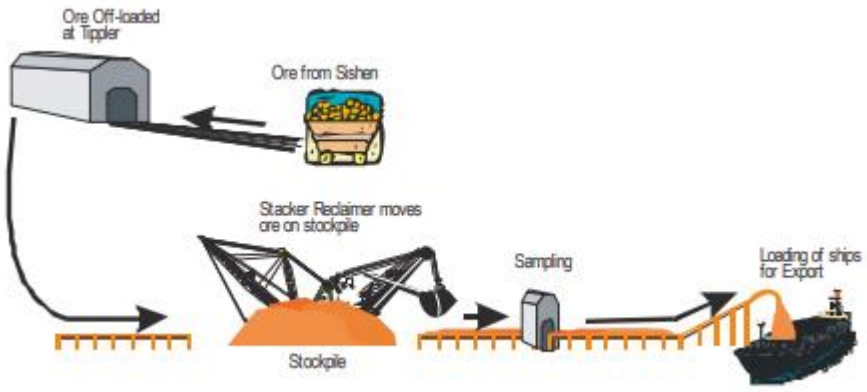

Figure 2: The current iron ore handling process at the Transnet Terminal in Saldanha Bay (PD Naidoo & Associates & SRK Consulting Engineers and Scientists, n.d.)

The iron ore is transported in open-top carts via the Sishen-Saldanha railway line from the mine to the Saldanha Bay Municipality. Tian, Liang and Li (2019) have reported that the dust that was tested in their study consisted of dust from many sources, one of them being truck leakage, where material was transported in uncovered trucks from the mines. Approximately 228 wagon trains that arrive via the Sishen-Saldanha railway line arrive at the Salkor Shunting Yard, located approximately 5 km north of the Transnet Terminal. Here, these wagon trains are broken down into shorter units, which subsequently allows them to be manageable (PD Naidoo & Associates & SRK Consulting Engineers and Scientists, n.d.). Once this is complete, the shorter units leave the Salkor Shunting Yard for the port for the unloading of their cargo. The tippler system, which has been designed to turn the units upside down, allows for the ore to be offloaded onto the conveyor belt system. The conveyor belt system transports the ore to the stockpile areas, where the iron ore is stacked onto the stockpiles by three stacker-reclaimers. These stacker-reclaimers are also used to retrieve the stockpiled ore by placing the ore onto the conveyor belts for loading onto the iron-ore carriers for export (PD Naidoo & Associates & SRK Consulting Engineers and Scientists, n.d.). According to a report by the World Health Organisation (1999), it is at this stage when large amounts of dust is produced.

2.3. Particulate Matter (PM) – An Air Pollutant

According to the United States Environmental Protection Agency (2022), particulate matter (PM), also known as particle pollution, is the term that is commonly used to describe the mixture of solid and liquid particles that are found in the air. Although PM has been defined, the definition of the term “dust” remains ambiguous. Petavratzi, Kingman and Lowndes (2005) have reported that the term “dust” is used generically to describe particles that are suspended in the air. This includes particles that are more commonly referred to as Total Suspended Particles (TSP), with aerodynamic diameters of up to 100 µm. The United States Environmental Protection Agency (2022) differentiates PM according to aerodynamic size. Inhalable course particles are particles that have an aerodynamic diameter between 2.5 µm and 10 µm, also known as PM_{10}. Particles with an aerodynamic diameter of less than 2.5 µm,

also known as $PM_{2.5}$, are classified as fine particles (Figure 3). Additionally, there is another subdivision of PM, known as ultrafine particles. These particles have an aerodynamic diameter of less than 0.1 µm (Gautam et al., 2016; Kant et al., 2016).

The United States Environmental Protection Agency (n.d.) has defined dust as particles, of any solid material, that are suspended in air, usually with a particle size less than 100 µm. In this study, the definitions of $PM_{2.5}$, PM_{10} and dust made by the United States Environmental Protection Agency (US EPA) are used.

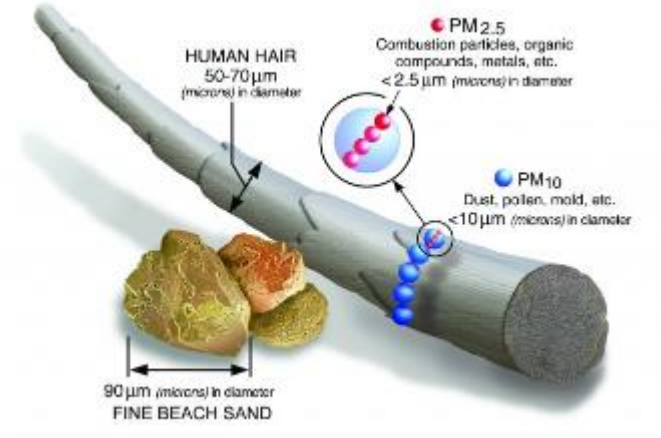

Figure 3: Size comparisons of $PM_{2.5}$ and PM_{10} particles (United States Environmental Protection Agency, 2022a)

PM can originate from both natural and anthropogenic sources (Csavina et al., 2012). Figure 4 below indicates the potential contaminant concentration against the potential particulate emissions and the potential risk to both human health and the environment. Csavina et al. (2012) reported that, although there are many anthropogenic and natural sources of particulate emissions, mining operations have the highest potential of risk to the environment and human health (Figure 4). Thornton (1996), has reported that mining-related activities such as smelting and handling large amounts of material, contribute to the contamination of the air, soil, and water. The contamination from these mining-related activities can be as a result of either controlled emissions, or the transport and storage of mineral-rich materials (Thornton, 1996). Entwistle et al. (2019) reports that potentially toxic elements are commonly associated with mined material and or gangue minerals in ores, such as arsenic, lead, copper, mercury, uranium, and zinc.

Activities associated with mining, including ore transportation, loading, off-loading and storage, generate airborne particulate suspension when exposed to wind (Boente et al., 2022). Csavina et al. (2012) reports that contaminated particulates emitted from mining-related activities are mostly in the finer size range with aerodynamic diameters less than 2 µm. These finer particulates travel a further distance than coarser particulates (Csavina et al., 2012).

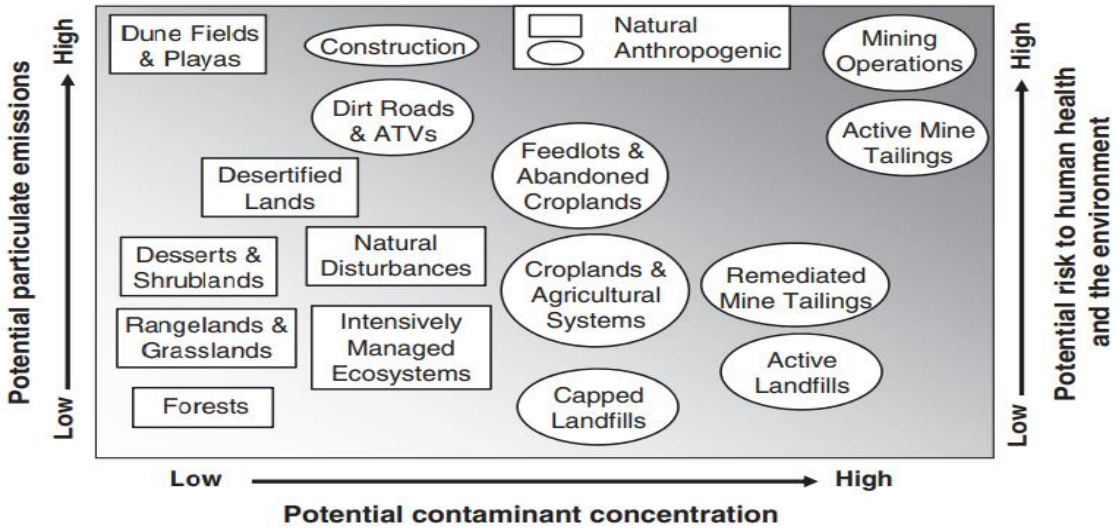

Figure 4: The anthropogenic and natural sources of dust associated with the relative amounts of potential particulate emissions, contaminant concentration and risk to the environment and human health (Csavina et al., 2012)

2.4. The Impact of Particulate Matter on Human Health

There is a relationship between adverse health effects and PM (Gautam et al., 2016). Composition of PM vary as PM absorbs and transfers multiple pollutants, therefore, when humans are exposed to PM, the different compositions of these mixtures as well as the concentration, contribute to adverse effects on human health (Gautam et al., 2016). Voutsa and Samara (2002) state that the size and shape of a particle are the two critical factors which control the extent to which airborne particles penetrate the respiratory tract in humans. However, it is emphasized that the size of the particle is the most important parameter in determining the different health implications (Gautam et al., 2016). Aerodynamic properties are used to express the size of a particle, since they help control the transport and removal of particles from air (Gautam et al., 2016). The aerodynamic properties also assist in governing the deposition of the particles in the respiratory system and are associated with both the composition and source(s) of the particles (Gautam et al., 2016).

Although coarse (PM_{10}), fine ($PM_{2.5}$), and ultrafine particulates are known as the three main subclasses of PM, PM is also classified in groups according to its deposition in the respiratory tract of mammalian species (ISO, 1995). These particulates are assigned as inhalable, thoracic, or respirable fractions (Petavratzi, Kingman & Lowndes, 2005). Jimenez, van Tongeren and Cherrie (2011) have reported the internationally agreed sampling curve criteria for inhalable, thoracic, and respirable fractions which is used to define these fractions (Figure 5).

Petavratzi, Kingman and Lowndes (2005) and Brown et al. (2013) have defined the inhalable, thoracic and respirable size fractions based on the reporting from the European Committee

for Standardisation (CEN). The inhalable size fraction is the mass fraction of the total airborne materials that are inhaled into the body through the mouth and nose, and these particulates are able to settle anywhere along the upper respiratory tract (World Health Organisation, 1999; Petavratzi, Kingman & Lowndes, 2005; Brown et al., 2013). These particles might not have pulmonary health effects but can pose as an irritant (Gautam et al., 2016). As indicated in Figure 5 , the inhalable fraction has 100% penetration for particles with aerodynamic diameters less than 10 µm. The penetration drops to 50% for particles with an aerodynamic diameter of 100 µm. The inhalable fraction also has no median cut-off aerodynamic diameter.

The thoracic fraction is the mass fraction of the inhaled particulates that penetrate beyond the larynx (Petavratzi, Kingman & Lowndes, 2005; Brown et al., 2013). These particles may be up to 30 µm in size but the criterion for this fraction is that 50% of the particles with an aerodynamic diameter of 11.54 µm will enter the larynx. The larynx is a hollow tube that connects the throat to the rest of the respiratory system, therefore, the thoracic fraction of particulates is able to penetrate the airways of the lung (Gautam et al., 2016). However, according to Petavratzi, Kingman and Lowndes (2005), this varies according to breathing patterns and individuals. The respirable fraction is the mass fraction of particulates that penetrates the unciliated airways and the gas exchange area of the lung (Petavratzi, Kingman & Lowndes, 2005; Brown et al., 2013). The criterion for this fraction includes a 4.25 µm median diameter. Gautam et al. (2016) have reported that toxins present in the respirable fraction may have a chemical reaction with the respiratory system as well as allow the transfer of the toxins into bloodstream via the alveolar walls. Petavratzi, Kingman and Lowndes (2005) have also reported that similar to thoracic particulates, respirable particulates vary by individual and breathing patterns.

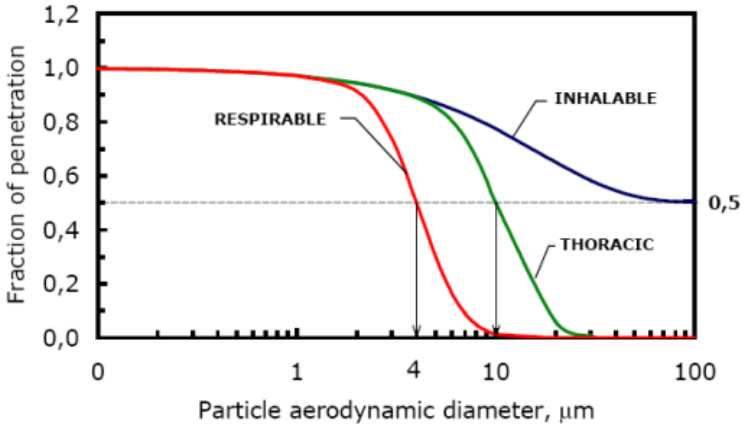

Figure 5: Probability for aerosol penetration as a function of particle aerodynamic diameter (Jimenez, van Tongeren & Cherrie, 2011)

The US EPA has outlined the effects of both short and long-term exposures to PM. Short-term particle exposures include exposures over a few hours or days. This type of exposure is shown to aggravate different types of lung disease such as asthma, acute bronchitis as well as increase respiratory infections (United States Environmental Protection Agency, 2022b). The US EPA has also reported that people who suffer with heart disease are more susceptible to

heart attacks, through PM exposure. According to Brook et al. (2010), results from many previous studies have indicated that exposure to PM is associated with adverse cardiovascular complications. Hassanvand et al. (2017) investigated the effects of PM on systematic inflammation biomarkers, which have been previously linked to the risk of both cardiovascular mortality as well as morbidity. Hassanvand et al. (2017) indicated that short-term exposure to $PM_{1\text{-}2.5}$, $PM_{2.5}$, $PM_{2.5\text{-}10}$ and PM_{10} were found to be associated with coagulation blood markers as well as inflammation. However, Hassanvand et al. (2017) also reported that the associations were largely dependent on the size of the PM and differences were found across time. Another study carried out by Hertel et al. (2010) also investigated the associations between inflammatory markers and exposure to PM and reported that the results of the study indicated that short-term exposure of PM can have adverse effects on cardiovascular health through an inflammatory mechanism.

Long-term exposure includes exposure experienced over many years. This exposure has been associated with health complications such as reduced function of the lung, chronic bronchitis as well as premature death (United States Environmental Protection Agency, 2022b). Studies were also carried out to investigate the effect of long-term exposure to air pollution and inflammatory markers in midlife women (Ostro et al., 2014; Green et al., 2016). The results from both studies indicated that long-term exposures of $PM_{2.5}$ were associated with high levels of the inflammatory markers, which subsequently may have adverse cardiovascular effects (Ostro et al., 2014; Green et al., 2016).

2.5. The Impact of Particulate Matter on the Environment

PM is known to have caused, in association with other gaseous compounds, several global, regional, and local environmental impacts. These include cloud modification, climate change, acid rain, ozone depletion, visibility reduction as well as destruction of property (Gautam et al., 2016). Some elements in trace amounts, such as arsenic, chromium and lead, have been found in cloud, fog, rain, and snow with mining-related activities alluded to as the sources (Csavina et al., 2011). Metal contamination in airborne PM also affects the surrounding fauna and flora (Huertas, Huertas & Solís-Casados, 2012).

According to Petavratzi, Kingman & Lowndes (2005), dust can be classified based on its effects on the environment, occupational health and effects, and physiological health effects. Petavratzi, Kingman and Lowndes (2005) have also reported that there are different sub-classes of dust that have an effect on the environment and these sub-classes may affect the environment in different ways depending on their physical characteristics. These sub-classes include generated dust, TSP, and nuisance dust. TSP has been defined previously in Section 2.3. Generated dust, defined by Petavratzi, Kingman and Lowndes (2005), is dust that is produced when solid materials are broken down by mechanical processes. However, not all this dust is capable of becoming airborne and entrained in the air. The portion of the generated dust that remains entrained in the air is known as TSP. Nuisance dust, which consists of larger, coarser, and settleable particulates has an aerodynamic diameter of more than 10 µm

(Khuzestani & Souri, 2012). Apart from physiological effects, these particulates are known to cause damage to infrastructure, machinery as well as reduce environmental amenities. Other effects of this type of dust include the reduction of visibility and the possibility of becoming an irritant substance in the atmosphere (Meyer, Du Plessis & Oberholzer, 1996).

Another class of atmospheric dust is fugitive dust, which occurs from the mechanical disturbance of material which is exposed to the air (United States Environmental Protection Agency, 2022b). This type of dust is defined as fugitive dust due to that it enters the atmosphere directly without first passing through either a duct or stack that is designed to control or direct the flow of the particulates. Some sources of fugitive dust include stockpiling of material, industrial processes as well as transportation and utilities (United States Environmental Protection Agency, 2022b;Ma et al., 2022). According to Organiscak and Randolph Reed (2004), fugitive dust that is generated includes particulates that become airborne and can consist of all sizes. Cao et al. (2008) have reported that fugitive dust is a major contributor to $PM_{2.5}$, which suggests that fugitive dust can also occur as inhalable dust. According to the Michigan Department of Environmental Quality (2016), most of fugitive dust particulates are, however, greater than 10 µm. This suggests that fugitive dust can also be classified as nuisance dust with regards to the larger and coarser particulates. As in the case of nuisance dust, fugitive dust particles are known to affect the environment by reducing visibility, which subsequently can result in vehicle and/or site accidents leading to either fatal injury or even death (Michigan Department of Environmental Quality, 2016).

2.6. The Effect of Meteorological Conditions on PM

To investigate the impact that meteorological conditions have on PM concentrations, several studies have been carried out to analyse the correlations between meteorology and PM concentrations (Huang et al., 2015; Li et al., 2015; He et al., 2017; Pope, Ezzati & Dockery, 2009). Some of these meteorology conditions include wind speed and direction, precipitation, and relative humidity, and have been found to exhibit complex interactions with PM.

Numerous studies have been conducted to investigate the influence of wind speed on the dispersion of PM (Huang et al., 2015; Sekuła et al., 2021; Dubey et al., 2022). According to some studies, it has been concluded that that there exists an inverse relationship between wind speed and $PM_{2.5}$ concentrations (Vassilakos et al., 2005; Huang et al., 2015). This alludes to that higher wind speeds assist in dispersing $PM_{2.5}$, while lower wind speeds would allow the accumulation of $PM_{2.5}$, subsequently resulting in higher concentrations.

Similarly to wind speed, studies have indicated that there is a negative correlation between precipitation and PM concentrations (Virgianto et al., 2021;Singh, Singh & Biswal, 2021). This is due to the scavenging effect that precipitation has on PM, where particles are scavenged from the atmosphere through wet deposition. Results regarding relative humidity have been inconsistent across studies. Akyüz & Çabuk (2009) concluded that there is a negative correlation between relative humidity and $PM_{2.5}$. Conversely, the results from a study by Huang et al. (2015) showed a positive correlation between relative humidity and $PM_{2.5}$.

Another factor to consider are temperature inversions, which are defined as natural occurrences, whereby temperature increases with altitude and forms distinct layers in the atmosphere (Nidzgorska-Lencewicz & Czarnecka, 2020). One of the effects of surface-based temperature inversions (SBTIs) is the increase in PM concentration at night. Niedźwiedź et al. (2021) concluded in their research that SBTIs are a key factor in the elevated concentration of PM in the near ground-layer of the atmosphere in winter months. Furthermore, Niedźwiedź et al. (2021) also indicate that this had also occurred during low PM emissions.

2.7. Managing, Monitoring and Mitigation of PM

There are a number of areas in South Africa that have been flagged as areas with air quality problems. Some of these are areas where various industrial activities take place, resulting in emissions of pollutants at different levels. The National Environmental Management: Air Quality Act (NEMAQA) Act No. 39 of 2004 outlines the 2017 National Framework for Air Quality Management in the Republic of South Africa, which stipulates that these levels depend on the amount of pollutant that is emitted and the number of sources per area (Department of Environmental Affairs, 2018). All South Africans have a right to know the status of the air quality that is monitored by air quality monitoring stations that have been commissioned by the government. According to the World Health Organisation (2022), there is strong evidence on the negative health effects associated with PM exposure, with one of the major components of PM being mineral dust. The 2017 National Framework for Air Quality Management also states that since there is a close and quantitative relationship between exposure to PM and increased mortality, it is important to limit the exposure to allow the related mortality to decrease (Department of Environmental Affairs, 2018).

2.7.1. South African Legislation on Air Quality Management

The 2017 National Framework for Air Quality Management is influenced by policies and legislative laws that are developed at international, national, provincial as well as municipal levels (Department of Environmental Affairs, 2018). The approach to control air pollution in South Africa was promulgated in 1965 by the Atmospheric Pollution Prevention Act, 1965 (Act 45 of 1965), also known as APPA. However, standards and targets that would ensure the achievement of an environment that is not harmful to health or well-being, were not set by the APPA (Department of Environmental Affairs, 2018). The APPA was replaced by the National Environmental Management: Air Quality Bill of 2003 (Department of Environmental Affairs and Tourism, 2003). The Bill established South African norms and standards, an air quality management framework, planning and reporting system as well as regulatory instruments to control air pollution, enforcement, and compliance (Department of Environmental Affairs and Tourism, 2003). The Department of Environmental Affairs (2018) have also outlined in the National Framework, that it is a Constitutional Right for the surrounding environment to be safe to health and well-being. To uphold this right, it was necessary that air quality legislation regarding cleaner air was required (Department of Environmental Affairs, 2018).

The National Environmental Management: Air Quality Act (NEMAQA) of 2004 addresses the adverse effects on ambient air pollution and outlines the acceptable concentration limit values and standards for pollutants found in ambient air (Department of Environmental Affairs, 2018). The objectives of the Air Quality Act (AQA) are to prevent air pollution, enhance and protect the quality of air in South Africa. It also aims to achieve sustainable development, subsequently promoting economic and social development. Another objective of the AQA is to ensure that all South Africans have access to clean air and an environment that is not harmful to health and well-being (Department of Environmental Affairs, 2018;Department of Environmental Affairs, 2009). The averaging period is the period of time whereby an average value is determined. The concentration limit values are defined as numerical values that have a unit of measurement, and the frequency of exceedance is a frequency that is related to a limiting value that represents the allowable exceedance of that limit value. The compliance time frames refer to date(s) when compliance with the standard is required (Department of Environmental Affairs, 2018).

The air quality guidelines that are introduced by the World Health Organisation is set out to offer health-based recommendations on a quantitative level (World Health Organisation, 2021). These guidelines are for both short- and long-term concentrations for key pollutants. The WHO has stated that, while these guidelines are not legally binding, they serve as an evidence-informed tool, which can be used during policymaking and legislation. Ultimately, the most important goal of these air quality guidelines is to play a significant role in reducing the high levels of air pollution, which subsequently allows for the decrease of the global health burden that is associated with air pollution (World Health Organisation, 2021).

Due to the health risk associated with PM, many international bodies have introduced statutory guidelines with regards to ambient PM pollution (Kim, Kabir & Kabir, 2015). These guidelines are presented in Table 1 below (European Commission, n.d.; Department of Environmental Affairs, 2009; Department of Environmental affairs, 2012; World Health Organisation, 2021; United States Environmental Protection Agency, 2023). The WHO has the strictest $PM_{2.5}$ and PM_{10} concentration guideline value for both 24-hour and annual averaging periods. South African concentration limits for $PM_{2.5}$ are lower than those of China and the EU but higher than the US standards. In the case of PM_{10}, the South African 24-hour concentration limit is higher than the WHO and the EU standard, but lower than that of China and the US. According to South African legislation, there are a total number of four allowed exceedances for a 24-hour cycle for both $PM_{2.5}$ and PM_{10}. Compliance dates are dates by which compliance with $PM_{2.5}$ and PM_{10} concentration limit values are required. South African standards for the current 24-hour and annual $PM_{2.5}$ concentrations are valid until the 31st of December 2029, whereafter new and stringent concentration limit values will be in effect (Table 2). New compliance dates for PM_{10} concentrations have not yet been specified.

Table 1: $PM_{2.5}$ and PM_{10} guidelines according to South African and International Governments

	Averaging Period	South Africa	WHO	EU	China	US
$PM_{2.5}$ ($\mu g/m^3$)	24 hours	40	15	n.a	75	35
	1 year	20	5	25	35	15
	Allowed frequency of exceedance per annum	0	n.a	n.a	n.a	n.a
PM_{10} ($\mu g/m^3$)	24 hours	75	45	50	150	150
	1 year	40	15	40	70	n.a
	Allowed frequency of exceedance per annum	0	n.a	n.a	n.a	1

*n.a stands for not available

Table 2: 24-hour and annual $PM_{2.5}$ concentration limits for 2030 compliance dates (Department of Environmental Affairs, 2009)

Pollutant	Averaging Period	Concentration Limit Values ($\mu g/m^3$)	Frequency of Exceedance	Compliance Date
$PM_{2.5}$ ($\mu g/m^3$)	24-hour	25	4	1 January 2030
	1 year	15	-	

Few national concentration limit values exist for pollutants when considering the NAAQS set out by NEM: AQA Act 39 of 2004 (United States Environmental Protection Agency, 2023a). The European Commission (EU) has outlined air quality standards for a variety of pollutants in its Four Daughter Directives (Environmental Protection Agency, n.d.). However, the focus is specifically on the 4th Daughter Directive which outlines ambient air limits of pollutants such as arsenic (As), nickel (Ni) and cadmium (Cd) (Table 3).

Table 3: Limit values for arsenic, cadmium and nickel outlined by the EU in the 4th Daughter Directive (Environmental Protection Agency, n.d.)

Pollutant	Averaging period	Target value ($\mu g/m^3$)	Limit Value Attainment Date
Arsenic	1 calendar year	0.006	31 December 2012
Cadmium		0.005	
Nickel		0.02	

2.7.1.3. South African Air Quality Monitoring

The two types of monitoring technologies, satellite and ground-based monitoring has improved significantly over the last 50 years, which has subsequently allowed for a better understanding of sources and chemical composition of fine particulates, as well as their impact on both human health and the environment (Engel-Cox et al., 2013). Ground-based monitoring is carried out using filter-base sampling or semi-continuous sampling measurements, the latter using a range of PM sampling monitors (Engel-Cox et al., 2013). Sampling that makes use of a filter to collect the sample is usually carried out over a specific period, such as a 24-hour sampling period. The mass and concentration of the sample and different particulate sizes, such as $PM_{2.5}$, PM_{10} and/or larger particulates, are determined gravimetrically (Engel-Cox et al., 2013). Another ground-based monitoring method in South Africa is dust fall monitoring. The standards and regulations of dust fall monitoring is outlined in the NEM: AQA (Act no. 39 of 2004) (Department of Environmental Affairs, 2018).

The two reference methods that are used for ground-based monitoring $PM_{2.5}$ and PM_{10} concentrations in South Africa are EN 14907:2005 and EN 12341:1998, respectively (Department of Environmental Affairs, 2015a). The reference method EN 12341 refers to the use of filter-based gravimetric samplers, including superhigh volume, high volume, and low volume samplers (Pilling et al., 2005). These samplers comprise of a sampling inlet that allows for the sampling of particles with aerodynamic diameters less than 10 µm. The inlet of the sampler is connected to a filter substrate as well as a flow controller that is regulated. After sampling has been completed, the EN 12341 method states that the mass collected on the filter paper is determined gravimetrically. The filter paper is also required to be conditioned at 20 °C and 50% relative humidity before it can be weighed to determine the mass (Pilling et al., 2005). The reference method EN 14907 also refers to the use of filter-based gravimetric samplers, such as the three mentioned above for EM 12341. However, the only difference between EN 12341 and EN 14907 is that the sampling inlet for EN 14907 allows for the sampling of particles with aerodynamic diameters less than 2.5 µm.

The procedure followed for dust fallout monitoring in South Africa is the ASTM D1739, the American Standard to Testing and Materials method (Department of Environmental Affairs, 2013). This is the standard method for the collection as well as the measurement of dust fall. It is stated in NEM: AQA (Act no. 39 of 2004) under the Draft National Dust Control Regulations, that the method used in South Africa for the measurement of dust fall is ASTM D1739:2010 (Department of Environmental Affairs, 2018). The ASTM D1739: 2010 also outlines the acceptable dust fall rates for both non-residential and residential areas (Table 4).

Table 4: Acceptable dust fall rates for both non-residential and residential areas in South Africa (Department of Environmental Affairs, 2013;Department of Environmental Affairs, 2018)

Areas	30-day average dust fall rate (D) in mg/m^2/day	Frequency of exceedance
Non-residential	D < 600	Two within a year
Residential	D <= 1 200	Two within a year

2.7.2. Mitigation Measures of PM at Ports

Al-Thani, Koç and Isaifan (2018) have reported that mitigation strategies of PM is extremely significant to reduce the impact and effect that PM has on the surrounding environment. In particular at ports, it is important to control dust emissions to improve the working environment of employees and their health as well as to increase productivity at the workplace and to better public relations (Berry, 2014). One of the mitigation policies that Al-Thani, Koç and Isaifan (2018) have reported includes improving the management of different processes. Improving the design of processes, operations that are carried out, maintenance as well as housekeeping significantly reduces emission (Al-Thani, Koç & Isaifan, 2018). According to Berry (2014), there are five potential approaches when dealing with dust emissions at Ports. These include preventing dust emissions at the source, preventing dust emissions during handling of material containment of any dust that is emitted, suppression of dust emissions and lastly, extraction and collection of dust that is emitted.

When considering preventing dust emissions at the source, this refers to reducing the amount of dust that is emitted from materials at the port. Some of the methods that apply this approach include the addition of a suppressant as well as the application of appropriate material handling techniques which can subsequently reduce dust emissions and particle attrition (Berry, 2014). Prevention includes reduction of dust emissions during handling of materials, such as loading and off-loading. When off-loading materials from the ships/carriers, the preferred method includes the use of bucket wheel and screw elevator unloaders (Berry, 2014). These unloaders are known to provide better containment of dust once the material is in the conveyor tube. At transfer points on the conveyor belts, the preferred method is to use the hood and spoon method, at opposed to the traditional method, which includes using a wet spray when material is transferred from one conveyor to the next (Berry, 2014). The hood and spoon method involves the profile of the hood being matched to the trajectory of the material that is about to be transferred to another conveyor. The spoon is present to direct the material onto the next conveyor at the appropriate velocity to allow for the material and dust to be kept together in a packed stream. This method is known to reduce the impacts and severity, which subsequently reduces the attrition of particles (Berry, 2014). The use of cascades as well as slow down chutes is a good approach during ship loading and off-loading. These allow for the material to be kept in a dense stream, which allows for the reduction of dust emission and particle attrition (Berry, 2014).

Containment includes containing any dust that is emitted or generated at the port(s) in either storage vessels or conveyors, to ensure that emissions are minimised. The traditional method of suppression of dust in ports involves the use of wet sprays to damp down material to reduce emissions, however, the use of the wet sprays could result in the increase of moisture content in the material(s). A new and preferred method involves the use of fogging systems. These systems produce fog around the trajectory of the material that is moving, subsequently containing the material (Berry, 2014). The last suggestion made by Berry (2014) is extraction and collection of the dust. This is carried out using extraction ducts around the transfer points at the port to assist with dust control and emissions (Berry, 2014). With regards to stockpiling of material(s), the United States Environmental Protection Agency (2022b) has provided measures that can be put into place to reduce PM emissions. One of these measures indicate the use of a wet spray, which has been discussed above. The other measures include the installation of covers, stockpiling the material(s) in an enclosed environment or installing wind breaks around the stockpiles. According to the United States Environmental Protection Agency (2022b), these measures contribute significantly to reducing emissions.

2.8. Saldanha Bay: An Area of Challenges

The Saldanha Bay Municipality is situated within the West Coast District Municipality in the Western Cape province, along the West Coast of South Africa (Figure 6). The are several large towns in the municipality, such as Vredenburg, Saldanha and Langebaan as well as other fishing and holiday towns situated along the coast of the Municipality.

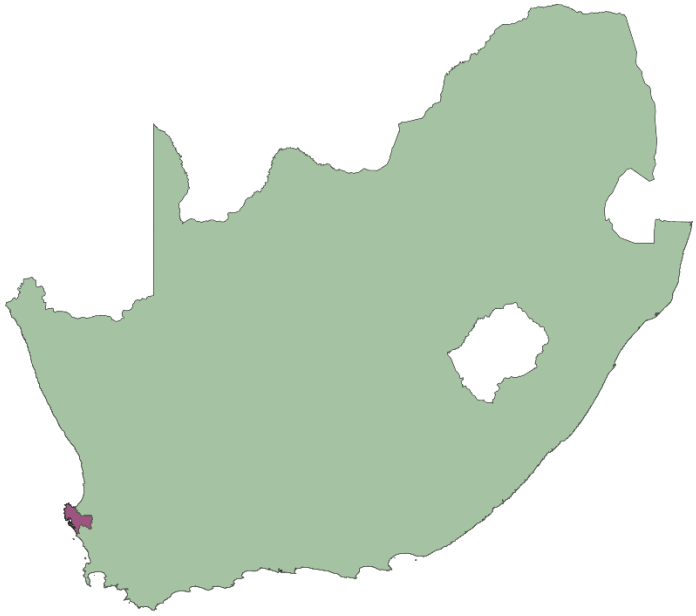

Figure 6: A map of the Saldanha Bay Municipality along the West Coast of South Africa

2.8.1. Modern-Day Saldanha Bay

During the 19th century, Saldanha Bay was primarily a fishing village and was of interest only to fishermen and whalers (FEWLB Nexus, 2021;South African History Online, n.d.). The town of Saldanha was founded on this lucrative fishing industry and was further developed by the construction of the port. In 1976, the Port of Saldanha Bay developed into a modern harbour, when the export of iron ore from the mines in the Northern Cape province became necessary (CCH, 2018). Welman and Ferreira (2016) have reported that the establishment of Saldanha has been, and will always be, linked to the evolution of the port. In 2011, Saldanha was listed as a presidential priority development region and two years later it was declared an Industrial Development Zone (IDZ). This was important for the envisaged oil and gas industry on the West Coast as well as the broader west coast of Africa (Welman & Ferreira, 2016). A year later, the government announced the strategy Operation Phakisa. This aim of Operation Phakisa was to unlock the economic potential that the South African ocean areas have (Department of Forestry Fisheries and the Environment, n.d.). With regards to the geology of the area, Le Roux, Bezuidenhout and Smit (2019) have reported that two main towns, Saldanha and Vredenburg, are the largest settlements situated in the West Coast Peninsula which forms part of the Cape Granite Suite. The dimension of the Peninsula is approximately 20 km in width and 40 km in length. The dominant geology of the Peninsula is granite, with both Saldanha and Vredenburg built on granite hills, with granite rocks present amongst houses in the suburbs (Le Roux, Bezuidenhout & Smit, 2019) (Figure 7).

Figure 7: Granite rocks present amongst houses in Vredenburg (Le Roux, Bezuidenhout & Smit, 2019)

With regards to aquaculture in Saldanha Bay, according to Anchor Environmental (2023), mussel and oyster farming was established in Saldanha Bay in 1981 and the early 2000s, respectively. Since then, aquaculture activities have developed and extended in the region, which subsequently resulted in these activities requiring an Environmental Impact Assessment (EIA). The EIA is carried out to acquire Environmental Authorisation (EA) provided by the Department of Forestry, Fisheries, and the Environment, which proves to be costly (Anchor

Environmental, 2023). Therefore, to prevent the laborious and costly barrier to the development and expansion of aquaculture activities, the Department of Agriculture, Forestry and Fisheries established the Aquaculture Development Zone (ADZ). Some of the aquaculture activities in the ADZ include the maintaining of structures, cultivated species harvesting, processing of bivalves and vessel trips (Anchor Environmental, 2023).

In addition to all the industrial development occurring in the Saldanha area which creates employment opportunities and the alleviation of poverty, Saldanha is also a famous tourist attraction. Saldanha is a picturesque coastal town, situated on the northern corner of one of South Africa's largest natural bays. The ideal location of the bay attracts both local and international water-sport enthusiasts (Anchor Environmental, 2023). Over the last few years, there has been an increase in the number of tourists visiting Saldanha Bay due to the West Coast National Park and Langebaan Lagoon, a Ramsar Site. The economy of the region thus is largely dependent on fishing, the harbour trade, tourism.

2.8.2. The Port of Saldanha

The Port of Saldanha is South Africa's largest natural, deepest port and is regarded important for economic growth along the West Coast of South Africa. The port was initially built for the export of iron ore, but today, various other metal ores such as lead, manganese and zinc are also exported. Blue Bay, Langebaan, Saldanha Bay and Vredenburg are the surrounding communities which are in close proximity to the port and other industries.

The iron ore terminal is the largest iron ore export facility in Africa and the only iron ore terminal in South Africa (Transnet, 2013). Feasibility studies for the export of iron ore started in 1969, with the construction of the port commencing in 1973. The very first ship load of iron ore was exported on the vessel, Fern Sea, in September 1976. By this time, the Saldanha Bay harbour became an international port and could accommodate large ore-carriers (Anchor Environmental, 2017). In 1979, diversification of the terminal occurred to include the handling and export of bulk commodities such as copper, lead, and zinc concentrates. Almost 20 years later, steel, and heavy minerals were also incorporated into the handling and exports (Transnet, 2013).

There are two key terminals at the port: the Iron Ore Terminal and the Multi-Purpose Terminal (MPT). The Iron Ore Terminal is South Africa's only dedicated iron ore terminal and contributes to almost 96% of South Africa's iron ore exports. The Iron Ore Terminal has the capacity to handle approximately 60 million tonnes per annum (tpa) of iron ore. However, Transnet intends to increase the throughput to 65 million tpa (Transnet, 2013). The ore that is exported from the Iron Ore terminal arrives from iron mines situated in the Northern Cape Province, 861 km from the Port of Saldanha. The MPT services mainly bulk clients and has the capacity to handle up to 8.5 million tpa of break bulk cargo. Initially, the MPT was used for the export of lead and zinc. In 2011 and 2013, the export of iron ore and manganese from the MPT commenced, respectively. It was found that by 2016, 15% of the total amount of manganese exported from South Africa, had been exported from the MPT (Anchor Environmental, 2017).

The MPT has four berths in total with two berths dedicated to manganese and iron ore vessels. The MPT channels approximately 4% of South Africa's iron ore exports (Figure 8). The other two berths are dedicated to bulk cargo, excluding manganese and iron ore (Transnet, 2013).

Figure 8: The aerial view of the Transnet MPT at the Port of Saldanha (Transnet, 2013)

2.8.3. Concerns from the Community

Issues that have been highlighted by the communities around Saldanha include the dust emissions from the transportation of the metal ores through these communities via the railway line, the handling and open stockpiling of the ore, as well as the effect of poor air quality on human health (WSP, 2018). According to a comments and response document compiled by the WSP Consulting Firm, one of the members of the Blue Water Bay community highlighted that the port does not employ an independent third party to carry out the dust fall monitoring in and around the port, but rather carries out its own monitoring (WSP, 2018). This has led to distrust from members of the community, which has been highlighted previously (Chetty & Grüning, 2018). According to an article by Ludidi (2021), a spokesperson for the Transnet Port Terminals has said that for last forty years, the dust emissions have been below the limit of 1 200 mg/m^3 and that the terminals continue to employ mitigation measures to ensure operations are environmentally compliant. The spokesperson has also reported that the visible dust is classified as nuisance dust and does not pose a threat to the health of members of the community. However, as mentioned above, since there is no third party involved, there is a great sense of distrust between the members of the community and the results from the monitoring carried out by the port (WSP, 2018).

The WSP report also mentioned that several members of the community suffer from respiratory problems and that no further action has been taken to research whether there exists a link between the dust emissions and respiratory implications (WSP, 2018). Members of the community are also concerned over the red/pink stain from the iron ore dust. There

have been reports that houses, cars, plants as well as animals, such as birds and sheep, are stained. The staining of properties has resulted in financial implications on members of the community. A member of the Blue Water Bay community has reported that the cottages located in Blue Water Bay are required to have a power wash every six months to maintain their colour (WSP, 2018). In addition to the red iron ore dust, a significant amount of black dust has now been noticed at Blue Water Bay as well. Given that Blue Water Bay is one of the closest communities to the port, many residents are now demanding the comparison of the PM concentration levels to the limits set out by the WHO, instead of those set out in NEM: AQA (Act 39 of 2004) (WSP, 2018). Another area of concern is the impact of the emissions on tourism, the fishing industry and the mussel and oyster industry (WSP, 2018). A member of the community has reported that filter feeders such as mussels depend on good water quality. However, there has also been reports that the presence of heavy metals has been found in mussels, although not at a level that is dangerous to human health (WSP, 2018).

2.9. Current Monitoring and Sampling by the Saldanha Bay Municipality

The Saldanha Bay Municipality carries out dust sampling measures and air quality monitoring at different locations around the municipality (Saldanha Bay Municipality, n.d.). This network consists of seven dust fallout bucket sites and two air quality monitoring (AQM) stations, although it should be noted that one dust fallout bucket is installed at the Saldanha AQM Station. The AQM stations were installed to sample for sulphur dioxide (SO_2), nitrogen oxide (NO), nitrogen dioxide (NO_2), oxides of nitrogen (NO_X), ozone (O_3), $PM_{2.5}$ and PM_{10} concentrations (Saldanha Bay Municipality, n.d.). The municipality's sampling/monitoring sites are indicated below (Figure 9). There are two sites in Saldanha (Blue Bay and the Saldanha AQM Station), three in Vredenburg (the Vredenburg Reservoir, the Vredenburg Electricity Department and the Vredenburg AQM Station), one between Vredenburg and Saldanha (the Airport), one just out of Vredenburg (Juffroushoogte) and one in Langebaan (Curro School). Dust fallout buckets are located at all of these sites, except at the Vredenburg AQM Station.

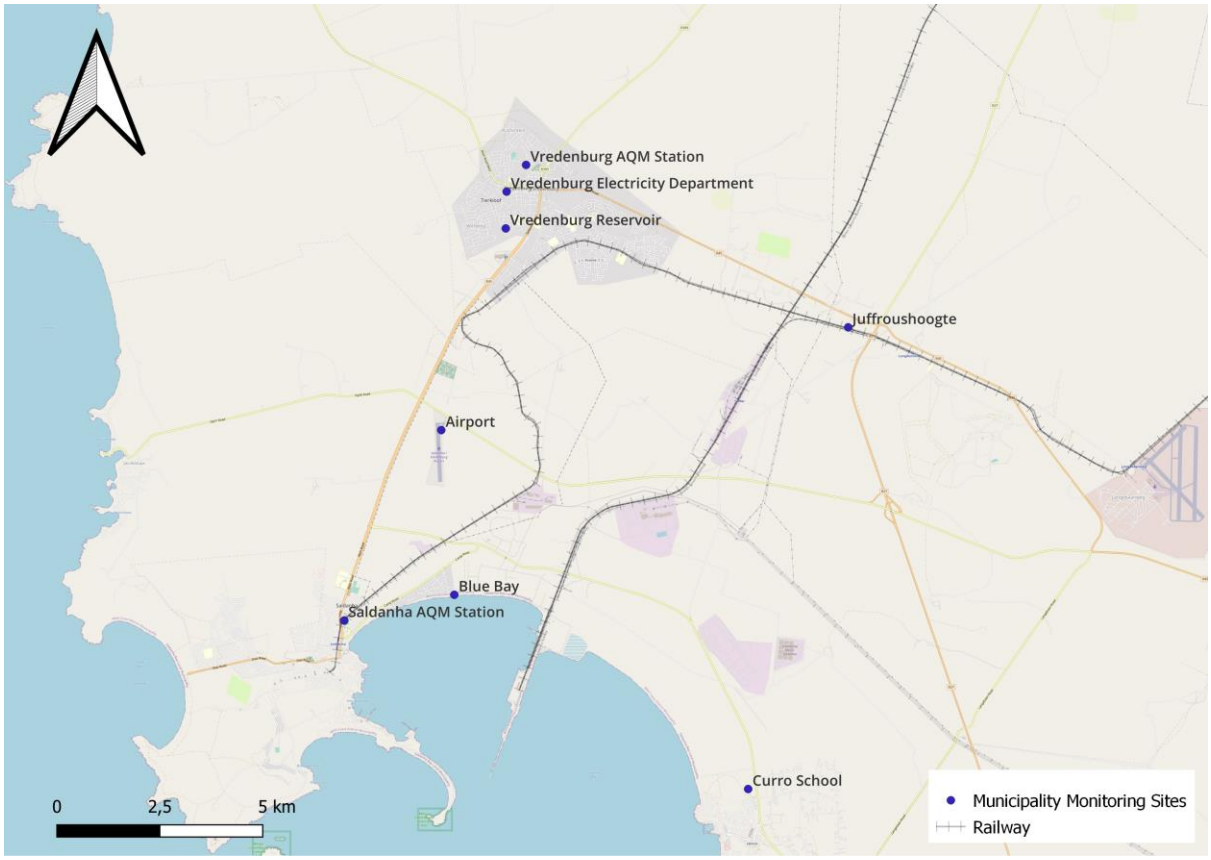

Figure 9: Saldanha Bay Municipality's sampling/monitoring sites

According to reports on the briefing by the Department of Forestry, Fisheries and the Environment and the Civil Society, the challenge that is faced across many South African Municipalities is that environmental concerns are not prioritised as budgetary items (Parliamentary Monitoring Group, 2014). The concern around the municipality's sampling and monitoring are the gaps present in the data collection (Saldanha Bay Municipality, n.d.). Some of these gaps are a result of contamination from other sources, some are due to equipment failure, while some are from no monitoring/sampling being carried out. It had been visible that the delay in the repairing of the equipment had been significantly lengthy, however the reasons for these delays are unknown.

2.10. Monitoring Approaches for Air Quality Monitoring

Air pollution has become the forefront in global discussions on pollution control, driven by significant evidence of its harmful effects on both human health and the overall ecosystem (Yang et al., 2021; Araújo & Costa, 2022). There have been several methodologies that have been developed to monitor and sample PM, which include the traditional use of gravimetric samplers to modern low-cost PM sensors. Presented below is a review of the different approaches used in PM monitoring which include, gravimetric samplers, BSNEs (Big Spring Number Eights), dust fallout buckets and low-cost PM sensors.

Gravimetric sampling includes the use of filters and is regarded as a standard reference monitoring approach, which further allows for physicochemical analysis of the collected samples in a laboratory (Araújo & Costa, 2022). While the analysis of the samples collected from gravimetric samplers can yield both qualitative and quantitative data, this approach tends to be costlier and does not account for the real-time dispersion of PM (Khamraev, Cheriyan & Choi, 2021). Previous studies have indicated that by using size inlets, gravimetric samplers are able to capture both $PM_{2.5}$ and PM_{10} (Charron, 2004; Almeida et al., 2006). Furthermore, gravimetric samplers are also able to sample TSP, by not using a particulate size inlet, as discussed by Yuwono et al. (2016) in their study.

Passive sampling of airborne dust, using air monitoring equipment without a flow meter, is a common method used in wind erosion and dust storm studies (Goossens & Buck, 2012). Developed in 1986 by Fryrear, the BSNE (Big Spring Number Eight) is the most widely used passive sampler in aeolian research (Goossens & Buck, 2012). Initially, the BSNE was developed to measure the horizontal sediment flux by capturing the suspended particles that pass through the 0.001 m^2 opening positioned directly facing the wind (Sharratt & Pi, 2018). Although initially developed for use in soil and wind erosion studies, over the years, there has been an increase in application of BSNEs in air quality studies, such as the one carried out by (Waza et al., 2019). At higher wind speeds, BSNEs are known to be less effective at capturing particulates < 30 µm, which subsequently can result in underestimating the amount of dust that is emitted in this fraction (von Holdt et al., 2021). Furthermore, the study carried out by von Holdt et al. (2021) also indicated variability in BSNE performance when compared to the PI-SWERL (Portable In Situ Wind Erosion Lab), with one BSNE showing a lower capture rate of particles <20 µm and the other indicating a higher capture rate of particles <10 µm but a lower capture rate in the 10-20 µm size range. According to another study, BSNE performance was seen to be similar to other automated gravimetric samplers when wind speeds were relatively low (<5 m/s) (Goossens & Buck, 2012). In addition, Goossens and Buck (2012) concluded that at low wind speeds, BSNEs could be reliable air monitoring equipment for measuring PM_{10}.

Dust fallout monitoring involves measuring the deposition of dust in ambient air as a component of air quality assessment (Dudu, Mathuthu & Manjoro, 2018a). This type of monitoring has been described as an efficient and cost-effective method for analysing dust deposition trends over time. It also assists in identifying key dust generation areas and can be used for both health-related and nuisance assessments (Engelbrecht et al., 2013). Dust fallout monitoring has gained significance amongst industries following the introduction of the Dust Control Regulations (DCR), issues under the National Environmental Management: Air Quality Act (Act No. 39 of 2004) (Kornelius et al., 2015). Similar to gravimetric sampling, this method does not account for the real-time dispersion of PM, although Endjambi et al. (2016) have concluded in their study that dust fallout sampling combined with real-time measurements is a valuable approach for assessing the real-time, variation and chemical composition of airborne particulates that are inhaled to allow for a better understanding of the potential human health impacts. Dust fallout buckets typically indicate low resolution of smaller size fractions,

due to gravity. This is explained by Sibanda (2009) in his study, where he indicates that, due to gravity, particles sized between 10-100 µm lose altitude. While strong winds are able to lift these larger particles, they settle one the wind subsides. However, in contrast, smaller particles (<10 µm) are influenced by factors such as turbulence and Brownian motion, which indicates that they will not settle like the larger particles (Sibanda, 2009).

With regards to low-cost sensors, they provide real-time PM measurements at a lower cost compared to traditional monitoring equipment, which enables higher spatial coverage when monitoring air pollutants (Karagulian et al., 2019). According to Snyder et al. (2013), the introduction of low-cost particulate sensors for air pollution monitoring has transformed the traditional reliance on complex equipment by providing high-resolution, real-time data, in a portable and user-friendly manner. While there are quite a few benefits of low-cost sensor use, Giordano et al. (2021) have reported in their study that low-cost sensors may overestimate PM concentrations compared to local air quality reference stations, due to aerosol growth at high relative humidity. This is because PM concentrations measured by governmental reference stations report data between low to intermediate relative humidity (Giordano et al., 2021). Furthermore, low-cost sensors, such as the PurpleAir Particulate Sensor, provides real-time concentrations of PM_1, $PM_{2.5}$ and PM_{10} (Ardon-Dryer et al., 2020).

2.11. Potential Sources of Metal-Bearing Emissions in the Saldanha Bay Municipality

With regards to concerns from the community and that air quality monitoring is carried out by the municipality, it was important to establish the potential sources of metal-bearing emission. According to the Atmospheric Emissions Licenses (AELs) found on the South African Atmospheric Emission Licensing and Inventory Portal (SAAELIP), two of the potential sources of emission include the Transnet Iron Ore Port Terminal and Tronox Namakwa Sands (Department of Forestry Fisheries and the Environment, n.d.). In addition to these established activities, Costa (2022) concluded that there was also the concern regarding non-listed activities in the municipality. According to a report by Anchor Environmental (2017), the establishment of these smaller storage facilities not requiring an AEL has resulted in cumulative impacts on the quality of air in the municipality. Non-listed sources are a concern since without an AEL, regulation of emissions is not strictly monitored, which can subsequently impact surrounding communities and the environment. Costa (2022) reported on three non-listed companies: Company 1 (with two storage facilities, A and B), Company 2 and Company 3 (Transnet MPT) (Table 5). Costa (2022) also provided the combined (minimum and maximum) storage of the different metal types at the non-listed companies. The combined minimum is approximately 290 000 tonnes, while the combined maximum is approximately 305 000 tonnes.

Table 5: Metal type, mode of transport storage capacity and monthly throughput of the three non-listed companies (Adapted from: Costa (2022))

Non-listed Companies	Metal ore type	Mode of transport	Storage capacity	Monthly throughput
Company 1 (A and B) (Two storage facilities)	Manganese	Rail	55 000 – 60 000 tonnes at each property Combined = 110 000 – 120 000 tonnes	165 000 – 180 000 tonnes
Company 2	Manganese, ilmenite and garnet sand	Truck	90 000 – 95 000 tonnes	100 000 – 110 000 tonnes
Company 3 (Transnet MPT)	Manganese	Rail	90 000 tonnes	125 000 – 133 334 tonnes

A previous study conducted by Chetty and Grüning (2018) was carried out around the municipality to determine whether the presence of industrial, mining-related and metal-ore transportation activities contribute towards the overall metal contamination levels in the soil. The study concluded that the presence of the mentioned activities contributed to the increase in metal contamination at two sites, one located in Vredenburg and the other at the Port terminal. Chetty and Grüning (2018) also reported that the soil samples from the Pindulo VDM site presented moderately contaminated soils. The five main metals that Chetty and Grüning (2018) discussed in their findings included iron (Fe), manganese (Mn), zinc (Zn), titanium (Ti) and lead (Pb). According to the study carried out by Chetty and Grüning (2018) as well as further investigations during fieldwork visits, another company which has been highlighted as potential sources of emission is Pindulo VDM. Conrad and Naicker (2019) have highlighted in their report that there exists a threat of contamination of the soil in the area, as the soil type is classified as sandy, which is permeable in nature. While Chetty and Grüning (2018) have concluded in their study that there are elevated levels of metal in the soils around Saldanha, it is important to acknowledge that soil itself is the source for many elements (Kabata-Pendias, 2001). These include elements such as lead, arsenic, iron, manganese, and vanadium, to mention a few. The locations and descriptions of these potential sources of emission are presented below (Figure 10).

Figure 10: Potential sources of emission in the Saldanha Bay Municipality

The ore handling facilities in the municipality include the Transnet Iron Ore Terminal and the non-listed companies (Company 1 and 2) and the Transnet MPT, which have been discussed previously in Section 2.8.3 and above, respectively. The metal ores of concern from the Transnet Facilities include iron, manganese, lead, zinc, and copper. The metal ores of concern from the non-listed companies are iron and manganese. The other ore handling facility in the municipality is Pindulo VDM, which is known to store and handle metal ores such as manganese prior to export, therefore the metal ore of concern is manganese. Pindulo VDM is also contracted by Lime Sales Ltd to mine lime at the Tabakbaai Quarry (National Portland Cement Saldanha, 2020).

Tronox Namakwa Sands is a smelting operation that processes ilmenite to produce pig iron and titanium dioxide slag. The concentrates are separated at the Mineral Separation Plant to produce ilmenite, rutile and zircon (Tronox, 2020). Thereafter, these products are transported via rail trucks to the smelter in Saldanha Bay. At the smelter, the ilmenite is processed to produce pig iron as well as titanium dioxide slag. The rutile and zircon are also stored at the smelter for export (Tronox, 2020). During the smelting process, carbon monoxide (CO) gas is produced by the furnace and passes through to gas-cleaning plants (Gous, 2006). The gas-cleaning plants are responsible for scrubbing and washing of the cooled gas, to assist in removing any dust that is entrained from the furnace. The clean gas stream re-routes to a gas holder, where it is used to preheat ilmenite and to dry anthracite, however, any excess gas is

flared into the atmosphere (Gous, 2006). This is an area of concern, as it is possible that there are harmful metals present in this excess gas, which potentially could be respirable. In 2011, AfriSam proposed to construct a plant near the iron ore terminal and the Saldanha Steel plant, in Saldanha. At the time, NPC was already known to mine at least 40 000 tpa of aeolinite (dune limestone) in the Southern Limestone Quarry area, also known as Tabakbaai Quarry (Halkett, 2011). According to the Department of Mineral Resources & Energy (n.d.), the Tabakbaai Quarry is currently still listed as an operating mine. The proposal included Phase 1 (2014-2021) which involved mining ~170 000 tpa of limestone by extending the Tabakbaai Quarry. However, there also exists a Northern Limestone Quarry area. This naturally occurring limestone quarries contain natural sources of excess calcium, which could also contribute to the contamination of PM (Chetty & Grüning, 2018). The other quarries present in the municipality include the two Afrimat quarries, known as the “De Kop” quarries and are known to mine quarzitic sandstone (Afrimat, n.d.). The mining of the sandstone could also potentially contribute to the high levels of PM and the release of naturally occurring minerals.

2.12. Summary of Literature Review

Although South African ports play a vital role in the national economy by allowing maritime trade between the country and its global trading partners, the ports are also one of the main sources of environmental pollution in coastal areas. With increases in international shipping, there is subsequently an increase of environmental impact by air pollution, with the main pollutants emitted by shipping terminals include PM, nitrogen oxides and sulphur oxides. Particulate matter is the term often used to describe the mixture of solid and liquid particles in the air. Although PM can originate from both natural and anthropogenic sources, PM from mining operations have the highest potential risk to the environment and human health. PM impacts on human health and is known to have both short- and long-term effects. PM has been defined by size fractions such as inhalable, thoracic, and respirable, based on where it settles along the respiratory tract. The inhalable fraction includes particulates that are inhaled through the mouth and nose and are able to settle anywhere along the upper respiratory tract. The thoracic fraction includes particulates that is able to penetrate into the airways of the lung. Lastly, the respirable fraction includes particulates that penetrates the unciliated airways and gas exchange area of the lung. Apart from the size of the particulates, the impact that PM has on health also depend on its chemical compositions, with PM emitted from the handling, storage, and processing of ore, potentially containing elevated levels of harmful metal pollutants. PM also has adverse effects on the environment, potentially affecting local ecosystems. Nuisance dust can impact the quality of life and the economy of local communities by irritating the eyes, skin and nasal passages as well as reducing visibility, staining, and damaging infrastructure.

Despite concerns, there are large gaps that still exist in ground-based monitoring, particularly with regards to $PM_{2.5}$ and PM_{10}, on a global level. There are also uncertainties around the sources of the PM emissions, which subsequently poses a challenge to establish meaningful action to mitigate these effects. There is also very limited information available regarding the

acceptable concentration levels for individual airborne contaminants. An area that is affected significantly by PM emissions from an ore export terminal is Saldanha Bay. The Port of Saldanha is South Africa's largest natural, deepest port and is regarding important for economic growth along the West Coast of South Africa. The port was initially built for the export of iron ore, but today, various other metal ores such as lead, manganese and zinc are also exported. The existence of the port has given rise to other industries over the years, which potentially contribute to air pollution in the municipality. There is also the concern of the non-listed companies in the area which could potentially contribute to PM emissions as well. Blue Bay, Langebaan, Saldanha Bay and Vredenburg are the surrounding communities which are in close proximity to the port and these other industries. Although ground-based monitoring is carried out around the municipality in the form of dust fallout buckets and filter-based PM sampling, there have been extensive periods where sampling has not been carried out, which subsequently does not provide assurance to members of the community. Members of the community are concerned about their health regarding the quality of the air that they breathe. Furthermore, the constant staining of infrastructure around the municipality has financial effects on members of the community who are required to constantly maintain/paint their businesses and homes. Another area of concern from the community includes the impact of emissions on tourism, the fishing industry as well as the mussel and oyster industry.

CHAPTER 3: METHODOLOGY

As indicated in Chapter 1, this study is comprised of three phases, which are collectively designed to address the aim and the objectives of the study. The first phase includes the selection of the sampling/monitoring sites for this study, and collection of background data. The second phase includes the generation of primary data by dust monitoring and physical sample collection and analysis. Lastly, the third phase includes the processing and interpretation of the primary data with a view to understanding the nature and patterns of PM pollution and the potential sources and health risks associated with these emissions. This chapter provides a detailed description of the methods used in the execution of the three study phases.

3.1. Phase 1: Monitoring/Sampling Site Selection and Description around the Saldanha Bay Municipality

In this study, receptor sites refer to the main areas/suburbs around the Saldanha Bay Municipality that were investigated, and include Saldanha, Blue Bay, Vredenburg, Louwville, Langebaan and St Helena Bay. The study sites are the AQMs, private homes and businesses situated within the respective receptor sites, where the air sampling equipment were installed. For this study, the sampling period commenced in January 2021 and concluded in February 2022. The receptor as well as the study sites were chosen with the help of the AQO at the municipality and the active participation by members of the community. These sites are listed in Table 6 and shown on Figure 11.

Table 6: Receptor Sites and Study Sites chosen within selected Receptor Sites for equipment installation in the Saldanha Bay Municipality

Receptor Sites	Saldanha	Blue Bay	Vredenburg	Louwville	Langebaan	St. Helena Bay
Study Sites within selected Receptor Sites	Saldanha AQM Station	Blue Bay Lodge	West Coast Mall and Vredenburg AQM Station	Louwville Private Home	Langebaan Private Home	St. Helena Bay Private Home

The two AQM stations were chosen to compare the concentration results that were obtained for this study to the results obtained by the municipality, in addition to their prime locations in the two different areas. However, as the fieldwork progressed, it was discovered that that the particulate sensors installed at the AQM stations for the measurement of $PM_{2.5}$ and PM_{10} had been damaged and there were delays in having the equipment repaired, resulting in no data being available from the reference stations for the duration of the study period. Blue Bay was considered due to its ideal location directly across the port and also due to the reassurance of

security in terms of the safety of the equipment. Therefore, both monitoring and sampling equipment was installed at Blue Bay Lodge. Management at the West Coast Mall were approached, since there had been reports of the mall requiring to be repainted as a result of the stain from the red iron ore dust. As a result, sampling/monitoring equipped was also installed on the roof of the mall.

The installation of equipment at the private homes was a courtesy extended to this study by members of the community. Louwville, St. Helena Bay and Langebaan were considered to be ideal receptor sites. Louwville, being a suburb was important for air quality sampling to identify PM concentrations in a residential area. Like the mall, reports were made based on the red iron ore dust stains as far as Langebaan and St. Helena Bay. However, the challenge was to find functional study sites for equipment installation and sampling. In addition, the study sites needed to accommodate the safety of the equipment as well as provide a power source and accessibility. The property owners of the potential study sites were approached, with the help of the AQO. Permission was granted to carry out sampling, while ensuring that the equipment was of no hindrance to the respective property owners.

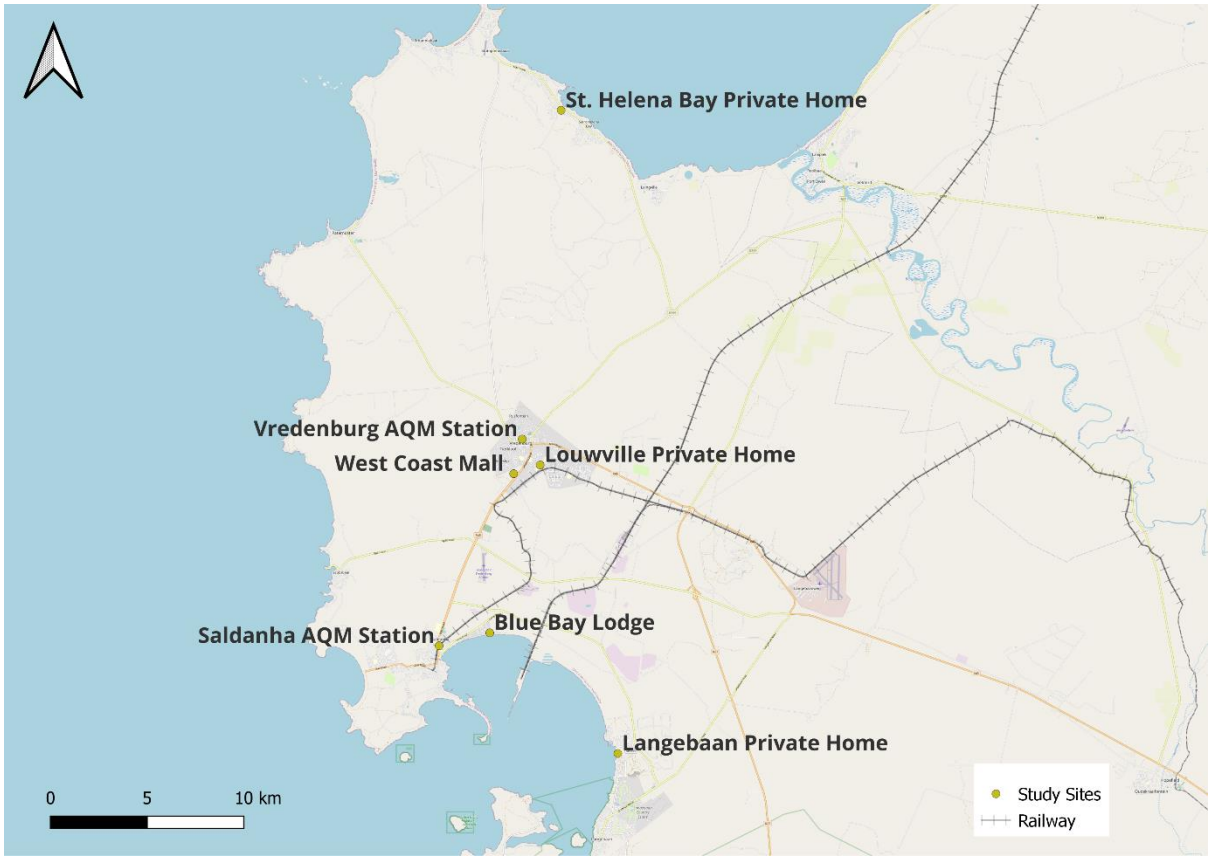

Figure 11: Study sites where air quality equipment was installed during fieldwork

3.2. Phase 2: Fieldwork and Laboratory Analysis: Primary Data Collection

The fieldwork study comprised of installing the PurpleAir Particulate Sensors, gravimetric samplers, dust fallout buckets and the BSNEs at the study sites to measure PM concentrations and collect samples. The monitoring and sampling equipment is described below in Section 3.2.1, and the monitoring and sample collection campaign is outlined in Section 3.2.2. The methods used to process the raw PM data and samples are described in Section 3.2.3. The analytical methods applied to determine the elemental and mineralogical composition of the physical samples are presented in Section 3.2.4.

3.2.1. Selection and Description of PM Monitoring and Sampling Equipment Installed

The fieldwork study included the installation of the sampling equipment at the chosen study sites (Figure 11). There were various types of air quality sampling equipment that had been selected to carry out the PM sampling and data capture. These included gravimetric samplers, particulate sensors, dust fallout buckets, and Big Spring Number Eights (BSNEs). The seven identical low-cost particulate sensors were installed to measure PM concentration around the municipality. Whereas, the gravimetric samplers, dust fallout bucket and BSNE were chosen for the physical PM capture, to determine composition, and where possible concentration. However, one of the limitations in this study was the number of identical gravimetric samplers available for use. Therefore, the ARA N-FRM sampler, the MiniVolTM Tactical Air Sampler and the MiniVolTM Portable Air Sampler VER 4.2, and Gilian GilAir-3 Sampling Pumps were chosen and deployed at the different study sites, as they all carry out the same function. Dust fallout is regulated, and the regulatory limits provides a measure of the extent of dust pollution and management. It was intended for dust fallout buckets to be installed at all study sites, however, due to installation limitations and security, this could only be achieved at Blue Bay Lodge. Table 7 below indicates the different pieces of equipment that were installed at each site. The reason(s) as well as description of each type of monitoring and sampling equipment used during fieldwork are presented below.

Table 7: The different types of PM monitoring and sampling equipment used at each study site

Study Site	Air Sampling Equipment			
	Gravimetric sampler	PurpleAir Sensor	Dust fallout bucket	BSNE
Saldanha AQM Station	✓	✓		✓
Blue Bay Lodge	✓	✓	✓	✓
West Coast Mall	✓	✓		
Vredenburg High School (Vredenburg AQM Station)		✓		
Louwville Private Home	✓	✓		
Langebaan Private Home	✓	✓		
St. Helena Bay Private Home	✓	✓		

3.2.1.1. Dust Fallout Buckets

The dust fallout buckets were used as per South African regulations outlined in Section 2.6.2. The use of the dust fallout bucket was to capture dust fall in the Blue Bay area for elemental and mineralogical analysis. The dust fallout buckets that were used had a diameter of 150 mm and a depth of 300 mm. The buckets were placed on a dust fallout bucket stand which had a height of 2 m. This was necessary as the method followed in South Africa for the measurement of PM deposition is ASTM: 1739-98 (Department of Environmental Affairs, 2013). It also states that the bucket is required to be at least 2 m above ground level, with a wind shield that is at the same level of the lip of the bucket. The ASTM: 1739-2010 version does not require for the addition of water to the bucket, however, previous versions ASTM: 1739-90 and ASTM 1739-82 does allow for water to be added. Therefore, water was added to the bucket, along with bleach to avoid the growth of bacteria. The stand had been hooked into the ground and sandbags were placed on top of the hooks to ensure additional security (Figure 12). When the buckets were required to be replaced, the old bucket was sealed tightly, and the same procedure was carried out for the new bucket.

Dust fallout buckets have been deployed around the municipality since 2015. It is important to monitor dust fallout to ensure that the dust fallout measurements are in accordance with legislation (Table 4). Additionally, the captured fallout dust provides information on the composition of the dust present in an area, which can further be used in health risk assessments to evaluate population exposures (Dudu, Mathuthu & Manjoro, 2018b).

Figure 12: Dust fallout bucket in a stand for fallout sampling installed at Blue Bay Lodge

3.2.1.2. Big Spring Number Eights (BSNEs)

Due to only being able to install the dust fallout buckets at Blue Bay Lodge, BSNEs were used due to their easier installation to collect physical samples of dust at Blue Bay Lodge and at the Saldanha AQM Station. The BSNE is a wind aspirated sampler that collects airborne dust that enters the opening of the sampler, regardless of wind velocity or direction. The BSNE sampler is able to sample a whole range of particle sizes, including both course and fine particulates. The installation of the BSNEs is straightforward, as a mounting pole is required to be installed and secured such that it is upright at 90°. A bracket(s) was placed on the mounting road and secured with clamps which ensures it stayed in place. The BSNE was then placed in the bracket and secured, if necessary, with cable ties (Figure 13). At Blue Bay Lodge, the BSNEs were placed at 1.2 m high and at the Saldanha AQM Station, the BSNEs were placed in the existing BSNE bracket that belonged to the station. This bracket was mounted onto a rod, on the roof of the station. When the BSNEs were required to be replaced, the BSNEs were taken out of the bracket and sealed in a zip lock bag to avoid any contamination. New and clean BSNEs were then placed into the bracket and secured for sampling.

(a) (b)

Figure 13: BSNE on its mounting pole installed at the Saldanha Bay AQM Station (a and b)

3.2.1.3. PurpleAir Particulate Sensors

The PurpleAir Particulate Sensors that were installed was the PA-II-SD device. This device is an air quality sensor that measures and stores real time concentrations of PM_1, $PM_{2.5}$ and PM_{10} and is suitable for residential, commercial, and industrial use. The sensor is equipped with a pair of laser-scattering particle sensors and a pressure, temperature, and relative humidity sensor. The sensor has a built-in Wi-Fi-enabled processor which allows for data to be uploaded to the PurpleAir map and can be downloaded in 2-minute intervals(Stavroulas et al., 2020; PurpleAir, n.d.).

The sensors were installed at all the study sites. Two out of the seven were connected to Wi-Fi, however, the sensor is equipped with an SD (Secure Digital) card and real-time clock that stores measurement in 2-minute intervals in CSV (comma-separated values) format. Therefore, with or without Wi-Fi connection, the SD card proved extremely reliable in storing all the data that had been collected. To extract the data, the SD card was inserted into an SD card reader. The sensor is relatively small with dimensions of 85 mm x 85 mm x 125 mm and therefore is easy to install, however, it does require a constant power source. Figure 14 below provides a graphical representation of the sensor.

Figure 14: The PurpleAir Particulate Sensor installed at the Saldanha AQM Station

3.2.1.4. Gravimetric Samplers and Filter Papers

There were four types of gravimetric samplers that were used in this study. These include an ARA N-FRM, a MiniVol™ Tactical Air Sampler (TAS), MiniVol™ Ver 4.2 and Gilian GilAir-3 Sampling Pumps. The gravimetric samplers that were used during fieldwork were all filter-based samplers. Gravimetric samplers were useful in that different particle sizes ($PM_{2.5}$, PM_{10} and TSP) could be collected, depending on the particle size inlet that was used during a specific sampling period. This allowed for the elemental and/or mineralogical analysis for the different particle sizes, which is explained further in Section 3.2.4.

All four samplers had a very similar set up with regards to the filter paper loading and PM collection. Both reference methods EN 14907 and EN 12341 were followed for $PM_{2.5}$ and PM_{10} sampling, respectively, which have been discussed in Section 2.6.2. Prior to being installed in the gravimetric samplers, all filter papers were placed in the filter paper cassette that are associated with each gravimetric sampler. This was done to avoid the contamination of the filter paper when replacing the old one with a new one. Once the filter paper cassette which contained a sample-filled filter paper was removed from the gravimetric sampler, it was sealed to prevent any contamination or compromise to the filter paper.

- *The ARA N-FRM (Federal Reference Method) Sampler*

The N-FRM portable sampler from ARA Instruments has established a new class of air sampler called “Near FRM” (Figure 15) (ARA Instruments, 2017). FRMs are methods that Environmental Protection Agency (EPA) scientists have developed and evaluated to accurately and reliably measure pollutants such as $PM_{2.5}$ and PM_{10} in outdoor air (United States Environmental Protection Agency, 2023b). The FRMs are known as the “gold standard” with regards to monitoring systems and also ensure that the data collected from air quality

monitoring at various study sites are collated in the same manner (United States Environmental Protection Agency, 2023b). The sampler is the first of its kind to deliver FRM accuracy at a lower cost compared to certified US EPA FRM samplers (ARA Instruments, 2017). The sampler is able to complete 24-hour sampling periods with a flowrate of 16.7 LPM (litres per minute). The sampler can be connected to a power source, however, in the event of disconnection, the sampler is equipped with rechargeable batteries. The ARA N-FRM is able to collect 24-hour filter samples of $PM_{2.5}$, PM_{10} and courser particles that are greater than 10 µm, using the appropriate impactors, while simultaneously measure and log real-time parameters, particulate counts and meteorological data (ARA Instruments, 2017). To record wind speed and direction, an anemometer and a wind vane were attached to the sampler. The temperature was also recorded by the sampler. The ARA N-FRM was installed at Blue Bay Lodge. The reason for this was that the ARA N-FRM, although cheaper than most samplers, is still expensive and Blue Bay Lodge was able to provide the security. The sampler was attached to the dust fallout bucket stand.

Figure 15: The ARA N-FRM sampler from ARA Instruments (ARA Instruments, n.d.)

- *The MiniVol™ Tactical Air Sampler (TAS)*

The MiniVol™ TAS samples ambient air at a flowrate of 5 LPM for $PM_{2.5}$, PM_{10} and TSP (Figure 16) (AirMetrics, n.d.). Similar to the ARA N-FRM, the MiniVol™ TAS is not a FRM sampler, but also provides results that closely approximate data obtained from FRM samplers. It is also portable and does require a power source for long-term sampling but is equipped with a rechargeable battery in the case of power disconnection (AirMetrics, n.d.). The MiniVol™ TAS sampler was installed at the West Coast Mall. The sampler was installed on the roof of the mall for security purposes to prevent theft and vandalism.

Figure 16: The MiniVol™ TAS by AirMetrics (AirMetrics, n.d.)

- *The MiniVol™ Portable Air Sampler VER 4.2*

The MiniVol™ Ver 4.2 (Figure 17) is simply an older version of the MiniVol™ TAS. The operation of both is very similar. This sampler was installed at the Saldanha AQM Station and later at the WC Mall when the MiniVol™ TAS malfunctioned. It must be noted that it was intended for the MiniVolTM Portable Air Sampler VER 4.2 to be installed at both the Saldanha AQM Station and the West Coast Mall for the same amount of time that the PurpleAir Particulate Sensors were installed, at those study sites. However, this did not occur due to the samplers malfunctioning shortly after installation.

Figure 17: The MiniVol^{TM} Ver 4.2 by Air Metrics installed at the Saldanha AQM Station

- *<u>The Gilian GilAir-3 Sampling Pump</u>*

The GilAir-3 (Figure 18) is a simple, yet reliable sampling pump sourced from Sensidyne®. It also can be considered a personal sampling pump and can be worn on one's person. However, in this study, it was installed for outdoor sampling. A clear hose connects the pump to a filter house installed with a filter paper, which allows for the collection of material at a flowrate of approximately 3 LPM. The pump is equipped with a built-in battery but can also be plugged into a power source for long-term sampling (Sensidyne, n.d.). These samplers were installed at the three private homes.

Figure 18: The Gilian GilAir-3 Sampling Pump (inteccon.inc, n.d.)

It must be noted that the gravimetric samplers used in this study only provided physical filter paper samples, and no PM concentrations. For all the gravimetric samplers, when filter papers were collected and replaced, the additional filter paper cassette was used, loaded with the new filter paper. This proved to be the easiest method to exchange the filter papers in the sampler without introducing any foreign contamination. The three types of filter paper that was used in this study was quartz by Millipore, polycarbonate by Whatman®, and micro cellulose ester provided by Sensidyne®. The polycarbonate was initially used in all the gravimetric samplers, excluding the GilAir-3 samplers. According to da Cruz and Magondo (2018), it was reported that when using NanoSEM, particles found on polycarbonate paper were more easily distinguishable. However, it was found that the samplers could not handle the delicacy of the polycarbonate filters and would therefore stop running. Therefore, the polycarbonate filters in the ARA were replaced with quartz filters. Most of the samplers, except the ARA N-FRM and the GilAir-3 samplers, had stopped running early into sampling and collection. The GilAir-3 samplers were equipped with mixed cellulose ester filters from Sensidyne®. These types of filter papers were recommended for the GilAir-3 samplers. Support pads for the mixed cellulose filters were also used to support the filters during sampling. The details regarding the filter papers used during sampling can be found in Appendix B.

3.2.2. Description of Dust Monitoring and Sample Collection Campaigns

One of the main challenges faced in this study, was carrying out fieldwork during the COVID19 pandemic. This subsequently resulted in a delay with the fieldwork only commencing in 2021. Although there were less restrictions, most of the fieldwork was carried out with caution, especially at the private homes. The first sampling campaign took place over two weeks at the end of February 2022. In these two weeks, installation of all the sampling equipment mentioned in Section 3.2.1 took place. Frequent inspections of the sampling equipment were made to ensure all the equipment was running smoothly and were replaced if necessary. After the first sampling campaign, trips to the West Coast were made monthly, if possible. This was highly dependent on COVID19 restrictions. The details regarding each sample are explained

further in Section 3.2.3, however a summary table regarding the sampling dates of each piece of equipment is presented below (Table 8).

Table 8: Details of each sample collected at the seven study sites

PurpleAir Particulate Sensors		
Sensor	Location	Sampling Period
PurpleAir 1	Blue Bay Lodge	28/01/2021 – 24/02/2022
PurpleAir 2	Saldanha AQM Station	05/02/2021 – 22/10/2021
PurpleAir 3	Louwville Private Home	23/02/2021 – 14/05/2021
PurpleAir 4	St. Helena Bay Private Home	03/03/2021 – 04/08/2021
PurpleAir 5	West Coast Mall	28/01/2021 – 03/04/2021
PurpleAir 6	Langebaan Private Home	23/02/2021 – 08/07/2021
PurpleAir 7	Vredenburg AQM Station	26/02/2021 – 30/06/2021
Dust Fallout Bucket Samples		
Dust Fallout Bucket 1	Blue Bay Lodge	25/02/2021 – 23/03/2021
Dust Fallout Bucket 2		23/03/2021 – 08/06/2021
Dust Fallout Bucket 3		08/06/2021 – 09/07/2021
Dust Fallout Bucket 4		09/07/2021 – 05/08/2021
BSNE Samples		
BSNE 1a	Blue Bay Lodge	25/02/2021 – 23/03/2021
BSNE 1b	Saldanha AQM Station	
BSNE 2a	Blue Bay Lodge	23/03/2021 – 08/06/2021
BSNE 2b	Saldanha AQM Station	
BSNE 3	Blue Bay Lodge	08/06/2021 – 09/07/2021
BSNE 4	Blue Bay Lodge	09/07/2021 – 05/08/2021
Filter Paper Samples		
Filter Paper 1c	Blue Bay Lodge	23/02/2021 – 01/03/2021
Filter Paper 2a	Saldanha AQM Station	01/03/2021 – 08/03/2021
Filter Paper 3a	West Coast Mall	23/03/2021 – 12/04/2021
Filter Paper 4b	Louwville Private Home	16/05/2021 – 08/06/2021
Filter Paper 5b	Langebaan Private Home	09/05/2021 – 08/06/2021
Filter Paper 6a	St. Helena Bay Private Home	11/04/2021 – 09/05/2021
Filter Paper 6b		09/05/2021 – 08/06/2021

3.2.3. PM Data Processing

3.2.3.1. R: A Programming Language

The CSV files that were collected from the SD cards at each receptor site were processed using the programming language R. The use of a programming language, R allowed for easy and quicker data manipulation. R is a programming language used for graphics as well as statistical computing and is highly extensible. Another advantage to using R is the ease with which well-designed graphs can be plotted that are of publication-quality.

3.2.3.2. Analysis of the PM Concentration Data using R

The 2-minute interval data provided by the PurpleAir Particulate Sensor was aggregated to 24-hour, 1-hour averages. This was done to establish whether the concentrations measured exceeded the concentration limits set out by NAAQS (Department of Environmental Affairs, 2009;Department of Environmental affairs, 2012). Additionally, the limits set out by the WHO, were also taken into consideration (World Health Organisation, 2021). The concentration limits have been presented in Chapter 2; however, the table below summarises the $PM_{2.5}$ and PM_{10} concentration limits according to both the NAAQS and WHO standards. The 24-hour aggregated $PM_{2.5}$ and PM_{10} concentration data was compared to both the NAAQS and WHO standards, presented in the table below. Visual presentations of the concentrations and exceedances are shown in Chapter 4.

Table 9: NAAQS and WHO $PM_{2.5}$ and PM_{10} concentration limits (Department of Environmental Affairs, 2009;Department of Environmental affairs, 2012;World Health Organisation, 2021)

Pollutant	Averaging Period	NAAQS Concentration Limit (µg/m^3)	Frequency of exceedance for NAAQS	WHO Concentration Limit (µg/m^3)
$PM_{2.5}$	24 hours	40	4	15
PM_{10}	24 hours	75	4	45
$PM_{2.5}$	1 year	20	0	5
PM_{10}	1 year	40	0	15

According to Barkjohn, Gantt and Clements (2021), PurpleAir Particulate Sensors overestimate $PM_{2.5}$ concentrations by ~40%. Apart from the overestimation of $PM_{2.5}$ concentrations, it was also necessary to correct for relative humidity. Therefore, it was necessary to correct the raw concentration data, using the Correction Equation Method provided below. These results of the data corrected using this method are presented in Section 4.1.1.

- *The Correction Equation Method*

The second approach was using a correction equation from a study conducted in the United States where a correction equation was developed, tested, and applied to datasets collected with a PurpleAir Particulate Sensor across the United States (Barkjohn, Gantt & Clements, 2021). The study concluded that the relative humidity (RH) model summarized the data more optimally compared to a linear correction. This equation is presented below:

$$PM_{2.5} = 0.524 \text{ x } PA_{cf1} - 0.0862 \text{ x RH} + 5.75 \quad (2)$$

Where:

PA_{cf1} = The higher correction factor, which is the $PM_{2.5}$ averages from channels A and B, as provided by the PurpleAir Particulate Sensor

RH = Relative Humidity, as provided by the PurpleAir Particulate Sensor

PA_{cf1} is the higher correction factor that is provided per $PM_{2.5}$/PM_{10} concentration measurement by the PurpleAir Particulate Sensor. For this method specifically, the higher correction factor for only $PM_{2.5}$ concentrations were considered. The SD card, from which the PM data is obtained provides PM_{1cf1}, $PM_{2.5cf1}$ and PM_{10cf1}, as an output from the sensor for both channels A and B. For Equation 2 above, PA_{cf1} is the average of $PM_{2.5cf1}$A and $PM_{2.5cf1}$B.

Barkjohn, Gantt and Clements (2021) concluded that only a relative humidity correction was required for their dataset due to that impacts of humidity on the light scattering of particles are known. However, the same cannot be said for temperature as no principle explaining the influence that temperature has on the scattering of particles exists yet. Barkjohn, Gantt and Clements (2021), believe that temperature may assist in accounting for local seasonal or diurnal patterns in aerosol properties that are found within smaller geographical areas, however, they also suggest that more studies should be carried out.

The correction equation provided in Equation 2 above was then used to correct all the $PM_{2.5}$ data in R. Unfortunately, the same could not be carried out for PM_{10} concentrations as there is not yet a correction equation for those measurements. However, it must be emphasized that the correction equation used also accounted for relative humidity.

3.2.4. Chemical and Mineralogical Analysis of Physical PM Samples

In this section, the different types of analytical procedures that were used to analyse the collected PM samples are described. These include X-Ray Powder Diffraction (XRD), X-Ray Fluorescence (XRF), Inductively Coupled Plasma – Mass Spectrometry (ICP-MS), Inductive Coupled Plasma – Atomic Emission Spectrometry (ICP-AES), Scanning Electron Microscopy (SEM) and Quantitative Evaluation of Materials by Scanning Electron Microscopy (QEMSCAN). The roadmap of the methods used to analyse the different samples collected as well as the description of said methods are presented below.

3.2.4.1. Roadmap on the Methods used to Analyse the Different Samples Collected

Figure 19 below indicates the roadmap which provides the type of analysis used to analyse the samples collected from their respective piece of equipment. Each sample is then explained further below.

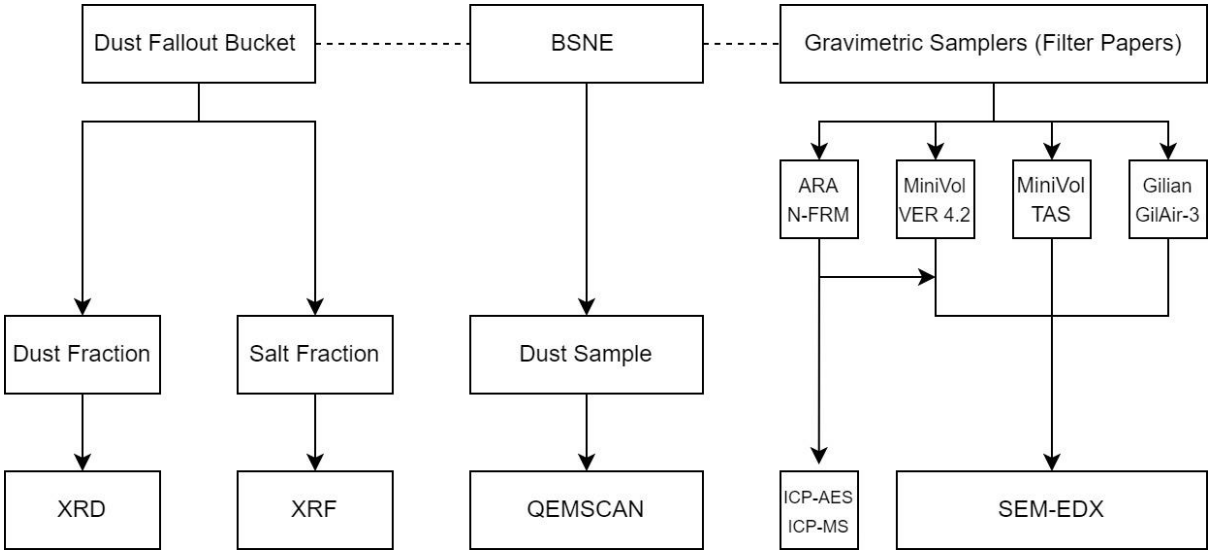

Figure 19: Roadmap on methods used to analyse samples collected by the different pieces of equipment

- *<u>The Dust Fallout Bucket Sample</u>*

The combined sample from the dust fallout bucket was separated into dust and salt samples by means of centrifugation, prior to analysis. This is explained in detail in Section 3.2.4.2.The dust and salt samples obtained from the dust fallout bucket were analysed using XRD and XRF, respectively (Table 10). The initial choice of analysis for these samples was QEMSCAN, however, due to the possible content of salt in the dust sample and salt content in the salt sample, it was decided that XRD would rather be used to analyse the dust fallout bucket samples. The reason for this was the potential risk of ridges in the resin block (if QEMSCAN was used), which is required to have a smooth surface for accurate measurements. Both the dust and salt samples were analysed by XRD, however, after an unsuccessful attempt at analysing the salt sample using XRD, the salt sample was then analysed using XRF.

Table 10: Information on the dust fallout bucket samples analysed by XRD and XRF

Sample	ID	Study Site	Sampling Period	Sampling Equipment	Analysis
Dust Sample	X	Blue Bay Lodge	25/02/2021 – 05/08/2021	Dust Fallout Bucket	XRD
Salt Sample	Y				XRF

- *Analysis of the Filter Papers by ICP-MS, ICP-AES and SEM-EDX*

All the filter papers used in the gravimetric samplers were conditioned in the laboratory between 20-25 °C for at least 24 hours (United States Environmental Protection Agency, n.d.). To ensure that the laboratory was humidity controlled, the DHT11 Temperature and Humidity Sensor was used. This normalises the absorbed water content that could affect the measurements. Moisture was removed from the filter papers by being dessicated for about 30 minutes and then weighed using an analytical balance. Once all the filter papers were weighed, they were placed into petri dish and sealed. To ensure that there was no introduction of foreign materials onto the filter paper, gloves and ethanol were used during the handling of the filter papers.

Two quartz filter papers used for sampling at Blue Bay lodge were analysed using ICP-MS and ICP-AES. The reason being that these two analyses, combined, provided elemental data on major, minor and trace elements in a sample. The range of elements that the sample/samples are analysed for are aluminium, calcium, iron, magnesium, potassium, sodium, vanadium, chromium, cobalt, nickel, copper, arsenic, selenium, strontium, molybdenum, cadmium, tin, antimony, barium and lead. ICP-MS and ICP-AES were also selected to verify if any additional elements were present that had not been detected in the results of other tests from samples in that location. In addition to qualitative analysis of the filter papers, quantitative analysis was also carried out to provide the concentrations of each element found.

The rest of the filter papers in Table 11 below, were analysed using SEM-EDX. The initial choice of analysis for the filter papers was QEMSCAN, however, a previous study carried out by da Cruz and Magondo (2018) indicated that their attempt at analysing filter papers with QEMSCAN had been unsuccessful. There was also the concern of possible damage from the filter papers to the QEMSCAN machine. It was then decided to analyse the filter papers using SEM-EDX.

Table 11: Information on the filter papers analysed using ICP-MS, ICP-AES and SEM-EDX

ID	Study Site	Sampling Period for 2021	Sampling Equipment	Filter Paper Type	Method of Analysis
1a	Blue Bay Lodge	09/07 – 05/08	ARA N-FRM	Quartz	ICP-MS & -AES
1b	Blue Bay Lodge	30/09 – 22/10	ARA N-FRM	Quartz	ICP-MS & -AES
1c	Blue Bay Lodge	23/02 – 01/03	ARA N-FRM	Polycarbonate	SEM
1d	Blue Bay Lodge	08/06 – 09/07	ARA N-FRM	Quartz	SEM
1e	Blue Bay Lodge	05/08 – 30/09	ARA N-FRM	Quartz	SEM
2a	Saldanha AQM Station	01/03 – 08/03	MiniVol™ Ver 4.2	Polycarbonate	SEM
3a	West Coast Mall	23/03 – 12/04	MiniVol™ TAS	Polycarbonate	SEM
4a	Louwville	10/04 – 16/05	GilAir-3	Mixed-Cellulose	SEM
4b	Louwville	16/05 – 08/06	GilAir-3	Mixed-Cellulose	SEM
5a	Langebaan	10/04 – 09/05	GilAir-3	Mixed-Cellulose	SEM
5b	Langebaan	09/05 – 08/06	GilAir-3	Mixed-Cellulose	SEM
6a	St. Helena Bay	11/04 – 09/05	GilAir-3	Mixed-Cellulose	SEM
6b	St. Helena Bay	09/05 – 08/06	GilAir-3	Mixed-Cellulose	SEM

- *The BSNE Sample*

The BSNE sample was analysed by using QEMSCAN such that the mineralogical data could be obtained (Table 12). The dust material from the BSNE was collected by washing the BSNE with de-ionised water and collecting water and the sample in a glass beaker. The glass beaker was weighed prior to the rinsing of the BSNEs, using an analytical balance. The beaker was then placed in an oven at to allow for dehydration. Once the water had dried-up the beaker was once again weighed to determine the mass of the material that remained. The beaker was sealed with parafilm to prevent any contamination of the sample. Although this preparation process is standard and unavoidable, it is important to note that it does affect the mineralogical and elemental composition of the sample. De-ionsed water lacks ions, which

allows for the dissolving of soluble salts and minerals. Therefore, should there be any soluble or partially soluble salts and/or minerals present, the possibility of the leaching of these salts and/or minerals may occur, which subsequently alters the composition of the sample. Another potential impact is the washing away of fine-grained material, which could also affect the representation of the sample.

Table 12: Information on the BSNE sample analysed by QEMSCAN

ID	Location	Sampling Period	Sampler	Analysis
Z	Blue Bay Lodge Saldanha AQM Station	25/02 – 05/08	BSNE	QEMSCAN

3.2.4.2. Descriptions of the Analytical Methods

- *<u>Dust Fallout Bucket Sample Preparation and Description of Analysis of Dust Sample by XRD</u>*

<u>Dust Fallout Bucket Material Preparation</u>

The first attempt at collecting the material from the dust fallout bucket followed the same procedure as the one for the BSNE material. However, when the sample achieved dehydration, it was found it contained a large amount of salt. This was justified as the dust fallout bucket was installed at Blue Bay Lodge, very close to the ocean. However, the challenge faced was that the dust particles had been trapped between the salt particles and needed to be separated. This was achieved through centrifugation. Once the samples were centrifuged, a plastic dropper was used to separate the liquid layer on top, from the settled dust layer in the centrifuge tube. The separated samples were transferred to a clean glass beaker before being dried in the oven and weighed to determine their respective masses. The equation for determining the time for centrifugation of the samples is presented below (Norman White & Dixon, 2003).

$$\mathrm{tmin} = \frac{(63.0 \times 10^{8})(\eta)(\log_{S}^{R})}{(N_m)^2 (D_u)^2 (S_p - S_l)}$$

Where:

Tmin (min) = Centrifuging time in minutes

η (Pa.s) = Viscosity at a given temperature. The initial dehydration of the sample indicated that it contained a large amount of salt, as mentioned above. Therefore, an assumption was made that the viscosity of the sample would be that of sea salt at room temperature of 25 °C, which is 0.00097 Pa.s

R (cm) = Radius of rotation of the top of the sediment in the centrifuge tube

S (cm) = Radius of rotation of the top of the suspension in the centrifuge tube

Nm (rev/min) = Revolutions of the centrifuge per minute

Du (µm) = Particle Diameter in microns. 1000 µm was used as the particle diameter as the BSNE openings are reported to be 0.001 m according to Sharratt and Pi (2018).

Sp – Sl (kg/m^3) = Difference between the density of the particle and the density of the liquid. The dust in the initial dehydrated sample also presented a red-like colour such as the one seen around the municipality from the red iron ore stains. Therefore, another assumption was made to use the density of iron as the density of the particle. Since de-ionised water was used as the liquid, the density of water was used as the density of the liquid.

As mentioned in Section 1.4, one of the limitations of this study included the combination of the dust and salt samples from all four dust fallout buckets into one. The reason for this was that the amount of dust that was achieved post centrifugation per dust fallout bucket would not be sufficient for XRD analysis. Therefore, the four samples of dust and salt each, were combined into one dust sample and one salt sample to be analysed by XRD and XRF, respectively. The details regarding each individual sample can be found in Appendix B. These beakers were also sealed to prevent any contamination. These samples were then transferred to the Electron Microscope Unit at the University of Cape Town and the Central Analytical Facilities at Stellenbosch University for dust and salt analysis, respectively.

Analysis of dust and salt samples from the Dust Fallout Bucket by XRD

The procedure below had been provided by the Electron Microscope Unit at the University of Cape Town in South Africa. The samples were analysed using a Bruker D8 Advanced powder diffractometer equipped with a LynxEye detector with a Co tube. The phase identification was carried out using the Bruker EVA software, which provided the qualitative data of the sample. The conditions for analysis are presented in Table 13.

Table 13: Analysis conditions for XRD

Condition	Unit	Value
Scan Range	θ	5 - 120
Time/Step	s	1.000
Steps		3 766
Time	s	3 862

Salt Sample from Dust Fallout Bucket Description of Analysis by XRF

The procedure below had been provided by the Central Analytical Facilities at Stellenbosch University in South Africa. Samples that are subjected to XRF analysis were first crushed into a fine powder using a jaw crusher. The crushed material was then milled in a tungsten zib mill prior to the preparation of a fused disc for both trace and major element analysis. This is done to prevent any trace and rare earth element contamination. The jaw crusher as well as the mill

were cleaned with uncontaminated quartz between two samples to prevent any cross contamination.

Trace Element Analytical Procedure

Pressed powder pellets were prepared for XRF analysis using approximately 8 g of the salt sample and a few drops of Movial (a poly vinyl alcohol) for bounding. The trace element and sulphur compositions were determined by XRF spectrometry, using a PANalytical Axios Wavelength Dispersive spectrometer. The spectrometer is fitted with an Rh tube and the following analysing crystals: LIF200, LIF220, LIF420, PE and PXI. The instrument is fitted with a scintillation detector and a gas-flow proportional counter. The proportional counter uses gas mixture which consists of 90% argon and 10% methane. Elements were analysed on a fused glass disk with tube operating conditions of 50 kV and 50 mA.

Major Element Analytical Procedure

Glass disks were prepared for this analysis using 7 g of high purity trace element and rare earth element-free flux mixed with 0.7 g of the powder sample. The flux consisted of 32.83% $LiBO_2$, 66.67% $Li_2B_4O_7$, and 0.50% LiI. The sample mixture and the flux were fused in platinum crucibles with a Claisse M4 gas fluxer at temperatures between 1 100 °C and 1 200 °C. Whole-rock major element compositions were determined by XRF Spectrometry using a PANalytical Axios Wavelength Dispersive spectrometer. The spectrometer is fitted with an Rh tube and the following analysing crystals: LIF200, LIF220, PE 002, Ge 111 and PXI. The instrument is fitted with a scintillation detector and a gas-flow proportional counter. The proportional counter uses gas mixture which consists of 90% argon and 10% methane. Major elements were analysed on a fused glass disk using a 2.4 kW Rhodium tube.

The Matrix effects in the sample was corrected for by applying theoretical alpha factors and measured the line overlap factors to the raw intensities that were measured with the SuperQ PAnalytical software. The control standards used in the calibration procedures for trace element analyses were NIM-G (Granite from the Council for Mineral Technology, South Africa) and BHVO-1 (Basalt from the United States Geological Survey, Reston). The control standards used in the calibration procedures for major element analyses were NIM-G and BE-N (Basalt from the Internation Working Group).

- *Description of Analysis of Quartz Filter Papers by ICP-MS and ICP-AES*

The procedure below had been provided by the Central Analytical Facilities at Stellenbosch University in South Africa.

Majors and Trace Analysis by ICP-MS

To digest the solid samples, approximately 0.1 g of dried homogenous sample was weighed directly into the Microwave Digester Teflon vessels. 6 ml UP HNO3 as well as 2 ml Supra pure HCL was added and digested using the MARS microwave digester. The vessels were then

cooled and diluted to a final volume of 50 ml. The instrument used was the Agilent 7900 ICPMS. The conditions for the microwave method are listed in Table 14 below.

Table 14: Microwave method conditions for ICP-MS

Condition	Unit	Value
Power level	W	1 600
Ramp time	min	25
Pressure	Psi	800
Hold time	min	10

The instrument conditions are listed in Table 15 below.

Table 15: Instrument conditions for ICP-MS

Condition	Unit	Value
RF Power	W	1 600
Carrier gas (Argon)	L/min	0.83
Sample depth	mm	10
Make-up gas	L/min	0.15
Helium flow	ml/min	5
Hydrogen flow	ml/min	6
Nebuliser (micro mist)	ml/min	0.4

Unknown samples are analysed against NIST Traceable Standards and independent quality control solutions. Calibration acceptance criteria of R2>0.9995 is used.

Majors and Trace Analysis by ICP-AES

To digest the solid samples, approximately 0.1 g of dried homogenous sample was weighed directly into the Microwave Digester Teflon vessels. 6 ml UP HNO3 as well as 2 ml Supra pure HCL was added and digested using the MARS microwave digester. The vessels were then cooled and diluted to a final volume of 50 ml with 1% HCL. The instrument used was the Thermo iCap 6000 Series that had been supplied by Thermo Scientific. The microwave conditions were the same at which the analysis for ICP-MS were carried out. The instrument conditions are listed in Table 16 below.

Table 16: Instrument conditions for ICP-AES

Condition	Unit	Value
RF Power	W	1 350
Carrier gas (Argon)	L/min	0.65
Aux gas (Argon)	L/min	1.0
Nebuliser (micro mist)	ml/min	2
Internal standard used	Ppm Yttrium	1

Digested solid samples were introduced into the instrument via auto sampler by peristaltic pump. The sample then passes through the nebuliser which produces a fine aerosol. As with ICP-MS, the large droplets were removed by a spray chamber, while the small droplets passed through to the plasma. The solvent was then evaporated, and the residual sample was

atomised and ionised. The ions excite in the plasma and emit a characteristic light. This light was measured by the Echelle Optical Design and Charge Injection Device (CID) solid state detector to provide elemental analysis. The instrument is controlled, and the data is processed by iTEVA software. Unknown samples are analysed against NIST Traceable Calibration Standards that range between 0.25-100 ppm and are prepared in 2% HNO3 from NIST-traceable multi-element stock solutions and Supra pure, double distilled acids. This is paired with independent quality control solutions. Calibration acceptance criteria of R2>0.9995 is used.

- *Filter Paper Description of Analyses by SEM*

Scanning Electron Microscopy (SEM) is considered as an effective method for analysing both organic and inorganic material at scales ranging from nanometres to micrometres (Mohammed & Abdullah, 2018). This technique provides structural, elemental as well as topographical information. It can be shown at both low and high magnifications up to 200 000x. The procedure below had been provided by the Electron Microscope Unit at the University of Cape Town in South Africa. The sample preparation included coating aluminium stubs with carbon glue. 1 cm x 1 cm filter paper blocks were attached to the stubs and carbon coated with a Balzers Carbon Coater.

Nova NanoSEM

The Nova NanoSEM is a high-resolution Field Emission SEM. The SEM combines low kV imaging and analytical capabilities with unique low vacuum performance. The Nova NanoSEM was used to obtain Energy Dispersive Spectroscopy (EDS). This was done for all the papers subjected to SEM analysis.

- *BSNE Sample Preparation and Description of Analysis by QEMSCAN*

Similar to the dust fallout bucket, another limitation of this study included the combination of the samples collected from both Blue Bay Lodge and the Saldanha AQM Station, into one sample. The reason for this was also similar to the one for the XRD sample, as the individual amounts of dust from the BSNEs were insufficient for QEMSCAN analysis. The procedure below was provided by the Centre for Minerals Research (CMR) Unit at the University of Cape Town. A representative of 1 g of sample was mixed with carbon nano powder, epoxy resin and hardener. The mixture was then cured in a 30 mm x 10 mm cylindrical mould. The cured sample was labelled and thereafter underwent a series of grinding and polishing steps. The final polished sample was dried, and carbon coated using a Quoram Q150T E-coater. The prepared sample was run on a FEI FEG QEMSCAN 650F which is equipped with two Bruker XFlash 6130 EDS. The accelerating voltage was set to 25 kV and the beam current to 10 nA. The back-scattered electron (BSE) brightness was calibrated using three standards: quartz (SiO_2) at 42 BSE, copper (Cu) at 130 BSE and gold (Au) at 232 BSE. The dust sample was

analysed using the particle mineral analysis (PMA) measurement mode set to a magnification of 200X and a point spacing of 3.0 µm.

3.3. Phase 3: Data Analysis and Interpretation

In this section, the percentage (%) capture at the seven study sites was calculated as it is important to authenticate results. The wind rose, pollution roses and polar plots were constructed to provide information on the PM concentrations as a function of wind direction and speed. The pollution roses and polar plots were used to provide information on the potential sources of the measured PM concentrations. This assessment was further assisted by data on the chemical compositions of the collected samples. This data was also used to provide information on the potential health impacts associated with the PM emissions.

3.3.1. PM Data Analysis and Interpretation

3.3.1.1. Percentage (%) Capture at the Seven Study Sites

The % capture of data of both $PM_{2.5}$ and PM_{10} concentrations were calculated at all seven sites where the PurpleAir Particulate Sensors were installed. This was necessary as it is required of the emission monitoring system to be maintained to yield a minimum of 80% capture (Department of Environmental Affairs, 2015). The % capture was calculated using the real-time $PM_{2.5}$ and PM_{10} concentrations measured at each study site, during the respective sampling periods. The calculation considered the gaps in the data, based on when the sensor was disconnected from its power source, this included a check if there were any $PM_{2.5}$ or PM_{10} concentrations that were not recorded. The data from the PurpleAir Particulate Sensors was also normalised by the number of days per month that the sensor was running (Table 24). Equation 3 below provides the equation used to calculate the percentage capture of both $PM_{2.5}$ and PM_{10}.

Percentage Capture of $PM_{2.5}$ (%)=

$$\frac{Actual\ number\ of\ PM2.5\ Concentrations\ recorded\ by\ the\ sensor}{Intended\ number\ of\ PM2.5\ concentrations\ recorded\ by\ the\ sensor} \text{x}100 \quad (3)$$

$PM_{2.5}$ concentrations were measured in 2-minute intervals. The numerator was calculated for each study site based on how many $PM_{2.5}$ concentrations that should have been recorded over the sampling period. The denominator is the actual number of $PM_{2.5}$ concentrations that were recorded by the sensor, based on the fact that some sensors were disconnected from its power source or were not in operation during loadshedding. For example, if the sampling period for a sensor was 24 hours, this would imply that the sensor was installed for 1 440 minutes and the intended number of $PM_{2.5}$ concentrations recorded by the sensor would be 720, given that the sensor measures in 2-intervals. However, in the event of a 2-hour period of loadshedding, this would imply that the sampling period was 22 hours, which implies that the actual number of $PM_{2.5}$ concentrations recorded by the sensor, in 2-minute intervals was 660. Therefore, the percentage capture would be 660 divided by 720, which results in a percentage capture of 92%.

3.3.1.2. Meteorology Data from a Local Weather Station

A meteorology analysis was necessary to establish wind and pollution roses to assist in identifying the potential sources of dust emissions, this is discussed further in Section 3.3.1.3. Since there was no meteorological data available from the two AQM stations in the municipality due to equipment malfunction, other stations were considered. Data was used from two NOAA (National Oceanic and Atmospheric Administration) stations using the worldmet package in R (Carslaw, 2020). The first station that was considered was the Langebaanweg Station (Figure 20). However, the topography of the area where the station is situated was an influencing factor and therefore, the data from this station was not considered as it would not be a true representation of the meteorological conditions that were experienced at the study sites. The meteorological variables that were used from the data downloaded was wind speed (m/s) and wind direction (°). The second station that was considered was the Geelbek Station (Figure 20). Although this station was further southeast of all the study sites, the absence of any topography allowed for data from this station to be used. The variables downloaded were the same as those downloaded from the Langebaanweg Station.

Figure 20: The Langebaanweg and the Geelbek weather stations

3.3.1.3. Wind Roses, Pollution Roses and Polar Plots

Wind roses show the wind direction and speed for a certain period. The circular format indicates the direction that the wind blew from, while the length of each spoke indicates how

often the wind blew from that direction. The windRose function in the openair package was used in R to plot the wind rose of hourly wind speed data obtained from the Geelbek Station. Although wind roses provide significant information regarding wind direction and speed, more detail was required to analyse the direction from which PM was coming from. Therefore, plots such as pollution roses and polar plots were considered. A pollution rose is a variant of the more commonly used wind rose and proves to be very useful by considering the concentrations of the pollutant(s) by wind direction (Carslaw & Davison, 2023). The pollution rose also provides the percentage time that a concentration is in a specific range (Carslaw & Davison, 2023). In R, using the openair package, the pollutionRose function was used to plot the pollution roses for each study site, using the hourly PM concentrations and meteorological data.

In R, the polarPlot function plots a bivariate polar plot of pollutant concentrations. These concentrations vary by wind direction and wind speed. Polar plots indicate both the wind direction and wind speeds that pollutants are associated with. The polar plot code calculates the mean PM concentrations based on hourly data associated with certain wind directions. It also assists in investigating the dependence of a particular pollutant on both wind direction and speed (Habeebullah et al., 2015). One of the enhancements that make Polar Plots different is that the plots are shown as a continuous surface, which are calculated through modelling processes using various smoothing techniques (Carslaw & Davison, 2023). These plots have also proved to be very useful for obtaining a graphical impression of potential sources influences at a particular location. Carslaw and Davison (2023) have reported that polar plots generally indicate interesting features at higher wind speeds. However, at higher wind speeds, it is possible that there exist few measurements, which subsequently results in higher uncertainty when the surface is calculated. Carslaw and Davison (2023) explicitly explain the code required to generate polar plots. The code, being a one-line code, requires only the dataset and the PM concentrations. Adding “uncertainty = TRUE” to the one-line code ensures using the most robust method. The result will provide the predicted surface, along with the lower (5%) and the upper (95%) confidence intervals (Carslaw & Davison, 2023). These uncertainty plots are presented in Appendix I.

3.3.2. Physical Sample Analysis and Interpretation

3.3.2.1. Dust Fall Rate Calculation

Equation 4 was used to calculate the dust fall rate for each sample obtained from the dust fallout bucket, with a sample calculation shown in Appendix H. The equation considered the mass of the sample obtained from the dust fallout bucket (post drying), the cross-sectional area of the dust fallout bucket and the number of sampling days. However, the rate for each sample was normalised over a period of 30 days to allow for appropriate comparison of each sample, due to the dust fallout bucket being in the field for more than 30 days during some months as a result as COVID19 restrictions (Equation 5).

Dust fall Rate = $\frac{Mass\ of\ Sample\ (mg)}{Cross\ Sectional\ Area\ of\ Dust\ Bucket\ (m^2) x\ Number\ of\ sampling\ days\ (day)}$ (4)

Normalised Dustfall Rate = $\frac{Dustfall\ Rate\ (mg/m^2/day)}{Number\ of\ sampling\ days\ (day)}$ x 30 days (5)

3.3.2.2. Filter Paper Metal Unit Conversion

The metals from the filter papers that were analysed by ICP-MS and ICP-AES were provided either in µg/kg (ppb) or mg/kg (ppm) and are presented as ppm and ppb in the results. However, to compare the metals to standards set out by NAAQS or the 4th Daughter Directive in the discussion, the units were required to be in µg/m^3. The concentration of the metals (µg/kg) were multiplied by the mass of the sample collected on the filter paper, in g. The concentration of the metal(s) was divided by the flowrate of air (16.7 LPM), which was converted to m^3/min. The number of days that the filter paper was also introduced into the dominator. This is indicated by Equation 6 below. To achieve the desired units, the appropriate unit conversions were used, with a sample calculation indicated in Appendix H.

Concentration of element = $\frac{Concentration\ of\ element(\mu g/kg)\ \ x\ Mass\ of\ sample\ on\ filter\ paper(g)}{Flowrate\ of\ air\ into\ sampler\left(\frac{L}{min}\right) x\ Number\ of\ sampling\ days(day)}$ (6)

CHAPTER 4: RESULTS

This chapter presents the results obtained during this study and consists of three main sections. Section 4.1. presents the time plot series of the PM data obtained from the PurpleAir Particulate Sensors installed at the seven study sites. The percentage capture and exceedances are also presented in this section. Section 4.2. presents the PM concentrations as a function of wind direction and speed, in the form of pollution roses and polar plots. Section 4.3. presents the results of the physical PM samples obtained from the dust fallout buckets, BSNEs and the gravimetric samplers.

4.1. PM Concentration Profiles

As previously mentioned in Section 3.2.1, PurpleAir monitors were installed at all the key study sites (Figure 21).

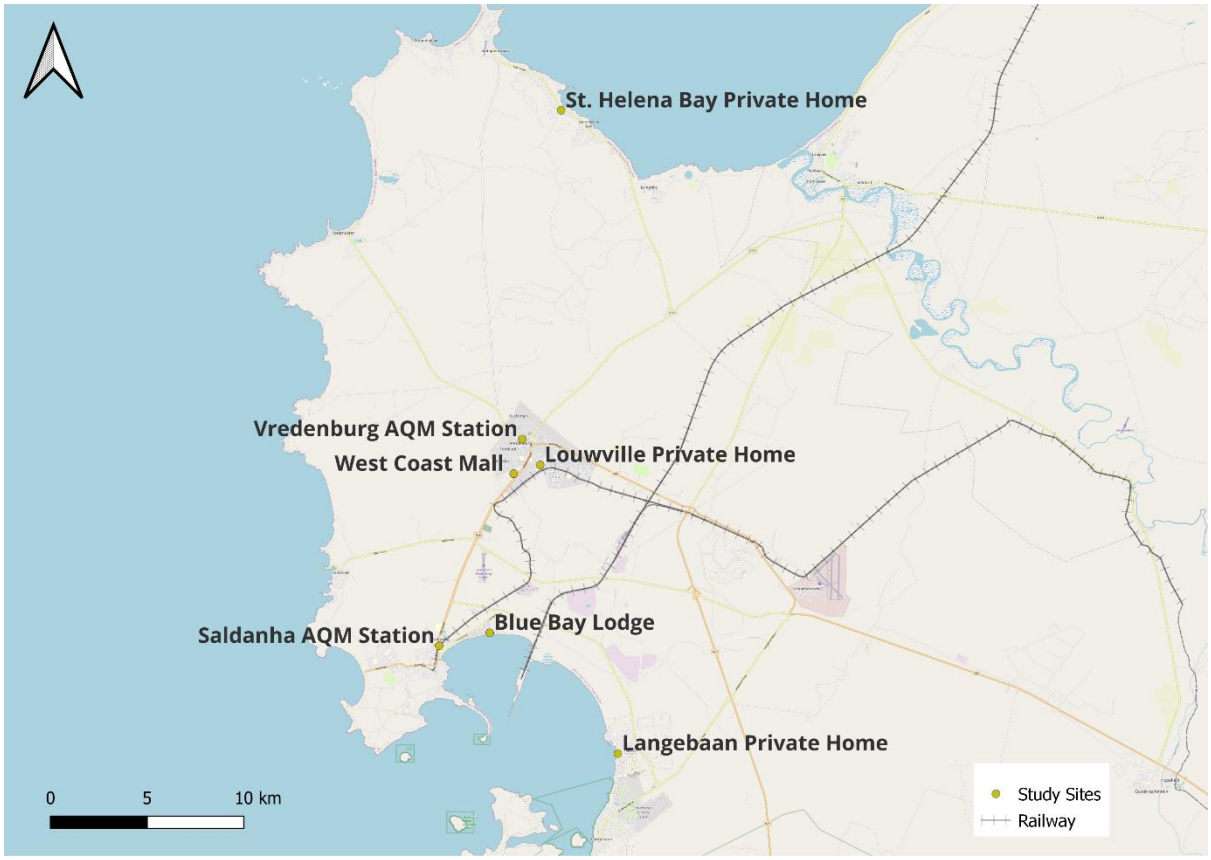

Figure 21: Study sites where the PurpleAir Particulate Sensors were installed

4.1.1. PM Concentrations Results at all Study Sites

The correction equation provided in Section 3.2.3.2 was used to correct all the $PM_{2.5}$ data measured by the PurpleAir Particulate Sensors. The data is analysed and presented by comparing the frequency of exceedances according to both the NAAQS and WHO guidelines, to indicate the significant differences between the two. According to NAAQS, only 24-hour and annual PM averages are considered. However, in this study, hourly averages are also

presented, as hourly averages are the basis to estimate short-term exposure of $PM_{2.5}$ concentrations, subsequently allowing for a faster response to pollution events that are of concern (Wu et al., 2021). The time series point plots for the different monitoring sites are presented in Sections 4.1.1.1-7. It should be noted that both $PM_{2.5}$ and PM_{10} annual averages were not included in this study. This was due to limited access to study sites, which resulted in the PurpleAir Particulate Sensors being removed before the 1-year duration.

4.1.1.1. Blue Bay Lodge Results: PM Concentrations

Both $PM_{2.5}$ and PM_{10} time series plots are presented; however, it should be noted that there is concern regarding the PM_{10} concentrations measured by the PurpleAir Particulate Sensor and is discussed further. The time plot series (Figure 22a/b and Figure 23a/b) presents the uncorrected and corrected $PM_{2.5}$ as well as the uncorrected PM_{10} concentrations over the entire sampling period at Blue Bay Lodge (28th January 2021 – 24th February 2022). However, during the month of August and September, no sampling took place due to the disconnection from the power source to the monitor. The concentration limits have been indicated on the time plot series by the horizontal lines for all the 24-hour average plots for each study site.

The uncorrected data for the $PM_{2.5}$ concentrations are illustrated only for Blue Bay Lodge, to indicate the effect of correcting the $PM_{2.5}$ data. For the rest of the sampling sites, only corrected $PM_{2.5}$ concentrations are presented. From this, the corrected PM concentrations are lower than the uncorrected PM concentrations, as expected as PurpleAir Particulate Sensors are known to overestimate PM concentrations by ~40% (Barkjohn, Gantt & Clements, 2021). As mentioned previously, Barkjohn, Gantt and Clements (2021), in their study have mentioned that humidity impacts the light scattering of particles, and therefore, the results obtained by using the correction equation, taking humidity into account, has proven to be consistent with what was expected. Over the entire sampling period at Blue Bay Lodge, there was no exceedances according to the NAAQS guidelines for both $PM_{2.5}$ (uncorrected and corrected) and PM_{10} (uncorrected). According to the WHO guidelines, there were 4 exceedances for the corrected $PM_{2.5}$ concentrations and 27 exceedances for the uncorrected $PM_{2.5}$ concentrations (Table 17).

As mentioned above, the NAAQS and WHO guidelines do not take into account hourly PM concentrations, and therefore, there are no limits that can be used to indicate exceedances of $PM_{2.5}$ and PM_{10} concentrations using hourly averages. However, when analysing the hourly and 24-hour average concentrations, it can be seen that the concentrations at various hours in the day are higher than the 24-hour average of that respective day. Hourly averages also provide a higher temporal resolution than the 24-hour averages, this is discussed further in Section 5.1.1.

- $PM_{2.5}$ Concentrations at Blue Bay Lodge

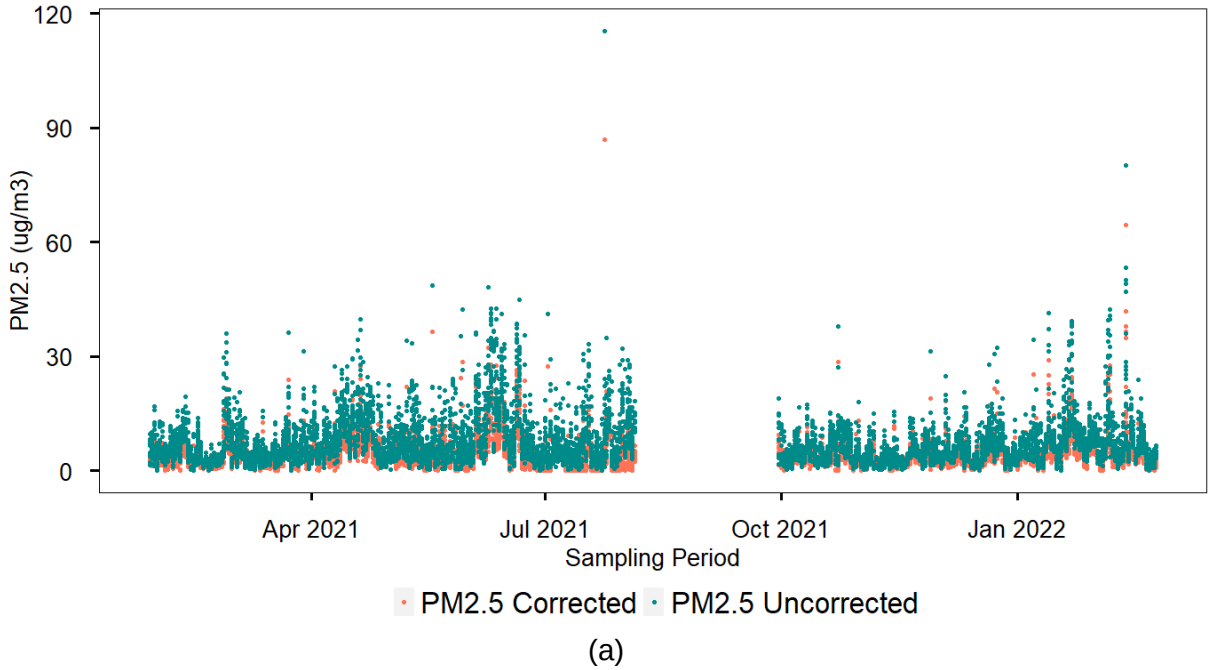

(a)

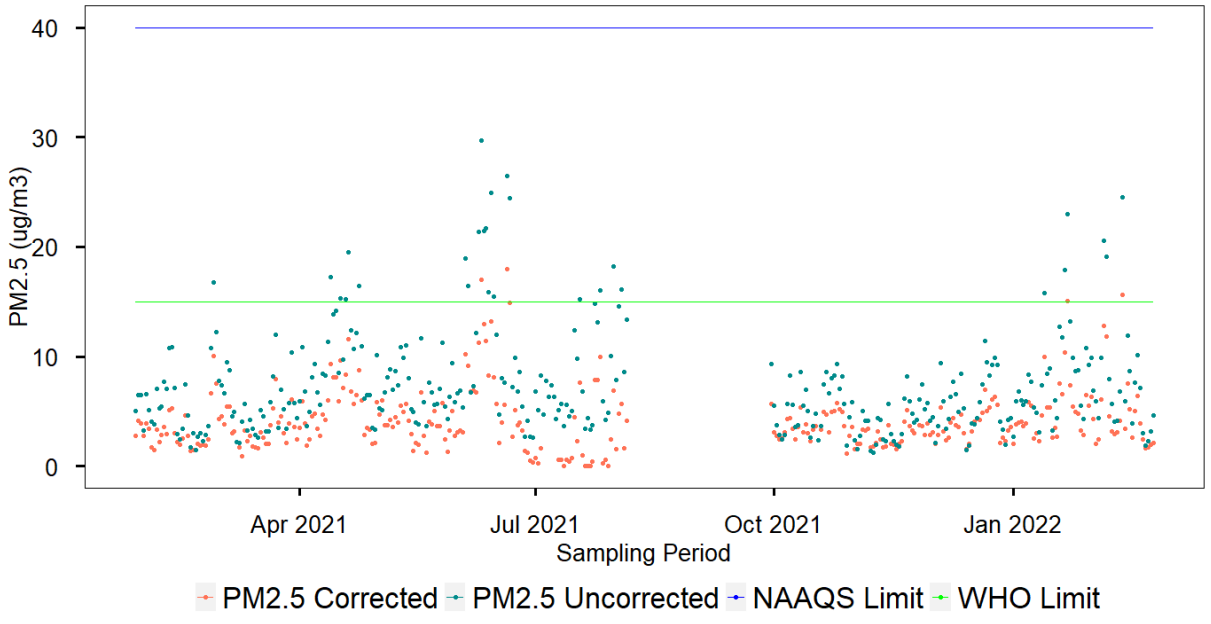

(b)

Figure 22: Uncorrected and corrected $PM_{2.5}$ concentrations (µg/m³) at Blue Bay Lodge (January 2021-February 2022) (a) hourly averages and (b) 24-hour averages

- PM_{10} Concentrations at Blue Bay Lodge

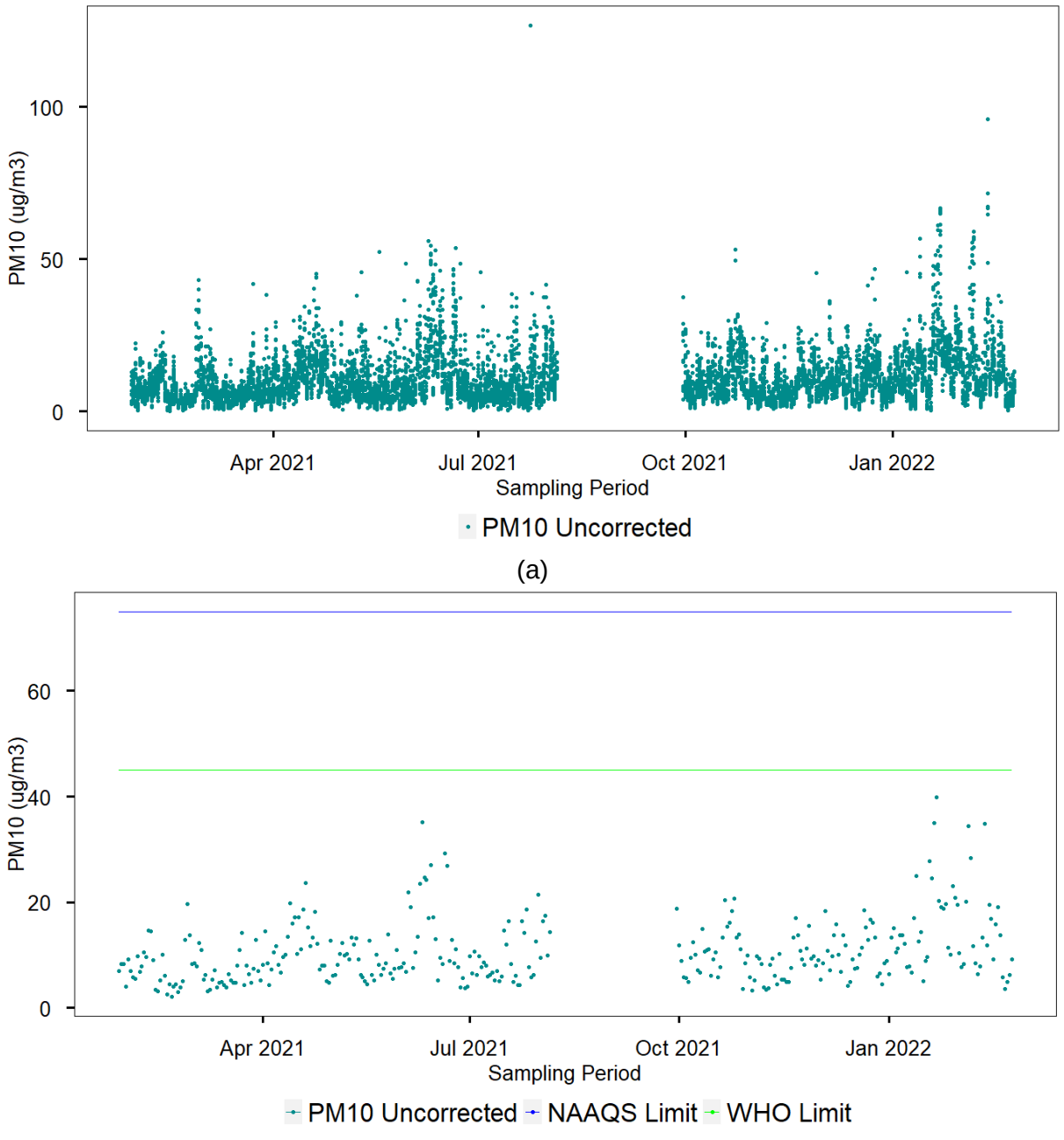

Figure 23: Uncorrected PM_{10} concentrations ($\mu g/m^3$) at Blue Bay Lodge (January 2021-February 2022) (a) hourly averages and (b) 24-hour averages

Table 17: Frequency of exceedances of 24-hour averages of $PM_{2.5}$ and PM_{10} concentrations ($\mu g/m^3$) measured at Blue Bay Lodge (January 2021-February 2022)

	$PM_{2.5}$ Corrected	$PM_{2.5}$ Uncorrected	PM_{10} Uncorrected
NAAQS	0	0	0
WHO	4	27	0

4.1.1.2. Saldanha AQM Station Results: PM Concentrations

The sampling period for PM concentrations at the Saldanha AQM Station commenced on the 25th of February 2021 until the 22nd of October 2021. The time plot series for both $PM_{2.5}$ and PM_{10} over the entire sampling period is presented in Figure 24a/b and Figure 25a/b. It was found that there were no $PM_{2.5}$ nor PM_{10} exceedances according to NAAQS, and 9 exceedances of $PM_{2.5}$ according to the WHO guidelines (Table 18).

- $PM_{2.5}$ Concentrations at the Saldanha AQM Station

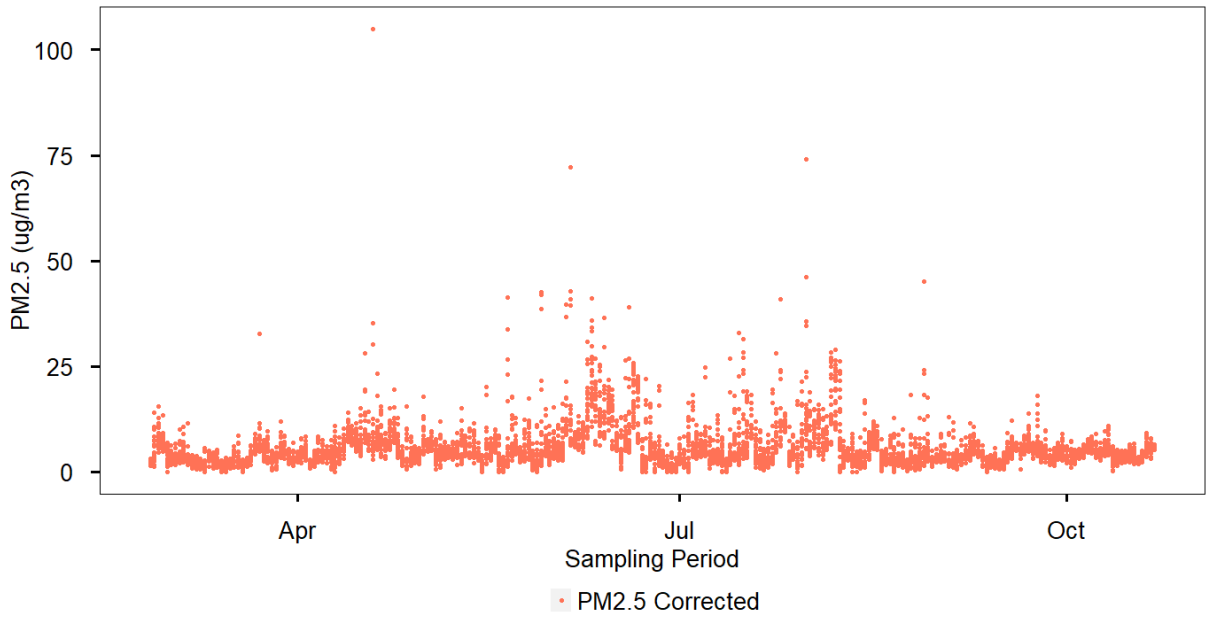

(a)

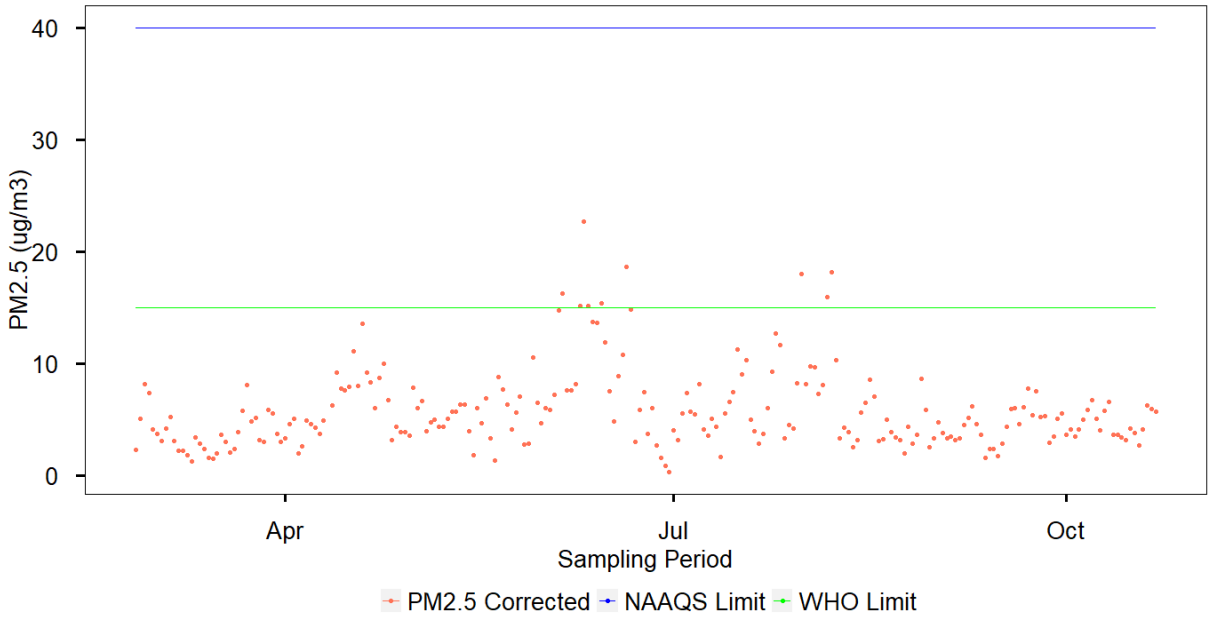

(b)

Figure 24: Corrected $PM_{2.5}$ concentrations (µg/m³) at Saldanha AQM Station (February-October 2021) (a) hourly averages and (b) 24-hour averages

- PM_{10} Concentrations at the Saldanha AQM Station

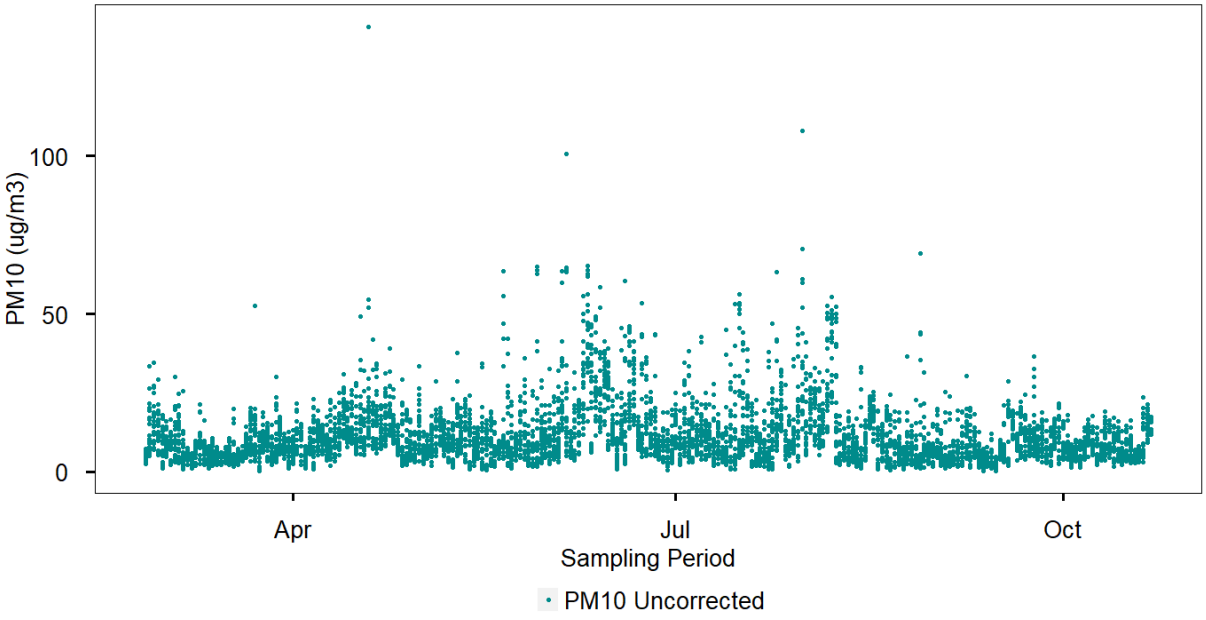

(a)

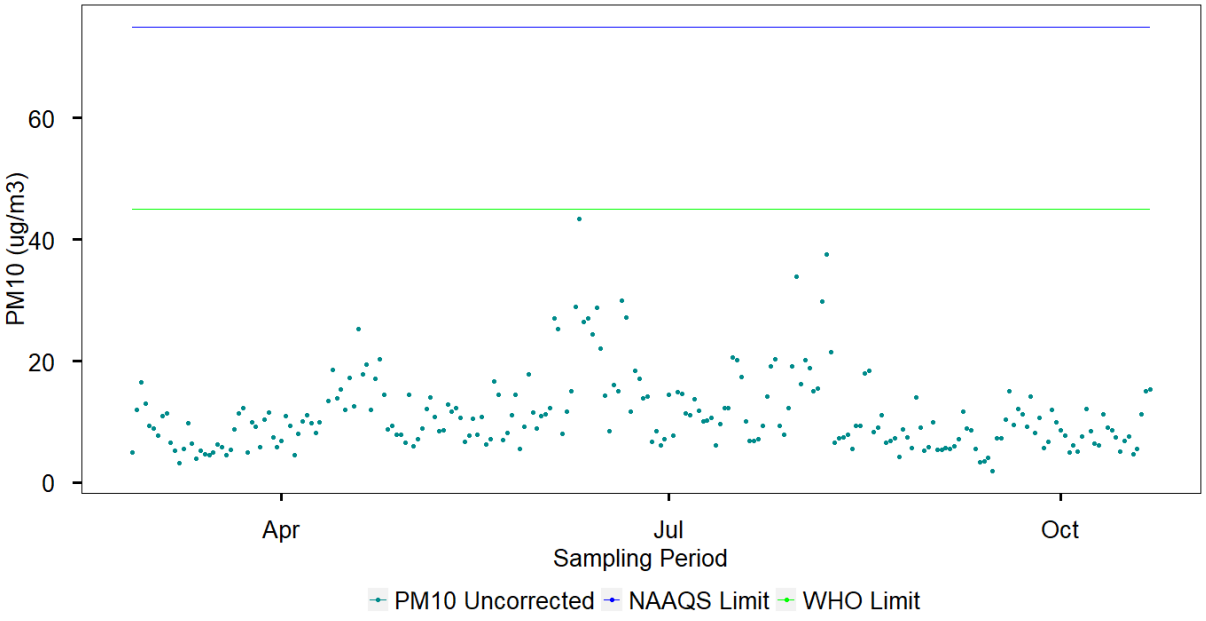

(b)

Figure 25: Uncorrected PM_{10} concentrations (µg/m³) at Saldanha AQM Station (February-October 2021) (a) hourly averages and (b) 24-hour averages

Table 18: Frequency of exceedances of 24-hour averages of $PM_{2.5}$ and PM_{10} concentrations (µg/m³) measured at the Saldanha AQM Station (February-October 2021)

	$PM_{2.5}$ Corrected	PM_{10} Uncorrected
NAAQS	0	0
WHO	9	0

4.1.1.3. Louwville Private Home: PM Concentrations

The sampling period for PM concentrations at the Louwville Private Home commenced on the 23rd of February 2021 until the 14th of May 2021. The time plot series for both $PM_{2.5}$ and PM_{10} over the entire sampling period is presented in Figure 26a/b and Figure 27a/b. It was found that there were no $PM_{2.5}$ nor PM_{10} exceedances according to NAAQS and the WHO guidelines (Table 19).

- $PM_{2.5}$ Concentrations at the Louwville Private Home

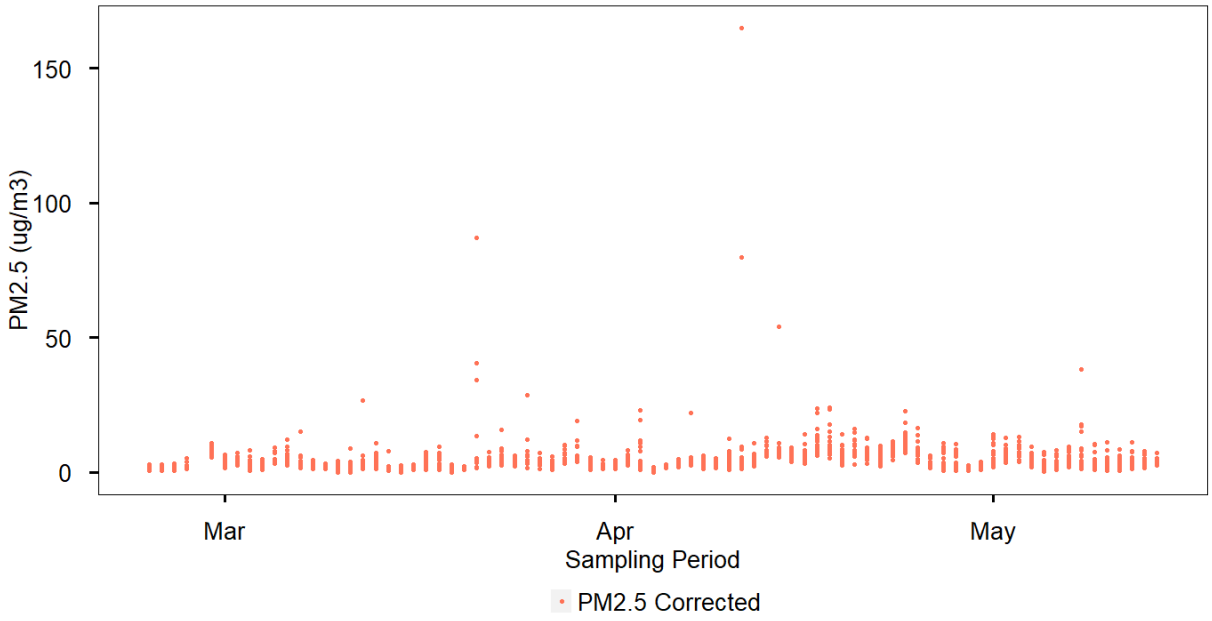

(a)

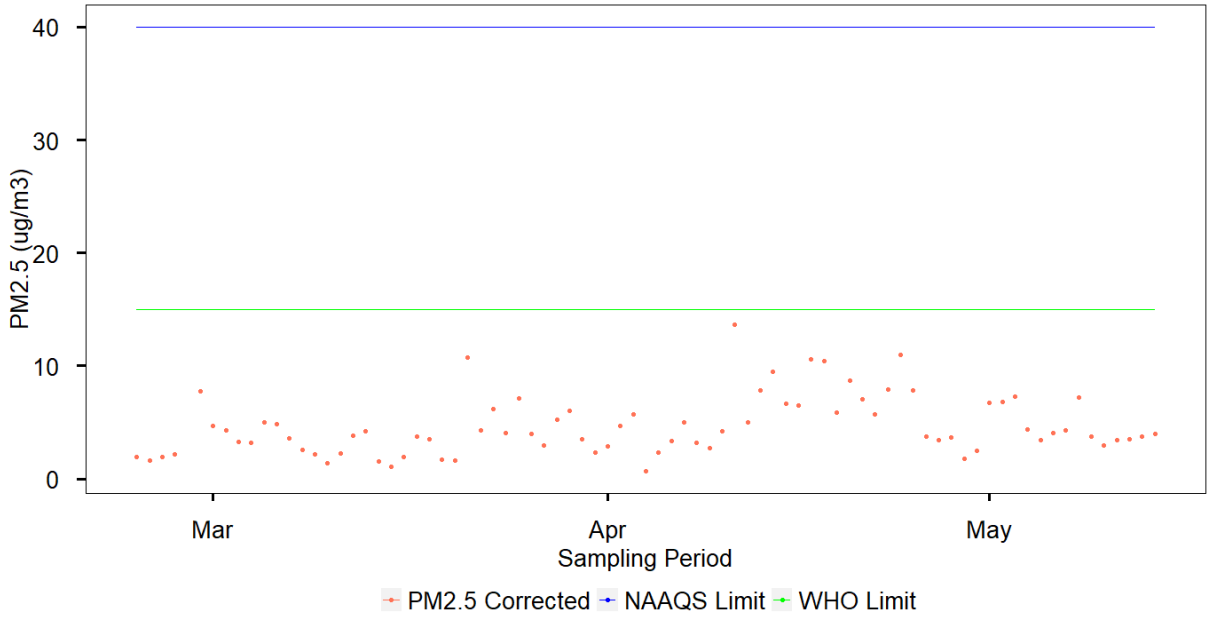

(b)

Figure 26: Corrected $PM_{2.5}$ concentrations (µg/m³) at Louwville Private Home (February-May 2021) (a) hourly averages and (b) 24-hour averages

- PM_{10} Concentrations at the Louwville Private Home

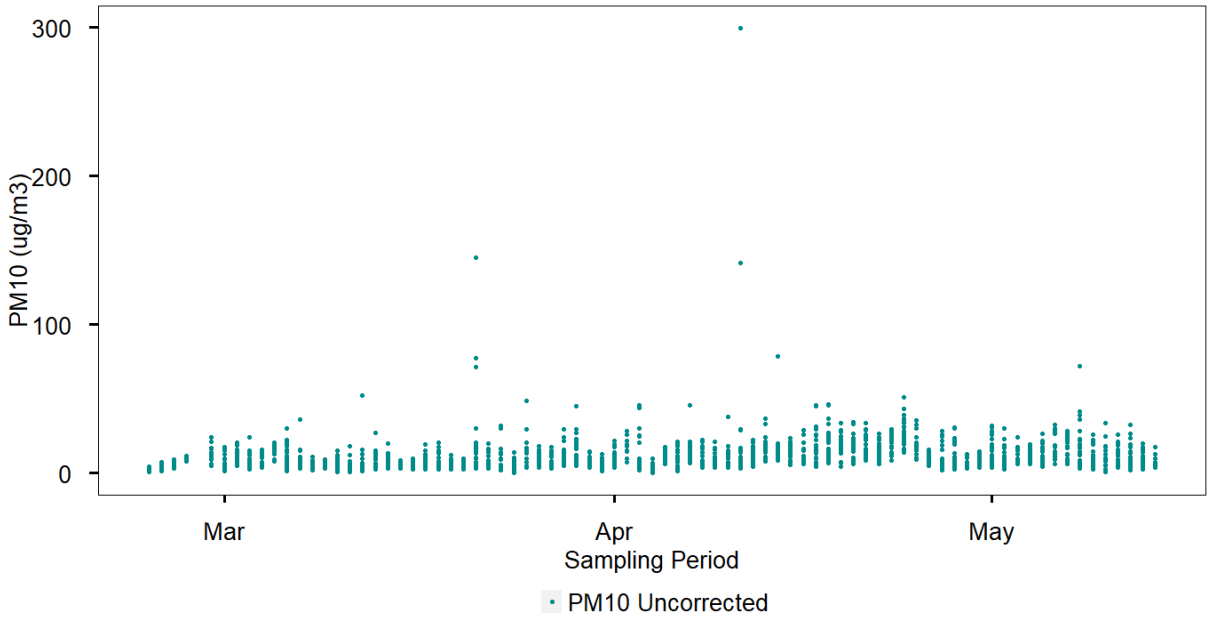

(a)

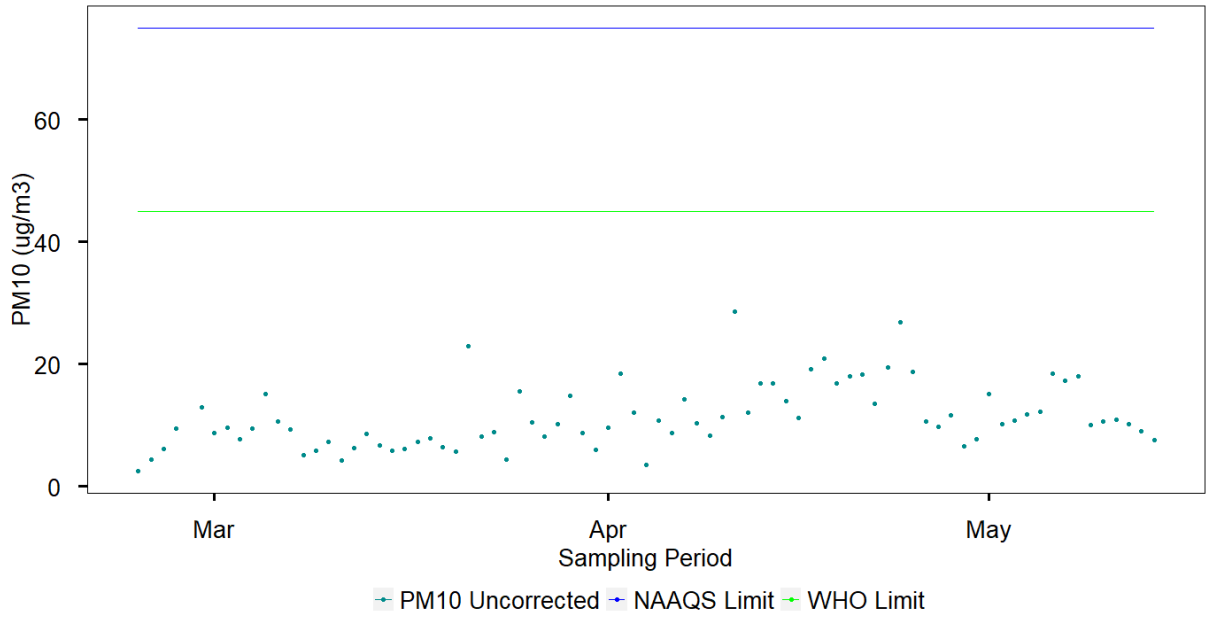

(b)

Figure 27: Uncorrected PM_{10} concentrations ($\mu g/m^3$) at Louwville Private Home (February-May 2021) (a) hourly averages and (b) 24-hour averages

Table 19: Frequency of exceedances of 24-hour averages of $PM_{2.5}$ and PM_{10} concentrations ($\mu g/m^3$) measured at the Louwville Private Home (February-May 2021)

	$PM_{2.5}$ Corrected	PM_{10} Uncorrected
NAAQS	0	0
WHO	0	0

4.1.1.4. St. Helena Bay Private Home: PM Concentrations

The sampling period for PM concentrations at the St. Helena Bay Private Home commenced on the 3rd of March 2021 until the 4th of August 2021. The time plot series for both $PM_{2.5}$ and PM_{10} over the entire sampling period is presented in Figure 28a/b and Figure 29a/b. It was found that there were no $PM_{2.5}$ nor PM_{10} exceedances according to NAAQS, and 4 exceedances of $PM_{2.5}$ and 1 PM_{10} exceedance according to the WHO guidelines (Table 20).

- $PM_{2.5}$ Concentrations at the St. Helena Bay Private Home

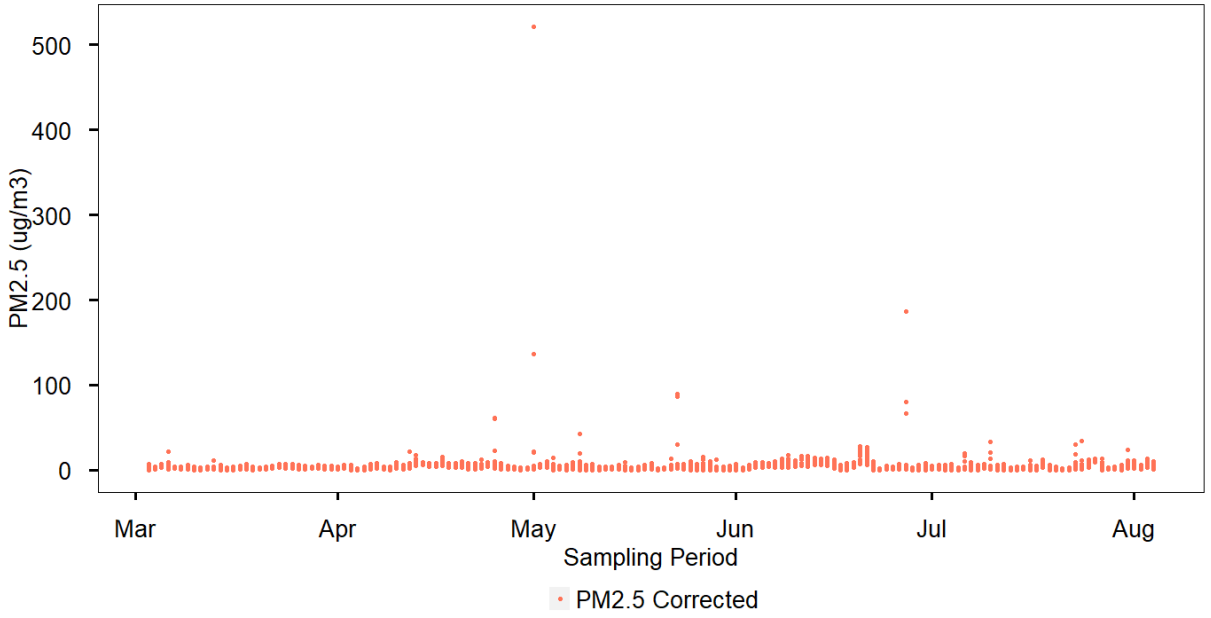

(a)

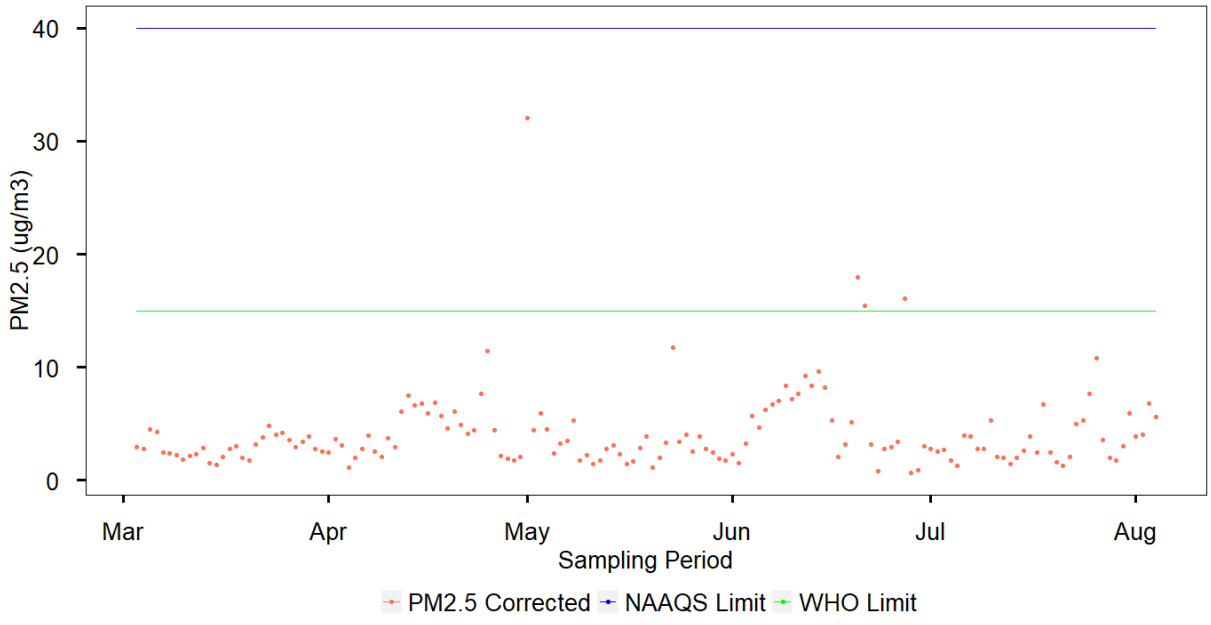

(b)

Figure 28: Corrected $PM_{2.5}$ concentrations (µg/m³) at St. Helena Bay Private Home (March-August 2021) (a) hourly averages and (b) 24-hour averages

- PM_{10} Concentrations at the St. Helena Bay Private Home

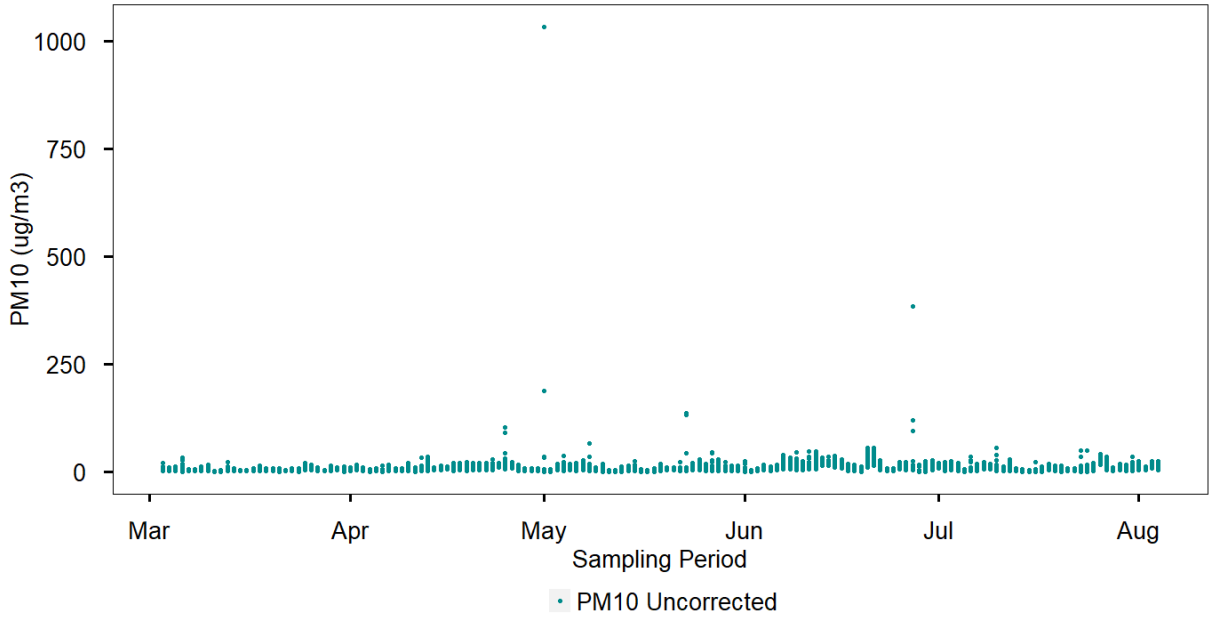

(a)

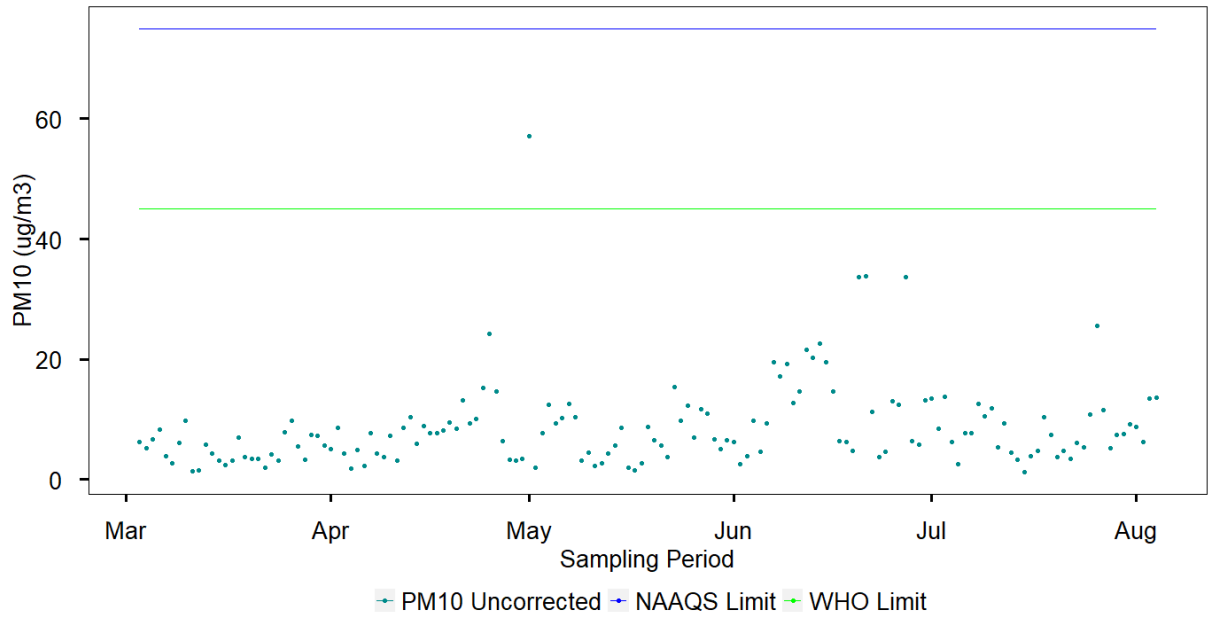

(b)

Figure 29: Uncorrected PM_{10} concentrations (µg/m³) at St. Helena Bay Private Home (March-August 2021) (a) hourly averages and (b) 24-hour averages

Table 20: Frequency of exceedances of 24-hour averages of $PM_{2.5}$ and PM_{10} concentrations (µg/m³) measured at the St. Helena Bay Private Home (March-August 2021)

	$PM_{2.5}$ Corrected	PM_{10} Uncorrected
NAAQS	0	0
WHO	4	1

4.1.1.5. West Coast Mall: PM Concentrations

The sampling period for PM concentrations at the West Coast Mall commenced on the 28th of January 2021 until the 3rd of April 2021. The time plot series for both $PM_{2.5}$ and PM_{10} over the entire sampling period is presented in Figure 30a/b and Figure 31a/b. It was found that there were no $PM_{2.5}$ nor PM_{10} exceedances according to NAAQS and the WHO guidelines (Table 21).

- $PM_{2.5}$ Concentrations at the West Coast Mall

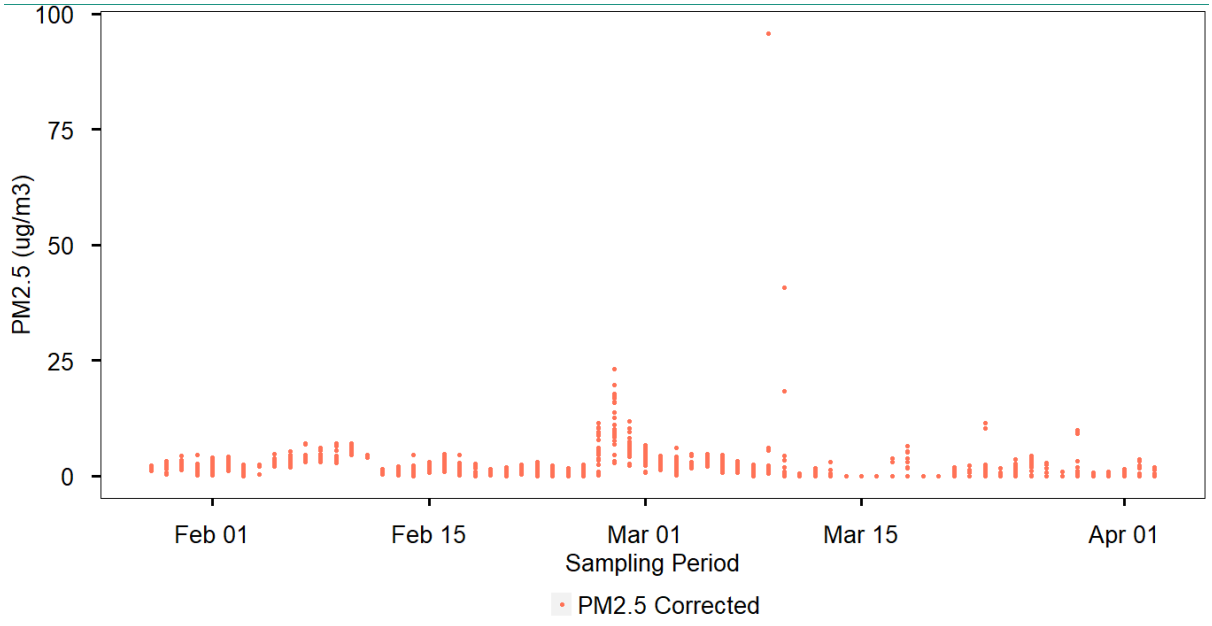

(a)

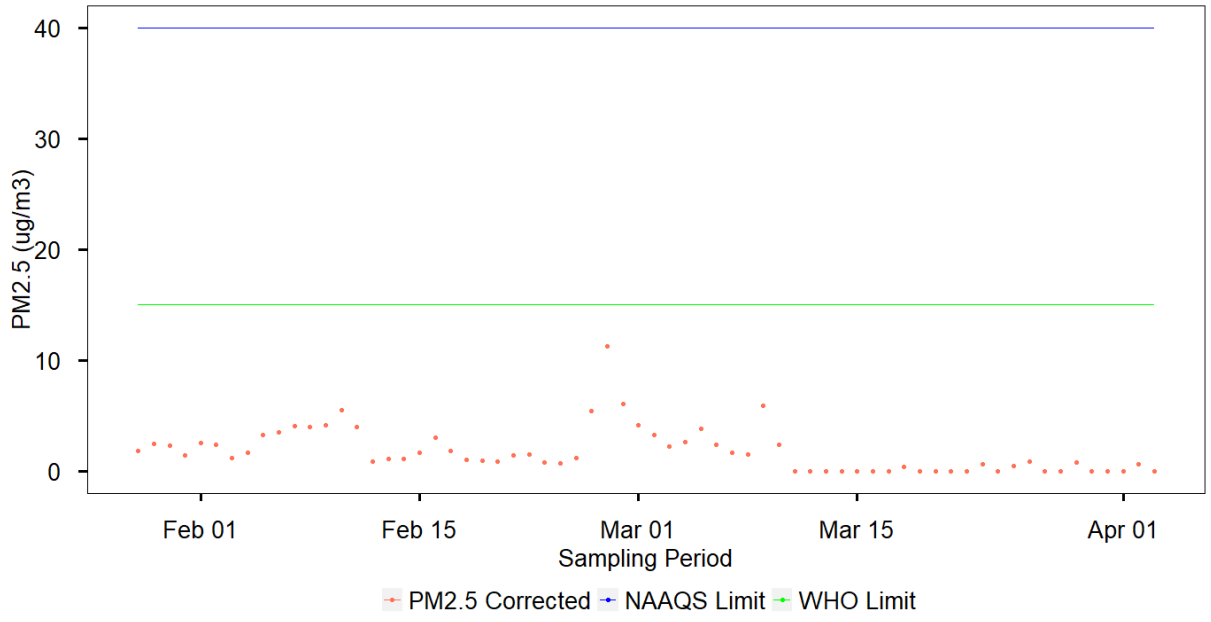

(b)

Figure 30: Corrected $PM_{2.5}$ concentrations (µg/m^3) at the West Coast Mall (January-April 2021) (a) hourly averages and (b) 24-hour averages

- PM_{10} Concentrations at the West Coast Mall

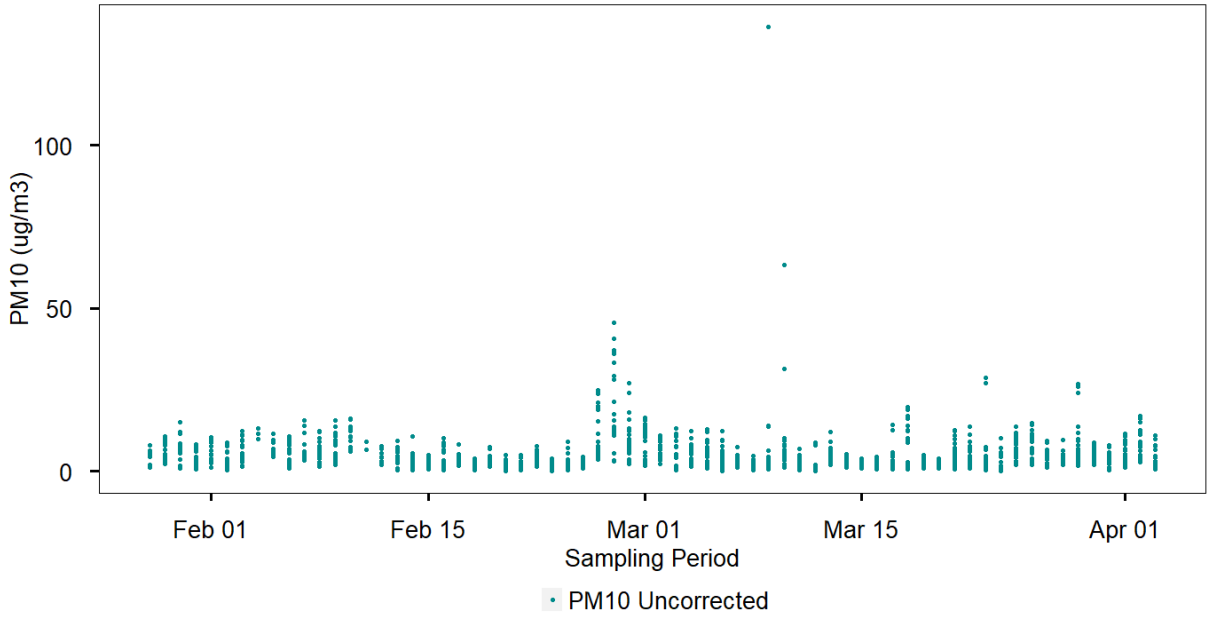

(a)

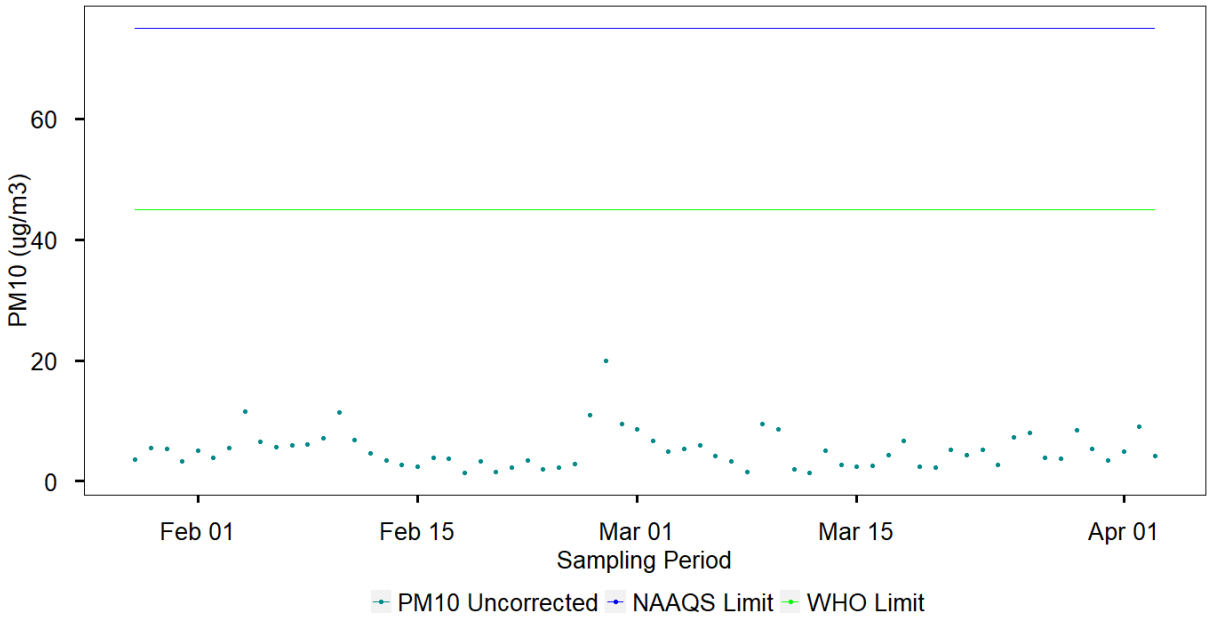

(b)

Figure 31: Uncorrected PM_{10} concentrations (µg/m³) at the West Coast Mall (January-April 2021) (a) hourly averages and (b) 24-hour averages

Table 21: Frequency of exceedances of 24-hour averages of $PM_{2.5}$ and PM_{10} concentrations (µg/m³) measured at the West Coast Mall (January-April 2021)

	$PM_{2.5}$ Corrected	PM_{10} Uncorrected
NAAQS	0	0
WHO	0	0

4.1.1.6. Langebaan Private Home: PM Concentrations

The sampling period for PM concentrations at the Langebaan Private Home commenced on the 23rd of February 2021 until the 8th of July 2021. The time plot series for both $PM_{2.5}$ and PM_{10} over the entire sampling period is presented in Figure 32a/b and Figure 33a/b. It was found that there were no $PM_{2.5}$ nor PM_{10} exceedances according to NAAQS, and 3 exceedances of $PM_{2.5}$ according to the WHO guidelines (Table 22).

- $PM_{2.5}$ Concentrations at the Langebaan Private Home

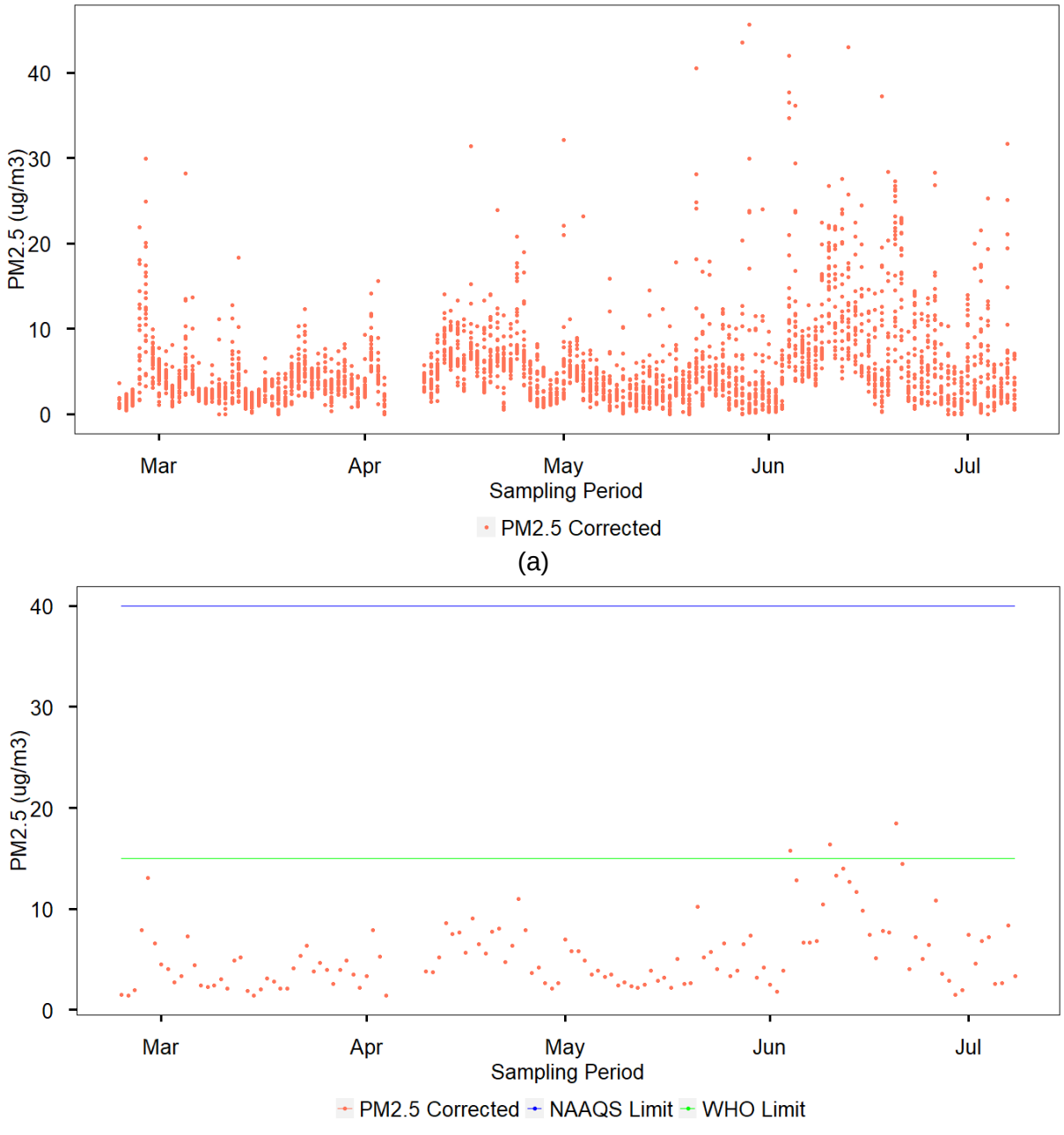

Figure 32: Corrected $PM_{2.5}$ concentrations (µg/m³) at the Langebaan Private Home (February-July 2021) (a) hourly averages and (b) 24-hour averages

- PM_{10} Concentrations at the Langebaan Private Home

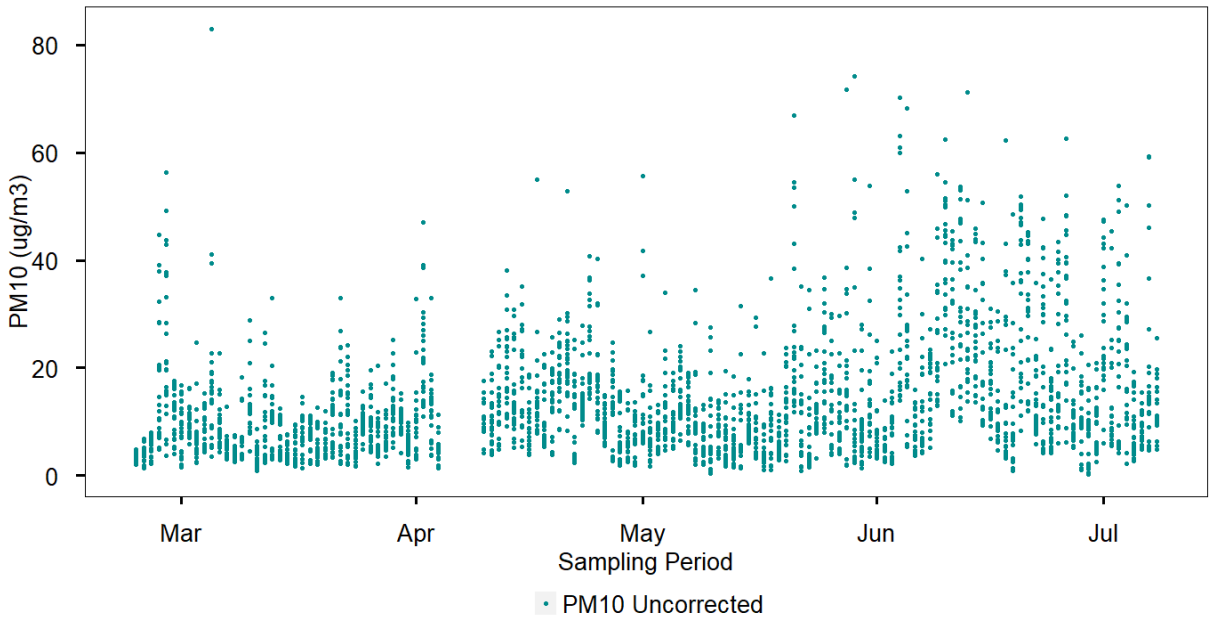

(a)

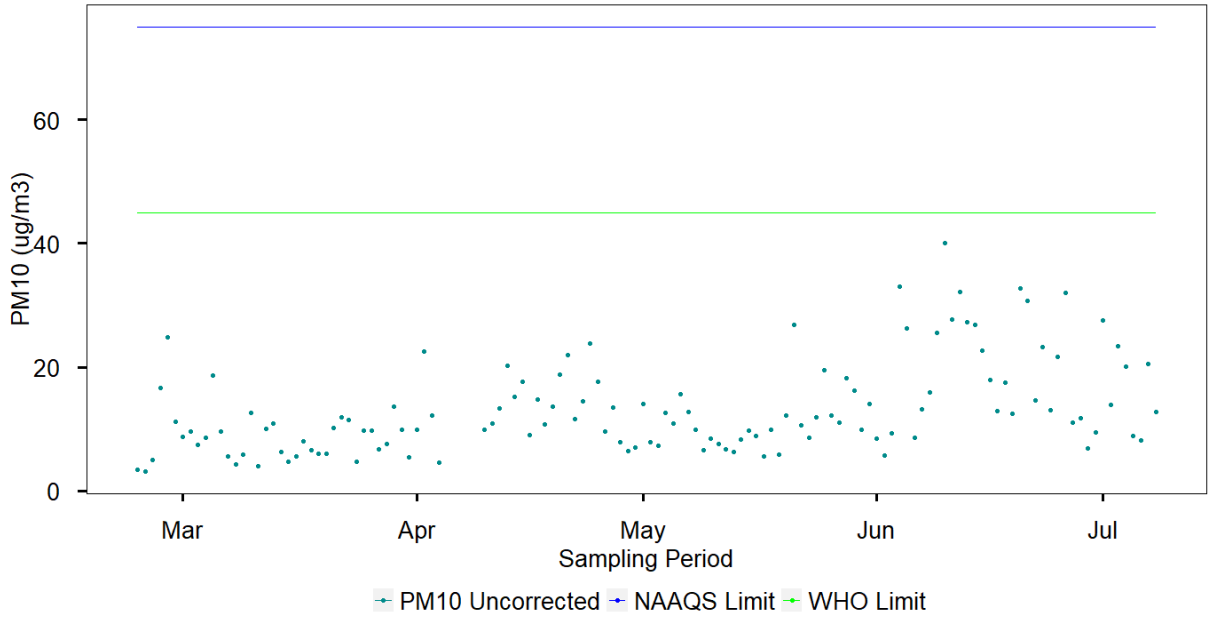

(b)

Figure 33: Uncorrected PM_{10} concentrations (µg/m³) at the Langebaan Private Home (February-July 2021) (a) hourly averages and (b) 24-hour averages

Table 22: Frequency of exceedances of 24-hour averages of $PM_{2.5}$ and PM_{10} concentrations (µg/m³) measured at the Langebaan Private Home (February-July 2021)

	$PM_{2.5}$ Corrected	PM_{10} Uncorrected
NAAQS	0	0
WHO	3	0

4.1.1.7. Vredenburg AQM Station: PM Concentrations

The sampling period for PM concentrations at the Vredenburg AQM Station commenced on the 26th of February 2021 until the 30th of June 2021. The time plot series for both $PM_{2.5}$ and PM_{10} over the entire sampling period is presented in Figure 34a/b and Figure 35a/b. It was found that there were no $PM_{2.5}$ nor PM_{10} exceedances according to NAAQS, and 1 exceedance of $PM_{2.5}$ according to the WHO guidelines (Table 23).

- $PM_{2.5}$ Concentrations at the Vredenburg AQM Station

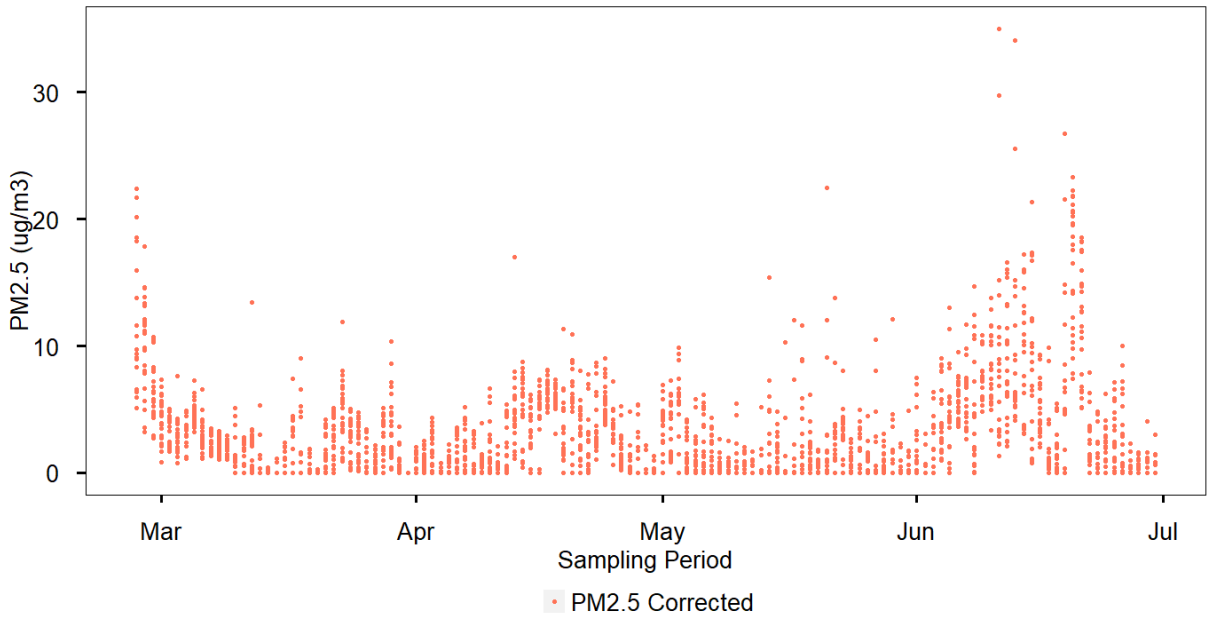

(a)

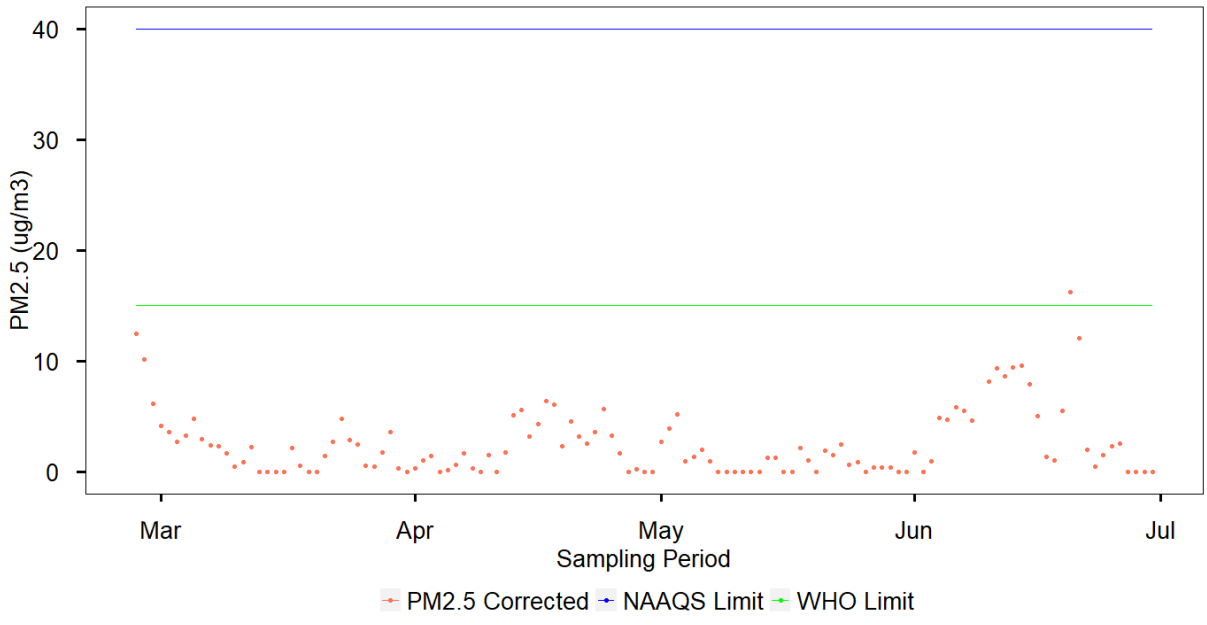

(b)

Figure 34: Corrected $PM_{2.5}$ concentrations (µg/m³) at the Vredenburg AQM Station (February-June 2021) (a) hourly averages and (b) 24-hour averages

- PM_{10} Concentrations at the Vredenburg AQM Station

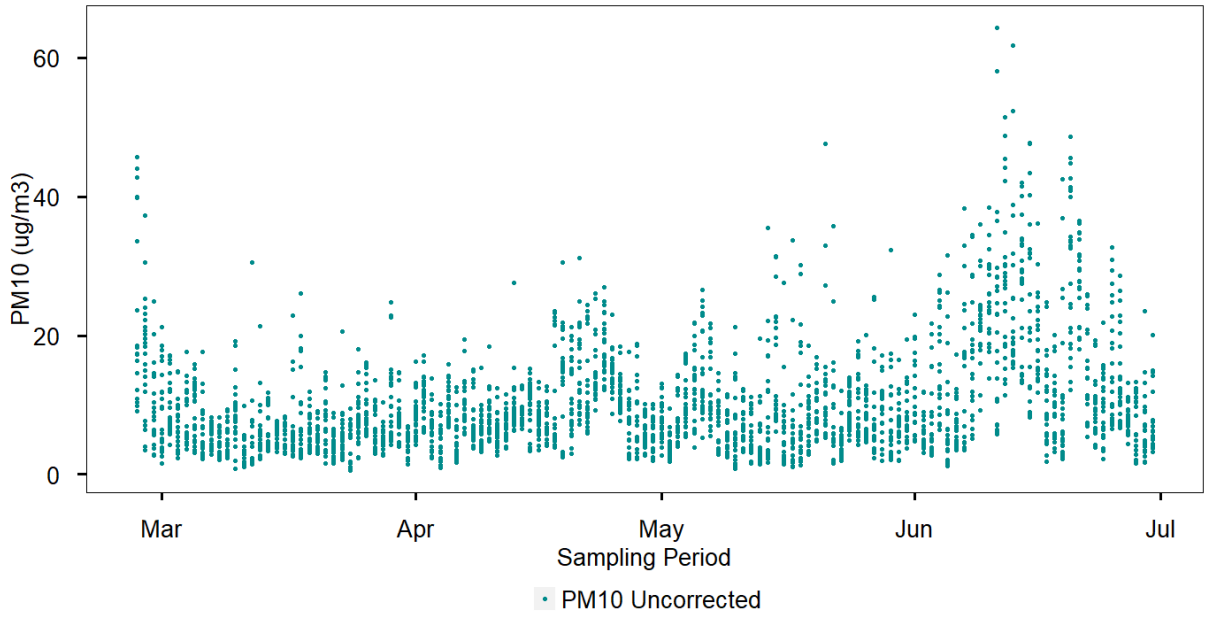

(a)

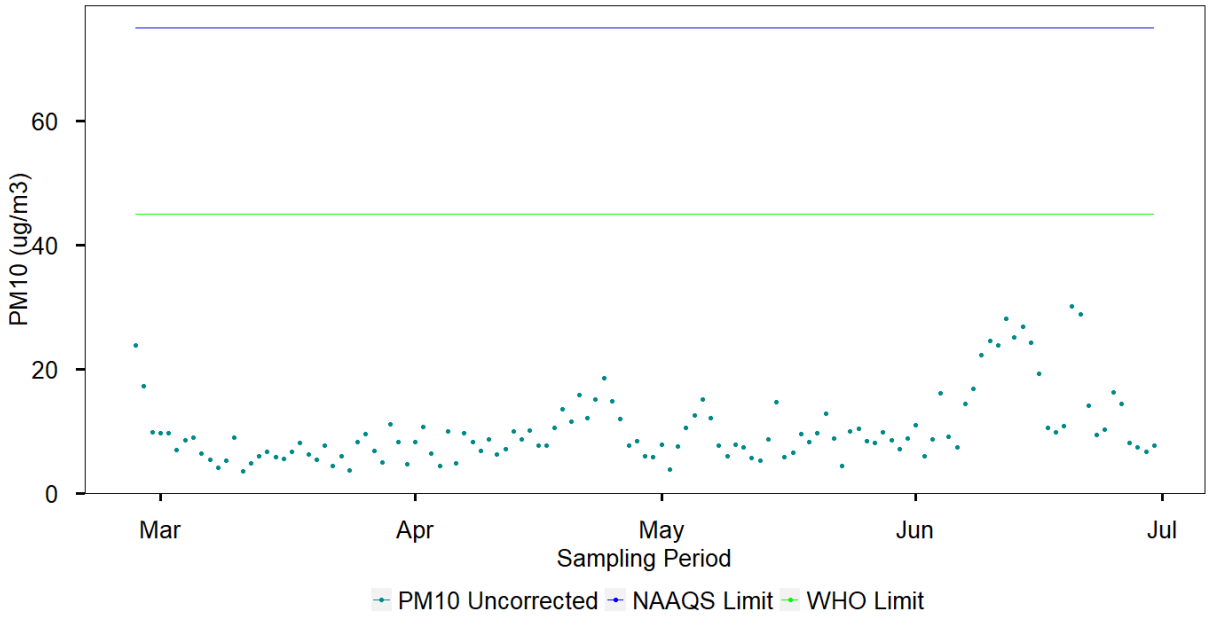

(b)

Figure 35: Corrected $PM_{2.5}$ concentrations (µg/m³) at the Vredenburg AQM Station (February-June 2021) (a) hourly averages and (b) 24-hour averages

Table 23: Frequency of exceedances of 24-hour averages of $PM_{2.5}$ and PM_{10} concentrations (µg/m³) measured at the Vredenburg AQM Station (February-June 2021)

	$PM_{2.5}$ Corrected	PM_{10} Uncorrected
NAAQS	0	0
WHO	1	0

4.1.2. Percentage Capture in the Saldanha Bay Municipality and at the Study Sites

The % capture per month per study site for $PM_{2.5}$ and PM_{10} is presented in Table 24. At each study site, it was important to determine the percentage capture of both the $PM_{2.5}$ and PM_{10} concentrations, to confirm that the capture was 80.0% or above, for the authenticity of the concentrations. According to (Department of Environmental Affairs, 2015b), the emission monitoring system is required to be maintained to yield a minimum of 80.0% capture. However, it is important to emphasise that the limitations and restrictions faced due to COVID19. With regards to incomplete months, such as months where the sensor was installed or uninstalled halfway or a few days into a month, the exceedances were normalised over the number of days in that respective month. This was done to allow for a fair comparison between the months where the sampler was in operation. The three study sites where % capture was <80% included Blue Bay Lodge, the Louwville Private Home, and the West Coast Mall. At Blue Bay Lodge, the % capture was 14.0% and 1.75% during August 2021 and September 2021, respectively. This was due to sensors disconnection from its power source. However, this was unknown at the time because the sensor was not connected to Wi-Fi and therefore, it could not be tracked on the PurpleAir Map. There were also no trips made to the West Coast during this time. The sensor was only installed at the Louwville Private Home on the 23rd of February 2021 and although the data was normalised over 28 days, only five days of sampling could possibly be the reason for the 62.9% capture.

Table 24: Monthly percentage capture and number of 24-hour exceedances of $PM_{2.5}$ and PM_{10} concentrations (µg/m³) at all seven sampling sites

	Blue Bay Lodge		Saldanha AQM Station		Louwville Private Home	St. Helena Bay Private Home			West Coast Mall	Langebaan Private Home		Vredenburg AQM Station	
2021	% Capture of $PM_{2.5}$ and PM_{10}	WHO $PM_{2.5}$ Exceedances	% Capture of $PM_{2.5}$ and PM_{10}	WHO $PM_{2.5}$ Exceedances	% Capture of $PM_{2.5}$ and PM_{10}	% Capture of $PM_{2.5}$ and PM_{10}	WHO $PM_{2.5}$ Exceedances	WHO PM_{10} Exceedances	% Capture of $PM_{2.5}$ and PM_{10}	% Capture of $PM_{2.5}$ and PM_{10}	WHO $PM_{2.5}$ Exceedances	% Capture of $PM_{2.5}$ and PM_{10}	WHO $PM_{2.5}$ Exceedances
January	100	0	-	No sampling	-	-	No sampling	No sampling	100	-	No sampling	-	No sampling
February	99.2	0	100	0	62.9	-	No sampling	No sampling	87.0	99.8	0	99.8	0
March	99.4	0	100	0	93.6	95.9	0	0	99.0	95.4	0	97.1	0
April	100	0	100	0	95.6	100	0	0	100	80.6	0	100	0
May	100	0	100	0	98.6	99.0	1	1	-	98.9	0	98.4	0
June	100	2	99.9	6	-	96.4	3	0	-	95.7	3	96.3	1
July	100	0	99.9	1	-	99.8	0	0	-	100	0	-	No sampling
August	14.0	0	99.0	2	-	100	0	0	-	-	No sampling	-	No sampling
September	1.75	0	100	0	-	-	No sampling	No sampling	-	-	No sampling	-	No sampling
October	99.6	0	100	0	-	-	No sampling	No sampling	-	-	No sampling	-	No sampling
November	99.9	0	-	No sampling	-	-	No sampling	No sampling	-	-	No sampling	-	No sampling
December	99.9	0	-	No sampling	-	-	No sampling	No sampling	-	-	No sampling	-	No sampling
2022	% Capture of $PM_{2.5}$ and PM_{10}	WHO $PM_{2.5}$ Exceedances											
January	99.9	1											
February	97.5	1											

*The “no sampling” indicates the months where the sensor was not installed.

As a comparison, the percentage capture of both the Saldanha and Vredenburg Stations were also analysed. This was carried out using the reports issued by the Saldanha Bay Municipality (Saldanha Bay Municipality, n.d.). The sampling and reporting of the results obtained from the reference stations are carried out by Argos Scientific. However, as previously mentioned, over the years, there has been significant gaps in data with regards to $PM_{2.5}$ and PM_{10} measurements at both sites. Percentage capture for 2015 until 2018 was recorded at the Saldanha AQM Station (Figure 36). Since 2018, there has been no measurements recorded for $PM_{2.5}$ and PM_{10} at both stations. From Figure 36, the significant gap in data collection is indicated. At both stations, $PM_{2.5}$ only commenced in 2017. At the Saldanha AQM station, there is a 90.0% and above data capture for PM_{10} in 2016, 2017 and 2018. At the Vredenburg AQM Station, PM_{10} data was only available in June 2015, with a 65.0% capture for that month. This raises concern as PM capture should be regarded as a priority in the area. Furthermore, data that is acceptable (>90.0% capture) is very limited and does not provide assurance to the communities in the Saldanha Bay Municipality.

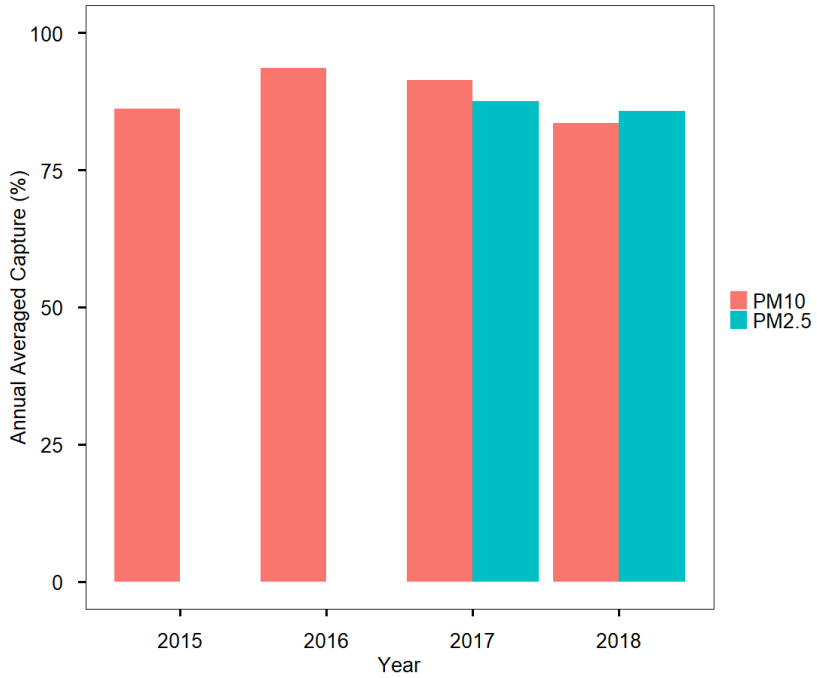

Figure 36: Percentage capture for $PM_{2.5}$ and PM_{10} at the Saldanha AQM Station

4.2. PM Concentrations as a Function of Wind Direction

The wind rose from the meteorological data obtained from the Geelbek Station is shown below (Figure 37). This wind rose covers the sampling period from January 2021 to February 2022. The wind rose for the Geelbek Weather Station covers the entire sampling period for all seven study sites from the 28th of January 2021 until the 24th of February 2022. The wind rose indicates that for the entire sampling period, 35% of the wind came from the south (S). It also shows the existence of a south southeaster (SSE), south southwester (SSW), west northwester (WNW) as well as a north northwester (NNW). The southeaster (SE) and the northwester (NW) are known to be the dominant wind directions in the municipality during the summer and winter months, respectively. The sampling period was divided per season to show the differences in wind conditions that are experienced in the municipality (Figure 38).

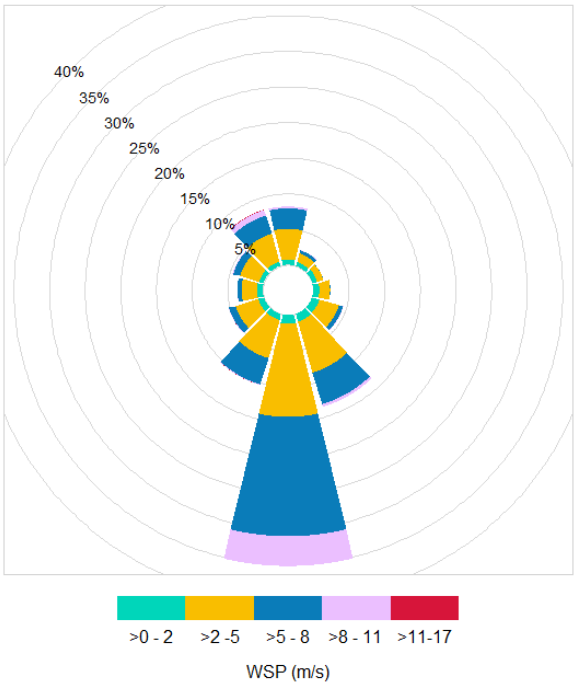

Figure 37: The Wind Rose for the Geelbek Weather Station (January 2021-February 2022)

During the summer (January-February 2021 and November 2021-December 2022), approximately 47% of the wind came from the S (Figure 38a). The wind rose for summer also indicated that there was a SSW (15%) and SSE (10%) wind component. The wind speeds also reached a high between 8-11 m/s from the S and the SSE. During autumn, approximately 35% came from the S and 13% from the SSE (Figure 38b). However, during autumn, there was also a shift in wind direction, where there were wind components from the N (north) and NNW. Wind speeds during autumn also reached a high between 8-11 m/s from the S and the NNW.

The shift from the S and SSE can be seen in the wind rose for winter (Figure 38c). Most of the wind in Winter came from the SSE (18%). 15% of wind came from the N, 14% from the S and

12% from the NNW. During winter, the wind speeds reached a high between 11-17m/s from the NNW and the N. The wind rose for spring was similar to the one for autumn. Approximately 33% of the wind came from the S and 18% from the SSE. During spring, there also existed wind components from both the N and NNW (Figure 38d). Wind speeds between 8-11 m/s were experienced from the east southeast (ESE), SSE, S and NNW. Using the meteorological from the Geelbek Station, the $PM_{2.5}$ and PM_{10} concentrations were expressed as a function of wind direction. This will be illustrated by the pollution roses and the polar plots in Sections 4.2.1 - 4.2.7.

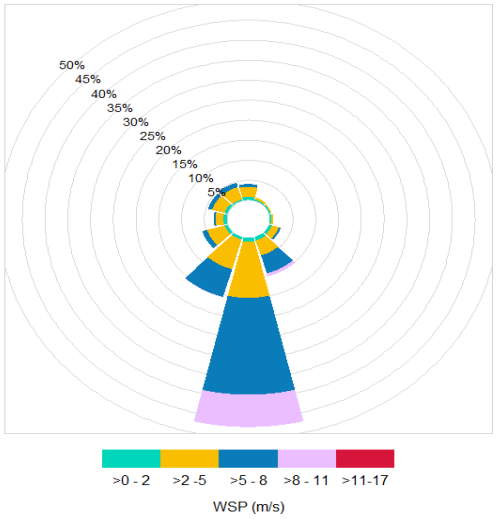

(a) Summer

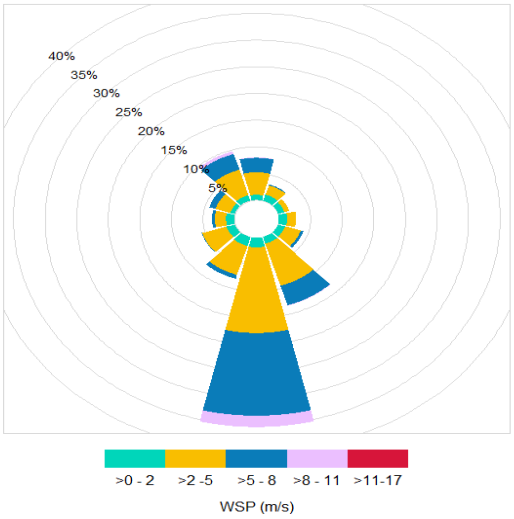

(b) Autumn

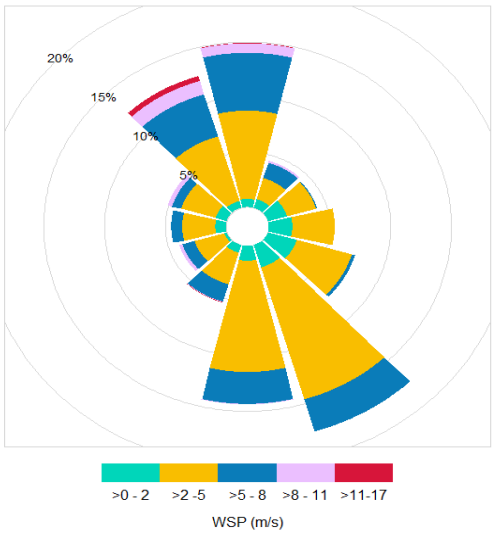

(c) Winter

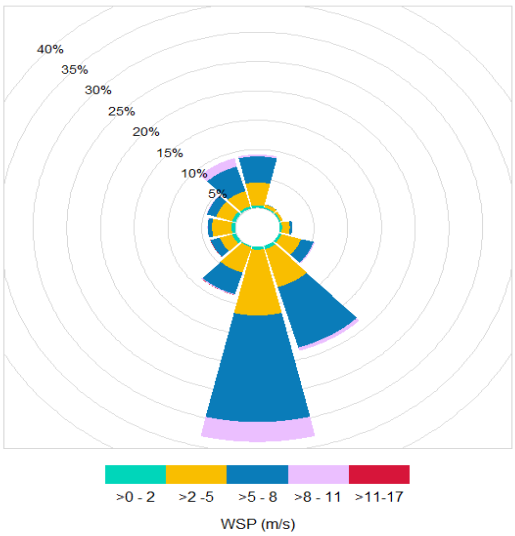

(d) Spring

Figure 38: Geelbek Station Meteorological Results for Saldanha Bay Municipality (a) Summer 2021/2020, (b) Autumn 2021, (c) Winter 2021 and (d) Spring 2021

4.2.1. Blue Bay Lodge Results: PM as a Function of Wind Direction

As previously mentioned, there is concern regarding PM_{10} concentrations measured by the PurpleAir Particulate Sensor, therefore, pollution roses and polar plots only for $PM_{2.5}$ concentrations are presented in this chapter. However, the pollution roses and polar plots for the PM_{10} concentrations are presented in Appendix C.

During the entire sampling period at Blue Bay Lodge (February 2021-March 2022), the pollution rose indicates that ~35% of $PM_{2.5}$ emissions were associated with wind from the S (Figure 39a). ~8% and ~7% of the $PM_{2.5}$ emissions from the S were between 1-2 $\mu g/m^3$ and 2-3 $\mu g/m^3$, respectively. ~14% and ~10% of the $PM_{2.5}$ emissions were also associated with wind from the SSE and the SSW, respectively. ~7% of the $PM_{2.5}$ emissions was associated with wind from both the N and the NNW.

The polar plot constructed for each study site indicates the mean $PM_{2.5}$ concentration per each wind speed-wind direction bin indicated by the scale on the right of the plot (Figure 39b). The polar plot wind directions were interpreted based on the width of the spoke shown on the pollution roses, for a particular direction. For Blue Bay Lodge, the polar plot indicates $PM_{2.5}$ concentrations from all directions between wind speeds of 0-14 m/s. The polar plot also indicates mean $PM_{2.5}$ concentrations between 10-15 $\mu g/m^3$ associated with wind between 7-10 m/s from the north northeast (NNE). Although the pollution rose indicates that approximately only 3% of $PM_{2.5}$ emissions were associated with wind from the NNE, it must be emphasised that the polar plots present the mean $PM_{2.5}$ concentrations for both wind speed and wind direction size bins. Although the wind from the NNE accounts for only 3%, the mean PM2.5 concentrations peak (10-15 $\mu g/m^3$) when it blows from the N/NNE direction (Figure 39b).

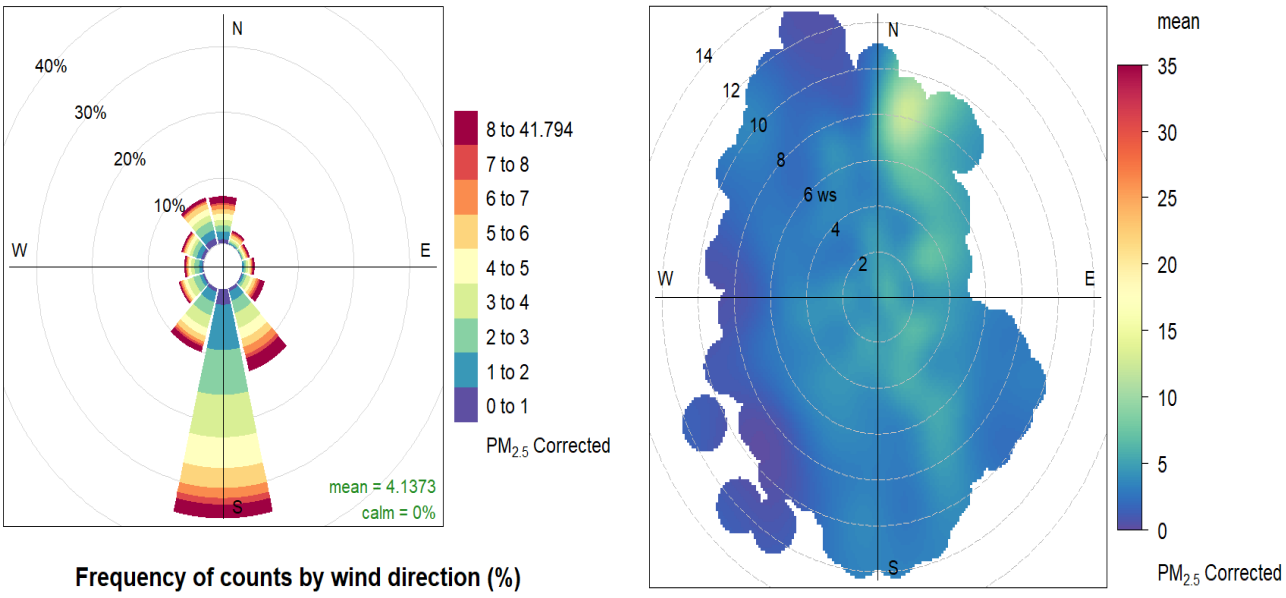

(a) (b)

Figure 39: The effect of wind direction and speed (m/s) on $PM_{2.5}$ concentrations ($\mu g/m^3$) captured at Blue Bay Lodge (January 2021-February 2022) using (a) a pollution rose and (b) a polar plot

Seasonal Pollution Roses and Polar Plots at Blue Bay Lodge

To analyse the shift in wind direction at each study site, seasonal illustrations of the pollution roses were produced for each study site. Blue Bay Lodge was the only study site where PM data was collected for all four seasons of 2021 and summer 2022 (Figure 40a/b - Figure 44a/b). The seasons were analysed as follows: Spring (September-November), Summer (December-February), Autumn (March-May) and Winter (June-August). During Summer 2021, it was found that ~60% of the $PM_{2.5}$ emissions were associated with wind from the S (Figure 40a). $PM_{2.5}$ emissions between 7-21.6 $\mu g/m^3$ were experienced with wind blowing from the east (E), east southeast (ESE), SSE, S and the SSW, with ~4% of $PM_{2.5}$ emissions between 7-21.6 $\mu g/m^3$ from the SSE. With regards to the polar plot constructed for Summer 2021, mean $PM_{2.5}$ concentrations were experienced from all directions between 0-9 m/s (Figure 40b). It was also found that the highest mean $PM_{2.5}$ concentrations (~10-15 $\mu g/m^3$) were associated with wind blowing from the SSE.

During Autumn, $PM_{2.5}$ emissions were experienced with wind from all directions (Figure 41a). ~35% of the emissions were associated with wind from the S. There were also emissions associated with wind from the SSE (14%), NNW (9%), SSW (8%) and the north (N) (7%). $PM_{2.5}$ emissions between 8-36.4 $\mu g/m^3$ were experienced from all directions, with ~3% of emissions in this range associated with wind from the S and the SSE. The polar plot indicates that most mean $PM_{2.5}$ concentrations were experienced between 0-10 m/s (Figure 41b). The

highest mean concentrations (5-10 µg/m^3) were experienced when the wind was blowing from the SSE.

The pollution rose and polar plot for Winter presents $PM_{2.5}$ concentrations experienced during June and July. During Winter at Blue Bay Lodge, although ~14% of $PM_{2.5}$ emissions were associated with wind from the SSE, there exists the shift in wind direction from the S to the N (Figure 42a). Emissions were also associated with wind from the N (13.5%), ESE (7%), S (8.5%) and from the NNW (10.5%). $PM_{2.5}$ emissions between 12-32.3 µg/m^3 were associated with wind from all directions, except the west southwest (WSW). ~2.5% of emissions in this range (12-32.3 µg/m^3) are associated with wind from the N. The polar plot indicates that mean $PM_{2.5}$ concentrations were experienced at wind speeds between 0-14 m/s (Figure 42b). The highest mean concentrations were experienced when the wind was blowing from the N/NNE (~15-20 µg/m^3) between 7-9 m/s.

The pollution rose and polar plot for Spring presents $PM_{2.5}$ concentrations experienced during October and November. During Spring, the shift in wind direction from wind blowing in the N to wind blowing in the S (Figure 43a). ~36% of the $PM_{2.5}$ emissions were associated with wind from the S during Spring. Emissions were also associated with wind from the SSE (18%), SSW (10.5%), with 7% from the NNW and N. Emissions between 6-28.6 µg/m^3 were experienced from all directions, except for the NNE, east northeast (ENE) and the west (W). ~1.5% of emissions in the 6-28.6 µg/m^3 range were associated with wind from the SSE and the S. From the polar plot, it can be seen that $PM_{2.5}$ concentrations were experienced at wind speeds between 0-12 m/s (Figure 43b). The mean $PM_{2.5}$ concentrations are approximately in the 0-5 µg/m^3 range.

During Summer (December 2021-February 2022), ~41% of the $PM_{2.5}$ emissions were associated with wind from the S (Figure 44a). ~15% of emissions were associated with wind from the SSW and 10.5% from the SSE. Emissions between 8-41.8 µg/m^3 were associated with wind blowing from all directions, except for the ENE. ~1.5% of emissions in the 8-41.8 µg/m^3 range were experienced when the wind was blowing from the S and the SSE. $PM_{2.5}$ concentrations were experienced during Summer 2021/2022 between 0-5 µg/m^3 at wind speeds between 0-11 m/s (Figure 44b). However, concentrations approximately between 5-10 µg/m^3 were experienced when the wind was blowing from the SSE.

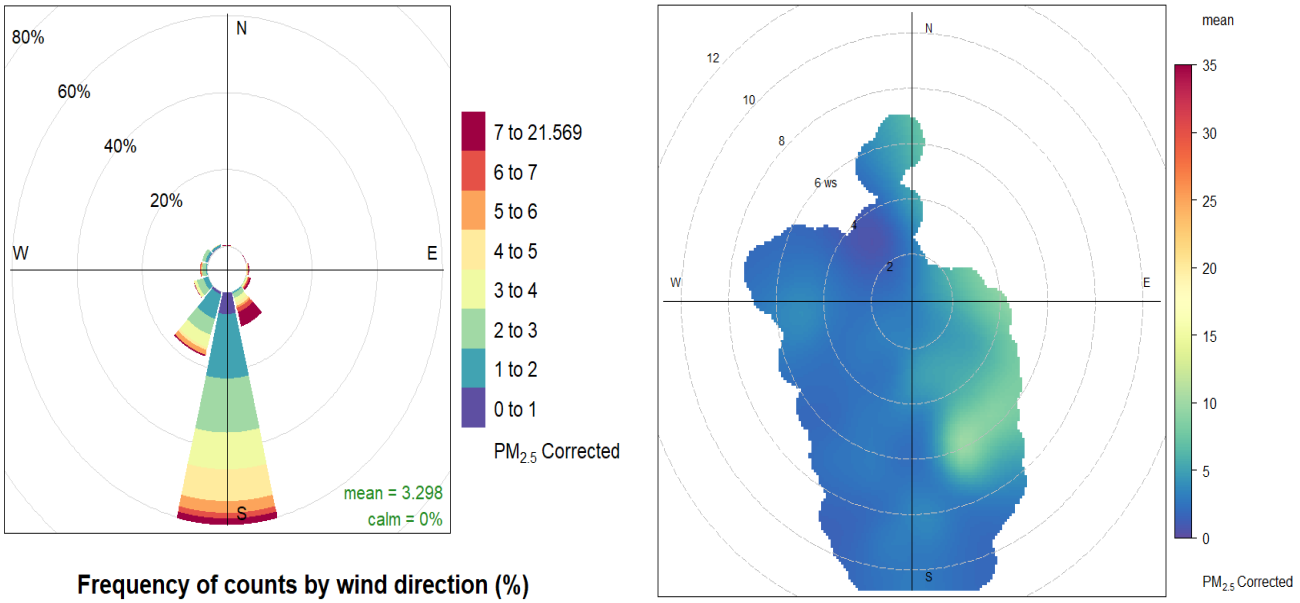

(a) (b)

Figure 40: Summer 2021 (January-February) at Blue Bay Lodge (a) $PM_{2.5}$ pollution rose and (b) $PM_{2.5}$ polar plot

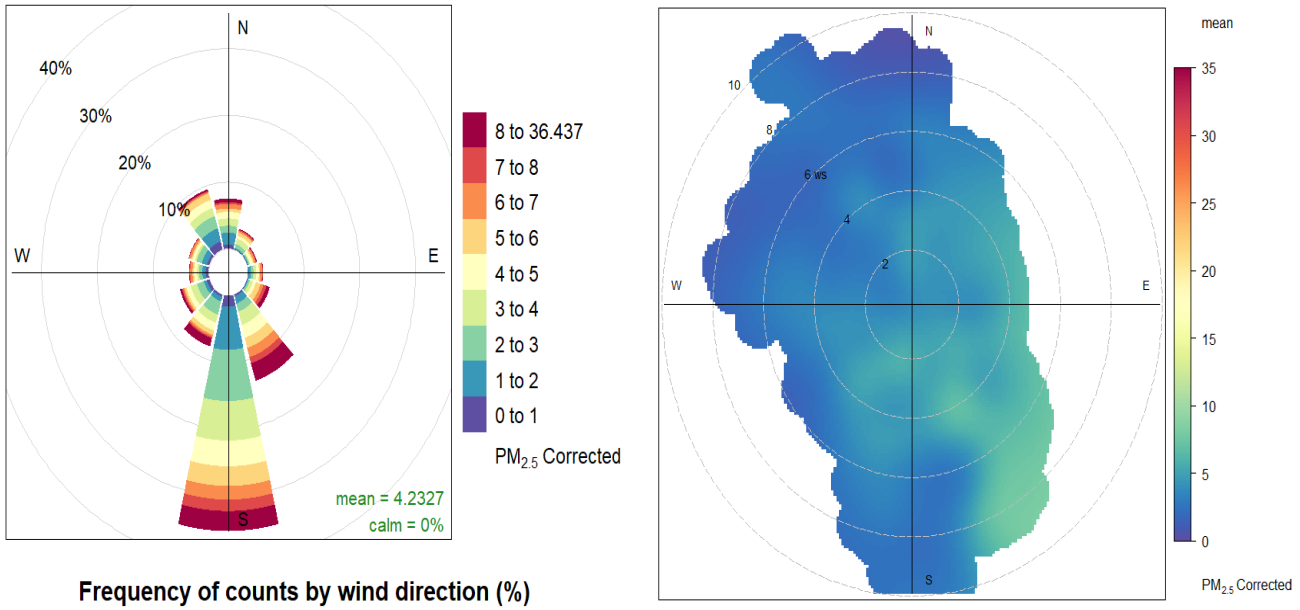

(a) (b)

Figure 41: Autumn 2021 (March-May) at Blue Bay Lodge (a) $PM_{2.5}$ pollution rose and (b) $PM_{2.5}$ polar plot

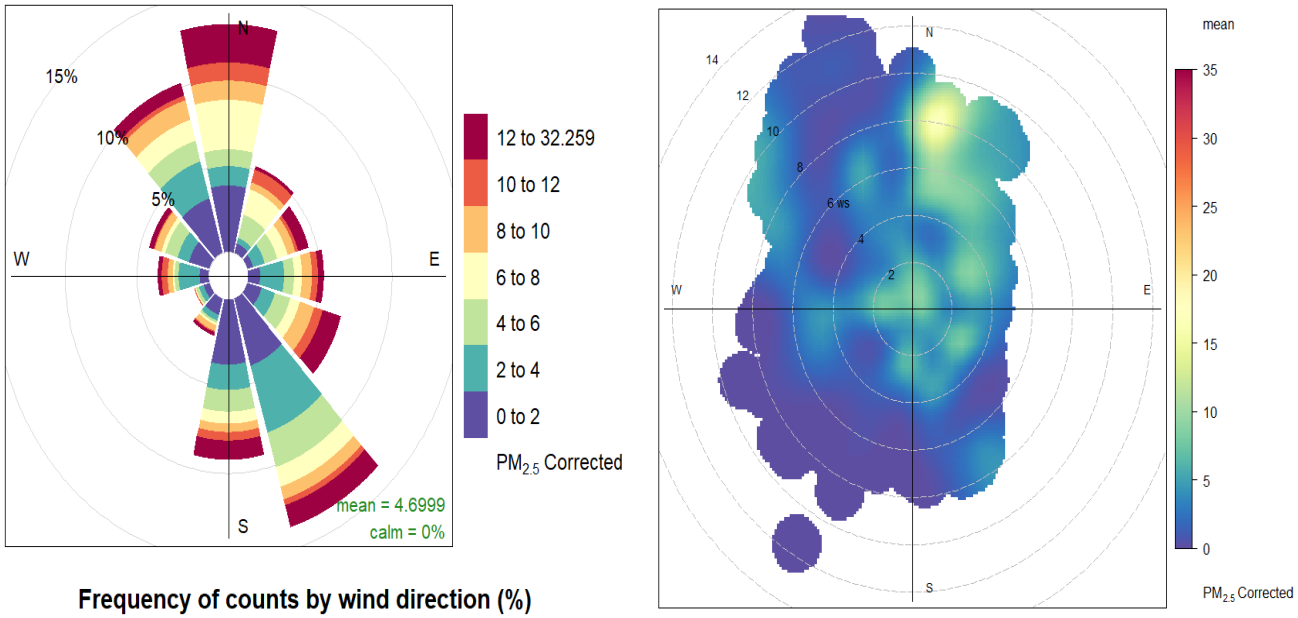

(a) (b)

Figure 42: Winter 2021 (June-August) at Blue Bay Lodge (a) $PM_{2.5}$ pollution rose and (b) $PM_{2.5}$ polar plot

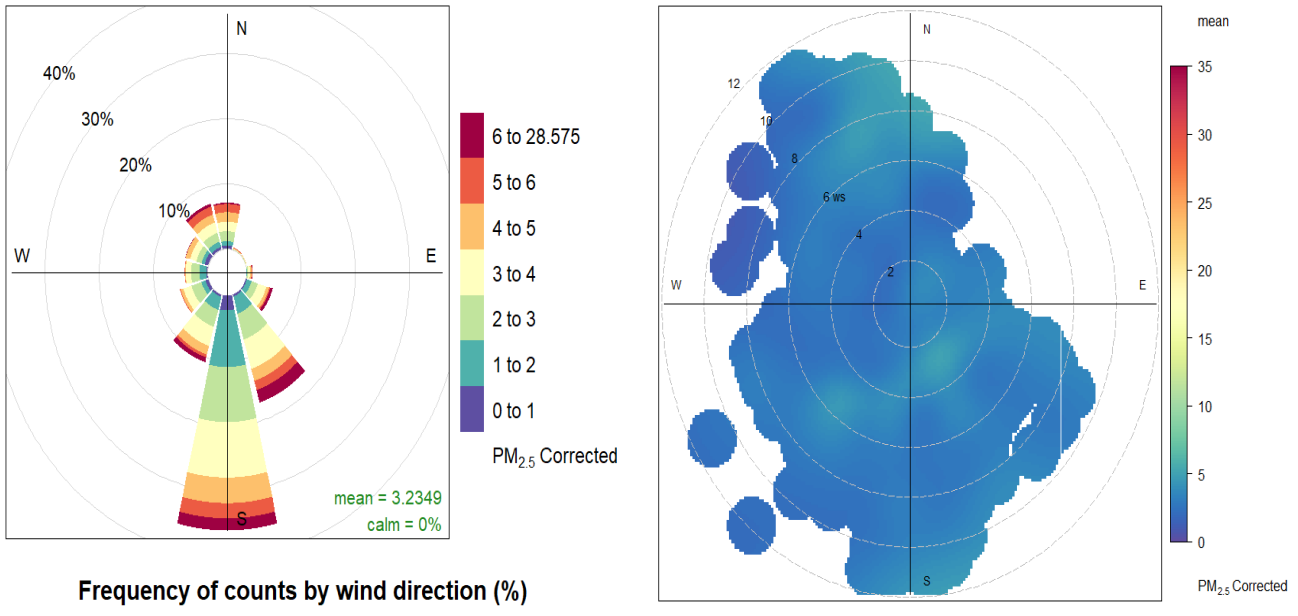

(a) (b)

Figure 43: Spring 2021 (September-November) at Blue Bay Lodge (a) $PM_{2.5}$ pollution rose and (b) polar plot

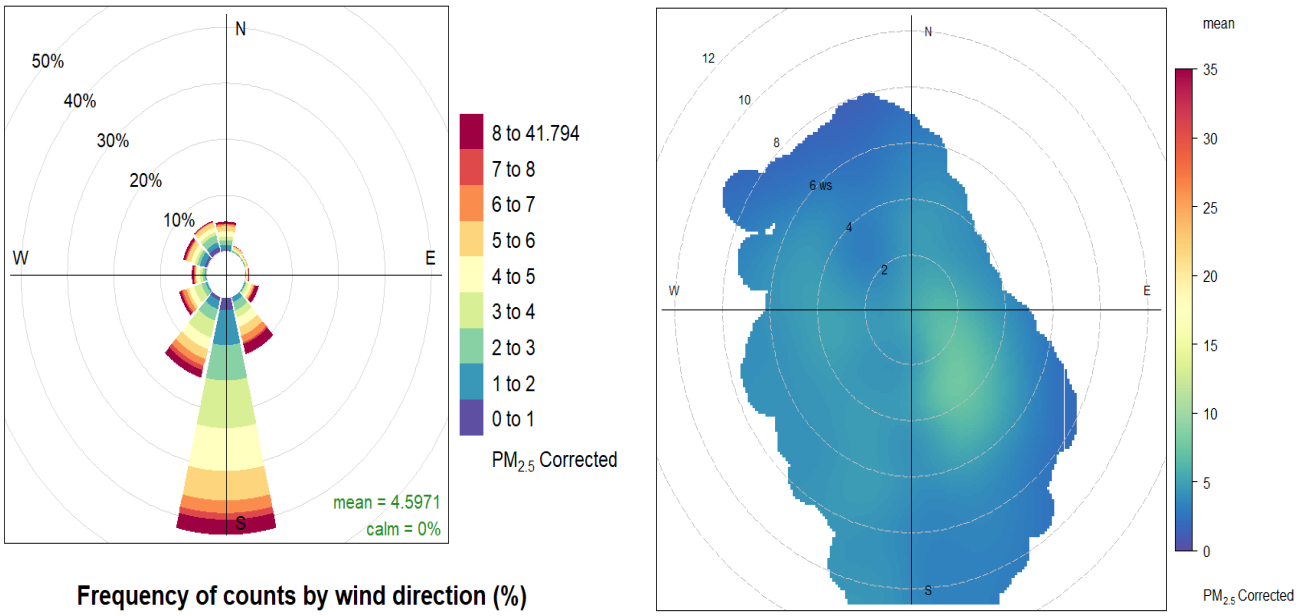

(a) (b)

Figure 44: Summer 2021/2022 (December-January) at Blue Bay Lodge (a) $PM_{2.5}$ pollution rose and (b) $PM_{2.5}$ polar plot

4.2.2. Saldanha AQM Station Results: PM as a Function of Wind Direction

At the Saldanha AQM station, it was found that during the entire sampling period (January-October), $PM_{2.5}$ emissions were experienced from all directions (Figure 45a). Emissions were experienced from the S (25%), SSE (17%), N (11%) and the NNW (10.5%). Of the 25% of emissions from the S, 10% was in the 2-4 µg/m^3 range and 6% in the 4-6 µg/m^3 range. $PM_{2.5}$ emissions between the ranges 12-46.1 µg/m^3 were also experienced from all directions. In the 12-46.1 µg/m^3 range, ~1.5% was associated with wind from the SSE and 1% from the S. From the polar plot (Figure 45b), it was found that the mean $PM_{2.5}$ concentrations were experienced between the wind speeds 0-14 m/s. It was also found that mean $PM_{2.5}$ concentrations between 0-5 µg/m^3 were experienced from all directions, with 5-110 µg/m^3 associated with wind from the N (0-2 m/s and 4-10 m/s) and NNE (4-10 m/s), ENE (0-6 m/s), ESE (0-4 m/s), S (0-4 m/s), SSE (0-4 m/s and 6-10 m/s), SSW (0-4 m/s) and W, WSW, WNW and NNW at 0-2 m/s.

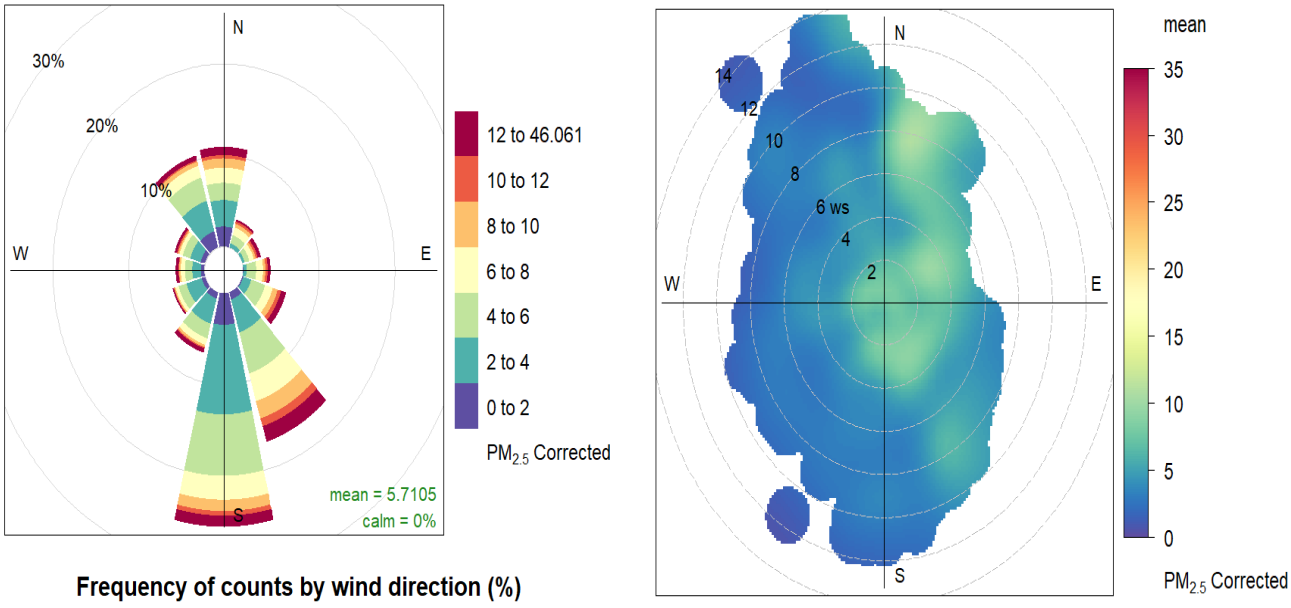

(a) (b)

Figure 45: The effect of wind direction and speed (m/s) on $PM_{2.5}$ concentrations (µg/m³) captured at the Saldanha AQM Station (February-October 2021) using (a) a pollution rose and (b) a polar plot

Seasonal Pollution Roses and Polar Plots at the Saldanha AQM Station

At the Saldanha AQM Station, the seasonal data available ranges from Summer 2021 until Spring 2021. During Summer, it was found that approximately 43% of the $PM_{2.5}$ emissions came from the SSE and 30% from the S (Figure 46). Emissions experienced in the 10-15.5 µg/m³ range were associated with wind from the SSE, S and the WSW. In the 10-15.5 µg/m³ range, ~9% was experienced when the wind was blowing from the SSE and 2% from the S. Unfortunately, the polar plot for Summer was unable to be plotted, due to insufficient data. During Autumn, $PM_{2.5}$ emissions were experienced from all directions at the Saldanha AQM Station (Figure 47a). Compared to the pollution rose for Summer (Figure 46), during Autumn, ~9.5% and ~7% of $PM_{2.5}$ emissions were experienced from the NNW and the N, respectively. ~35% of emissions were experienced from the S and 13% from the SSE. Emissions in the 10-42.5 µg/m³ range were experienced from all directions, except from the E, while at least 2% in the 10-42.5 µg/m³ range was experienced from the SSE. The polar plots indicates that $PM_{2.5}$ concentrations were experienced from all directions between 0-10.5 m/s (Figure 47b). From the plot, it can also be seen that majority of the $PM_{2.5}$ concentrations from most directions were between 0-5 µg/m³. However, in the ENE, ESE, SSE and SSW, the mean $PM_{2.5}$ concentrations are in the 5-10 µg/m³ range.

In Winter, the shift in wind direction is seen with ~14.5% and ~12% of $PM_{2.5}$ emissions associated with wind from the N and NNW, respectively (Figure 48a). However, ~17.5% and

~13.5% of the emissions were associated with wind from the SSE and the S, respectively. The largest range of $PM_{2.5}$ emissions (16-46.1 µg/m^3) was experienced at the Saldanha AQM Station from all directions. In this range, ~2% was from the N and the S, while 2.5% was associated with wind from the SSE. From the polar plot constructed for the Winter data at the Station, it was found that mean $PM_{2.5}$ concentrations in the 10-15 µg/m^3 range were associated with wind from the N/NNE (6-10 m/s), ENE (0-6 m/s), ESE, SSE and SSW (0-4 m/s), WSW, WNW and NNW (0-2 m/s) (Figure 48b). During Spring, there was still evidence of $PM_{2.5}$ emissions associated with wind from the N (10.5%) and the NNW (10%) (Figure 49a). ~28% of the $PM_{2.5}$ emissions were experienced when the wind was blowing from the S and 21% when the wind was blowing from the SSE. Emissions in the 7-17.9 µg/m^3 range was experienced from all directions, with at least 3% from the SSE. The polar plot show that $PM_{2.5}$ concentrations were experienced from all directions between 0-11 m/s (Figure 49b). Mean concentrations were experienced in the 5-10 µg/m^3 range from almost all directions, although at different wind speeds.

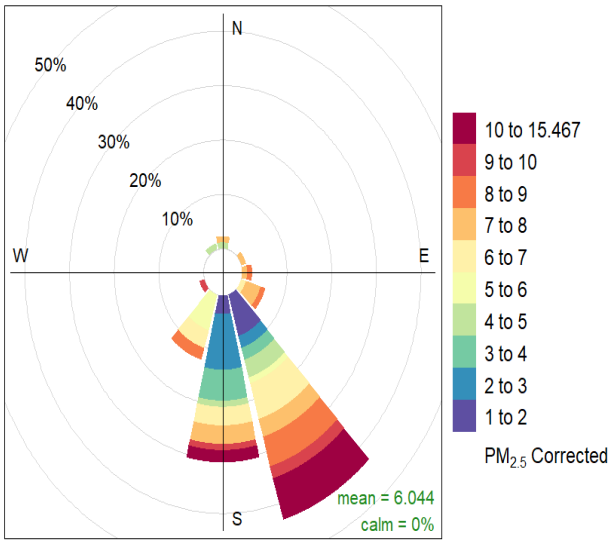

Figure 46: $PM_{2.5}$ pollution rose during Summer 2021 (January-February) at the Saldanha AQM Station

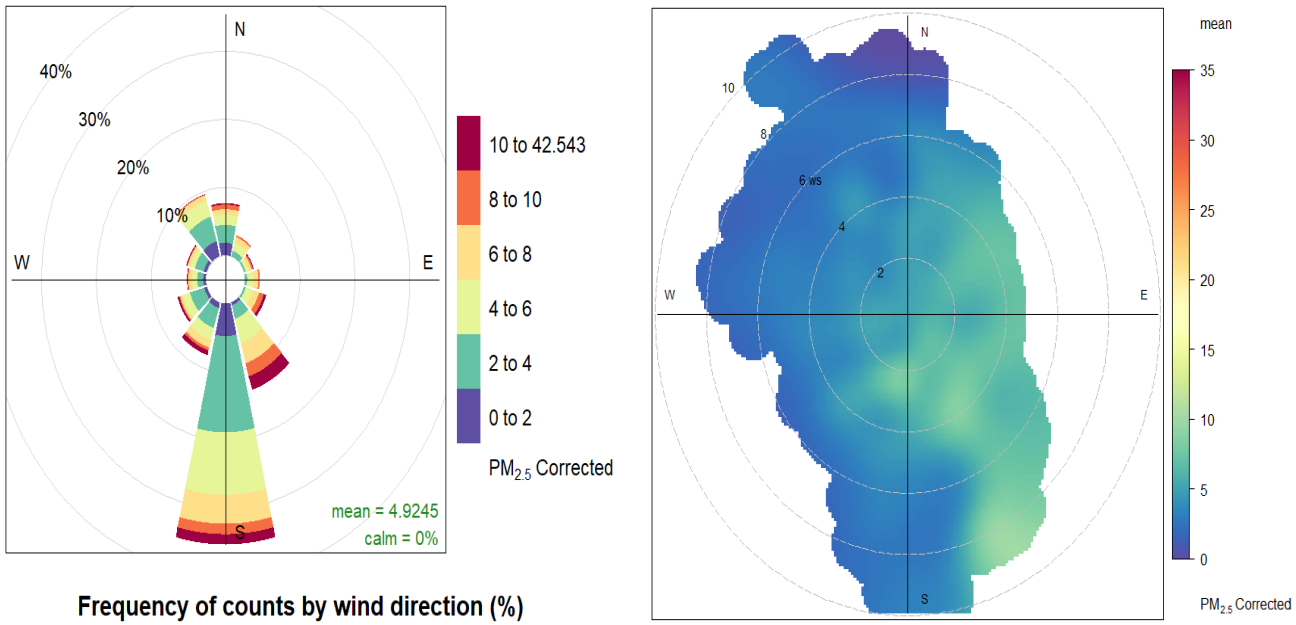

(a) (b)

Figure 47: Autumn 2021 (March-May) at the Saldanha AQM Station (a) $PM_{2.5}$ pollution rose and (b) $PM_{2.5}$ polar plot

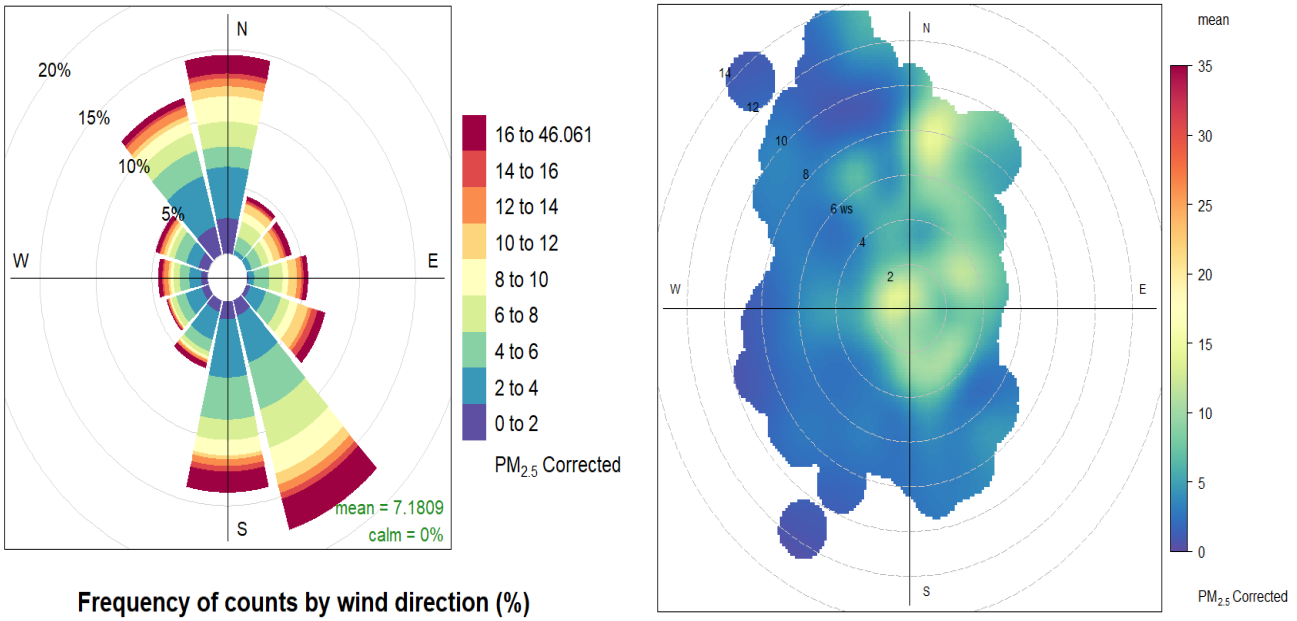

(a) (b)

Figure 48: Winter 2021 (June-August) at the Saldanha AQM Station (a) $PM_{2.5}$ pollution rose and (b) $PM_{2.5}$ polar plot

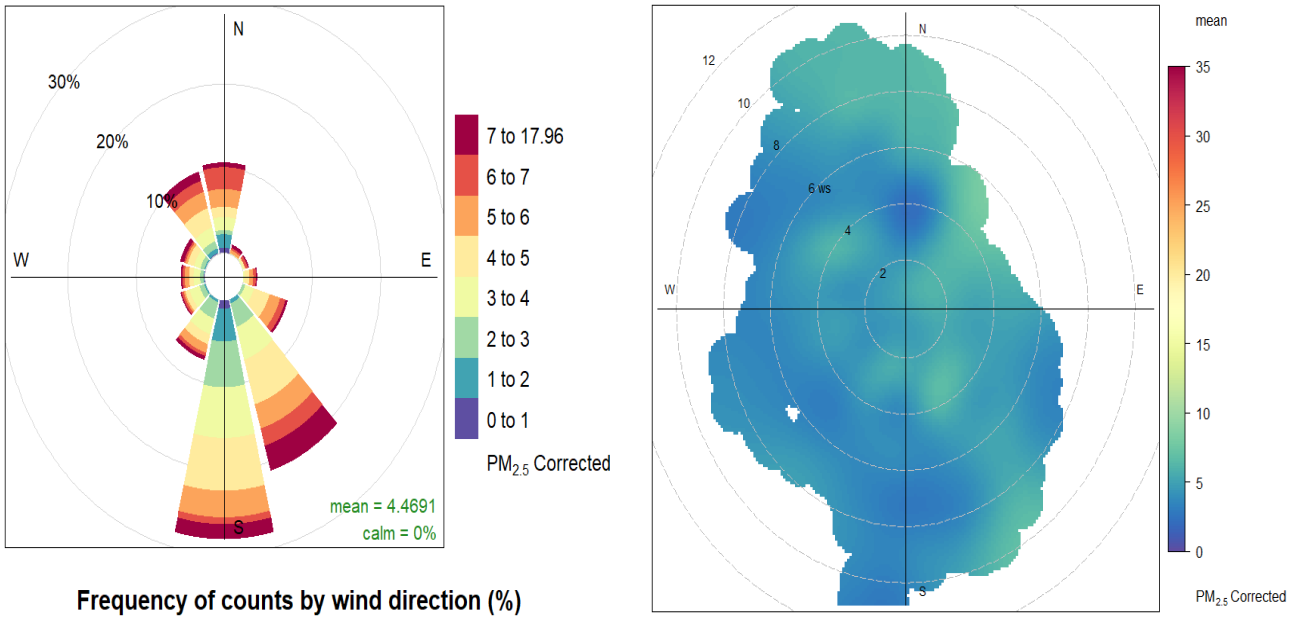

(a) (b)

Figure 49: Spring 2021 (September-October) at the Saldanha AQM Station (a) $PM_{2.5}$ pollution rose and (b) $PM_{2.5}$ polar plot

4.2.3. Louwville Private Home Results: PM as a Function of Wind Direction

At the Louwville Private Home, the PurpleAir Particulate Sensor was only installed from February until May, therefore, no Winter data was measured. Approximately 41% of $PM_{2.5}$ emissions were associated with wind from the S (Figure 50a). PM emissions were also associated with wind from the SSE (~15%), NNW (~8) and the N (7%). Emissions in the 9-40.7 µg/m^3 range were experienced from all directions except the west (W). The polar plot constructed for the Louwville Private Home, indicates that mean $PM_{2.5}$ concentrations in the 10-15 µg/m^3 range were experienced when the wind was blowing from the ENE (Figure 50b).

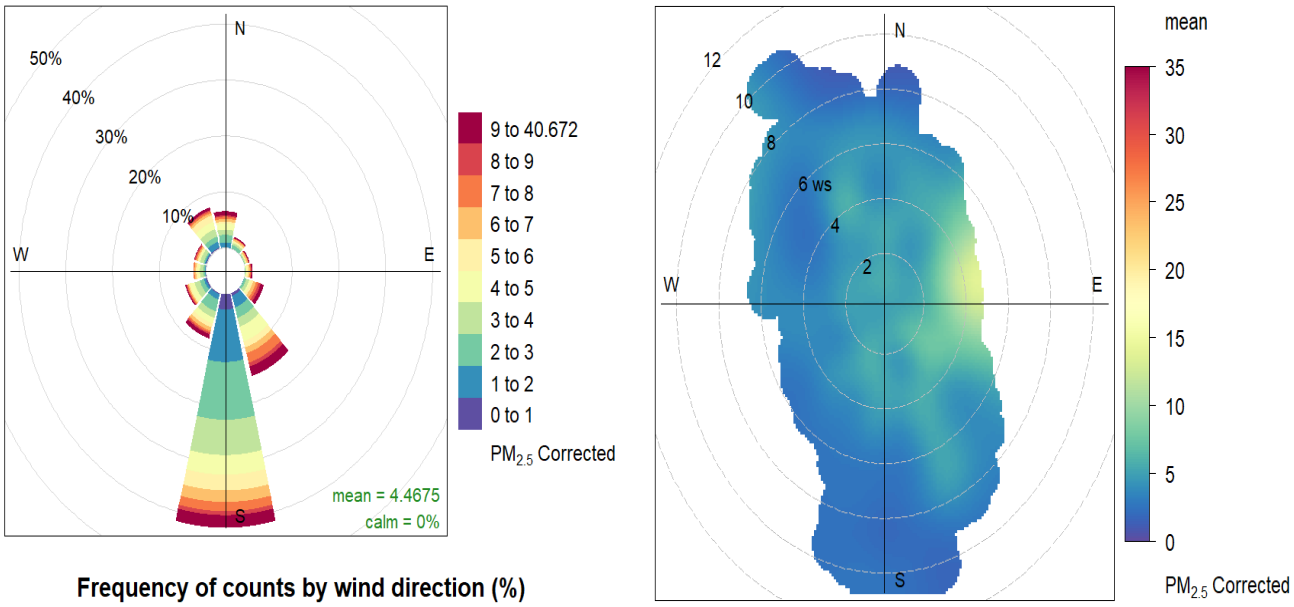

(a) (b)

Figure 50: The effect of wind direction and speed (m/s) on $PM_{2.5}$ concentrations (µg/m^3) captured at the Louwville Private Home (February-May 2021) using (a) a pollution rose and (b) a polar plot

Seasonal Pollution Roses and Polar Plots at the Louwville Private Home

Due to insufficient data during the month of January, a polar plot could not be constructed for Summer at the Louwville Private Home. However, the pollution rose indicates that approximately 55% of the $PM_{2.5}$ emissions were associated with wind from the S (Figure 51). From this 55%, ~23% of the emissions were between 1-2 µg/m^3, while ~14% were between 2-3 µg/m^3. ~21% of the emissions were also associated with wind from the NNW. Emissions in the 8-10.8 µg/m^3 range were experienced from the E, ESE, SSW and WSW. However, ~2.5% of the emissions from the SSW were in the 8-10.8 µg/m^3 range. During Autumn, the pollution rose indicated $PM_{2.5}$ emissions from the N (7%) and the NNW (8%) (Figure 52a). However, ~41% of the emissions were associated with wind from the S. Emissions were also associated with wind from the SSE (16%). Emissions in the 9-40.7 µg/m^3 range were experienced from all directions during Autumn, except from the W. The polar plot for Autumn shows that in the 10-15 µg/m^3 range, mean $PM_{2.5}$ concentrations were experienced when the wind was blowing from the ESE at wind speeds between 1-5 m/s (Figure 52b).

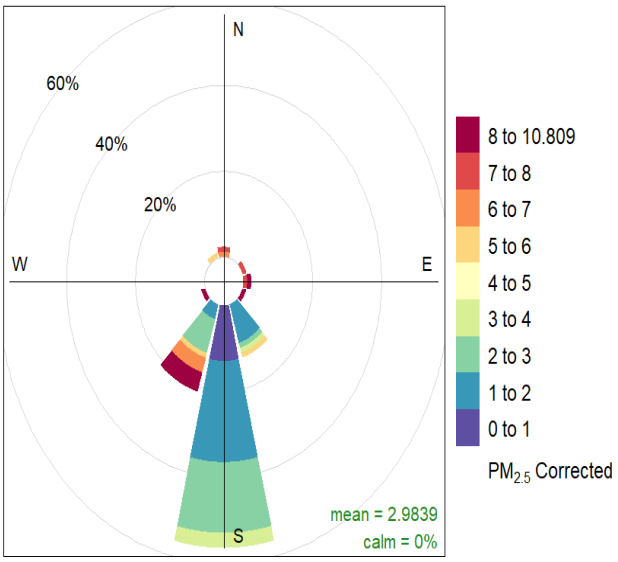

Figure 51: $PM_{2.5}$ pollution rose during Summer 2021 (February) at the Louwville Private Home

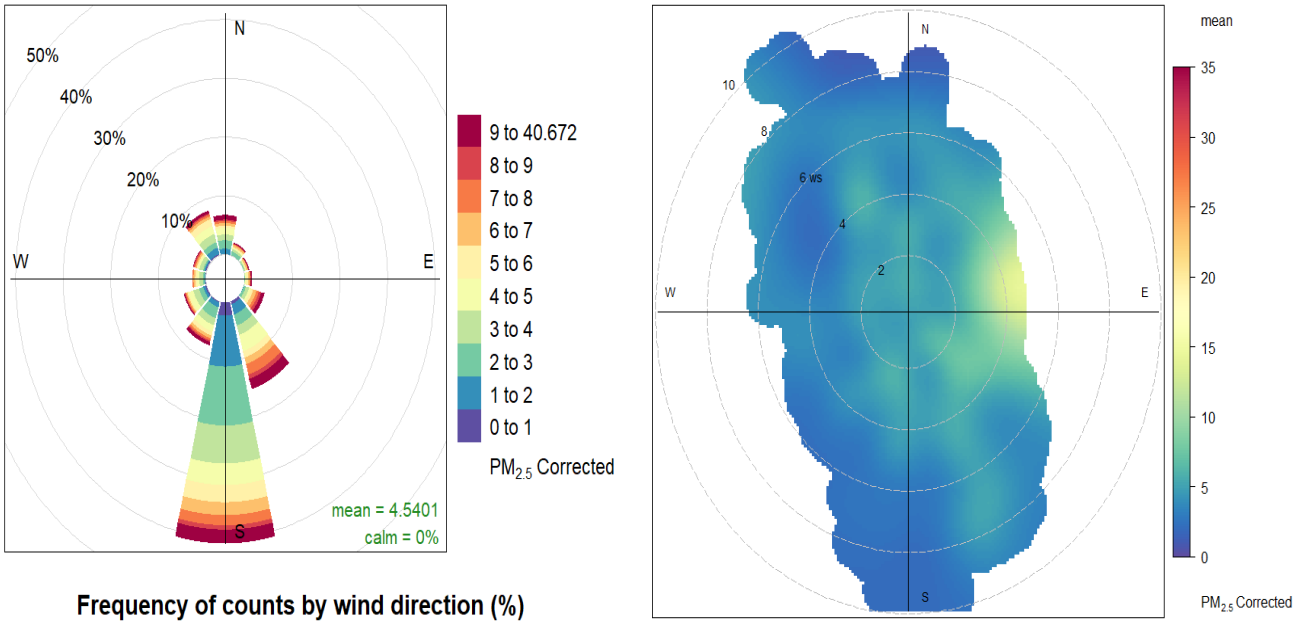

(a) (b)

Figure 52: Autumn 2021 (March-May) at the Louwville Private Home (a) $PM_{2.5}$ Pollution Rose and (b) $PM_{2.5}$ Polar Plot

4.2.4. St. Helena Bay Private Home Results: PM as a Function of Wind Direction

At the St. Helena Bay Private Home, the pollution rose presented, indicates that $PM_{2.5}$ emissions were experienced from all directions (Figure 53a). During the sampling period (March-August), ~26% of the emissions were associated with wind from the S, while ~14% was experienced when the wind was blowing from the SSE. Emissions were also experienced associated with wind from the N (~11%) and the NNW (10.5%). The largest range of emissions (8-61.8 µg/m^3) were experienced from all directions. However, ~3% of emissions in the 8-61.8 µg/m^3 were associated with wind from the N. The polar plot for the St. Helena Bay Private Home shows that mean $PM_{2.5}$ concentrations were experienced from all directions at wind speeds between 0-14 m/s (Figure 53b). Mean concentrations between 10-15 µg/m^3 were also experienced with wind blowing from the N/NNE between 6-10 m/s.

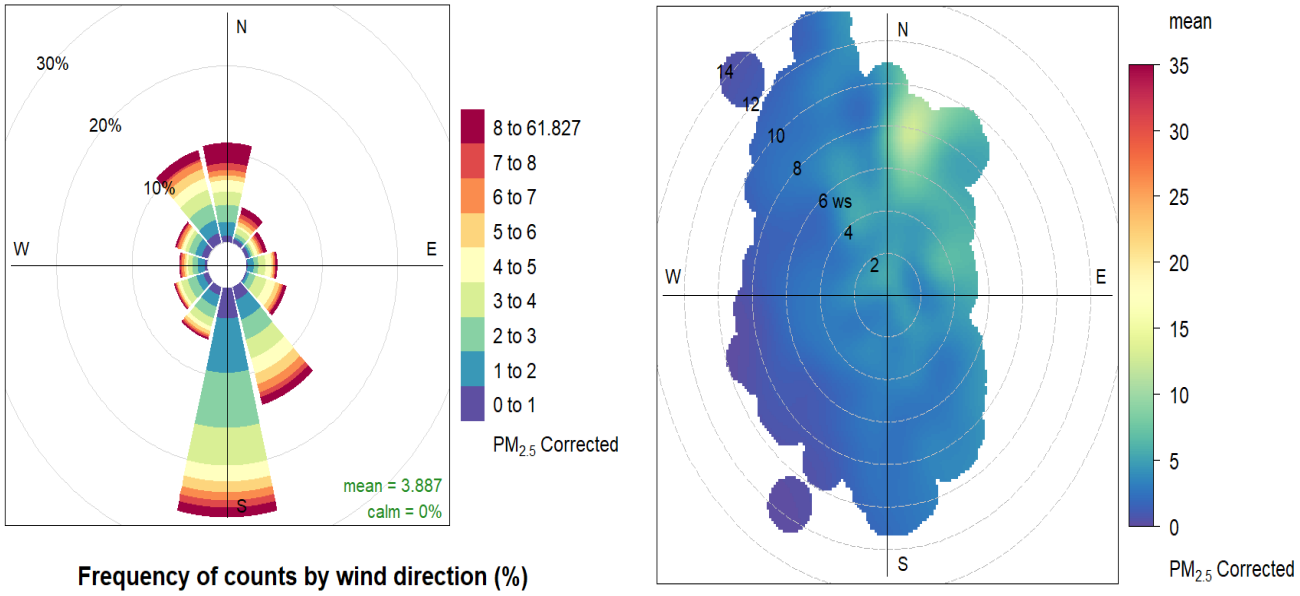

(a) (b)

Figure 53: The effect of wind direction and speed (m/s) on $PM_{2.5}$ Concentrations (µg/m^3) captured at the St. Helena Bay Private Home (March-August 2021) using (a) a pollution rose and (b) a polar plot

<u>Seasonal Pollution Roses and Polar Plots at the St. Helena Bay Private Home</u>

During Autumn (March-May) at the St. Helena Bay Private Home, ~36% of the $PM_{2.5}$ emissions were associated with wind from the S, ~14% from the SSE, ~9% from the NNW and ~7% from the N (Figure 54a). From the ~36% from the S, ~10% of these emissions were in the 1-2 µg/m^3 range and ~7% in the 2-3 µg/m^3 range. $PM_{2.5}$ emissions in the largest range (7-61.8 µg/m^3) were experienced from all directions, with ~2% in this range from the S. Mean $PM_{2.5}$ concentrations were experienced from all directions between wind speeds of 0-10.5 m/s (Figure 54b). Mean concentrations between 5-10 µg/m^3 were experienced from the ENE (4-5

m/s) and the NNW (4-5 m/s). During Winter, the shift in wind direction is presented by the pollution rose in Figure 55a. $PM_{2.5}$ emissions were associated with wind from the N (~17%), SSE (~14.5%), S (~12.5%) and the NNW (~13.5%). Emissions in the largest range (10-34.1 µg/m^3) was experienced from all directions, except from the WSW. However, in this range (10-34.1 µg/m^3), the emissions were associated with wind from the N (~3%) and NNW (~2%). The polar plot for Winter at St. Helena Bay indicates that $PM_{2.5}$ concentrations (15-20 µg/m^3) are experienced with wind blowing from the N/NNE (Figure 55b).

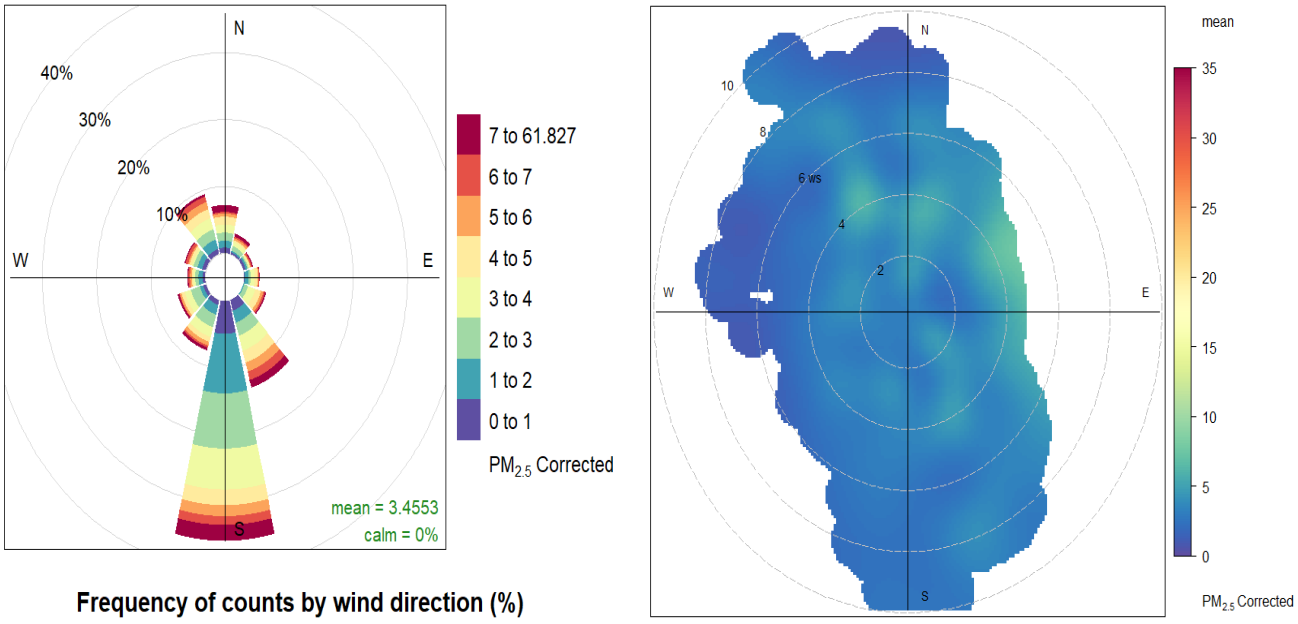

(a) (b)

Figure 54: Autumn 2021 (March-May) at the St. Helena Bay Private Home (a) $PM_{2.5}$ pollution rose and (b) $PM_{2.5}$ polar plot

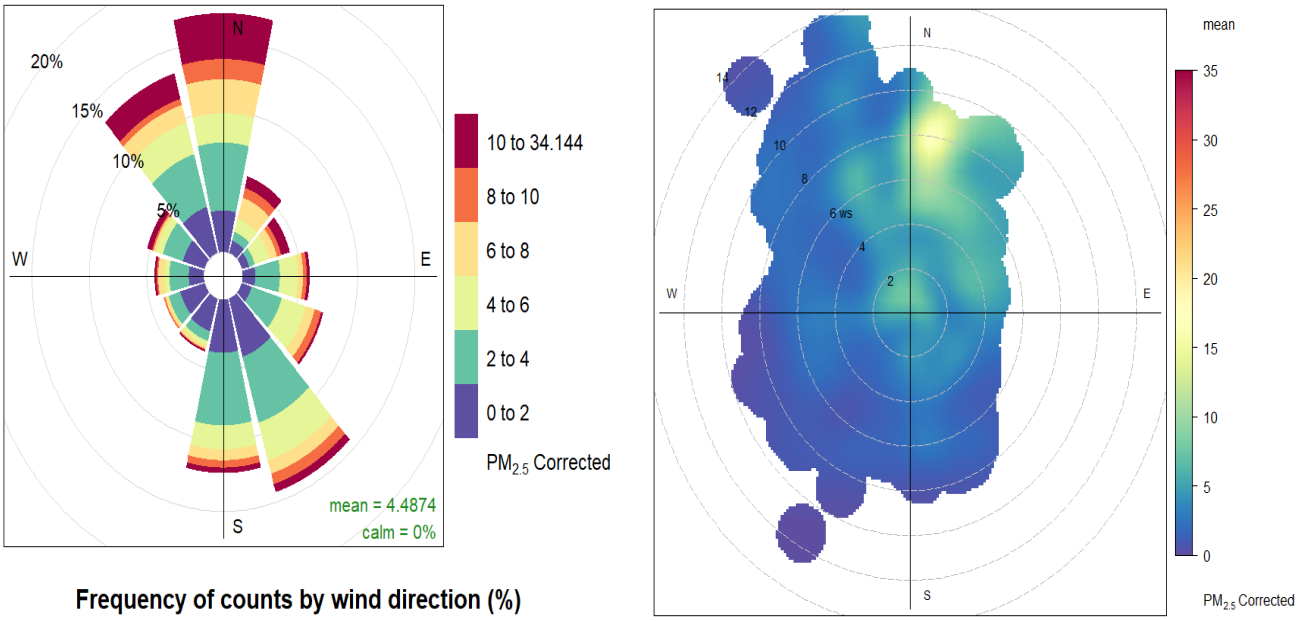

(a) (b)

Figure 55: Winter 2021 (June-August) at the St. Helena Bay Private Home (a) $PM_{2.5}$ pollution rose and (b) $PM_{2.5}$ polar plot

4.2.5. West Coast Mall Results: PM as a Function of Wind Direction

During the sampling period at the West Coast Mall (January-April), ~32% of $PM_{2.5}$ emissions were associated with wind from the S (Figure 56a). ~11% and ~7% of the emissions were associated with wind from the SSW and the SSE, respectively. Furthermore, ~2% of the emissions in the largest range (4.5-23.1 µg/m^3) were experienced when the wind was blowing from the SSE. The polar plot for the West Coast Mall indicates that mean $PM_{2.5}$ Concentrations were experienced from all directions between 0-5 µg/m^3 and at wind speeds of 0-12 m/s (Figure 56b).

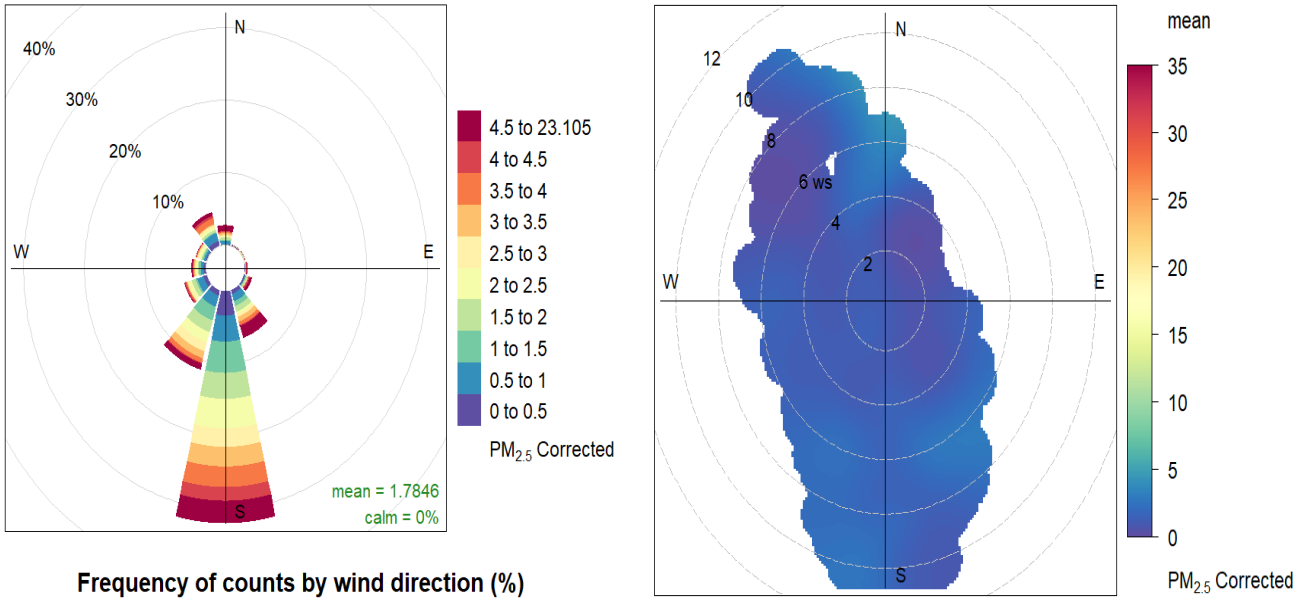

(a) (b)

Figure 56: The effect of wind direction and speed (m/s) on $PM_{2.5}$ concentrations ($\mu g/m^3$) captured at the West Coast Mall (January-April 2021) using (a) a pollution rose and (b) a polar plot

Seasonal Pollution Roses and Polar Plots at the West Coast Mall

During Summer at the West Coast Mall, ~52%, ~18% and ~10% of $PM_{2.5}$ emissions were associated with wind from the S, SSW and SSE, respectively (Figure 57a). In the largest range (6-23.1 $\mu g/m^3$), $PM_{2.5}$ emissions were experienced with wind blowing from the N, E, ESE, SSE, S, SSW and WSW. Furthermore, ~2% and ~1.5% in this range (6-23.1 $\mu g/m^3$) were associated with wind from the SSE and the S. The polar plot for the West Coast Mall in Summer indicates mean $PM_{2.5}$ concentrations between 10-15 $\mu g/m^3$ at wind speeds between 4-8 m/s from the SSE (Figure 57b). Mean concentrations between 5-10 $\mu g/m^3$ between 4-8 m/s were also present, associated with wind from the N. Compared to Summer (Figure 57a), the pollution rose for Autumn indicates the shift in wind direction, where PM emissions were also associated with wind from the N (Figure 58a). $PM_{2.5}$ emissions were associated with wind from the S (~17%), SSW (~5.5%), SSE (~4%), NNW (~7.5%) and the N (~4.5%). Emissions in the largest range (3.5-18.4 $\mu g/m^3$) were experienced from all directions, except from the ENE and the E. Furthermore, emissions in the 3.5-18.4 $\mu g/m^3$ range were experienced from the N (~2%), NNW (~3.5%) and the S (~2%). The polar plot for Autumn indicates that mean $PM_{2.5}$ concentrations were experienced between 0-5 $\mu g/m^3$ at wind speeds between 0-10.5 m/s (Figure 58b).

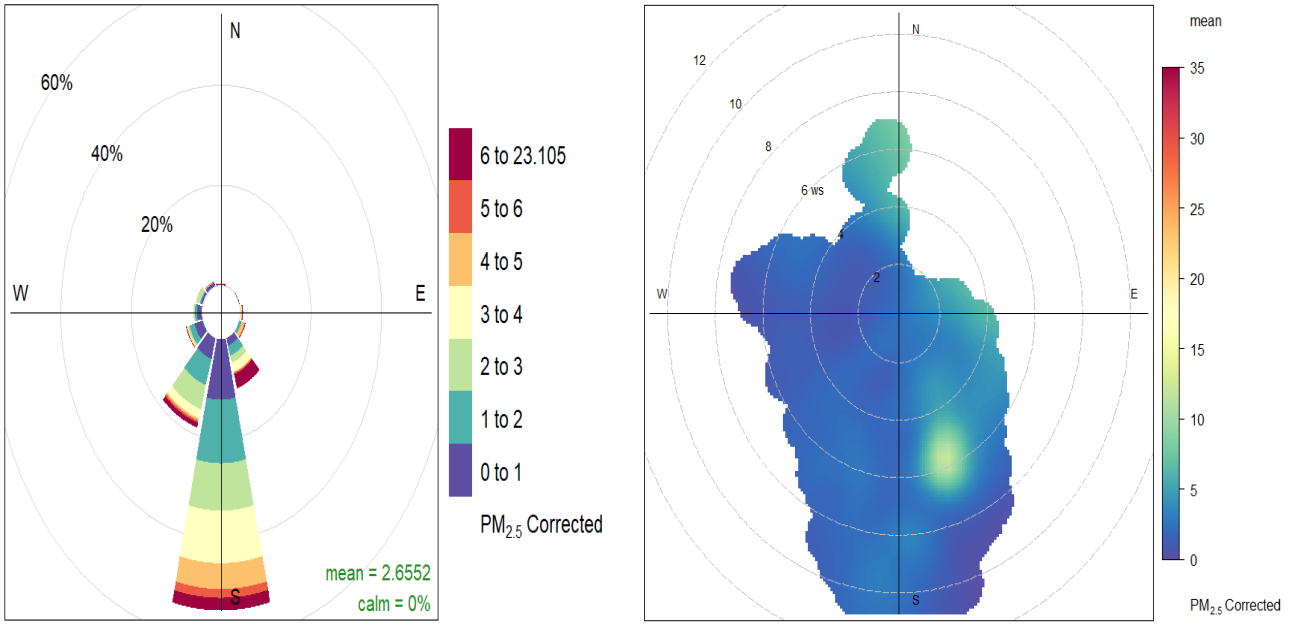

(a) (b)

Figure 57: Summer 2021 (January-February) at the West Coast Mall (a) $PM_{2.5}$ pollution rose and (b) $PM_{2.5}$ polar plot

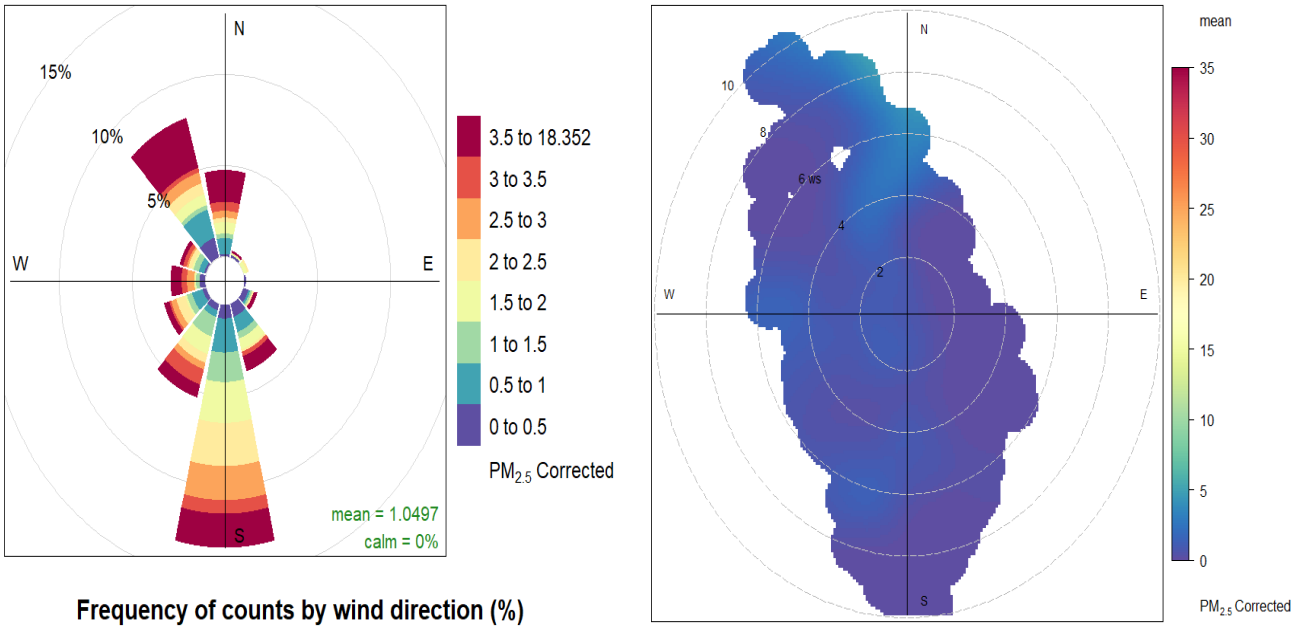

(a) (b)

Figure 58: Autumn 2021 (March-April) at the West Coast Mall (a) $PM_{2.5}$ pollution rose and (b) $PM_{2.5}$ polar plot

4.2.6. Langebaan Private Home Results: PM as a Function of Wind Direction

At the Langebaan Private Home, ~26%, ~15% and ~11% of $PM_{2.5}$ emissions were associated with wind from the S, SSE, N and NNW, respectively (Figure 59a). Of the ~26% from the S, ~8% of the emissions were each in the 0-2 µg/m^3 and the 2-4 µg/m^3 range. Furthermore, emissions in the largest range (12-45.6 µg/m^3), were experienced from all directions. From the polar plot, mean $PM_{2.5}$ concentrations were experienced in the 0-5 µg/m^3 range from all directions (Figure 59b). However, concentrations between 10-15 µg/m^3 were also experienced from the N/NNE (6-10 m/s), W (4-6 m/s), and ESE (2-4 m/s).

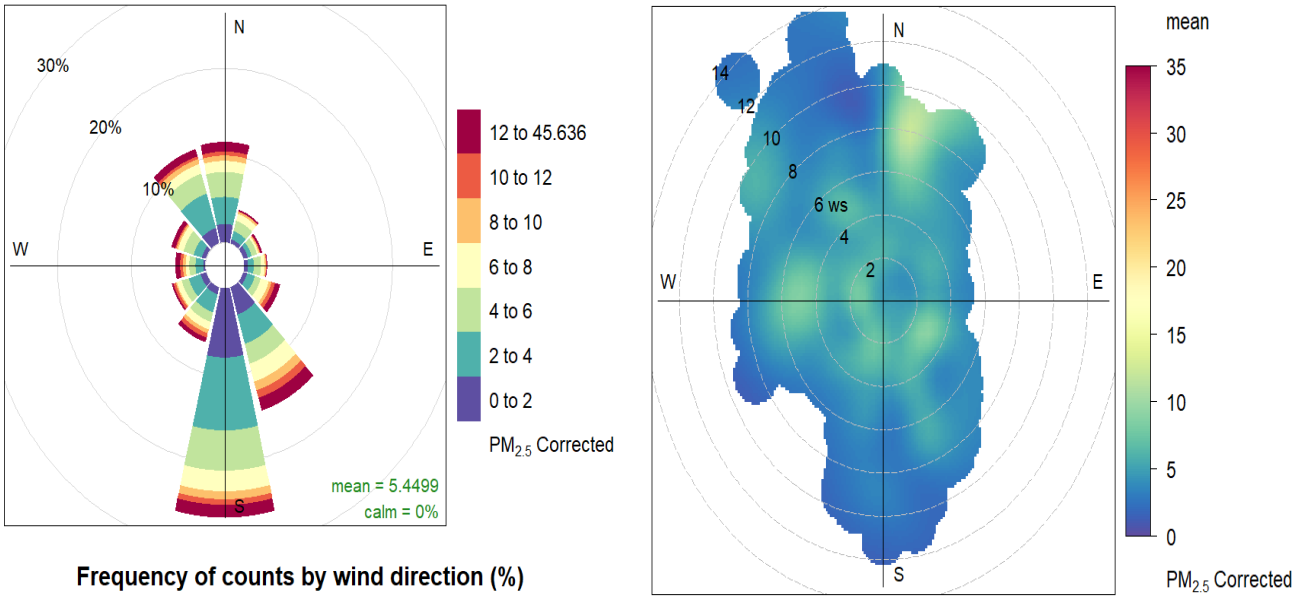

(a) (b)

Figure 59: The effect of wind direction and speed (m/s) on $PM_{2.5}$ concentrations (µg/m^3) captured at the Langebaan Private Home (February-July 2021) using (a) a pollution rose and (b) a polar plot

<u>Seasonal Pollution Roses and Polar Plots at the Langebaan Private Home</u>

Due to insufficient data, only the pollution rose for Summer was constructed at the Langebaan Private Home. The pollution rose shows that ~48% of $PM_{2.5}$ emissions were associated with wind from the S (Figure 60). Almost 30% and ~12% of emissions were also associated with wind from the SSE and the SSW. The largest range of $PM_{2.5}$ emissions in Summer (14-29.9 µg/m^3), was only experienced when the wind was blowing from the SSE and the S. Furthermore, ~9% of this range was associated with wind from the SSE. During Autumn, the shift in wind direction is confirmed by the N and NNW wind component on Figure 61a. $PM_{2.5}$ emissions were associated with wind from the S (~32%), SSE (~13.5%), NNW (~10%), and the N (~8%). The largest range of $PM_{2.5}$ emissions (9-45.6 µg/m^3) were experienced from all directions, except for ENE and E. The polar plot for Autumn indicates that mean $PM_{2.5}$

concentrations between 0-5 µg/m^3 were experienced from all directions (Figure 61b). However, concentrations between 5-10 µg/m^3 were also experienced with wind from the NNE (2-6 m/s), ESE (3.5-4.5 m/s), SSE (2-8 m/s) and SSW (2-4 m/s). During Winter, it was found that 20% of the $PM_{2.5}$ emissions were associated with wind from the N, 15% from the NNW and the SSE and ~9.5% from the S (Figure 62a). Furthermore, the largest range of emissions (20-42.9 µg/m^3) were experienced at the Home, from all directions, except the E and the WSW. In this range (20-42.9 µg/m^3), ~2% of the $PM_{2.5}$ emissions were from the N. With regards to the polar plot, it was found that the mean $PM_{2.5}$ concentrations in the 15-20 µg/m^3 range were associated with wind from the N/NNE (6-10 m/s) and the W (0-2 m/s) (Figure 62b).

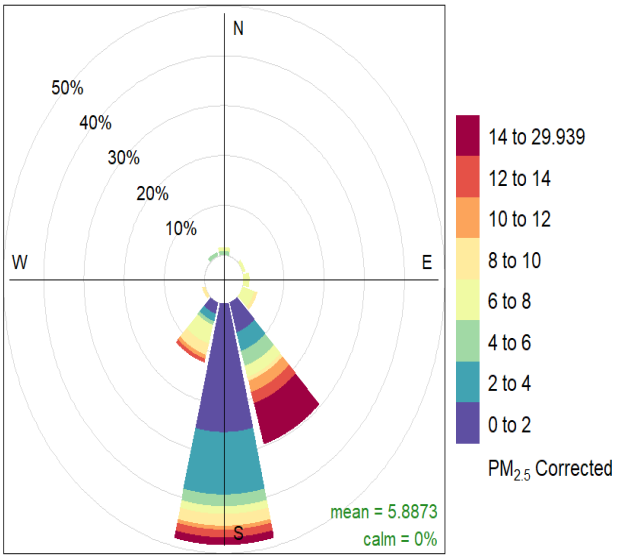

(a)

Figure 60: $PM_{2.5}$ pollution rose during Summer 2021 (February) at the Langebaan Private Home

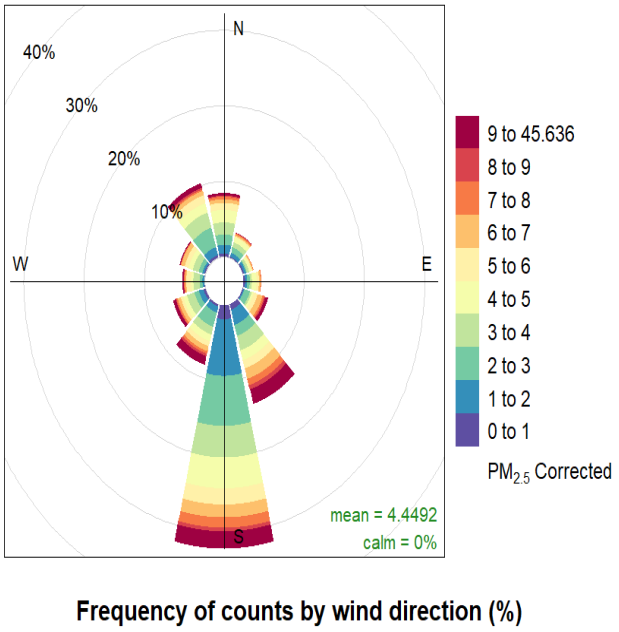

(a)

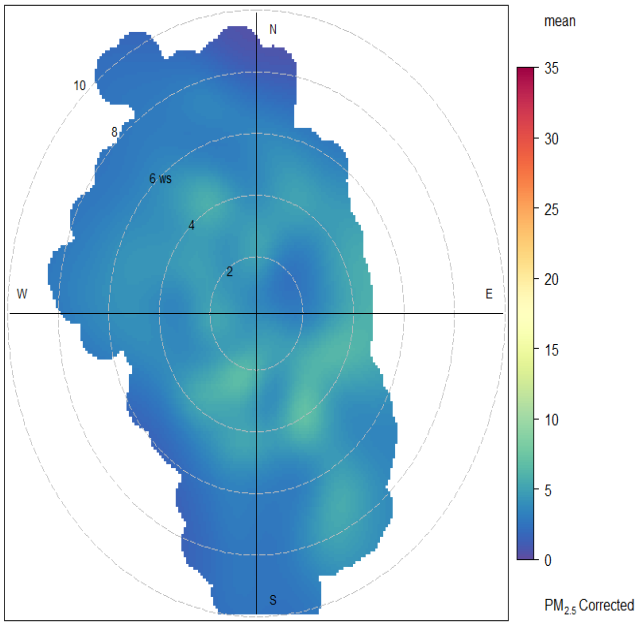

(b)

Figure 61: Autumn 2021 (March-May) at the Langebaan Private Home (a) $PM_{2.5}$ pollution rose and (b) $PM_{2.5}$ polar plot

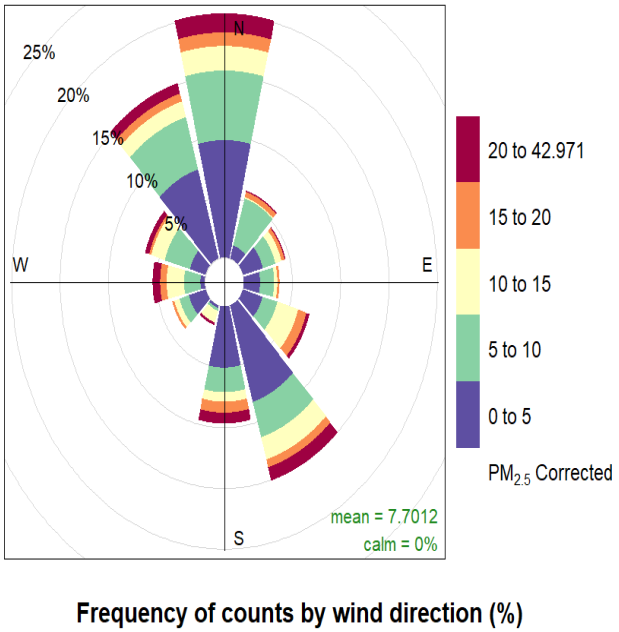

(a)

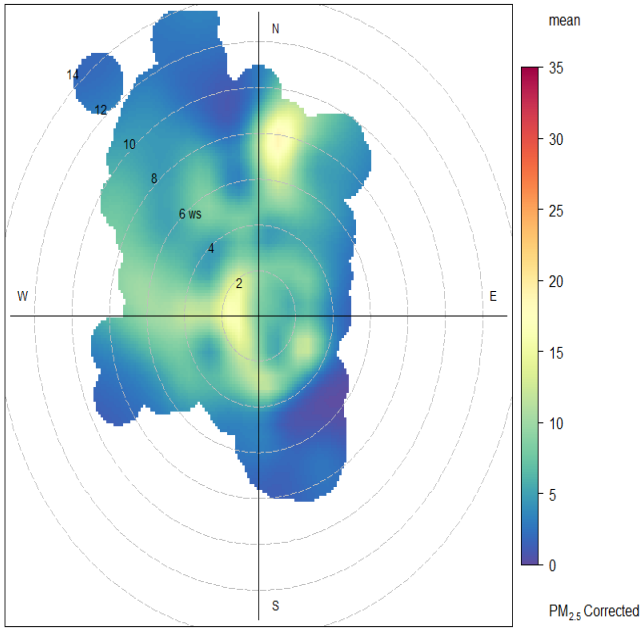

(b)

Figure 62: Winter 2021 (June-July) at the Langebaan Private Home (a) $PM_{2.5}$ pollution rose and (b) $PM_{2.5}$ polar plot

4.2.7. Vredenburg AQM Station Results: PM as a Function of Wind Direction

At the Vredenburg AQM Station, the PurpleAir Particulate Sensor measured PM from February until June. From the pollution rose, it was found that ~17% of the $PM_{2.5}$ emissions were associated with wind from the S, ~10.5% from the SSE, ~9% from the N and ~7% from the NNW (Figure 63a). $PM_{2.5}$ emissions in the 8-35.0 µg/m^3 range was experienced at the Station from all directions. This range (8-35.0 µg/m^3) made up at least 1.5% from the N, S and the SSE and ~2% from the NNW. The polar plot indicates that mean $PM_{2.5}$ concentrations were experienced between 0-5 µg/m^3 at wind speeds between 0-14 m/s (Figure 63b). However, mean concentrations between 5-10 µg/m^3 were associated with wind from the N/NNE between 8-10 m/s.

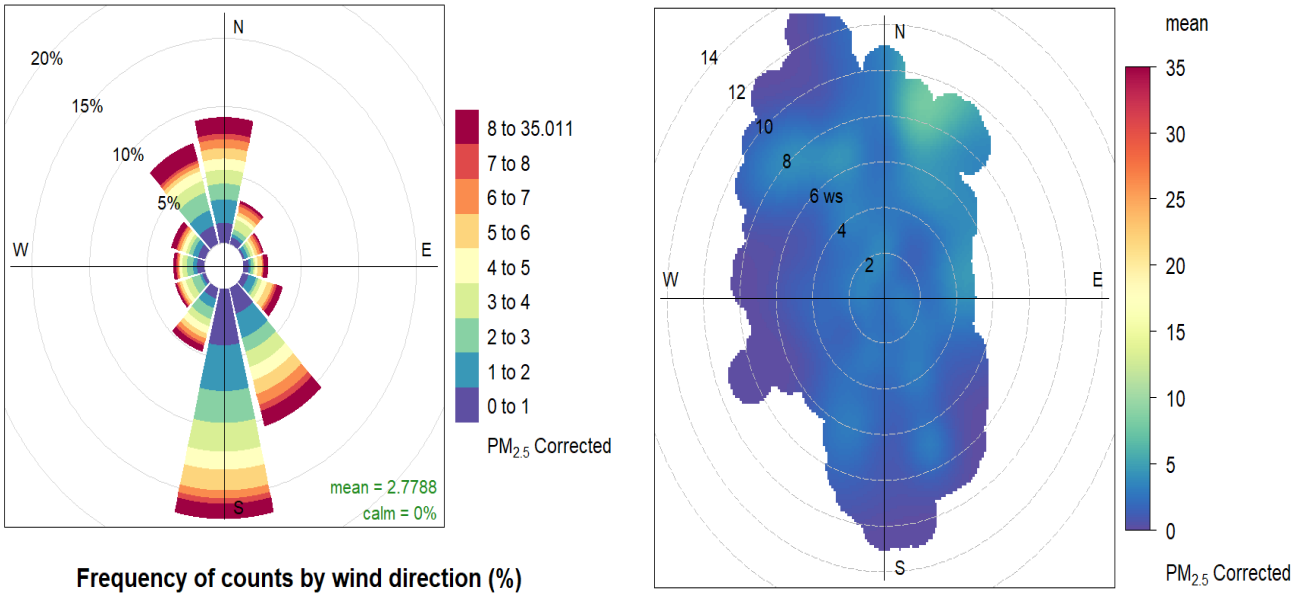

(a) (b)

Figure 63: The effect of wind direction and speed (m/s) on $PM_{2.5}$ Concentrations (µg/m^3) captured at the Vredenburg AQM Station (February-June 2021) using (a) a pollution rose and (b) a polar plot

<u>Seasonal Pollution Roses and Polar Plots at the Vredenburg AQM Station</u>

Due to insufficient information during Summer at the Vredenburg AQM Station, only the pollution rose was constructed (Figure 64). ~44% of the $PM_{2.5}$ emissions were associated with wind from the SSE, with ~20.5% from the S and ~16.5% from the SSW. From the largest range of $PM_{2.5}$ emissions (16-22.4 µg/m^3), it was found that emissions in this range were associated with wind only from the S and the SSE. Furthermore, ~8% of emissions in the 16-22.4 µg/m^3 range were experienced with wind blowing from the SSE. Although a shift in wind direction indicated by the N and NNW wind component present in Figure 65a during Autumn, 20% of the $PM_{2.5}$ emissions were associated with wind from the S, ~8.5% from the SSE, ~7%

from the NNW and ~6% from the N. $PM_{2.5}$ emissions in the largest range (6-22.4 µg/m^3) were experienced from all directions. The polar plot shows that mean $PM_{2.5}$ concentrations between 0-5 µg/m^3 were experienced from all direction at wind speeds between 0-10.5 m/s (Figure 65b). During Winter, ~19% of the $PM_{2.5}$ emissions were associated with wind from the N (Figure 66a). ~10.5% and ~12.5% of the emissions were also associated with wind from the NNW and the SSE, respectively. The largest range of $PM_{2.5}$ emissions (12-35.0 µg/m^3) at the Station were experienced from all directions, except for the ENE, SSW and WSW. Furthermore, in this range (12-35.0 µg/m^3), ~5% of the emissions were associated with wind from the NNW. The polar plot shows that mean concentrations between 10-15 µg/m^3 were experienced with wind from the N/NNE (6-10 m/s), NNW and WSW (0-2 m/s and 6-8 m/s) (Figure 66b).

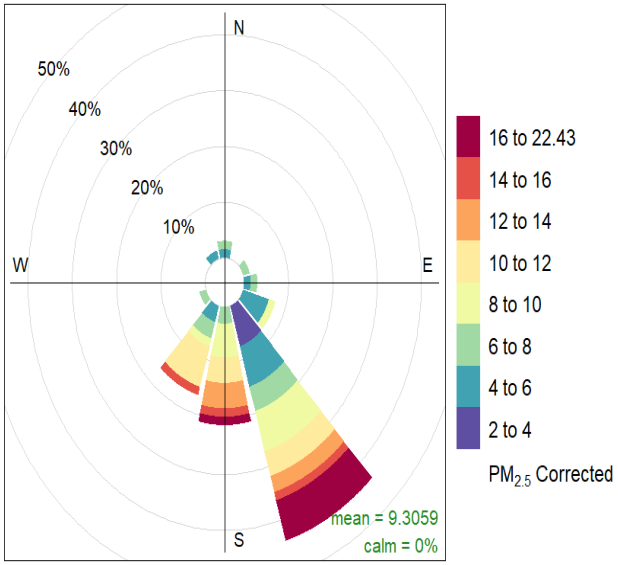

Frequency of counts by wind direction (%)

(a)

Figure 64: $PM_{2.5}$ pollution rose during Summer 2021 (February) at the Vredenburg AQM Station

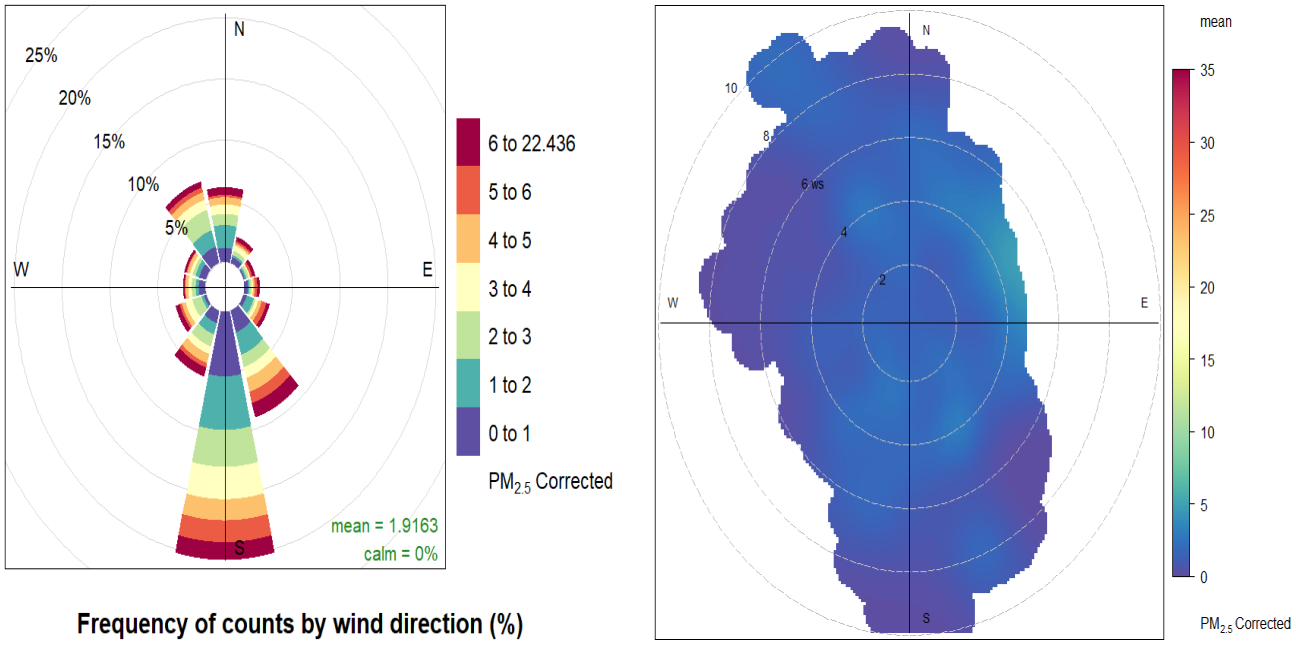

(a) (b)

Figure 65: Autumn 2021 (March-May) at the Vredenburg AQM Station (a) $PM_{2.5}$ pollution rose and (b) $PM_{2.5}$ polar plot

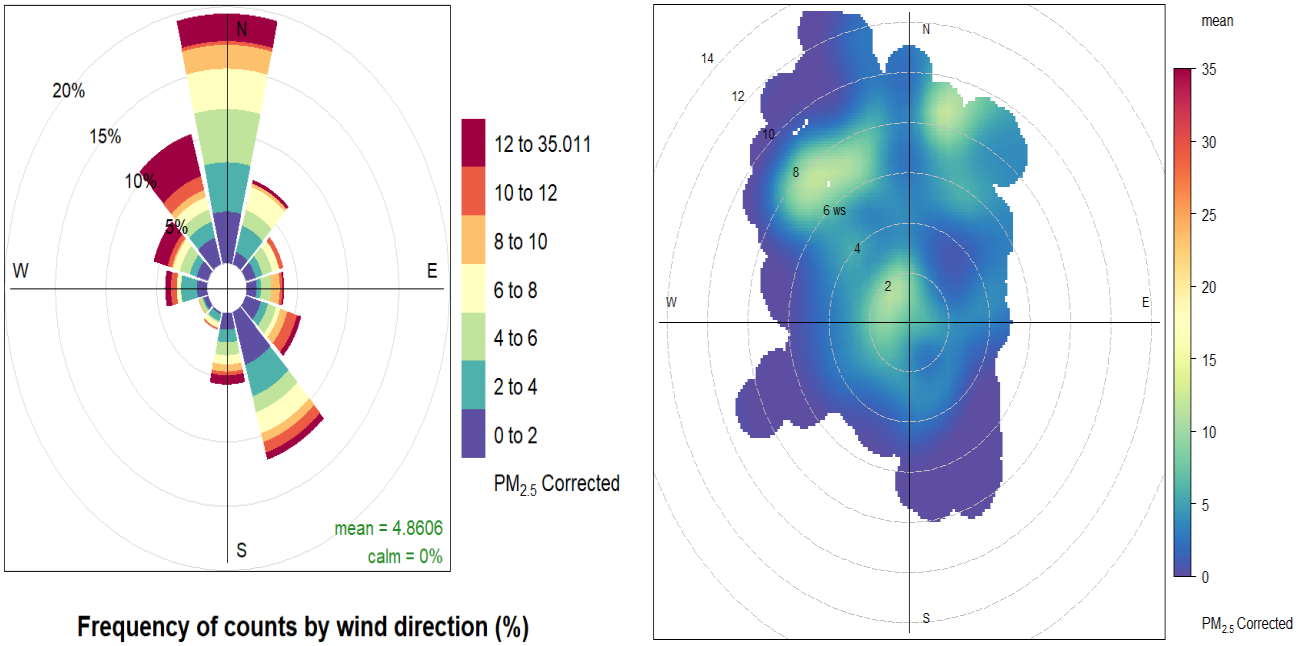

(a) (b)

Figure 66: Winter 2021 (June) at the Vredenburg AQM Station (a) $PM_{2.5}$ pollution rose and (b) $PM_{2.5}$ polar plot

4.3. Results from Physical Samples: Dust Composition: Outcomes of Phase 3b

4.3.1. Results of the PM Sample from the Dust Fallout Bucket: Blue Bay Lodge

Dust fallout Buckets were installed at Blue Bay Lodge from the 25th of February 2021 until the 5th of August 2021. A total of four dust fallout buckets were installed during this sampling period. The acceptable dust fall rate (D) is stipulated in Table 4 as D < 600 mg/m^2/day for residential areas and 600 < D < 1200 mg/m^2/day for non-residential areas. The dust fall rate that was calculated for each sample from the dust fallout buckets were all higher than the acceptable dust fallout standards (Table 25). However, according to South African Legislation, the dust fall rates are calculated based on a 30-day averages. Due to logistical as well as COVID19 restrictions, sometimes the dust fallout bucket was installed for longer or shorter periods of time. Therefore, the dust fall rate for each dust fallout bucket was normalised over a 30-day average (Table 25). A sample calculation of the dust fall rate is indicated in Section 3.3.2.

Table 25: The Net Mass and Dust Fall Rate (D) of samples collected from the Dust Fallout Bucket installed at Blue Bay Lodge

	Dust Fallout Bucket 1	Dust Fallout Bucket 2	Dust Fallout Bucket 3	Dust Fallout Bucket 4
Sampling Period (days)	27	78	32	28
Net Mass (g)	1.7	7.6	8.4	1.9
Dust fall Rate (D) (mg/m^2/day)	3 427	5 521	14 772	3 931
Normalised Dust fall Rate over a 30-day sampling period (mg/m^2/day)	3 808	2 123	13 849	4 211

The samples collected from dust fallout buckets were combined into one sample. The total mass of the combined sample was 19.6 g. As previously mentioned in Section 3.2.5.1, the sample was separated into dust and salt fractions to separate out the dust from the salt content in the sample. X-ray Diffraction (XRD) was used to analyse the dust fraction, while the salt fraction was analysed during X-ray Fluorescence (XRF). The samples were centrifuged twice to ensure that most of the salt was separated from the dust fraction.

4.3.1.1. The Dust Fraction

The total sample of dust that was obtained post-centrifugation was 0.23 g. Quantitative XRD was used to find the mass % of the minerals in the dust fraction (Figure 67). The results from the XRD analysis indicate that the dust sample consisted of six minerals: quartz (SiO_2 at

37.3%), calcite ($CaCO_3$ at 29.1%), hematite (Fe_2O_3 at 21.2%), biotite ($K(MgFe)_3AlSi_3O_{10}(OH)_2$ at 8.9%) and halite (NaCl at 3.6%) (Figure 67). The graph obtained from XRD analysis can be found in Appendix E.

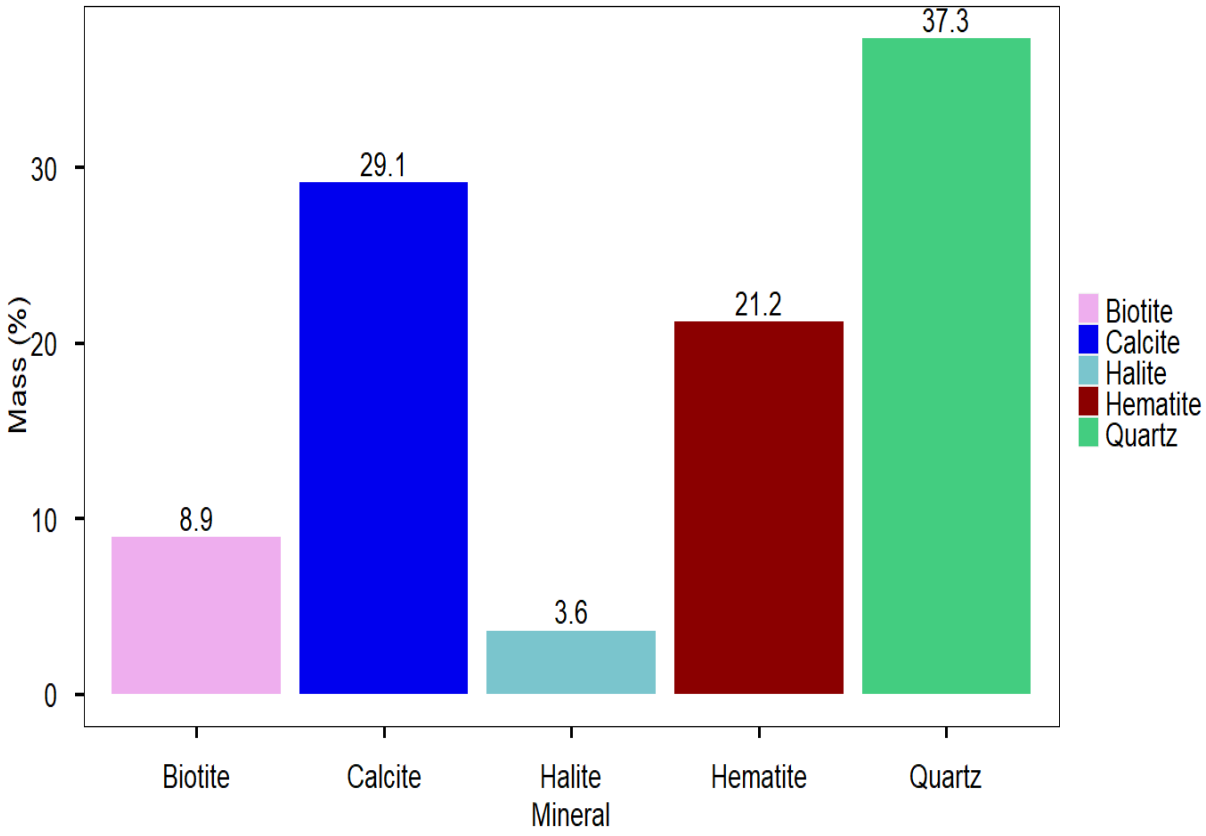

Figure 67: XRD Dust Sub-Sample Results from the Dust Fallout Bucket Samples Collected at Blue Bay Lodge

4.3.1.2. The Salt Fraction

The total amount of salt that was obtained post-centrifugation was 19.3 g. The salt sample was subjected to XRF analysis and the results from this analysis provided major, minor and trace elements and are listed along with their respective mass % and concentrations (Table 26). In this study, major elements are classified as those with a wt% greater than 0.1%. Minor elements are classified as those less than 0.1 wt%, but greater than 100 ppm. Trace elements are classified as those less than 100 ppm.

The element found most abundant in the major elements in the salt sample was chlorine (Cl) with a concentration of 37.5 wt% and the second most abundant major element was found to be sodium (Na) at 35.0 wt% (Table 26). The ideal wt% of sodium and chlorine are 39.3 wt% and 60.7 wt %, respectively. The value obtained for sodium is in the ballpark of the ideal value, however, the same cannot be said for chlorine. The one possible reason for this is that the chlorine concentration was above the detection limit and the calibration curve that was used to obtain the wt% of chlorine greatly underestimated its concentration. The minor elements found in the sample consisted of potassium (K) at 0.07 wt%, silica (Si) at 0.06 wt%, calcium

(Ca) at 0.02 wt%, sulphur (S) at 1 464 ppm and phosphorus (P) at 167 ppm (Table 26). There was also a total of 16 elements classified as trace elements in the sample and are presented in Table 26. Ultimately, from the results obtained, it can be said that both sodium and chlorine are the major constituents of this sample, with the halite obtained from the dust sample analysed by XRD above confirming the presence of sodium chloride (NaCl) (Table 26).

Table 26: Major, Minor and Trace Elements from XRF Analysis of the Salt Sub-Sample from the Dust Fallout Bucket sample at Blue Bay Lodge

Major Elements		Minor Elements		Trace Elements	
Element	Value	Element	Value	Element	Value (ppm)
Sodium (%)	35.0	Potassium (%)	0.07	Barium	15
Chlorine (%)	37.5	Silica (%)	0.06	Rubidium	10
		Calcium (%)	0.02	Strontium	10
		Sulphur (mg/kg)	1464	Zinc	9
		Phosphorus (mg/kg)	167	Chromium	8
				Nickel	8
				Zirconium	8
				Copper	7
				Lanthanum	7
				Lead	7
				Titanium	4
				Niobium	3
				Cobalt	2
				Uranium	2
				Gallium	1
				Thorium	1

4.3.2. Results of the PM Sample from the BSNEs: Saldanha Bay and Blue Bay Lodge

The BSNE sample that was analysed was a combined sample from the BSNEs that were installed at the Saldanha AQM Station and Blue Bay Lodge from the 25th of February 2021 to the 5th of August 2021 (Figure 68). The total combined amount of sample was 0.88 g. The sample was then measured with Quantitative Evaluation of Minerals by Scanning Electron Microscopy (QEMSCAN). The results from this analysis of the sample are presented below.

Figure 68: A map indicating the two study sites, Blue Bay Lodge and the Saldanha AQM Station, where the Big Spring Number Eights (BSNEs) were installed

4.3.2.1. Major, minor and trace minerals, total mass% and number of particles found in the BSNE sample

The major minerals that were found in the BSNE sample include: quartz (SiO_2) which made up 45.2% of the sample, feldspar ($KAlSi_3O_8$) at 16%, hematite (Fe_2O_3) at 12.8%, mica (AB_2-$3(XSi)_4O_{10}(OFOH)_2$) at 8.4%, carbonates at 7%, kaolinite ($Al_2O_32SiO_{22}H_2O$) at 2.6%, amphibole ($R_{14}[(OH)_4Si_{16}O_{44}]$) at 1.9%, sulphides at 1.1% and a group classified as “other” at 2.9% (Figure 69). The minerals present as minor minerals in the sample include: apatite ($Ca_5(PO_4)$) at 0.9%, chlorites ($((MgFe)_3(SiAl)_4O_{10}(OH)_2(MgFe)_3(OH)_6$) at 0.6%, epidote ($Al_2Ca_2FeH_2O_{13}Si_3$) and rutile/anatase ($TiO_2$) at 0.2% each and ilmenite ($((FeTi)_2O_3$) at 0.1% (Figure 69). The only mineral classified as trace was zircon (ZrSiO4) at 0.03% (Figure 69).

The sample is predominantly comprised of quartz, feldspar, and hematite. There is also the presence of aluminosilicates such as amphibole, chlorite as well as epidote; clay minerals such as kaolinite and mica; titanium minerals such as ilmenite and rutile/anatase; apatite, carbonates, sulphides, zircon and a group of unclassified minerals (Figure 69). Table 27 below indicates the different size bins in which particles in the sample were found, as well as the total mass% and number of particles in each size bin obtained from the results provided by the QEMSCAN.

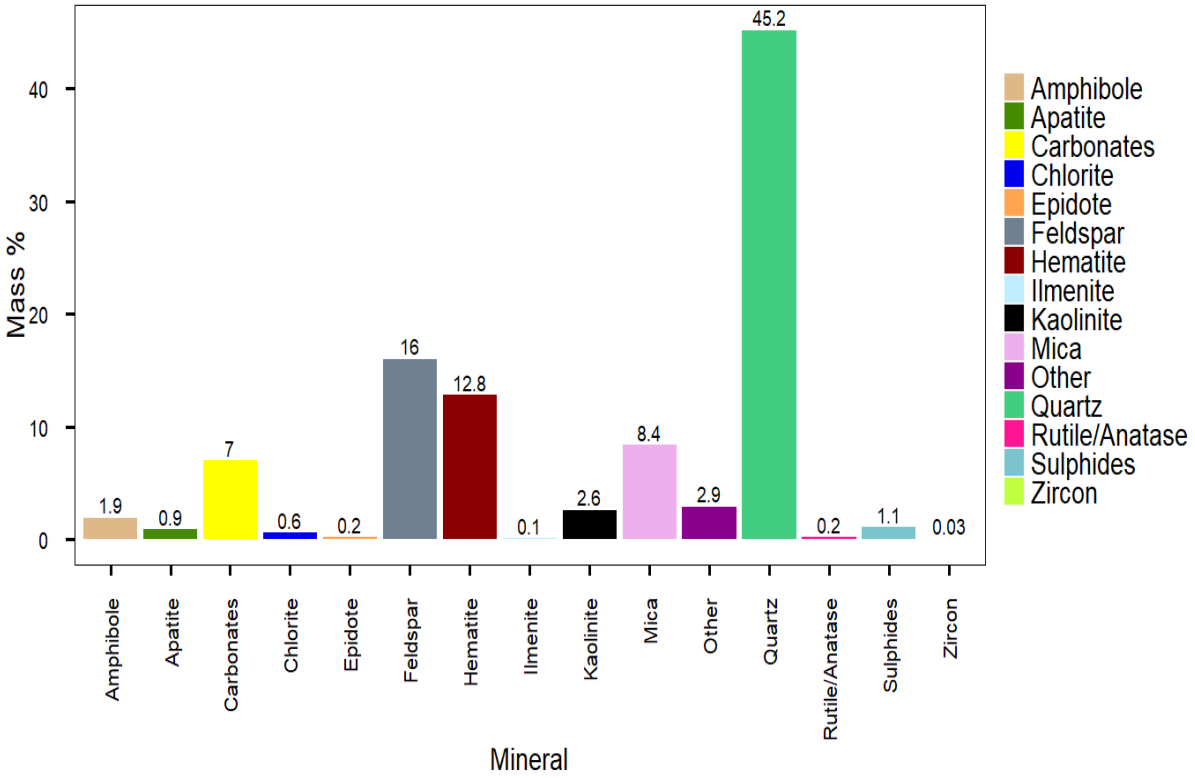

Figure 69: Mass% of minerals measured by the QEMSCAN from the BSNEs installed at Blue Bay Lodge and Saldanha AQM Station

A total number of 69 931 particles were scanned from the combined BSNE sample collected at Blue Bay Lodge and the Saldanha AQM Station. This measurement by the QEMSCAN produced the different sizes of the scanned particles as well as their mineralogy. The <5 µm size bin contained majority of the particles at 65.9%, while the 200-250 µm size bins contained the least particles. The relationship seen here is one that is inversely proportional, whereas the size bin increased, the number of particles in each size bin decreased. The sizes of the particles obtained from the measurements ranged from fine particles with a diameter less than 5 µm to course particles with a diameter less than and equal to 250 µm (Table 27). The 20-63 µm size bin contains the greatest mass% of particles in the sample. The majority of the mass% of particles are found in three bins covering the particle size ranges, 20-125 µm. 100% of the sample occur in the <250 µm, while 94.1% are <150 µm in size. Almost a third of the particles in the sample (28.5%) occur in the <20 µm size bins (Table 27).

Table 27: The total mass% of particles and number of particles in each particle size bin from the BSNE sample measured by the QEMSCAN

Size bins (µm)	Total mass%	Number of particles
<5	6.8	46 118
5-10	8.6	14 541
10-20	13.1	6 043
20-63	33.0	2 822
63-100	19.6	296
100-125	10.4	89
125-150	2.6	11
150-200	3.4	7
200-250	2.5	4
250-350	0	0
>350	0	0

4.3.2.2. Particle size distribution across the different size bins from the BSNE sample analysed by QEMSCAN

Figure 70 indicates the distribution of the minerals across the different size fractions, to compare the composition of particles across the different size bins, the results of the particle size analysis of minerals from the QEMSCAN was normalised (Figure 71). The normalised results are discussed below, with the mass% of each mineral presented in Table 28.

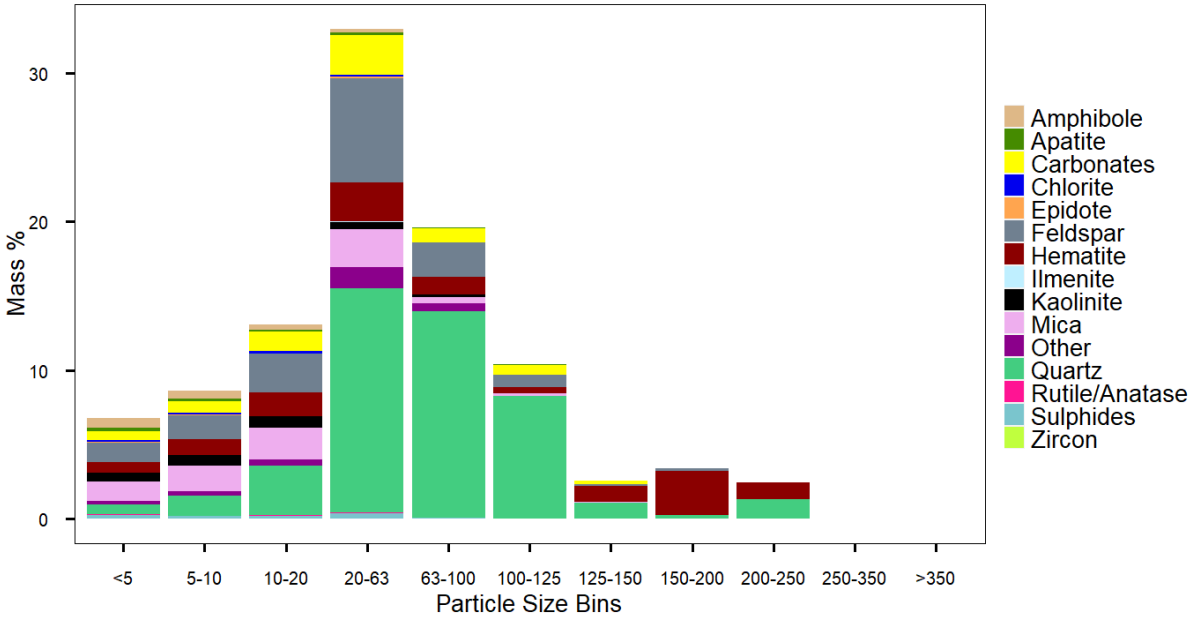

Figure 70: Particle size distribution of minerals from QEMSCAN analysis of BSNE sample collected at Blue Bay Lodge and the Saldanha AQM Station

Despite being present across all the particle size bins (except for the 250-350 µm and >350 µm, where no minerals were found), the percentage of quartz and hematite varied greatly between the size bins (Figure 71). Between the size fractions 10-20 µm and <5 µm and in the

size fraction 150-200 µm, the mass% of quartz varied compared to the mass% between the size fractions 20-63 µm and 125-150 µm as well as the 200-250 µm size fraction (Table 28). For hematite, between the <5 µm and 100-125 µm size fractions, the mass% was much lower compared to the mass% of hematite found between the 125-150 µm and the 200-250 µm size fractions. With regards to feldspar, the mass% was found to be higher between the <5 µm and 20-63 µm size fractions, thereafter, decreasing between the 63-100 µm and 150-200 µm size fractions. The same pattern can be seen for mica, where the mass% was found to be higher between the <5 µm and the 10-20 µm size fractions and thereafter decreasing between the 20-63 µm and the 100-150 µm size fractions. There was no presence of mica in the 150-200 µm, but 0.4% was found in the 200-250 µm size fraction (Table 28).

Kaolinite, amphibole and apatite were all found in the same size fractions (between <5 µm and 100-125 µm) (Figure 71) (Table 28). The trend that was seen for all three minerals was that a higher mass% for each was found in the smaller size fractions, thereafter, decreasing as the size fraction increased (Table 28). Chlorite, epidote, rutile/anatase and ilmenite were all found in the same size fractions (between <5 µm and 20-63 µm) (Figure 71) (Table 28). The mass% of chlorite was found to decrease as size fraction increased. The mass% of epidote increased between the <5 µm and 5-10 µm size fractions and thereafter decreased as size fraction increased. The mass% of rutile/anatase decreased between the <5 µm and the 5-10 µm size fractions, and thereafter increased as size fraction increased. For ilmenite, between the size fractions <5 and 5-10 µm, the mass% was 0.1% and increased to 0.2% in the 10-20 µm and the 20-63 µm size fractions. Zircon was only found in the 20-63 µm size fraction, with a mass% of 0.1% (Table 28).

Carbonates were found in all the size fractions, except for the 150-200 µm and the 200-250 µm size fractions (Figure 71) (Table 28). The mass% of carbonates increased between the <5 µm and the 10-20 µm size fractions and then decreased between the 20-63 µm and 100-125 µm size fractions. The mass% of carbonates then increased again in the 125-150 µm size fraction. Sulphides and the group “other” were both found in the same size fractions (between <5 µm and 63-100 µm) (Figure 71). With sulphides, it was found that the mass% decreased as the size fraction increased. With regards to “other”, the mass% decreased between the <5 µm and 10-20 µm size fractions, and then increased to 4.4% in the 20-63 µm size fraction. Thereafter, the mass% decreased to 2.6% in the 63-100 µm size fraction (Table 28).

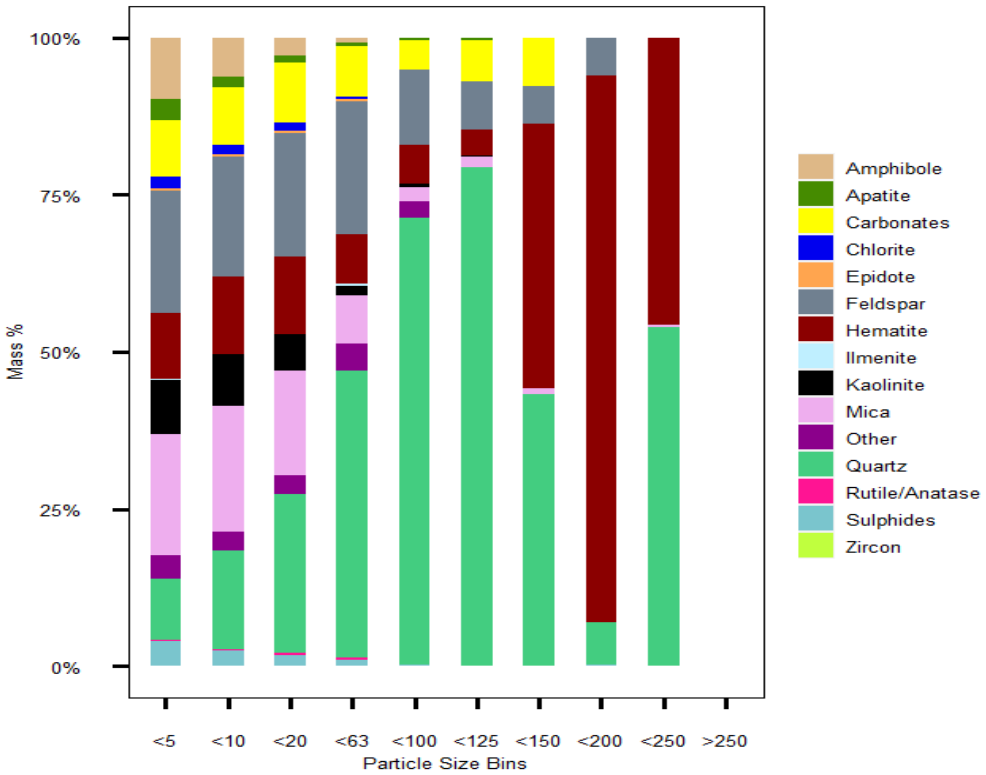

Figure 71: Normalised Particle Size Distribution of Minerals from QEMSCAN Analysis of BSNE Sample collected at Blue Bay Lodge and the Saldanha AQM Station

Table 28: The Normalised Results of the Mass% of Minerals found in the QEMSCAN Sample

Mineral	<5 µm	5-10 µm	10-20 µm	20-63 µm	63-100 µm	100-125 µm	125-150 µm	150-200 µm	200-250 µm	250-350 µm	350 µm
Quartz	9.7	15.7	25.4	45.6	70.9	79.4	43.4	6.7	53.8	-	-
Feldspar	19.3	18.9	19.6	21.3	11.9	7.7	5.9	6.1	-	-	-
Mica	19.3	20.1	16.7	7.7	2.2	1.6	0.8	-	0.4	-	-
Chlorite	1.9	1.5	1.4	0.5	-	-	-	-	-	-	-
Kaolinite	8.5	8.1	5.7	1.5	0.7	0.1	-	-	-	-	-
Amphibole	9.7	6.3	2.8	0.8	0.1	0.1	-	-	-	-	-
Epidote	0.4	0.5	0.4	0.2	-	-	-	-	-	-	-
Sulphides	4.0	2.4	1.8	1.0	0.4	-	-	-	-	-	-
Hematite	10.6	12.3	12.3	7.9	6.2	4.2	42.2	86.8	45.7	-	-
Rutile/ Anatase	0.3	0.2	0.3	0.3	-	-	-	-	-	-	-
Ilmenite	0.1	0.1	0.2	0.2	-	-	-	-	-	-	-
Carbonates	8.8	9.1	9.5	8.0	4.6	6.4	7.8	-	-	-	-
Zircon	-	-	-	0.1	-	-	-	-	-	-	-
Apatite	3.5	1.7	1.1	0.5	0.4	0.4	-	-	-	-	-
Other	3.7	3.0	2.9	4.4	2.6	-	-	-	-	-	-

*The dashes indicate that there were no minerals present in those size ranges.

4.3.3. Results from the Gravimetric Samplers PM Samples

Gravimetric samplers were installed at all the study sites, excluding the Vredenburg AQM Station, due to concern of vandalism (Figure 72).

Figure 72: A map indicating the six study sites where gravimetric samplers were installed

The filter papers that were collected during the fieldwork study were subjected to SEM-EDX as well as ICP-MS and ICP-AES for qualitative and quantitative analysis of elemental composition of major, minor and trace elements, respectively. ICP-MS and ICP-AES analysis was carried out on two quartz filter papers (1a and 1b) with sample collected at Blue Bay Lodge. The samples collected on 1a and 1b are TSP and PM_{10}, respectively. An extra blank filter paper (FP67) was also analysed. The details regarding these filter papers can be found in Appendix B. SEM-EDX analysis was carried out on all the remaining filter papers that were collected around the Municipality. Both these analyses provide elemental data and the decision to analyse the other filter papers with ICP-AES and ICP-MS was to confirm if there were any other elements that were present, that had not been picked up by the SEM analysis and vice versa.

4.3.3.1. ICP-MS and ICP-AES Results

The two filter papers analysed by ICP-MS and ICP-AES were obtained from the ARA N-FRM Sampler installed at Blue Bay Lodge. The details regarding these filter papers are tabulated below (Table 29).

Table 29: Filter Papers Information collected at Blue Bay Lodge for ICP-MS and -AES Analysis

Filter Paper ID	Receptor Site	Sampling Period	Number of days	Impactor	Mass of Material on Filter Paper (mg)
1a	Blue Bay Lodge	09/07/2021 – 05/08/2021	28	No impactor – collected TSP	32.3
1b		30/09/2021 – 22/10/2021	23	PM_{10}	14.0

The elements found on the filter papers 1a and 1b are presented according to their concentration. The elements found in high concentrations are sodium (Na), iron (Fe), magnesium (Mg), calcium (Ca), aluminium (Al), potassium (K) (Figure 73).

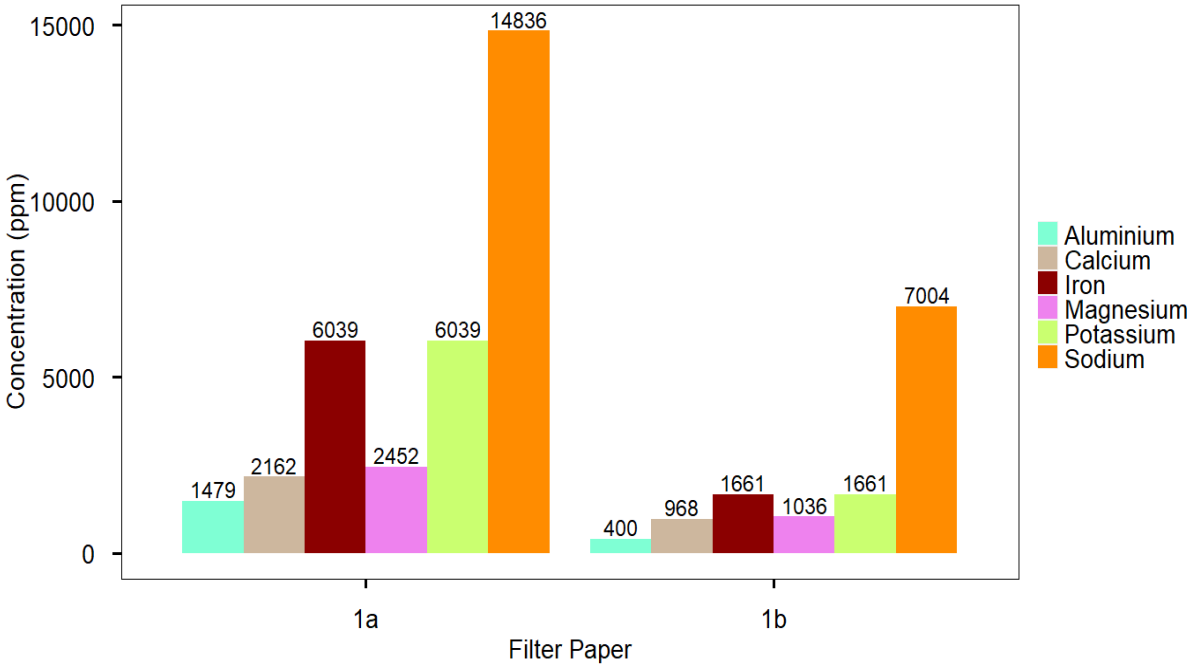

Figure 73: Major and Minor Elements from filter papers 1a (TSP) and 1b (PM_{10}), collected at Blue Bay Lodge and measured by ICP-AES

All of the elements found on filter papers 1a and 1b are classified as major elements, with the exception for aluminium and calcium on filter paper 1b, which classify as minor elements. There were fourteen elements measured by the ICP-MS which were found to be trace elements (Table 30).

Table 30: Trace Elements from Filter Papers 1a and 1b, collected at Blue Bay Lodge and measured by ICP-MS

Element	Symbol	Filter paper	
		1a – Concentration in ppb	1b – Concentration in ppb
Barium	Ba	41 245	13 474
Lead	Pb	40 072	13 706
Strontium	Sr	22 644	10 414
Copper	Cu	11 212	3 097
Arsenic	As	8 770	1 340
Nickel	Ni	7 775	2 651
Vanadium	V	7 562	3 426
Chromium	Cr	7 494	1 662
Selenium	Se	1 999	999
Tin	Sn	1 498	635
Cobalt	Co	919	218
Cadmium	Cd	613	101
Molybdenum	Mo	300	61
Antimony	Sb	138	117

4.3.3.2. SEM-EDX Results

All the filter papers that were collected were subjected to SEM-EDX analysis. This excludes the two quartz filter papers that were analysed by ICP-MS and -AES presented above. The table below indicates the filter papers that were analysed by the SEM-EDX.

Table 31: Filter Papers Information collected at all Receptor Sites for SEM Analysis

Filter Paper ID	Study Site	Sampling Period	Impactor	Mass of Material on Filter Paper (mg)
1c	Blue Bay Lodge	23/02/2021 – 01/03-2021	$PM_{2.5}$	1.30
2a	Saldanha AQM Station	01/03/2021 – 08/03/2021	TSP	2.30
3a	West Coast Mall	23/03/2021 – 12/04/2021	TSP	1.10
4b	Louwville Private Home	16/05/2021 – 08/06/2021	TSP	13.0
5b	Langebaan Private Home	09/05/2021 – 08/06/2021	TSP	21.8
6a	St. Helena Bay Private Home	11/04/2021 – 09/05/2021	TSP	15.2
6b	St. Helena Bay Private Home	09/05/2021 – 08/06/2021	TSP	22.6

The SEM-EDX results are presented qualitatively in this study. Based on the elements that have been found in the SEM-EDX analysis, and their associated stoichiometric ratios, the five main minerals that have been deduced stoichiometrically are sodium chloride (NaCl), quartz (SiO_2), hematite (Fe_2O_3), calcium carbonate ($CaCO_3$) and titanium dioxide (TiO_2). SEM-EDX analysis was carried out at all of the study sites, with the exception of the Vredenburg AQM Station, due to no gravimetric sampler being installed. The minerals that have been found based on the SEM-EDX results are tabulated below (Table 32). Sodium chloride, quartz and calcium carbonate was found at all six study sites. Hematite and titanium dioxide both were found at all the study sites, except for at the Langebaan Private Home.

Table 32: Results of SEM-EDX Analysis that was carried out on Filter Papers from six Study Sites

Filter Paper ID	Filter Paper Type	Study Site	Minerals found on Filter Paper
1c	Polycarbonate	Blue Bay Lodge	▪ Sodium chloride (NaCl) ▪ Quartz (SiO_2) ▪ Hematite (Fe_2O_3) ▪ Calcium carbonate ($CaCO_3$) ▪ Titanium dioxide (TiO_2)
2a	Polycarbonate	Saldanha AQM Station	▪ Sodium chloride (NaCl) ▪ Quartz (SiO_2) ▪ Hematite (Fe_2O_3) ▪ Calcium carbonate ($CaCO_3$)
3a	Polycarbonate	West Coast Mall	▪ Sodium chloride (NaCl) ▪ Quartz (SiO_2) ▪ Hematite (Fe_2O_3) ▪ Calcium carbonate ($CaCO_3$) ▪ Titanium dioxide (TiO_2) ▪ Manganese oxide (MnO)
4b	Mixed-Cellulose	Louwville Private Home	▪ Sodium chloride (NaCl) ▪ Quartz (SiO_2) ▪ Hematite (Fe_2O_3) ▪ Calcium carbonate ($CaCO_3$) ▪ Titanium dioxide (TiO_2)
5b	Mixed-Cellulose	Langebaan Private Home	▪ Quartz (SiO_2) ▪ Calcium carbonate ($CaCO_3$)
6a and 6b	Mixed-Cellulose	St. Helena Bay Private Home	▪ Sodium chloride (NaCl) ▪ Quartz (SiO_2) ▪ Hematite (Fe_2O_3) ▪ Calcium carbonate ($CaCO_3$) ▪ Titanium dioxide (TiO_2)

CHAPTER 5: DISCUSSION OF RESULTS

This chapter address the key research questions of this study and are listed below:

i. What are the concentration profiles of PM at the key study sites within the region?
ii. What are the chemical and physical characteristics of the collected PM samples?
iii. Based on the results from (i) and (ii), what are the potential sources of emission that contribute to PM contamination in the Saldanha Bay municipality?
iv. Based on the results from (i) and (ii), what are the potential health implications?

The first two key research questions are addressed based on the results obtained in this study. The first question (i) addresses the hourly and 24-hour averaged $PM_{2.5}$ and PM_{10} concentration profiles that were measured at the seven study sites during their respective sampling periods (Section 5.1.1). The question also addresses the PM concentration profiles at the seven study sites with regards to meteorological factors such as wind speed and wind direction (Section 5.1.2). The second question (ii) discusses the results obtained from the analysis of the physical PM samples from the salt and dust sub-samples from the dust fallout bucket, the combined dust sample from the BSNEs and the filter papers from the gravimetric samplers (Sections 5.2.1 and 5.2.2). The second question also discusses the potential origins of some of the metals/minerals found in the samples (Section 5.2.3). The third question (iii) discusses the potential sources that contribute to PM emission by considering the results from the pollution roses, polar plots and potential sources present in the municipality (Section 5.3). Based on the chemical and physical characteristics of the physical PM samples, the fourth question (iv) discusses the potential implications that the metals/minerals have on human health (Section 5.4).

5.1. PM Concentration Profiles at the Key Study Sites

5.1.1. Summary and Synthesis of PM Concentration Profile Results

The PurpleAir Particulate Sensors were installed at seven study sites, which were located in four receptor areas. The four receptor areas in which the study sites are located included: Saldanha, Vredenburg, St. Helena Bay and Langebaan. Blue Bay Lodge and the Saldanha AQM Station are located in Saldanha; the West Coast Mall, the Vredenburg AQM Station and the Louwville Private Home are located in Vredenburg; the Langebaan Private Home is located in Langebaan; and the St. Helena Bay Private Home is located in St. Helena Bay.

The PurpleAir Particulate Sensors measured $PM_{2.5}$ and PM_{10} concentrations at all seven study sites during the respective sampling periods, with the results presented in Chapter 4, Section 4.1. The raw concentrations obtained from the sensors were aggregated from 2-minute intervals to hourly and 24-hour averages. The $PM_{2.5}$ concentrations were corrected using a correction equation for humidity, while the PM_{10} concentrations remained uncorrected as there does not yet exist a correction equation for PM_{10} concentrations. However, the $PM_{2.5}$ concentrations were corrected for only relative humidity, as relative humidity impacts the light scattering of particles (Barkjohn, Gantt & Clements, 2021). Both the hourly and 24-hour averages of the corrected $PM_{2.5}$ concentrations and the uncorrected PM_{10} concentrations are

presented as time plot series in Section 4.1 for each study site, although it must be emphasised that there are concerns regarding the accuracy of the PM_{10} concentrations measured by the sensor.

The summary of the hourly (Figure 74) and 24-hour (Figure 75) uncorrected and corrected PM2.5 concentrations are presented below in the form of boxplots. Boxplots were used to represent the PM2.5 and PM10 concentrations, assuming that the data is log-normally distributed. Using a Shapiro test, if the p-value is less than the 0.05 threshold, then there is strong evidence against the null hypothesis that the data is normally distributed. Concentrations were tested, with p-values on 10-12 returned, indicating that the data is non-normally distributed and therefore, the log-normal distribution would work with this set of data and subsequently allow for a better presentation of the data. Although the boxplots below indicate outliers above the upper range limit, in this study, the outliers indicated are regarded as true PM concentrations (Figure 74 and Figure 75). In this study, the outliers were defined as Q3 + 1.5IQR, where Q3 is the third quartile and IQR is the interquartile range. Although both boxplots below,

Figure 74 and Figure 75, are log-normally presented, it is important to note that the discussion of the results in this section are interpreted in terms of the original scale. Both the log transformed and original scale data of Figure 74 and Figure 75 can be found tabulated in Appendix F. For all sites, except the Louwville and St. Helena Bay Private Homes, it was found that the hourly uncorrected PM2.5 concentrations were <200 µg/m3 (Figure 74)). However, the hourly corrected PM2.5 concentrations were <200 µg/m3 at all seven study sites. Furthermore, when comparing the hourly to the 24-hour averages, PM2.5 concentrations (corrected and uncorrected) were <40 µg/m3 at all study sites, which also indicates that there were no 24-hourly PM2.5 exceedances according to the NAAQS. There was, however, insufficient data to enable an assessment of compliance with the annual average standard. Although the NAAQS and the WHO guidelines do not consider hourly averages, however, presenting these averages highlighted the many hours where PM exposure was above the national average around the municipality. Ostro and Chestnut (1998) have in their paper stated that while $PM_{2.5}$ and PM_{10} have been associated with morbidity and mortality, it has been very difficult to identify a safe level of PM, in terms of exposure. It is important to consider hourly data as hourly PM exposure can be classified as short-term exposure and as reported by Wu et al. (2021), hourly averages are known as the basis to estimate short-term exposure of PM concentrations, which subsequently allow for a faster response to pollution events. Additionally, there are also serious health risks that are a consequence of short-term PM exposure, which are discussed further in Section 5.4.

For the hourly $PM_{2.5}$ concentrations, it was found that the first quartile (Q1), which represents the value under which 25% of the data is found, was highest at the Saldanha AQM Station for both uncorrected (3.57 µg/m^3) and corrected (2.94 µg/m^3) values. This was found to be the same for the 24-hour $PM_{2.5}$ concentrations, where Q1 was found to be highest at the Saldanha AQM Station with values of 5.12 µg/m^3 for uncorrected and 3.44 µg/m^3 for corrected concentrations (Table 46 and Table 48). This indicates that $PM_{2.5}$ concentrations for the 24-

hour averages were more spread out towards the higher end of 25% of the concentration's distribution, when compared to the hourly averages. The medians (Q2 or middle values) of both the hourly and 24-hour $PM_{2.5}$ concentrations also followed a common trend, where the median was found to be the highest for the uncorrected concentrations at the Langebaan Private Home at 6.59 µg/m^3 for hourly and 7.31 µg/m^3 for 24-hour averages. With regards to the corrected $PM_{2.5}$ concentrations, the median was found to be highest at the Saldanha AQM Station at 4.55 µg/m^3 for hourly and 4.95 µg/m^3 for 24-hour averages (Table 46 and Table 48). The medians for uncorrected and corrected 24-hour averages were higher than those for the hourly averages, which indicates that the central tendency of the 24-hour $PM_{2.5}$ concentrations were found to be shifted towards higher values compared to the hourly concentrations.

For the hourly $PM_{2.5}$ concentrations, it was found that the third quartile (Q3), which represents the value under which 75% of the data is found, was highest at the Langebaan Private Home for uncorrected concentrations (11.62 µg/m^3) and highest at the Saldanha AQM Station for corrected values (6.90 µg/m^3). This was found to be the same for the 24-hour $PM_{2.5}$ concentrations, where Q3 was found to be highest at the Langebaan Private Home at 11.99 µg/m^3 for uncorrected values and at the Saldanha AQM Station at 7.13 µg/m^3 for corrected concentrations (Table 46 and Table 48). This indicates that the upper 25% of the 24-hour averages are relatively larger than the upper 25% of the hourly averages of $PM_{2.5}$ concentrations. With regards to the upper limit (highest point of the upper whisker), it was found that the values for the hourly averages were higher than those for the 24-hour averages. This is indicative that the upper extreme values of the boxplots (outliers) in the hourly averages are higher than those in the 24-hour averages of $PM_{2.5}$ concentrations. It is also worth noting that the maximum values of the 24-hour averages were significantly higher than the hourly averages (Table 46 and Table 48).

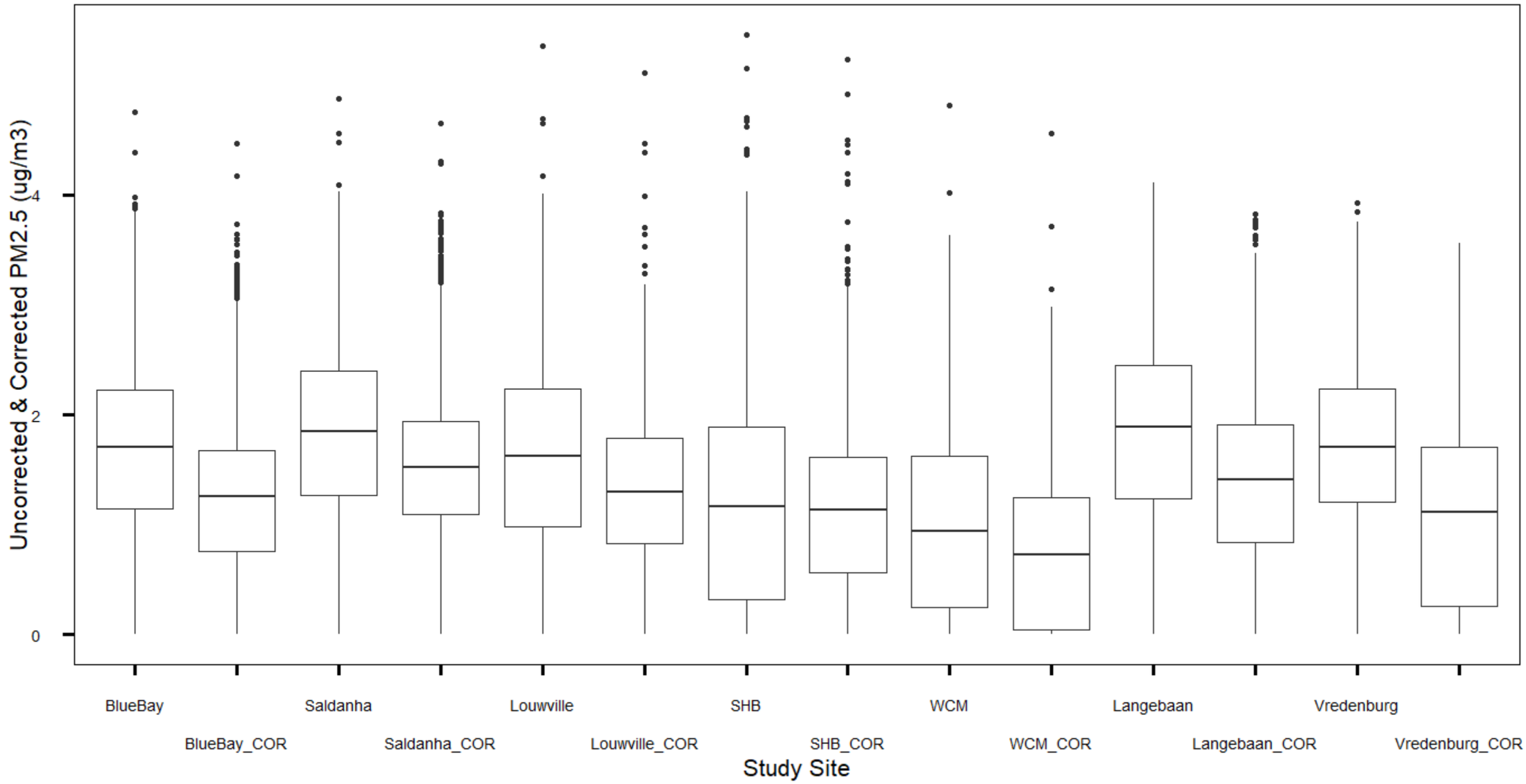

Figure 74: Summary of the hourly uncorrected and corrected $PM_{2.5}$ concentrations at all seven study sites

*BlueBay = Blue Bay Lodge, Saldanha = Saldanha AQM Station, Louwville = Louwville Private Home, SHB = St. Helena Bay Private Home, WCM = West Coast Mall, Langebaan = Langebaan Private Home, Vredenburg = Vredenburg AQM Station

*COR = Corrected $PM_{2.5}$ Concentrations

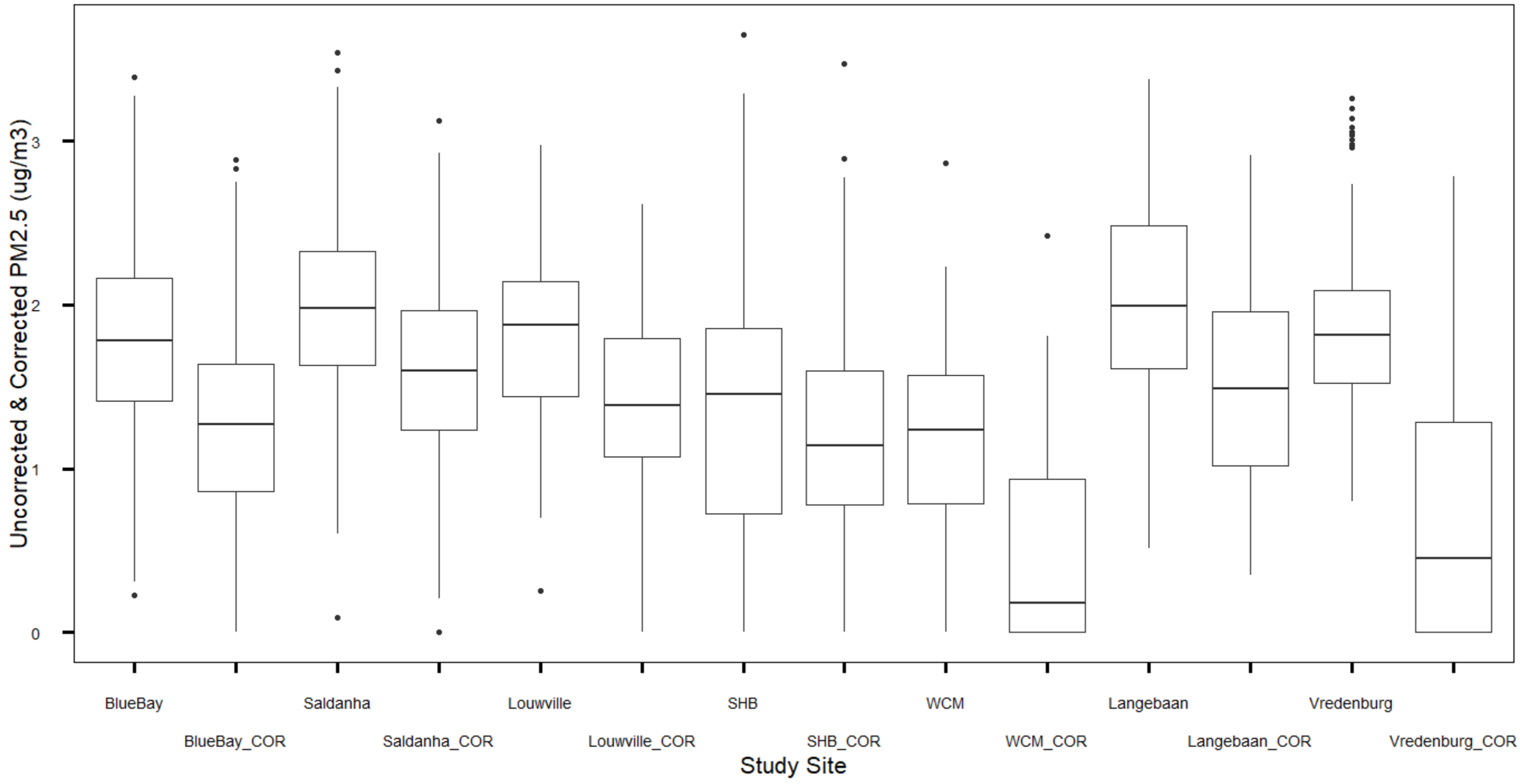

Figure 75: Summary of the daily uncorrected and corrected $PM_{2.5}$ concentrations at all seven study sites

*BlueBay = Blue Bay Lodge, Saldanha = Saldanha AQM Station, Louwville = Louwville Private Home, SHB = St. Helena Bay Private Home, WCM = West Coast Mall, Langebaan = Langebaan Private Home, Vredenburg = Vredenburg AQM Station

*COR = Corrected $PM_{2.5}$ Concentrations

$PM_{2.5}$ and PM_{10} Concentration Limit Exceedances

The 24-hour $PM_{2.5}$ and PM_{10} concentrations were compared to the concentration limits outlined by the NAAQS and WHO guidelines. There were no exceedances according to the NAAQS at any of the study sites. It was also found that there were no exceedances according to the WHO guidelines at both the Louwville Private Home and the West Coast Mall. However, there were exceedances, according to the WHO guidelines at the five other study sites. A summary of these exceedances is presented in Table 33 below. This summary includes all exceedances, including the ones considered anomalies as a result of potential faults from the sensor. The inclusion of the extreme outliers/anomalies are important as they highlight the shortcomings, such as faults experienced by the PurpleAir Particulate Sensor and the effect that such extreme outliers can have on the dataset. From Table 33 below, there was only one exceedance of PM_{10} at the St. Helena Bay Private Home. The rest of the exceedances were $PM_{2.5}$ concentrations and occurred during Autumn (May) and Winter (June-August) months. There were however 2 exceedances at Blue Bay Lodge during Summer 2021 (January-February). The NAAQS indicate that the frequency of exceedances of $PM_{2.5}$ concentrations in 24-hours are 4. This was another reason to aggregate the data to hourly averages, as these were used to check if there were 4 or more exceedances of both $PM_{2.5}$ and PM_{10} in 24-hours. Upon further investigation of the hourly concentrations, it was found that the frequency was not exceeded for both $PM_{2.5}$ and PM_{10} concentrations.

Table 33: $PM_{2.5}$ 24-hour exceedances according to WHO guidelines

	Study Sites					
	Blue Bay Lodge	Saldanha AQM Station	St. Helena Bay Private Home		Langebaan Private Home	Vredenburg AQM Station
2021	$PM_{2.5}$	$PM_{2.5}$	$PM_{2.5}$	PM_{10}	$PM_{2.5}$	$PM_{2.5}$
May	-	-	1	1	-	-
June	2	6	3	-	3	1
July	-	1	-	-	-	-
August	-	2	-	-	-	-
2022						
January	1	-	-	-	-	-
February	1	-	-	-	-	-

*The dashes indicate zero exceedances at the study sites.

NAAQS has also outlined $PM_{2.5}$ concentration limits of 25 µg/m^3, that will come into effect on the 1st of January 2030 (Table 2 in Chapter 2). Although the results indicate that there were no exceedances according to the current NAAQS limits, it was important to compare the results using the 2030 concentration limits to evaluate if the concentrations meet the future targets. The only study site where $PM_{2.5}$ concentrations were >25 µg/m^3 was at the St. Helena Bay during May. However, this would still be accepted as the frequency of exceedance is below the required amount of 4 exceedances in 24-hours.

With regards to the exceedances per month, it was found that there were more exceedances during Winter, compared to the rest of the seasons. It is interesting that the $PM_{2.5}$ exceedances were in fact higher in Winter, as this is the season where the most rainfall occurs in the municipality, which is known to have a wet scavenging effect on PM emissions (Liu et al., 2020). To further investigate this, uncorrected $PM_{2.5}$ concentrations vs. Relative Humidity correlations were calculated from the data obtained from the PurpleAir Particulate Sensor at each study site (Table 34). To label the strength of association, absolute values of r between 0-0.3 are regarded positively weak (Ratner, 2009). The positively weak correlations in Table 34 below indicate that humidity does indeed have an influence of PM concentrations.

While it is agreed that rain is expected to decrease concentrations, due to its scrubbing action, these higher concentrations could potentially be partially unrelated to mineral sources. For instance, temperature inversions are common during the winter months, where cool air is trapped near the ground by a layer of warm air. This subsequently prevents pollutants, such as PM, from dispersing. Furthermore, it should also be noted that during winter, there is an increase in heating and/or vehicles, which may inadvertently contribute to the levels of PM (Ha et al., 2023).

Table 34: PM vs. relative humidity correlation at each study site

Study Site	PM vs. Relative Humidity Correlation
Blue Bay Lodge	0.1
Saldanha AQM Station	0.04
Louwville Private Home	0.1
St. Helena Bay Private Home	0.003
West Coast Mall	0.05
Langebaan Private Home	0.08
Vredenburg AQM Station	0.1

5.1.2. PM Concentrations as function of wind speed and direction in the Saldanha Bay Municipality

Meteorological data from the Geelbek Weather Station was used to construct the wind rose, pollution roses and polar plots. The pollution roses and polar plots for $PM_{2.5}$ were constructed for each study site, with the results presented in Section 4.2.

The Wind Rose for the Geelbek Weather Station

Since both the Saldanha and Vredenburg AQM Stations were not in operation during this study's sampling period, the decision was made to use meteorological data from the weather stations available in the municipality. These included the Langebaanweg and the Geelbek Stations. The decision to use the data from the Geelbek Station was due to the topography that surrounds the Langebaanweg Station, which would have ultimately provided inaccurate wind data for the study sites. Table 35 below provides the dominant wind directions per season. The dominant wind direction in the municipality during all seasons, except Winter, was the S. In Winter, the dominant wind direction was the SSE. Using this data, the pollution roses and polar plots were constructed for each study site and are discussed further below.

Table 35: Dominant wind direction per season in the Saldanha Bay Municipality

	Frequency of Counts (%)				
Season	South (S)	South southeast (SSE)	South southwest (SSW)	North (N)	North northwest (NNW)
Summer	54.0	10.0	15.5	<5.0	<5.0
Autumn	35.0	13.5	7.5	7.5	9.5
Winter	14.0	17.5	6.0	15.0	13.5
Spring	33.5	18.0	8.0	9.0	8.5

The Saldanha Area: Blue Bay Lodge and the Saldanha AQM Station

The dominant wind directions associated with $PM_{2.5}$ concentrations in the Saldanha area (Blue Bay Lodge and the Saldanha AQM Station) are summarised in Table 36 below. At Blue Bay Lodge, the dominant direction of $PM_{2.5}$ pollution was associated with wind from the S during Summer 2021 (0-21.6 µg/m^3), Autumn (0-36.4 µg/m^3), Spring (0-28.6 µg/m^3) and Summer 2021-2022 (0-41.8 µg/m^3). Winter was the only season at Blue Bay Lodge where the SSE was the dominant direction of $PM_{2.5}$ pollution, with concentrations ranging between 0-32.3 µg/m^3. At the Saldanha AQM Station, the dominant direction of $PM_{2.5}$ pollution was associated with wind from the S in Autumn and Spring, where $PM_{2.5}$ concentrations ranged between 0-42.5 µg/m^3 and 0-17.9 µg/m^3, respectively. The dominant direction of $PM_{2.5}$ pollution was associated with wind from the SSE during Summer and Winter, where $PM_{2.5}$ concentrations ranged between 0-15.5 µg/m^3 and 0-46.1 µg/m^3, respectively. The $PM_{2.5}$ concentration ranges provided, indicate the concentrations measured at the study sites, through the entire respective season.

Table 36: Dominant wind directions associated with $PM_{2.5}$ concentrations in the Saldanha area

Blue Bay Lodge					
Season	Frequency of counts (%)				
	South (S)	South southeast (SSE)	South southwest (SSW)	North (N)	North northwest (NNW)
Summer (2021)	60.0	17.0	10.0	-	-
Autumn	35.0	14.0	8.0	7.0	9.0
Winter	8.0	14.0	2.0	13.5	10.5
Spring	36.0	18.0	10.5	7.0	7.0
Summer (2021-2022)	41.0	10.5	15.0	5.0	5.5
Saldanha AQM Station					
Season	Frequency of counts (%)				
	South (S)	South southeast (SSE)	South southwest (SSW)	North (N)	North northwest (NNW)
Summer	30.0	43.0	12.5	2.5	1.0
Autumn	35.0	13.0	7.5	7.0	9.5
Winter	13.5	17.5	5.0	14.5	12.0
Spring	28.0	21.0	6.5	10.5	10.0

The Vredenburg Area: Louwville Private Home, West Coast Mall and the Vredenburg AQM Station

The dominant wind directions associated with $PM_{2.5}$ concentrations in the Vredenburg area (Louwville Private Home, West Coast Mall and the Vredenburg AQM Station) are summarised in Table 37 below. At the Louwville Private Home, the dominant direction associated with $PM_{2.5}$ pollution was the S during both Summer (0-10.8 µg/m^3) and Autumn (0-40.7 µg/m^3). Similar to the Louwville Private Home, the dominant direction associated with $PM_{2.5}$ pollution at the West Coast Mall was also the S during Summer (0-23.1 µg/m^3) and Autumn (0-18.4 µg/m^3). At the Vredenburg AQM Station, the dominant direction associated with $PM_{2.5}$ pollution was the SSE during Summer (0-22.4 µg/m^3), S during Autumn (0-22.4 µg/m^3) and N during Winter (0-35.0 µg/m^3).

Table 37: Dominant wind directions associated with $PM_{2.5}$ concentrations in the Vredenburg area

Louwville Private Home					
Season	Frequency of counts (%)				
	South (S)	South southeast (SSE)	South southwest (SSW)	North (N)	North northwest (NNW)
Summer	55.0	13.0	20.5	2.0	21.0
Autumn	41.0	16.0	7.0	7.0	8.0
West Coast Mall					
Season	Frequency of counts (%)				
	South (S)	South southeast (SSE)	South southwest (SSW)	North (N)	North northwest (NNW)
Summer	52.0	10.0	18.0	-	-
Autumn	17.0	4.0	5.5	4.5	7.5
Vredenburg AQM Station					
Season	Frequency of counts (%)				
	South (S)	South southeast (SSE)	South southwest (SSW)	North (N)	North northwest (NNW)
Summer	20.5	44.0	16.5	3.0	2.0
Autumn	20.0	8.5	6.0	6.0	7.0
Winter	6	12.5	1.0	19.0	10.5

The Langebaan Area: Langebaan Private Home

The dominant wind directions associated with $PM_{2.5}$ concentrations in the Langebaan area (Langebaan Private Home) are summarised in Table 38 below. The dominant direction associated with $PM_{2.5}$ pollution was the S during Summer (0-29.9 µg/m^3) and Autumn (0-45.6 µg/m^3). The dominant direction associated with $PM_{2.5}$ pollution during Winter was the N, with $PM_{2.5}$ concentrations ranging between 0-42.9 µg/m^3.

Table 38: Dominant wind directions associated with $PM_{2.5}$ concentrations in the Langebaan area

Langebaan Private Home					
Season	Frequency of counts (%)				
	South (S)	South southeast (SSE)	South southwest (SSW)	North (N)	North northwest (NNW)
Summer	48.0	30.0	12.0	1.5	1.0
Autumn	32.0	13.5	7.5	8.0	10.0
Winter	9.5	15.0	2.0	20.0	15.0

The St. Helena Bay Area: St. Helena Bay Private Home

The dominant wind directions associated with $PM_{2.5}$ concentrations in the St. Helena Bay area (St. Helena Bay Private Home) are summarised in Table 39 below. The dominant direction associated with $PM_{2.5}$ pollution was the S during Autumn (0-61.8 µg/m^3) and the N during Winter (0-34.1 µg/m^3).

Table 39: Dominant wind directions associated with $PM_{2.5}$ concentrations in the St. Helena Bay area

St. Helena Bay Private Home					
Season	Frequency of counts (%)				
	South (S)	South southeast (SSE)	South southwest (SSW)	North (N)	North northwest (NNW)
Autumn	36.0	14.0	8.0	7.0	9.0
Winter	12.5	14.5	8.0	17.0	13.5

5.2. Chemical Composition of the Physical PM Samples

5.2.1. Mineralogical Composition of the Collected Physical PM Samples from the Dust Fallout Bucket and the BSNEs

The dust sub-sample from the dust fallout bucket contained 1.2% of the total sample collected. The dust fraction comprised mainly of quartz (37.3%), calcite (29.1%), hematite (21.2%), biotite (8.9%) and halite (3.6%) (Table 40). When compared to the major minerals found in the QEMSCAN analysis of the combined BSNE sample, it was found that the combined BSNE sample also contained a significant quantity of both quartz (45.2%) and hematite (12.8%) (Table 40) . Table 40 also indicates that the combined BSNE sample contains less carbonate minerals and a higher percentage of silicate minerals, which include feldspar (16.0%), mica (8.4%), kaolinite (2.6%), amphibole (1.9%), chlorite (0.6%) and epidote (0.2%). Other minerals found in the BSNE sample include carbonates (7.0%), apatite (0.9%), sulphides (1.1%), zircon (0.03%) as well as Ti-minerals such as, rutile and ilmenite at 0.2% and 0.1%, respectively (Table 40).

Table 40: Summary of the mineralogical composition of the dust fallout bucket (dust sub-sample) and the BSNE combined sample

Dust Fallout Bucket		BSNEs	
Dust Sub-Sample		Combined Sample	
Mineral	Mass%	Mineral	Mass%
Quartz	37.3	Quartz	45.2
Calcite	29.1	Feldspar	16.0
Hematite	21.2	Hematite	12.8
Biotite	8.9	Mica	8.4
Halite	3.6	Carbonates	7
		Other	2.9
		Kaolinite	2.6
		Amphibole	1.9
		Sulphides	1.1
		Apatite	0.9
		Chlorites	0.6
		Epidote	0.2
		Rutile/Anatase	0.2
		Ilmenite	0.1
		Zircon	0.03

By analysing the composition of the combined BSNE sample as a function of particle size, indicates that the minerals are not uniformly distributed across the different particle size fractions. The three smallest size fractions (<63 µm) make up 61.5% of the total mass and comprises most of the silicate minerals found in the sample. These include feldspar (78.2% of total of total), mica (92.5% of total), chlorite (100.0% of total), kaolinite (94.5% of total), amphibole (98.4% of total) and epidote (100.0% of total) (Table 41). The smaller size fractions

also contained the majority of the zircon (100 % of total), sulphides (93.0% of total), carbonates (74.8% of total), apatite (85.2% of total) and, Ti-minerals, rutile/anatase and ilmenite, both at 100.0% of total, as well as a significant quantities of the hematite (46.7% of total) and quartz (45.1% of total) (Table 41). This is indicative of the complexity across the different size fractions. Quartz and ilmenite were the only two minerals whose mass% consistently increased with increasing particle size from <5 to <63 µm, whereas minerals such as chlorite, kaolinite, amphibole, sulphides and apatite decreased with increasing particle size from <5 to <63 µm (Table 41). The three intermediate size fractions (63-100 µm, 100-125 µm and 125-150 µm) make up 19.6%, 10.4% and 2.6% of the total mass, respectively (Table 41). The size fraction 63-150 µm comprises of a variety of minerals and are distributed across these size fractions, with the % of distribution in brackets: quartz (51.5%), feldspar (20.5%), mica (7.4%), kaolinite (5.5%), amphibole (1.6%), sulphides (7.0%), hematite (21.4%), carbonates (25.2%), apatite (14.8%) and other (17.9%) (Table 41). The two largest size fractions (150-200 µm and 200-250 µm) make up 3.4% and 2.5% of the total mass, respectively. Hematite (31.9%) and quartz (3.5%) are also distributed across the 150-250 µm size fractions, with smaller amounts of feldspar (1.3%) and mica (0.1%) also found to be distributed in these size fractions (Table 41). In essence, the QEMSCAN analysis of the BSNE combined sample indicate that, while the silicates, heavy mineral sand minerals, apatite and sulphides occur largely as finer particles (<63 µm), hematite occurs in a range of particle sizes from <5-250 µm, with the majority (73.6%) occurring across the 20-125 µm size fractions. The majority of quartz (82.2%) and carbonates (59.8%) are distributed across the 20-125 µm size fractions (Table 41).

Table 41: The distribution of minerals across the different size fractions

Mineral	<5 µm	5-10 µm	10-20 µm	20-63 µm	63-100 µm	100-125 µm	125-150 µm	150-200 µm	200-250 µm	250-350 µm	350 µm
Quartz	1.5	3.0	7.4	33.3	30.7	18.3	2.5	0.5	3.0	-	-
Feldspar	8.2	10.1	16.0	43.9	14.6	5.0	1.0	1.3	-	-	-
Mica	15.6	20.6	26.0	30.3	5.1	2.0	0.2	-	-	-	-
Chlorite	21.3	21.3	30.2	27.2	-	-	-	-	-	-	-
Kaolinite	21.7	26.1	28.0	18.6	5.2	0.4	-	-	-	-	-
Amphibole	35.4	29.1	19.7	14.2	1.1	0.6	-	-	-	-	-
Epidote	14.4	22.8	27.8	35.0	-	-	-	-	-	-	-
Sulphides	24.2	18.4	21.0	29.4	7.0	-	-	-	-	-	-
Hematite	5.6	8.2	12.5	20.3	9.5	3.4	8.5	23.0	8.9	-	-
Rutile/ Anatase	11.6	9.8	22.3	56.3	-	-	-	-	-	-	-
Ilmenite	6.3	8.0	24.3	61.3	-	-	-	-	-	-	-
Carbonates	8.5	11.1	17.7	37.5	12.8	9.5	2.9	-	-	-	-
Zircon	-	-	-	100	-	-	-	-	-	-	-
Apatite	29.3	18.0	17.7	20.3	9.6	5.1	-	-	-	-	-
Other	8.8	9.0	13.3	50.9	17.9	-	-	-	-	-	-

*The values in the table are the % of the total mass of each mineral across the different size fractions. The extended table(s) can be found in Appendix J.

*The dashes indicate that there were no minerals present in those size ranges.

The variation in the distribution of the different minerals as a function of particle size as well as the tendency of minerals such as silicates (chlorite, kaolinite, and amphibole), sulphides, apatite and the Ti-minerals (rutile and ilmenite) to deport to the finer particle size fractions possibly explain the differences in composition of the BSNE and the dust fallout bucket samples. It was also found that the coarser particles in the BSNE sample containing lower to negligible concentrations of these minerals.

Some of the filter papers used in the gravimetric samplers were analysed using qualitative SEM-EDX. The analysis confirmed the presence of sodium chloride (halite), quartz, hematite, calcium carbonate (calcite), titanium dioxide (rutile/anatase) and manganese oxide around the municipality. Halite and hematite were found at most sampling sites, except the Langebaan Private Home. Quartz and calcite were found at all six sampling sites, while titanium dioxide was also found at most sampling sites, except the Saldanha AQM Station and the Langebaan Private Home. Manganese oxide was only found from filter papers collected at the West Coast Mall.

5.2.2. Elemental Composition of the Collected Physical PM Samples from the Dust Fallout Bucket and the Gravimetric Samplers

The salt fraction obtained from the dust fallout bucket at Blue Bay Lodge was analysed using quantitative XRF. The results indicate that the sample comprised largely of Na (35.0 wt%) and Cl (37.5 wt%). Minor elements found in the salt fraction include K (0.07 wt%), Si (0.06 wt%), Ca (0.02 wt%), S (1 464 ppm) and P (167 ppm) (Table 42). Trace of salts such as Ba, Rb and Sr were found between (10-15 ppm) and metals such as Zn, Cr, Ni, Zr, Cu and Pb were found between (7-9 ppm). Other metals including Ti, Ni, Co, U, Ga and Th were found between (1-4 ppm) (Table 42). The results indicate that from the major elements found, the salt fraction of the dust fallout bucket is largely comprised of sea salt, for which NaCl/Halite is the predominant mineral, which was also found in the dust sub-sample (Table 40). Other minor minerals found in the salt sub-sample, which are typically known to be present in sea salt include K, Ca and S (Canfield & Farquhar, 2009;Lee et al., 2017). As the salt fraction contained 98.8% of the total sample collected from the dust fallout bucket, it can be concluded that the dust fallout bucket at Blue Bay Lodge collected mainly sea salt from the dispersion of sea spray.

The filter papers that were analysed by ICP-MS and ICP-AES were two filter papers from the ARA N-FRM sampler at Blue Bay Lodge. One of the filter papers collected TSP and the other collected PM_{10}, with the major and minor element results presented in Table 42 below. From Table 42, it can be seen that the metal concentrations in the coarser TSP sample were significantly higher than the PM_{10} sample. It is likely that a significant portion of the Fe found is associated with hematite, which has been found both in the dust sub-sample of the dust fallout bucket and in the combined BSNE sample. The Ca and Mg could potentially present as the minerals calcite ($CaCO_3$) or dolomite ($CaMg(CO_3)_2$), although, another source of Mg is potentially the ocean. It is likely that the metals found on filter papers 1a and 1b are mainly associated with the silicate minerals found in the combined BSNE sample, based on the samples' mineralogy. The two main feldspar groups include plagioclase feldspars and alkali feldspars (Cairncross, 2004). The Al, Ca and Na found could possibly be associated to the plagioclase feldspars, which are known to comprise of Al and are both sodium- and calcium rich (Cairncross, 2004). The Al, Na and K could possibly be associated to the orthoclase feldspars, which are known to be potassium-bearing feldspars (Cairncross, 2004). The two common types of mica include biotite ($K(MgFe)_3AlSi_3O_{10}(OH)_2$) and muscovite ($KAl_2(Si_3Al)O_{10}(OH,F)_2$, with biotite present in the dust sub-sample of the dust fallout bucket. Therefore, the Al, K, Fe and Mg could potentially be associated with the minerals in the mica group mentioned above. The other two minerals that the metals in Table 42 below could also be associated to is the kaolinite ($Al_2O_32SiO_{22}H_2O$) and the amphibole group (containing Ca, Fe, Al and Mg) (Cairncross, 2004). Similar to the Mg, another source of Na could potentially be the halite in the sea spray and will be discussed further.

Table 42: Summary of the elemental composition of the salt sub-sample from the dust fallout bucket and the filter papers from the ARA N-FRM gravimetric sampler

Dust Fallout Bucket		ARA N-FRM Gravimetric Sampler		
Salt Sub-Sample				
Major Elements		Elements	Filter Paper 1a (TSP) ppm	Filter Paper 1b (PM_{10}) ppm
Element	wt%	Sodium	14 836	7 004
Sodium	35.0	Iron	6 039	1 661
Chlorine	37.5	Potassium	6 039	1 661
		Magnesium	2 452	1 036
Minor Elements		Calcium	2 162	968
Element	wt%	Aluminium	1 479	400
Potassium	0.07			
Silica	0.06			
Calcium	0.02			
Element	ppm			
Sulphur	1 464			
Phosphorus	167			
Trace Elements				
Element	ppm			
Barium	15			
Rubidium	10			
Strontium	10			
Zinc	9			
Chromium	8			
Nickel	8			
Zirconium	8			
Copper	7			
Lanthanum	7			
Lead	7			
Titanium	4			
Niobium	3			
Cobalt	2			
Uranium	2			
Gallium	1			
Thorium	1			

ICP-MS was also used to analyse for trace metal quantities on both filter papers 1a (TSP) and 1b (PM_{10}). Alkali earth metals such as Ba (41.2 and 13.5 ppm) and Sr (22.6 and 10.4 ppm) were found. Other trace metals were also found and included Pb (40.1 and 13.7 ppm), Cu (11.2 and 3.1 ppm), As (8.7 and 1.3 ppm), Ni (7.8 and 2.7 ppm), V (7.6 and 3.4 ppm), Cr (7.5 and 1.7 ppm), Se (2.0 and 1.0 ppm), Sn (1.5 and 0.6 ppm), Co (0.9 and 0.2 ppm), Cd (0.6 and

0.1 ppm), Mo (0.3 and 0.06 ppm) and Sb (0.01 and 0.01 ppm). Although present in trace amounts, it should be noted that toxic metals such as Pb and As were found, and will be discussed further.

5.2.3. Potential Origins of Dust-Bearing Minerals and Metals

It can be argued that many of the minerals and metals found in the physical PM samples can be attributed, at least partially to anthropogenic activities. The presence of both hematite (dust sub-sample of dust fallout bucket, combined BSNE sample and filter papers) as well as iron (filter papers) can almost be exclusively attributed to the transport, storage and handling of iron ore at the port as well as listed and non-listed facilities within the municipality. Apart from direct PM emissions, fugitive emissions have visibly contaminated the surrounding area, including both infrastructure and the soils. In addition to the storage facilities (listed and non-listed), the non-operational iron ore smelter (Arcelor Mittal) is also visibly contaminated with iron ore dust. At these sites, it is possible for the dust to become airborne either by anthropogenic activities such as handling, or by dispersion through meteorological conditions, such as wind (Gautam, Prusty & Patra, 2015). The Black Mountain Mine that is situated in the Northern Cape and run by Vedanta produces 40 000 tonnes of lead, 7 000 tonnes of copper and 250 000 tonnes of zinc concentrates annually (Global Africa Network, 2018;Vedanta, n.d.). Approximately a third of the annual concentrates that are produced are exported through the Port of Saldanha (Global Africa Network, 2018). Copper and lead were found in on both filter papers 1a and 1b from the gravimetric sampler (ARA N-FRM) at Blue Bay Lodge. Copper, lead and zinc were all found in the salt sub-sample from the combined dust fallout bucket sample also at Blue Bay Lodge. Manganese oxide was found from a filter paper obtained from the West Coast Mall. The possible origin of the manganese oxide could potentially be from the transport, handling and storage of the manganese oxide at the port as well as from the three non-listed companies.

Ti-minerals, such as ilmenite and rutile (found in the combined BSNE sample and on filter papers) as well as zircon are mined along the West Coast. The Tormin Mineral Sands Operation consists of beach as well as mineral sands deposits which comprise of high-grade garnet, ilmenite, magnetite, rutile and zircon (MRC Mineral Commodities, n.d.). The Namakwa Sands' mining operations include a mineral sand mine at Brand-se-Baai and a mineral separation plant, 7 km west of Koekenaap (Moumakwa, 2007). The mineral sand mine consists of a mine as well as a primary and secondary concentrate plant and the mineral separation plant separates the ilmenite, rutile and zircon products. The concentrates are then transported to the Tronox Namakwa Sands Smelter in Saldanha where they are processed (Tronox, 2020). Furthermore, the ilmenite produced is further processes to produce rutile/anatase slag and pig iron. Additionally, zircon and rutile and stored at the Tronox Namakwa Sands Smelter until export. Additionally, excess CO gas from the ilmenite smelting process is flared into at the atmosphere (Gous, 2006). Although the composition of the excess gas is unknown, it should be noted that this gas could potentially contain harmful toxins that

could cause health implications. The non-listed Company 2 is also known to store and transport ilmenite (Costa, 2022).

Activities such as mining, processing, transporting and handling of minerals, as well as meteorological conditions, contribute to the exposure and dispersion of the mineral ores. The carbonate mineral limestone (calcite and found in the dust sub-sample and the filter papers and Ca found in the salt sub-sample in the salt sub-sample) and the phosphorus mineral apatite (combined BSNE sample and P found in the salt sub sample) both occur naturally along the West Coast. According to Syers et al. (1967), apatite inclusions are commonly found in beach sands, which are mined along the West Coast. The limestone mine is known as the Tabakbaai Quarry and is owned by NPC (Halkett, 2011).

It is also likely that the majority of the quartz and other silica-bearing minerals, originate from natural sources. Quartz was found most abundantly in both the dust sub-sample from the dust fallout bucket (33.9%) and in the combined BSNE sample (45.2%). The Minerals Education Coalition (2022) has stated that beach sand is usually composed of quartz and since all the sites where quartz was found was near the ocean, it is likely that beach sand is the reason for the presence of quartz. The West Coast, along which the Saldanha Bay Municipality is located, forms part of the Cape Granite Suite (CGS) and is known as the West Coast Peninsula, which is dominated by a granite geology (Le Roux, Bezuidenhout & Smit, 2019). According to Cairncross (2004), granite mainly comprises of quartz and feldspar group silicates (which include potassium-bearing orthoclase as well as microcline). Another feldspar that is found in granite is albite, which is part of the plagioclase group (Cairncross, 2004). Some of the other minerals found in granite include mica (muscovite more commonly than biotite), and a mineral 'hornblende' which typically forms part of the amphibole group of minerals (Cairncross, 2004). Kaolinite, a clay mineral also found in granite, is formed through the chemical breakdown of alkali feldspars (Cairncross, 2004). Additionally, according to Broska et al. (2002), accessory minerals that occur in granite that have been found in the results obtained include apatite, rutile and zircon.

Analysis of the gravimetric PM samples that were collected at Blue Bay Lodge, indicated the presence of trace metals such as Cu and Pb. According to a study carried out by Palero-Fernández and Martín-Izard (2005), some of the trace metals that are typically found in galena, and have been found at Blue Bay Lodge include Fe, Zn, Sb, Cu, Ni, Cd, Sr, Co, As, and Se. However, these metals can also occur as trace metals in natural soils (Taylor & McLennan, 1995). Sulphides found in the combined BSNE sample, could potentially originate from pyrite present in the granitic soils and rocks around the municipality. The trace mineral barium is a naturally occurring element found in the earths' crust especially in coal, igneous rocks, sandstone and shale. It is also known to occur naturally in the environment through the weathering of minerals and rocks (United States Department of Health and Human Services, 2022a). Similarly, strontium is known to be ubiquitous in nature and is found in almost all rocks and soils (Höllriegl, 2019). The (United States Environmental Protection Agency, 2022c) have also stated that phosphorus and potassium are usually found in fertilizers.

5.3. Potential Anthropogenic Sources of PM Emissions

The Saldanha Area: Blue Bay Lodge and the Saldanha AQM Station

At Blue Bay Lodge, the pollution roses indicated that the dominant directions associated with $PM_{2.5}$ concentrations included the S and SSE during Summer 2021, Autumn and Spring. During Winter, the dominant directions included the SSE, N and NNW, and S and SSW during Summer 2021/2022. The polar plots indicate that during Summer 2021, mean $PM_{2.5}$ concentrations between 0-10 µg/m^3 were experienced between 0-7 m/s (N-E) and 0-12 m/s (S-E). Mean $PM_{2.5}$ concentrations between 0-5 µg/m^3 were experienced between 0-12 m/s (S-W) and 0-7.5 m/s (N-W), The polar plot for Autumn indicated that mean $PM_{2.5}$ concentrations between 0-5 µg/m^3 were experienced from all directions between wind speeds of 0-9 m/s (N-E), 0-10 m/s (S-E and S-W) and 0-10.5 m/s (N-W). Similarly for Spring, mean $PM_{2.5}$ concentrations between 0-5 µg/m^3 were experienced from all directions between wind speeds of 0-9 m/s (N-E), 0-12 m/s (S-E, S-W and N-W). Finally, for Summer 2021/2022, mean $PM_{2.5}$ concentrations between 0-5 µg/m^3 were experienced from all directions between wind speeds of 0-7 m/s (N-E), 0-11 m/s (S-E and S-W) and 0-9 m/s (N-W). During Winter, it was found that high mean concentrations of 15-20 µg/m^3 were experienced between 7-9 m/s associated with wind from the N/NNE. These wind speeds experienced at Blue Bay Lodge range between moderate to strong breezes (Northeastern Regional Association of Coastal Ocean Observing Systems, n.d.). It is generally agreed upon that the threshold value for PM to become airborne is between the range of 4-7 m/s (Visser & Cornelis, 2004). Therefore, is possible that all the potential sources of emission indicated on Figure 76 below could possibly contribute to $PM_{2.5}$ concentrations at Blue Bay Lodge. Based on the results from the pollution roses, the potential source of emission is the non-listed company 3 (MPT). However, based on the results from the dust fallout bucket, the BSNEs and the filter papers, the potential anthropogenic sources of emission include the Transnet Iron Ore Terminal, Tabakbaai Quarry, Tronox Namakwa Sands, non-listed company 2 and Pindulo VDM.

At the Saldanha AQM Station, the pollution roses indicated that the dominant directions associated with $PM_{2.5}$ concentrations included the S and SSE during Summer, Autumn and Spring and the S, SSE and N during Winter. Unfortunately, due to insufficient information, the polar plot for Summer could not be constructed. The polar plots indicate that during Autumn 2021, mean $PM_{2.5}$ concentrations between 0-10 µg/m^3 were experienced between 0-9 m/s (N-E), 0-10 m/s (S-E and S-W) 0-10.5 m/s (N-W). From the Winter polar plot, it was found that mean $PM_{2.5}$ concentrations in the 10-15 µg/m^3 range were associated with wind from the N/NNE (6-10 m/s), ENE (0-6 m/s), ESE, SSE and SSW (0-4 m/s), WSW, WNW and NNW (0-2 m/s). Lastly, the polar plot for Spring indicated that concentrations between 0-10 µg/m^3 were experienced between 0-9.5 m/s (N-E), 0-11 m/s (S-E) and 0-9 m/s (S-W and N-W). Although there are no anthropogenic sources in the dominant directions from the pollution roses, based on the mean $PM_{2.5}$ concentrations and wind speeds from the polar plots and the physical PM results, the potential sources of emission include the listed company, non-listed companies 1A, B and 2, Tronox Namakwa Sands, Pindulo VDM, Transnet Iron Ore Terminal, MPT and Tabakbaai Quarry.

Figure 76: Potential sources of emission relative to Blue Bay Lodge and the Saldanha AQM Station

The Vredenburg Area: Louwville Private Home, the West Coast Mall and the Vredenburg AQM Station

At the Louwville Private Home, the pollution roses indicated that the dominant directions associated with $PM_{2.5}$ concentrations included the S, SSW and NNW during Summer and S and the SSE during Autumn. Unfortunately, due to insufficient information, the polar plot for Summer could not be constructed. The polar plot for Autumn indicated that mean $PM_{2.5}$ concentrations between 0-5 µg/m^3 were experienced from all directions at the Louwville Private Home between wind speeds of 0-9 m/s (N-E), 0-10 m/s (S-E and S-W) and 0-11 m/s (N-W). This indicates that all the sources of emission in Figure 77 below could possibly contribute to $PM_{2.5}$ concentrations at the Private Home, as the wind speeds indicates fresh to strong breezes experienced (Northeastern Regional Association of Coastal Ocean Observing Systems, n.d.). Additionally, based on the pollution rose, there are no anthropogenic sources of emission SSW, SSE and NNW of the Private Home, however, from the S, the potential sources of emission include Pindulo VDM, the Transnet Iron Ore Terminal and the non-listed company 3 (MPT). Furthermore, the presence of hematite, calcium carbonate and titanium dioxide on the filter paper collected from the Louwville Private Home indicate potential sources of emission such as the Transnet Iron Ore Terminal and the non-listed company 3 (MPT),

Tabakbaai Quarry and Tronox Namakwa Sands. The Afrimat Aggregates and Quarry, where quarzitic sandstone is mined, could also potentially be sources of emission due to quartz found on the filter paper.

At the West Coast Mall, the pollution roses indicated that the dominant directions associated with $PM_{2.5}$ concentrations included the S and SSW during Summer and S during Autumn. The polar plot for Summer indicated that mean $PM_{2.5}$ concentrations between 0-5 µg/m^3 were experienced from all directions between the S-E and the S-W between 0-11 m/s. Whereas, mean $PM_{2.5}$ concentrations between 0-10 µg/m^3 were experienced between the N-W and the N-E between 0-7.5 m/s and 0-7 m/s, respectively. Additionally, the polar plot for Summer also indicated mean $PM_{2.5}$ concentrations between 10-15 µg/m^3 between 4-8 m/s from the SE. The polar plot for Autumn indicated that mean $PM_{2.5}$ concentrations of 0-5 µg/m^3 were experienced at 0-7 m/s (N-E), 0-10 m/s (S-E and S-W) and 0-10.5 m/s (N-W). This indicates that it is possible that all potential sources of emission south of the West Coast Mall (Figure 77), could potentially contribute to $PM_{2.5}$ concentrations measured at the Mall, as the wind speeds indicates a fresh breeze experienced (Northeastern Regional Association of Coastal Ocean Observing Systems, n.d.). Although low mean $PM_{2.5}$ concentrations were experienced from the ENE and the NE, the Afrimat Aggregates and Quarry could also potentially contribute to $PM_{2.5}$ concentrations at the West Coast Mall, it must be emphasized that they are approximately 19 km apart and wind speeds experienced from those directions are classified as a gentle breeze and lower (Northeastern Regional Association of Coastal Ocean Observing Systems, n.d.). With regards to the pollution roses, there are no anthropogenic sources of emission SSW of the West Coast Mall, however, Pindulo VDM, Transnet Iron Ore Terminal and the MPT are potential sources of emission from the S. Furthermore, based on the results from the filter paper, the potential sources of emission include the Transnet Iron Ore Terminal, MPT, Tabakbaai Quarry, Tronox Namakwa Sands and non-listed companies 1A, B and 2.

At the Vredenburg AQM Station, the pollution roses indicated that the dominant directions associated with $PM_{2.5}$ concentrations included the S, SSE and SSW during Summer, the S in Autumn and the SSE, N and NNW in Winter. Unfortunately, due to insufficient information, the polar plot for Summer could not be constructed. The polar plot for Autumn indicated that mean $PM_{2.5}$ concentrations between 0-5 µg/m^3 were experienced from all directions at 0-9 m/s (N-E), 0-10 m/s (S-E and S-W) and 0-10.5 m/s (N-W). This indicates that all potential sources of emissions shown in Figure 77 below could possibly contribute to $PM_{2.5}$ concentrations at the Vredenburg AQM Station, as the wind speeds experienced at the Station can be classified as a fresh breeze (Northeastern Regional Association of Coastal Ocean Observing Systems, n.d.). During Winter, mean $PM_{2.5}$ concentrations between 10-15 µg/m^3 were experienced from the N/NNE (6-10 m/s), NNW (0-2 m/s) and WSW (6-8 m/s). It is worth noting that although there are no anthropogenic sources in these directions, the Station was installed on the grounds of the Vredenburg High School and therefore, the high mean $PM_{2.5}$ concentrations could be a result of other activities unrelated to minerals, such as mowing the grounds and other school activities. From the pollution roses, the potential sources of emission include

Pindulo VDM, Transnet Iron Ore Terminal, MPT and Tabakbaai Quarry. Unfortunately, due to no gravimetric sampler installed at the Station, there are no results from physical samples.

Figure 77: Potential sources of emission relative to the West Coast Mall, Louwville Private Home and the Vredenburg AQM Station

The Langebaan Private Home

At the Langebaan Private Home, the pollution roses indicated that the dominant directions associated with $PM_{2.5}$ concentrations included the S and SSE during Summer and Autumn and the SSE, N and NNW during Winter. Unfortunately, due to insufficient information, the polar plot for Summer could not be constructed. The polar plot for Autumn indicated that mean $PM_{2.5}$ concentrations between 0-5 µg/m^3 were experienced from all directions at 0-9 m/s (N-E), 0-10 m/s (S-E and S-W) and 0-10.5 m/s (N-W). This indicates that all potential sources of emissions shown in Figure 78 below could possibly contribute to $PM_{2.5}$ concentrations at the Vredenburg AQM Station, as the wind speeds experienced at the Station can be classified as a fresh breeze (Northeastern Regional Association of Coastal Ocean Observing Systems, n.d.). Whilst for Winter the polar plot indicated mean high concentrations between 15-20 µg/m^3 between 6-10 m/s associated with wind from the N/NNE and from the W between 0-2 m/s. Wind speeds at 10 m/s and 2 m/s can be classified as fresh and light breeze, respectively (Northeastern Regional Association of Coastal Ocean Observing Systems, n.d.). Therefore, based on the results of the pollution roses, the potential sources of emission include the listed

company, non-listed companies 1A, 1B and 2 and Tronox Namakwa Sands. It must be noted that although the S and the SSE were dominant directions associated with $PM_{2.5}$ concentrations, there are no anthropogenic potential sources of emission in those directions. Based on the results from the filter papers which indicated the presence of calcium carbonate, the other potential source of emission includes the Tabakbaai Quarry, which although is situated NW of the Langebaan Private Home, is approximately 23 km away. The Afrimat Aggregates could potentially also contribute to $PM_{2.5}$ concentrations at the Langebaan Private Home, however, the wind speeds were between 0-9 m/s from that direction and is situated approximately 28 km away.

Figure 78: Potential sources of emission relative to the Langebaan Private Home

The St. Helena Bay Private Home

At the St. Helena Bay Private Home, the pollution roses indicated that the dominant directions associated with $PM_{2.5}$ concentrations included the S and SSE during Autumn and the S, SSE, N and NNW during Winter. The polar plot for Autumn indicated that mean $PM_{2.5}$ concentrations between 0-5 µg/m^3 were experienced from all directions at 0-9 m/s (N-E), 0-10 m/s (S-E and S-W) and 0-10.5 m/s (N-W). Whilst for Winter the polar plot indicated mean high concentrations between 15-20 µg/m^3 between 6-10 m/s associated with wind from the N/NNE, with these wind speeds classified as a fresh breeze (Northeastern Regional Association of Coastal Ocean Observing Systems, n.d.). Based on the pollution roses, the potential sources

of emission include the Transnet Iron Ore Terminal, Pindulo VDM, MPT, Tronox Namakwa Sands, the listed company and the non-listed companies 1A, B and 2. Additionally, based on the filter paper results, another potential source of emission includes the Tabakbaai Quarry. It must be emphasized that although wind speeds of up to 10.5 m/s were experienced at the Private Home, all the abovementioned potential sources of emission are situated far south, with the Transnet Iron Ore Terminal situated approximately 41 km away. It should also be noted that there are no anthropogenic sources N and NNW of the Private Home.

Figure 79: Potential sources of emission relative to the St. Helena Bay Private Home

5.4. Potential Human Health Implications of PM Contamination

5.4.1. Potential PM Health Implications

The following section focuses on discussing the potential health risks that could occur from PM exposure, however, it should be emphasized that a health risk assessment was not considered as part of the scope of the study. In terms of PM concentrations, no exceedances of $PM_{2.5}$ and PM_{10} were reported at any of the seven study sites over the respective sampling period according to NAAQS. However, there were exceedances according to the WHO guidelines (based on the results presented in Section 4.1.1). According to the World Health Organisation (2021), the effect of PM exposure can lead to major health risks, which include respiratory and cardiovascular complications, which are known to be two of the major causes of mortality on a global scale.

The combined BSNE sample analysed by QEMSCAN – which was the only sample for which the particle size distribution was analysed – displayed ~66% of the total particles in the <5 µm size bin. Although the QEMSCAN results do not provide the number of particles that are less than 2.5 µm, it is reasonable to assume that a proportion of the particles in the <5 µm bin could be classed as $PM_{2.5}$ and would therefore be categorised as respirable. Given the fact that particles less than 2.5 microns have the potential to enter into the bloodstream, such high proportions of particles in the category of <5 µm raises a concern on the potential downstream health effects that may result. As previously mentioned, Gautam et al. (2016) that toxins that fall into the respirable fraction (4.25 µm) might have a chemical reaction with the human respiratory system as well as allow the transfer of said toxins via the alveolar walls into the bloodstream. The PM_{10} size bin (5-10 µm) contains approximately 21% of the total particles and although it is not as high as the <5 µm size bin, it is also a concern regarding the impact that PM_{10} has on human health and its potential to enter into the lower lung. This is due to that these particles can be classified as inhalable, which can settle anywhere along the upper respiratory tract (World Health Organisation, 1999; Petavratzi, Kingman & Lowndes, 2005; Brown et al., 2013).

From the normalised dust fall rates, it was found that for each dust fallout bucket, the dust fall rate was significantly higher than the acceptable limit of 1200 mg/m^2/day, according to South African Legislation. Although the dust fall rates exceeded the acceptable limits, results from both the XRD and XRF did not provide any indication on particulate size of the dust and salt sub-samples. However, it is important to acknowledge that potentially toxic elements, such as lead and uranium, were found in the analysis of the salt sub-sample and therefore, it is important to highlight the potential health risk of these elements given the solubility of salts under biologically relevant conditions.

5.4.2. Potential Health Implications from Minerals/Elements found in the Physical PM Samples

According to Kamanzi et al. (2023), ~1.35 million deaths are due to chronic respiratory diseases caused by exposure to mineral dust. In discussing the factors leading to such diseases on a particle level, this study additionally highlighted the importance of determining the physical characteristics and mineral composition of dust to understand its risk potential. Based on this the mineral composition and dust concentration of the physical PM samples that were collected from the dust fallout buckets, the BSNEs and the filter papers from the gravimetric samplers were assessed. Based on the results obtained, the human health implications are discussed further.

Quartz was found in both the dust sub-sample from the dust fallout bucket and in the combined BSNE sample. However, from the QEMSCAN analysis of the BSNE sample, it was found that quartz was present in the <5 µm size fraction (9.7 mass%). As previously mentioned, this size category consists of both inhalable and respirable size fractions, with the focus on the respirable size fractions. In terms of health effects, silicosis has been identified as a major health challenge and is defined as an irreversible lung disease caused by the inhalation of crystalline silica, with the most common type being quartz (Mossman & Churg, 1998;Hoy et al., 2022). Furthermore, it has been reported that quartz particles that are respirable have been classified as a carcinogen (Hoy et al., 2022).

Hematite was also found in both the dust sub-sample from the dust fallout bucket and in the combined BSNE sample. In the combined BSNE sample, hematite was present in the <5 µm size fraction (10.6 mass%). The concern around both inhalable and respirable particulates in this size fraction is the same as those mentioned for quartz above. Lung cancer is one of the many diseases that are found amongst those exposed to iron ore particulates, as these particulates are known to coat the surface of the lungs (Oliveira, Cacodcar & Motghare, 2014; Senthil Kumar & Rajkumar, 2014). Boyd et al. (1970) have reported that over a period of 19 years, there were several deaths of miners employed at an iron ore mine: 47 deaths were attributed to lung cancer; 74 deaths to other types of cancer and 174 deaths due to respiratory diseases. Chronic inhalation of hematite dust particulates could also result in a lung disease called pneumosiderosis, also known as Welder's lung (Khalid, Khalid & Jennings, 2009; Senthil Kumar & Rajkumar, 2014).

According to the NAAQS, the only pollutant outlined, which was subsequently found in the results of this study, is lead. Lead was found at 7 ppm in the salt sub-sample of the dust fallout bucket and on filter papers 1a (0.0019 µg/m^3) and 1b (0.00035 µg/m^3). The acceptable concentration of lead according to NAAQS is 0.5 µg/m^3, and therefore, the concentrations of lead found on both filter papers are below the acceptable limit. However, it is important to highlight the potential health implications associated with exposure to lead. Some of the health risks associated with lead exposure includes effects on the brain and the central nervous system of children, which subsequently results in convulsions as well as death (World Health Organisation, 2019). Exposure to lead can also affect the development of the brain, anaemia, hypertension and is known to be toxic to the reproductive system, amongst other health effects

(World Health Organisation, 2019). Other sulphur-bearing minerals that exist in granitic rocks and soils is pyrite and based on the results from a study carried out by Harrington, Hylton and Schoonen (2012), it has been reported that pyrite particles, 1 µm in size, can exist in human lungs for more than a year. Additionally, it has been reported that pyrite is also responsible for the damage of human lung tissue (Harrington, Hylton & Schoonen, 2012).

Although it is not South African legislation, concentration limits values have been outlined by the EU in the 4th Daughter Directive for arsenic (0.006 µg/m^3 = 6 ng/m^3), cadmium (0.005 µg/m^3 = 5 ng/m^3) and nickel (0.02 µg/m^3 = 20 ng/m^3). Arsenic and cadmium (within filter paper-based samples) as well as nickel (on filter paper and salt sub-samples) were all found as trace metals. From Table 43 below, the concentrations of these three pollutants found on the two filter papers are lower than the acceptable concentrations outlined by the 4th Daughter Directive. However, it is important to highlight potential health implications based on exposure to these pollutants, which although are below acceptable limits, are still present. According to Hong, Song and Chung (2014), arsenic is the only known carcinogen that causes cancer via both gastrointestinal and respiratory exposure. Extensive research has been conducted on the health effects of arsenic and some of the cancers associated are skin, lung, bladder, liver, prostrate and leukaemia (Hong, Song & Chung, 2014). There are also other non-carcinogen health effects such as the impact on memory and neurological effects, diabetes, skin disorders, cardiovascular diseases and effects on the reproductive system (Hong, Song & Chung, 2014). Respirable cadmium-rich particulates can negatively affect human health by causing the build-up of fluid in the lungs and shortness of breath (Seidal et al., 1993). Furthermore, Barbier et al. (2005) have reported that chronic exposure to cadmium ultimately results in kidney damage. According to Genchi et al. (2020), exposure to nickel-rich particulates through inhalation results in toxicity of the immune system, lung as well as the respiratory tract.

Table 43: Concentrations of pollutants found on filter papers from ARA N-FRM for comparison to EU Standards

Pollutant	Filter Paper 1a (ng/m^3)	Filter Paper 1b (ng/m^3)
Arsenic	0.42	0.079
Cadmium	0.029	0.006
Nickel	0.38	0.17

Other trace metals which are potentially harmful and were found in the salt sub-sample include thorium and uranium. According to the Agency for Toxic Substances and Disease Registry (2015), the exposure to uranium through inhalation or ingestion of uranium and uranium compounds has resulted in kidney damage, found in both humans and animals. However, the Agency for Toxic Substances and Disease Registry (2015) has also reported that insoluble uranium compounds that have been inhaled can also damage the respiratory tract. According to the National Cancer Institute (2022), the inhalation of thorium-bearing dust increases the risk of contracting lung and pancreatic cancer. However, thorium may also be stored in the

bones of human, and therefore, exposure to thorium might also potentially increase the risk of contracting bone cancer (National Cancer Institute, 2022).

Other elements such as copper, zirconium, vanadium and manganese are essential at lower concentrations but could potentially cause harmful effects at higher concentrations and occur more abundantly in natural environments. According to the United States Department of Health and Human Services (2022b), copper is generally essential for good human health, however, exposure to higher doses of copper can have harmful effects on human health. Long-term exposure to copper-containing dust can cause nose, mouth and eye irritations. A study carried out by Yu et al. (2016) concluded that the health effects that are associated with the inhalation of zirconium dust includes injury of the respiratory system, pneumoconiosis, dysfunction of the immune system as well as the impairment of liver. According to the New Jersey Department of Health and Senior Services (2007), contact with vanadium dust can result in irritation of the skin, eyes, nose, throat and lungs. Continued exposure to dust-bearing manganese could potentially cause damage to organs such as the kidney, liver and the lungs. Exposure to dust containing manganese can also result in the development of manganism, which is a neurological condition whose symptoms are similar to Parkinson's disease (National Institute for Occupational Safety and Health, 2019). Ultimately, the extent of the health risks of these elements depends on whether they are able to travel to different organs through the blood. This implies that having a robust understanding of the host minerals and element profiles of respirable dust becomes key to managing the health risks associated with mineral dust.

CHAPTER 6: CONCLUSIONS AND RECOMMENDATIONS

Whilst mining contributes to both local and national economies, it can also have a significant impact on the surrounding environment. An example of one of these impacts is air pollution through the emission of particulate matter (PM). PM varies in size, however, PM with an aerodynamic diameter of less than 2.5 µm ($PM_{2.5}$) and 10 µm (PM_{10}) is of particular concern due to its ability to degrade air quality and pose health risks to surrounding communities. Although metal-bearing dust is typically linked to mining operations and large-scale waste deposits, activities such as the transport, stockpiling and handling of ores can also disperse metal-bearing dust, which can subsequently impact communities located far from the mine itself. The overarching aim of this study was to assess PM concentrations and compositions of ambient dust in the Saldanha Bay Municipality and based on these results, to assess the potential sources and health implications of these dust emissions. The aim of this study was accomplished through PM monitoring and physical PM sample collection to answer the following key research questions:

i. What are the concentration profiles of PM at the key study sites within the region?
ii. What are the chemical and physical characteristics of the collected PM samples?
iii. Based on the results from (i) and (ii), what are the potential sources of emission that contribute to PM contamination in the Saldanha Bay municipality?
iv. Based on the results from (i) and (ii), what are the potential health implications?

6.1. Research Findings

6.1.1. Concentration Profiles of PM at the Key Study Sites within the Region

The $PM_{2.5}$ and PM_{10} concentrations obtained from the PurpleAir Particulate Sensors were aggregated to hourly and 24-hour concentrations. However, it was found that by aggregating the data to 24-hour averages dampens the $PM_{2.5}$ and PM_{10} concentrations when comparing the upper range limits between hourly and 24-hour data. PurpleAir Sensors are known to overestimate $PM_{2.5}$ concentrations by ~40%, and therefore, the $PM_{2.5}$ concentrations were corrected for the overestimate as well as for humidity using a correction equation. Subsequently, it was found that the corrected $PM_{2.5}$ concentrations were lower than the uncorrected concentrations. When compared to the NAAQS, it was found that there were no exceedances for both $PM_{2.5}$ and PM_{10} at any of the study sites. It must be noted that due to the limited monitoring period, this could not be compared to the annual standard. According to the WHO guidelines, exceedances of $PM_{2.5}$ concentrations occurred at Blue Bay Lodge, the Saldanha and the Vredenburg AQM Stations as well as the St. Helena Bay and Langebaan Private Homes. There was also one PM_{10} exceedance at the St. Helena Bay Private Home. Based on the boxplots constructed using the hourly and 24-hour averages of both $PM_{2.5}$ and PM_{10} concentrations, it was found that Q1, Q2 and Q3 values were higher for the hourly $PM_{2.5}$ concentrations compared to the 24-hour concentrations. However, it was found that the upper range values for the hourly concentrations were higher than the upper range values for the

24-hour concentrations, which indicate that the outliers for hourly $PM_{2.5}$ concentrations are higher compared to the 24-hour values. It was also noted that the maximum values for the hourly concentrations were higher than the 24-hour concentrations. Another finding was the occurrence of extreme outliers, which in this study, are defined as random spikes in PM concentrations, possibly resulting from a fault within the sensor. These outliers were highlighted by investigating the PM concentrations measured at all seven study sites. It was also found that most of the exceedances of $PM_{2.5}$ and PM_{10} concentrations occurred in winter when rain is mostly experienced. However, this was purely an observation, as it is based on the concentrations measured by the PurpleAir Particulate Sensors. While it is agreed that rain is expected to decrease concentrations, due to its scrubbing action, these higher concentrations could potentially be partially unrelated to mineral sources. For instance, temperature inversions are common during the winter months, where cool air is trapped near the ground by a layer of warm air. This subsequently prevents pollutants, such as PM, from dispersing. Furthermore, it should also be noted that during winter, there is an increase in heating and/or vehicles, which may inadvertently contribute to the levels of PM (Ha et al., 2023).

The % capture for each month at each study site was also calculated to confirm that the capture was 80% and above, for the authenticity of the data. The three sites where the % capture was <80% was Blue Bay Lodge (2 months) and the Louwville Private Home (1 month). The reasoning behind the low % capture was disconnection from the power source at Blue Bay Lodge and the West Coast Mall and monitoring for a short period at the end of the month at the Louwville Private Home. The correlation between the uncorrected $PM_{2.5}$ concentrations and relative humidity at each study site were found to be very weak, which ultimately indicated that the particulates measured by the sensor were not water vapour droplets from the atmosphere.

PM concentrations were also plotted as a function of both wind direction and speed in the form of pollution roses and polar plots. The pollution roses were plotted using the $PM_{2.5}$ and PM_{10} concentrations from all study sites and provided the pollution direction that these concentrations were associated with. The polar plots were also constructed which indicated the pollution directions and wind speeds associated with mean $PM_{2.5}$ and PM_{10} concentrations. It was found that during Spring and Summer, the dominant directions that PM pollution were associated with included the S, SSE and SSW. However, significant PM pollution was also associated with wind from the N and the NNW during Autumn and Winter. The results from the pollution roses and the polar plots assisted in determining the potential sources of emission in the municipality.

6.1.2. Chemical and Physical Characteristics of the Collected PM Samples

Physical PM samples were collected using dust fallout buckets, BSNEs and gravimetric samplers. The normalised dust fall rate over a 30-day sampling period of the samples collected from the four dust fallout buckets were higher than the South African acceptable dust fall rate.

The four samples from the buckets were combined into one sample, which was further separated into dust and salt sub-samples. The dust sub-sample is predominantly comprised for quartz (37.3 mass%), calcite (29.1 mass%) and hematite (21.2 mass%). Biotite (8.9 mass%) and halite (3.6 mass%) were also found in the sample. It was found that the salt sub-sample was predominantly comprised of sodium chloride/halite, however, potentially toxic trace elements such as lead (7 ppm), uranium (2 ppm) and thorium (1 ppm) were also found in the salt sub-sample, amongst other elements.

The combined sample from the BSNE was comprised of samples collected from both Blue Bay Lodge and the Saldanha AQM Station. The sample is predominantly comprised of quartz (45.2 wt%), feldspar (16.0 wt%) and hematite (12.8 wt%). There is also the presence of aluminosilicates such as amphibole, chlorite as well as epidote; clay minerals such as kaolinite and mica; titanium minerals such as ilmenite and rutile/anatase; apatite, carbonates, sulphides, zircon and a group of unclassified minerals. A total number of 69 931 particles were scanned from the combined BSNE sample with size bins ranging from <5 - <250 µm. The relationship between particle size and the number of particles in each size bin is inversely proportional as the <5 µm size bin contained 65.9% of particles, whilst the 200-250 µm size bin contained 0.0057% of particles.

The two filter papers from the ARA N-FRM at Blue Bay Lodge analysed by ICP-MS and ICP-AES captured TSP (1a) and PM_{10} (1b). The results from the filter papers indicated that elements found in high concentrations included sodium, iron, potassium, calcium, and aluminium. However, trace elements were also found in the ICP-AES analysis, which included potentially toxic elements, such as arsenic and lead. The other filter papers analysed quantitatively by SEM-EDX indicated that minerals such as sodium chloride, quartz, and calcium carbonate at six of the study sites. Hematite and titanium dioxide both were found at all study sites, except for the Langebaan Private Home. Manganese oxide was only found at the West Coast Mall.

6.1.3. The Potential Anthropogenic Sources that Contribute to PM contamination in the Saldanha Bay Municipality

The potential sources of emission that are listed here have been concluded from the analysis of the pollution roses, polar plots, and the physical PM samples. In the Saldanha area, the potential sources of emission include the Transnet Iron Ore Terminal, the MPT (non-listed company 3), Tabakbaai Quarry, Tronox Namakwa Sands, Pindulo VDM and non-listed companies 1A, B and 2. In the Vredenburg area, the potential sources of emission highlighted were the same as those for the Saldanha area, with the addition of the Afrimat Aggregates and Quarry. The potential sources of emission for the Langebaan area included Tronox Namakwa Sands, Afrimat Aggregates, Tabakbaai Quarry and non-listed companies 1A, B and 2. In the St. Helena Bay area, the potential sources of emission include the Transnet Iron Ore Terminal, the MPT (non-listed company 3), Pindulo VDM, Tronox Namakwa Sands, Tabakbaai Quarry, the listed company and the non-listed companies 1A, B and 2.

6.1.4. The Potential Health Implications

Although no $PM_{2.5}$ and PM_{10} exceedances were reported at any sites according to the NAAQS, there were exceedances according to the WHO guidelines. The effect of PM exposure can lead to major health risks, which include respiratory and cardiovascular complications, which are known to be two of the major causes of mortality on a global scale (World Health Organisation, 2021). In the combined BSNE sample, 65.9% of particles were in the <5 µm size fraction, with a possibility that some of the particles could be <2.5 µm, which are classified as respirable particulates. Furthermore, 21.0% of the total particles were found in the 5-10 µm size fraction, which are classified as inhalable particulates, with the potential to enter the lower lung.

Quartz was the dominant mineral in both the dust sub-sample and the combined BSNE sample, with 9.7 mass% present in the <5 µm size fraction in the latter. Silicosis has been identified as a major health challenge and is defined as an irreversible lung disease caused by the inhalation of crystalline silica, with the most common type being quartz (Mossman & Churg, 1998; Hoy et al., 2022). According to Hoy et al. (2022), quartz particles that are respirable are also classified as a carcinogen. Hematite was found in the dust sub-sample, combined BSNE sample and quantitatively on filter papers and lung cancer is one of the many diseases that are found amongst those exposed to iron ore particulates, as these particulates are known to coat the surface of the lungs (Oliveira, Cacodcar & Motghare, 2014; Senthil Kumar & Rajkumar, 2014).

Lead was the only element found in this study, whose concentration limit has been outlined by the NAAQS. Although the concentrations of lead found in the salt sub-sample and on the filter papers from the ARA N-FRM were below the acceptable limit, it is important to highlight its presence and the potential health implications associated with it. Lead can affect the development of the brain, anaemia, hypertension and is known to be toxic to the reproductive system, amongst other health effects (World Health Organisation, 2019). Concentration limits for arsenic, cadmium and nickel have been outlined in the 4th Daughter Directives and although all concentrations of these three elements were found to be lower than the acceptable limit, there are toxic effects that they could potentially have on human health. These include cancer due to arsenic exposure, fluid build-up in the lung and kidney damage from cadmium and toxic effects on the lung and respiratory tract from nickel-rich particulate exposure (Hong, Song & Chung, 2014; Seidal et al., 1993; Barbier et al., 2005; Genchi et al., 2020). Other trace elements that are toxic that were found include uranium and thorium, which are known to cause kidney damage and cancer, respectively (Agency for Toxic Substances and Disease Registry, 2015; National Cancer Institute, 2022).

6.2. Concluding Remarks of this Study

As previously mentioned, the overarching aim of this study was to assess PM concentrations and compositions of ambient dust in the Saldanha Bay Municipality and based on these results, to assess the potential sources and health implications of these dust emissions. This

study has shown, through the monitoring of PM using PurpleAir Particulate Sensors, that although there were no exceedances according to the NAAQS, there were exceedances according to the more stringent WHO guidelines for both $PM_{2.5}$ and PM_{10}. Another concern is that the compositions of the physical samples that have been collected to date has not been sufficiently explored. The results from the physical samples obtained in this study from the dust fallout buckets, BSNEs and gravimetric samplers have indicated complex compositions in the finer fractions, which can potentially result in different mechanistic pathways in terms of inflammatory responses and cytotoxicity. The results of the compositions have also indicated potential sources of emission of PM within the municipality, as well as the potential human health implications associated with exposure to the pollutants.

It was envisioned to implement the master/slave concept by comparing PM concentrations measured by the PurpleAir Particulate Sensors to the concentrations measured by the AQM Stations in the municipality. However, this was one of the challenges faced during the study as the AQM stations were not in operation during the sampling period of this study. The fieldwork study was in progress during a time where the municipality was experiencing high stages of loadshedding, which directly impacted the sensors and samplers, as they both required electricity to operate. It was also observed that large plumes of dust were released by the ore-carriers in the harbour. This is particularly concerning as it not only affects the quality of air in the municipality but can also affect the surrounding seawater. This subsequently affects the fishing industry, which is very popular for its mussel and oyster industry in the municipality. With regards to the red staining of infrastructure, buildings and roads around the municipality, it is important to highlight that hematite was found to be a significant component of PM in the middle-coarser size fractions. These are classified as coarser and settleable particulates which are known to cause damage to infrastructure. This is particularly so, given the exceedances of the dust fall rates. However, in addition to infrastructure damage and staining, these particulates also result in irritation and contribute to the reduction of visibility. As a result of the staining, members of the community have been forced to bear the expense of maintenance by having to wash or paint their homes and businesses annually. On a final note, members of the community are concerned of the effect that air pollution has and will have on the tourism industry, as it plays a significant role in the municipality's economy. Recommendations for future and complimentary studies are provided in Section 6.3 below.

6.3. Recommendations

Based on the results and conclusions of this study, the following are recommended:

6.3.1. Recommendations for Future and Complimentary Studies:

- Future studies are recommended for the investigation of possibly installing a different low-cost particulate sensor alongside the PurpleAir Particulate Sensor for comparison of PM concentrations. The future studies are also recommended to install the sensors at the AQM station, if and once they are back in operation, also for the comparison of PM concentrations.
- Future studies are also recommended to install the PurpleAir Particulate Sensors at different study sites for the same amount of time, to allow for a fair comparison of PM concentrations. It is also recommended that the PurpleAir Particulate Sensors be installed for complete seasons, to provide a more holistic view on the exceedances that occur.
- It is also recommended that more BSNEs are installed around the municipality, to sample for a wider range of particulate sizes. Furthermore, it is also recommended that the samples collected be analysed by QEMSCAN, as it provides information regarding particle size distribution across different size fractions.
- Future studies should also consider a more detailed dispersion monitoring and health risk assessment, particularly regarding iron ore.
- A more holistic investigation needs to be carried out regarding the emissions associated with the Industrial Development Zone (IDZ) and the non-listed companies in the municipality.
- It is also recommended that future studies investigate potentially contaminated soils and stockpiles using PI-SWERL (Portable In-Situ Wind ERosion Lab). This device would be able to provide the potential for wind erosion and PM emissions in the municipality. It is also recommended that studies should carry out wind tunnel tests with collected soils and ore samples present in the municipality.
- Lastly, future studies should consider using observational data in an atmospheric dispersion model to simulate best- and worst-case scenarios of PM emissions. Furthermore, the observational and simulated PM data should be compared for the validation of the model.

6.3.2. Recommendations for Practice:

- Transparency regarding reporting of PM emissions from both listed and non-listed companies in the Saldanha Bay Municipality, as well as public accessibility of AELs of listed companies.
- Implementation of mitigation strategies, to reduce PM emissions.
- It is also recommended to investigate the possibility of South Africa implementing a pollution tax on industries that emit large volumes of air pollution.

References

Afrimat. n.d. *Construction Materials: Aggregates*. Available: https://www.afrimat.co.za/aggregates/ [2023, September 06].

Agency for Toxic Substances and Disease Registry. 2015. *Uranium*. Available: https://www.atsdr.cdc.gov/sites/toxzine/uranium_toxzine.html [2023, September 05].

AirMetrics. n.d. *MiniVol Tactical Air Sampler (TAS) Operation Manual*.

Akyüz, M. & Çabuk, H. 2009. Meteorological variations of PM2.5/PM10 concentrations and particle-associated polycyclic aromatic hydrocarbons in the atmospheric environment of Zonguldak, Turkey. *Journal of Hazardous Materials*. 170(1):13–21. DOI: 10.1016/j.jhazmat.2009.05.029.

Al-Thani, H., Koç, M. & Isaifan, R.J. 2018. A review on the direct effect of particulate atmospheric pollution on materials and its mitigation for sustainable cities and societies. *Environmental Science and Pollution Research*. 25(28):27839–27857. DOI: 10.1007/s11356-018-2952-8.

Anchor Environmental. 2017. The State of Saldanha Bay and Langebaan Lagoon. (October).

Anchor Environmental. 2023. *Saldanha Bay Aquaculture Development Zone (ADZ)*. Available: https://sbwqft.org.za/adz-monthly-summary-report-13-for-april-2023/ [2023, May 10].

Antin, D. 2013. *The South African Mining Sector: An Industry at a Crossroads*. Available: https://southafrica.hss.de/fileadmin/user_upload/Projects_HSS/South_Africa/170911_Migration/Mining_Report_Final_Dec_2013.pdf [2024, October 21].

ARA Instruments. 2017. Available: https://arainstruments.com/wp-content/uploads/N-FRM_Manual.pdf [2024, October 21].

ARA Instruments. n.d. *N-FRM Sampler*. Available: https://arainstruments.com/products/n-frm-sensor/ [2023, June 04].

Araújo, I.P.S. & Costa, D.B. 2022. Measurement and Monitoring of Particulate Matter in Construction Sites: Guidelines for Gravimetric Approach. *Sustainability*. 14(1):558. DOI: 10.3390/su14010558.

Ardon-Dryer, K., Dryer, Y., Williams, J.N. & Moghimi, N. 2020. Measurements of PM_{2.5} with PurpleAir under atmospheric conditions. *Atmospheric Measurement Techniques*. 13(10):5441–5458. DOI: 10.5194/amt-13-5441-2020.

Bailey, D. & Solomon, G. 2004. Pollution prevention at ports: clearing the air. *Environmental Impact Assessment Review*. 24(7–8):749–774. DOI: 10.1016/j.eiar.2004.06.005.

Ballini, F. & Bozzo, R. 2015. Air pollution from ships in ports: The socio-economic benefit of cold-ironing technology. *Research in Transportation Business & Management*. 17:92–98. DOI: 10.1016/j.rtbm.2015.10.007.

Barbier, O., Jacquillet, G., Tauc, M., Cougnon, M. & Poujeol, P. 2005. Effect of Heavy Metals on, and Handling by, the Kidney. *Nephron Physiology*. 99(4):p105–p110. DOI: 10.1159/000083981.

Barkjohn, K.K., Gantt, B. & Clements, A.L. 2021. Development and Application of a United States wide correction for PM2.5 data collected with the PurpleAir sensor. *Atmospheric Measurement Techniques*. 14(6):4617–4637. DOI: 10.5194/amt-14-4617-2021.

Berry, R. 2014. Dealing with Dust. *Port Technology International*. (64):82–86. Available: https://www.porttechnology.org/wp-content/uploads/2019/05/082.pdf [2024, October 21].

Boente, C., Millán-Martínez, M., Sánchez de la Campa, A.M., Sánchez-Rodas, D. & de la Rosa, J.D. 2022. Physicochemical assessment of atmospheric particulate matter emissions during open-pit mining operations in a massive sulphide ore exploitation. *Atmospheric Pollution Research*. 13(4):101391. DOI: 10.1016/j.apr.2022.101391.

Boyd, J.T., Doll, R., Faulds, J.S. & Leiper, J. 1970. Cancer of the Lung in Iron Ore (Haematite) Miner. *British Journal of Industrial Medicine*. 27(2). Available: https://www.jstor.org/stable/pdf/27722501.pdf?refreqid=excelsior%3Aec72817c0037ff9525473e0c03dfdf72&ab_segments=&origin=&initiator=&acceptTC=1 [2023, August 17].

Brook, R.D., Rajagopalan, S., Pope, C.A., Brook, J.R., Bhatnagar, A., Diez-Roux, A. V., Holguin, F., Hong, Y., et al. 2010. Particulate Matter Air Pollution and Cardiovascular Disease. *Circulation*. 121(21):2331–2378. DOI: 10.1161/CIR.0b013e3181dbece1.

Broska, I., Kubis, M., Terry Williams, C. & Konecny, P. 2002. The compositions of rock-forming and accessory minerals from the Gemeric granites (Hnilec area, Gemeric Superunit, Western Carpathians). *Bulletin of the Czech Geological Survey*. 77(2):147–155. Available: http://www.geology.cz/bulletin/fulltext/147-155broska.pdf [2023, September 15].

Brown, J.S., Gordon, T., Price, O. & Asgharian, B. 2013. Thoracic and respirable particle definitions for human health risk assessment. *Particle and Fibre Toxicology*. 10(1):12. DOI: 10.1186/1743-8977-10-12.

Cairncross, B. 2004. *Field Guide to Rocks & Minerals of Southern Africa*. L. Harvey & J. Hromnik, Eds. Cape Town: Struik Nature.

Canfield, D.E. & Farquhar, J. 2009. Animal evolution, bioturbation, and the sulfate concentration of the oceans. *Proceedings of the National Academy of Sciences*. 106(20):8123–8127. DOI: 10.1073/pnas.0902037106.

Cao, J.J., Chow, J.C., Watson, J.G., Wu, F., Han, Y.M., Jin, Z.D., Shen, Z.X. & An, Z.S. 2008. Size-differentiated source profiles for fugitive dust in the Chinese Loess Plateau. *Atmospheric Environment*. 42(10):2261–2275. DOI: 10.1016/j.atmosenv.2007.12.041.

Carslaw, D. 2020. *Worldmet: Import Surface Meteorological Data from NOAA Integrated Surface Database (ISD)*. Available: https://davidcarslaw.github.io/worldmet/ [2022, June 30].

Carslaw, D.C. & Davison, J. 2023. *The openair book: A Guide to the Analysis of Air Pollution Data*.

Cassim, Z., Goodman, S. & Rajagopaul, A. 2019. *Putting the shine back into South African mining: A path to competitiveness and growth*. Available: https://www.mckinsey.com/~/media/mckinsey/featured%20insights/middle%20east%20and%20africa/putting%20the%20shine%20back%20into%20south%20african%20mining/mck-putting-the-shine-back-into-south-african-mining-a-path-to-competitiveness-and-growth.pdf [2024, October 21].

CCH. 2018. *Saldanha Area Profile*. Available: https://www.cch.co.za/area-profiles/saldanha/ [2024, October 21].

Chetty, E. & Grüning, C. 2018. Dust Deposition Footprint & Impact on Saldanha Bay Soils. 144(November).

Conrad, J. & Naicker, P. 2019. *Geohydrological input into a Strategic Environmental Assessment for the Greater Saldanha Area, Western Cape*. Available: https://sbm.gov.za/wp-content/uploads/Pages/Air_Quality/Groundwater-Specialist-Report.pdf [2023, May 13].

Costa, C. 2022. Investigating the Non-Listed Activities Pertaining to the Storage and Handling of Mineral Ores in the Saldanha Bay Municipality. University of Cape Town.

da Cruz, C. & Magondo, N. 2018. Exposure Risk of Urban Industrial Particulate Matter: Are Our Monitoring Methods Effective? (November).

Csavina, J., Landázuri, A., Wonaschütz, A., Rine, K., Rheinheimer, P., Barbaris, B., Conant, W., Sáez, A.E., et al. 2011. Metal and Metalloid Contaminants in Atmospheric Aerosols from Mining Operations. *Water, Air, & Soil Pollution*. 221(1–4):145–157. DOI: 10.1007/s11270-011-0777-x.

Csavina, J., Field, J., Taylor, M.P., Gao, S., Landázuri, A., Betterton, E.A. & Sáez, A.E. 2012. A review on the importance of metals and metalloids in atmospheric dust and aerosol from mining operations. *Science of The Total Environment*. 433:58–73. DOI: 10.1016/j.scitotenv.2012.06.013.

Department of Environmental Affairs. 2009. *National Environmental Management: Air Quality Act 39 of 2004*.

Department of Environmental affairs. 2012. *National Environmental Management: Air Quality Act 39 of 2004*.

Department of Environmental Affairs. 2013. Available: https://cer.org.za/wp-content/uploads/2013/11/Dust-Control-Regulations.pdf [2023, May 15].

Department of Environmental Affairs. 2015a. National Ambient Air Quality Standard for Particulate Matter with Aerodynamic Diameter Less Than 2.5 Micron Metres. 2004(1):1–22.

Department of Environmental Affairs. 2015b. Available: https://www.saflii.org/za/legis/consol_reg/loawriaewhomhasdeoteihscececoch2046.pdf [2024, October 21].

Department of Environmental Affairs. 2018. National Framework for Air Quality Management in the Republic of South Africa. 7(41996).

Department of Environmental Affairs and Tourism. 2003. *National Environmental Management: Air Quality Bill*.

Department of Forestry Fisheries and the Environment. n.d. *Operation Phakisa - Oceans Economy*.

Department of Forestry Fisheries and the Environment. n.d. *South African Atmospheric Emission Licensing & Inventory Portal* .

Department of Mineral Resources & Energy. n.d. *Operating Mines in Western Cape*. Available: https://www.dmr.gov.za/mineral-policy-promotion/operating-mines/western-cape [2023, September 06].

Dubey, R., Patra, A.K., Joshi, J., Blankenberg, D. & Nazneen. 2022. Evaluation of vertical and horizontal distribution of particulate matter near an urban roadway using an unmanned aerial vehicle. *Science of The Total Environment*. 836:155600. DOI: 10.1016/j.scitotenv.2022.155600.

Dudu, V.P., Mathuthu, M. & Manjoro, M. 2018. Assessment of heavy metals and radionuclides in dust fallout in the West Rand mining area of South Africa. *Clean Air Journal*. 28(2). DOI: 10.17159/2410-972x/2018/v28n2a17.

Endjambi, K.W., Ameh, O.S., Kgabi, N., Maposa, I. & Hamatui, N. 2016. Particulate Matter Concentrations in the Vicinity of an Incinerator. *Journal of Geoscience and Environment Protection*. 04(12):88–100. DOI: 10.4236/gep.2016.412007.

Engelbrecht, J., Joubert, J., Harmse, J. & Hongoro, C. 2013. Optimising a fall out dust monitoring sampling programme at a cement manufacturing plant in South Africa. *African Journal of Environmental Science and Technology*. 7(4):128–139. Available: file:///C:/Users/user/Downloads/ajol-file-journals_389_articles_93766_submission_proof_93766-4633-240183-1-10-20130906%20(1).pdf [2024, October 19].

Engel-Cox, J., Kim Oanh, N.T., van Donkelaar, A., Martin, R. V. & Zell, E. 2013. Toward the next generation of air quality monitoring: Particulate Matter. *Atmospheric Environment*. 80:584–590. DOI: 10.1016/j.atmosenv.2013.08.016.

Entwistle, J.A., Hursthouse, A.S., Marinho Reis, P.A. & Stewart, A.G. 2019. Metalliferous Mine Dust: Human Health Impacts and the Potential Determinants of Disease in Mining Communities. *Current Pollution Reports*. 5(3):67–83. DOI: 10.1007/s40726-019-00108-5.

Environmental Protection Agency. n.d. *Air Quality Standards*. Available: https://airquality.ie/information/air-quality-standards [2023, May 13].

European Commission. n.d. *EU Air Quality Standards*.

FEWLB Nexus. 2021. History about the Berg River. Available: http://www.fewlbnexus.uct.ac.za/history-3#:~:text=Saldanha%20Bay's%20history%20is%20strongly,visited%20the%20Cape%20in%201503. [2022, November 07].

Gautam, S., Prusty, B.K. & Patra, A.K. 2015. Dispersion of respirable particles from the workplace in opencast iron ore mines. *Environmental Technology & Innovation*. 4:137–149. DOI: 10.1016/j.eti.2015.06.002.

Gautam, S., Patra, A.K., Sahu, S.P. & Hitch, M. 2016. Particulate matter pollution in opencast coal mining areas: a threat to human health and environment. *International Journal of Mining, Reclamation and Environment*. 32(2):75–92. DOI: 10.1080/17480930.2016.1218110.

Genchi, G., Carocci, A., Lauria, G., Sinicropi, M.S. & Catalano, A. 2020. Nickel: Human Health and Environmental Toxicology. *International Journal of Environmental Research and Public Health*. 17(3):679. DOI: 10.3390/ijerph17030679.

Giordano, M.R., Malings, C., Pandis, S.N., Presto, A.A., McNeill, V.F., Westervelt, D.M., Beekmann, M. & Subramanian, R. 2021. From low-cost sensors to high-quality data: A summary of challenges and best practices for effectively calibrating low-cost particulate matter mass sensors. *Journal of Aerosol Science*. 158:105833. DOI: 10.1016/j.jaerosci.2021.105833.

Global Africa Network. 2018. *Mine revivals under way in iron ore, zinc and copper*. Available: https://www.globalafricanetwork.com/mining/mine-revivals-under-way-in-iron-ore-zinc-and-copper/ [2023, August 17].

Goossens, D. & Buck, B.J. 2012. Can BSNE (Big Spring Number Eight) samplers be used to measure PM10, respirable dust, PM2.5 and PM1.0? *Aeolian Research*. 5:43–49. DOI: 10.1016/j.aeolia.2012.03.002.

Gous, M. 2006. An overview of the Namakwa Sands ilmenite smelting operations. *The South African Institute of Mining and Metallurgy*. 106. Available: https://journals.co.za/doi/pdf/10.10520/AJA0038223X_3100 [2023, August 18].

Green, R., Broadwin, R., Malig, B., Basu, R., Gold, E.B., Qi, L., Sternfeld, B., Bromberger, J.T., et al. 2016. Long-and Short-Term Exposure To Air Pollution and Inflammatory/Hemostatic Markers in Midlife Women. *Epidemiology*. (November):1. DOI: 10.1097/EDE.0000000000000421.

Ha, Y., Kim, J., Lee, S., Cho, K., Shin, J., Kang, G., Song, M., Lee, J.Y., et al. 2023. Spatiotemporal differences on the real-time physicochemical characteristics of PM2.5 particles in four Northeast Asian countries during Winter and Summer 2020–2021. *Atmospheric Research*. 283:106581. DOI: 10.1016/j.atmosres.2022.106581.

Habeebullah, T.M., Munir, S., Awad, A.H.A.A., Morsy, E.A., Seroji, A.R. & Mohammed, A.M.F. 2015. The Interaction between Air Quality and Meteorological Factors in an Arid Environment of Makkah, Saudi Arabia. *International Journal of Environmental Science and Development*. 6(8).

Halkett, D. 2011. Heritage Impact Assessment: Proposed Afrisam Cement Plant Mine and Associated Infrastructure in Saldanha, Western Cape. (September). Available: https://sahris.sahra.org.za/sites/default/files/heritagereports/CASE%20293.pdf [2023, August 17].

Harrington, A.D., Hylton, S. & Schoonen, M.A.A. 2012. Pyrite-driven reactive oxygen species formation in simulated lung fluid: implications for coal workers' pneumoconiosis. *Environmental Geochemistry and Health*. 34(4):527–538. DOI: 10.1007/s10653-011-9438-7.

Hassanvand, M.S., Naddafi, K., Kashani, H., Faridi, S., Kunzli, N., Nabizadeh, R., Momeniha, F., Gholampour, A., et al. 2017. Short-term effects of particle size fractions on circulating biomarkers of inflammation in a panel of elderly subjects and healthy young adults. *Environmental Pollution*. 223:695–704. DOI: 10.1016/j.envpol.2017.02.005.

He, J., Gong, S., Yu, Y., Yu, L., Wu, L., Mao, H., Song, C., Zhao, S., et al. 2017. Air pollution characteristics and their relation to meteorological conditions during 2014–2015 in major Chinese cities. *Environmental Pollution*. 223:484–496. DOI: 10.1016/j.envpol.2017.01.050.

Healy, R.M., O'Connor, I.P., Hellebust, S., Allanic, A., Sodeau, J.R. & Wenger, J.C. 2009. Characterisation of single particles from in-port ship emissions. *Atmospheric Environment*. 43(40):6408–6414. DOI: 10.1016/j.atmosenv.2009.07.039.

Hertel, S., Viehmann, A., Moebus, S., Mann, K., Bröcker-Preuss, M., Möhlenkamp, S., Nonnemacher, M., Erbel, R., et al. 2010. Influence of short-term exposure to ultrafine and fine particles on systemic inflammation. *European Journal of Epidemiology*. 25(8):581–592. DOI: 10.1007/s10654-010-9477-x.

von Holdt, J.R.C., Eckardt, F.D., Baddock, M.C., Hipondoka, M.H.T. & Wiggs, G.F.S. 2021. Influence of sampling approaches on physical and geochemical analysis of aeolian dust in source regions. *Aeolian Research*. 50:100684. DOI: 10.1016/j.aeolia.2021.100684.

Höllriegl, V. 2019. Other Environmental Health Issues: Strontium in the Environment and Possible Human Health Effects. In *Encyclopedia of Environmental Health*. Elsevier. 797–802. DOI: 10.1016/B978-0-12-409548-9.11195-9.

Hong, Y.-S., Song, K.-H. & Chung, J.-Y. 2014. Health Effects of Chronic Arsenic Exposure. *Journal of Preventive Medicine and Public Health*. 47(5):245–252. DOI: 10.3961/jpmph.14.035.

Horckmans, L., Swennen, R., Deckers, J. & Maquil, R. 2005. Local background concentrations of trace elements in soils: a case study in the Grand Duchy of Luxembourg. *CATENA*. 59(3):279–304. DOI: 10.1016/j.catena.2004.09.004.

Hoy, R.F., Jeebhay, M.F., Cavalin, C., Chen, W., Cohen, R.A., Fireman, E., Go, L.H.T., León-Jiménez, A. 2022. Current global perspectives on silicosis—Convergence of old and newly emergent hazards. *Respirology*. 27(6):387–398. DOI: 10.1111/resp.14242.

Huang, F., Li, X., Wang, C., Xu, Q., Wang, W., Luo, Y., Tao, L., Gao, Q., et al. 2015. PM2.5 Spatiotemporal Variations and the Relationship with Meteorological Factors during 2013-2014 in Beijing, China. *PLOS ONE*. 10(11):e0141642. DOI: 10.1371/journal.pone.0141642.

Huertas, J.I., Huertas, M.E. & Solís-Casados, D.A. 2012. Characterization of airborne particles in an open pit mining region. *Science of the Total Environment*. 423:39–46. DOI: 10.1016/j.scitotenv.2012.01.065.

inteccon.inc. n.d. *GilAir3/GilAir5*.

ISO. 1995.

Jimenez, A.S., van Tongeren, M. & Cherrie, J.W. 2011. *A review of Monitoring Methods for Inhalable Hardwood Dust*. Available: https://ec.europa.eu/social/BlobServlet?docId=10153&langId=en [2024, October 21].

Kabata-Pendias, A. 2001. *Trace Elements in Soils and Plants*. 3rd ed. CRC Press.

Kamanzi, C., Becker, M., Jacobs, M., Konečný, P., Von Holdt, J. & Broadhurst, J. 2023. The impact of coal mine dust characteristics on pathways to respiratory harm: investigating the pneumoconiotic potency of coals. *Environmental Geochemistry and Health*. (May, 2). DOI: 10.1007/s10653-023-01583-y.

Kant, N., Müller, R., Braun, M., Gerber, A. & Groneberg, D. 2016. Particulate Matter in Second-Hand Smoke Emitted from Different Cigarette Sizes and Types of the Brand Vogue Mainly Smoked by Women. *International Journal of Environmental Research and Public Health*. 13(8):799. DOI: 10.3390/ijerph13080799.

Karagulian, F., Barbiere, M., Kotsev, A., Spinelle, L., Gerboles, M., Lagler, F., Redon, N., Crunaire, S., et al. 2019. Review of the Performance of Low-Cost Sensors for Air Quality Monitoring. *Atmosphere*. 10(9):506. DOI: 10.3390/atmos10090506.

Khalid, I., Khalid, T.J. & Jennings, J.H. 2009. A welder with pneumosiderosis: a case report. *Cases Journal*. 2(1):6639. DOI: 10.1186/1757-1626-2-6639.

Khamraev, K., Cheriyan, D. & Choi, J. 2021. A review on health risk assessment of PM in the construction industry – Current situation and future directions. *Science of The Total Environment*. 758:143716. DOI: 10.1016/j.scitotenv.2020.143716.

Khuzestani, R.B. & Souri, B. 2012. Evaluation of heavy metal contamination hazards in nuisance dust particles, in Kurdistan Province, western Iran. *Journal of Environmental Sciences*. 25(7):1346–1354. DOI: 10.1016/S1001-0742(12)60147-8.

Kim, K.-H., Kabir, E. & Kabir, S. 2015. A review on the human health impact of airborne particulate matter. *Environment International*. 74:136–143. DOI: 10.1016/j.envint.2014.10.005.

Kornelius, G., Loans, C., Lotter, J.L. & Ramsuchit, D. 2015. Comparison of different dust fallout measurement techniques with specific reference to the standard ASTM D1739:1970 technique for the measurement of dust deposition in South Africa. (October). Available:

https://www.researchgate.net/profile/Gerrit-Kornelius/publication/283118774_COMPARISON_OF_DIFFERENT_DUST_FALLOUT_MEASUREMENT_TECHNIQUES_WITH_SPECIFIC_REFERENCE_TO_THE_STANDARD_ASTM_D17391970_TECHNIQUE_FOR_THE_MEASUREMENT_OF_DUST_DEPOSITION_IN_SOUTH_AFRICA/links/562b3ba708ae04c2aeb1f959/COMPARISON-OF-DIFFERENT-DUST-FALLOUT-MEASUREMENT-TECHNIQUES-WITH-SPECIFIC-REFERENCE-TO-THE-STANDARD-ASTM-D17391970-TECHNIQUE-FOR-THE-MEASUREMENT-OF-DUST-DEPOSITION-IN-SOUTH-AFRICA.pdf [2024, October 19].

Lee, B.-H., Yang, A.-R., Kim, M.Y., McCurdy, S. & Boisvert, W.A. 2017. Natural sea salt consumption confers protection against hypertension and kidney damage in Dahl salt-sensitive rats. *Food & Nutrition Research*. 61(1):1264713. DOI: 10.1080/16546628.2017.1264713.

Liu, Z., Shen, L., Yan, C., Du, J., Li, Y. & Zhao, H. 2020. Analysis of the Influence of Precipitation and Wind on PM2.5 and PM10 in the Atmosphere. *Advances in Meteorology*. 2020:1–13. DOI: 10.1155/2020/5039613.

Ludidi, N. 2021. *Watchdog for better air quality*.

Ma, W., Du, W., Guo, J., Wu, S., Li, L. & Zeng, Z. 2022. Dust Dispersion Characteristics of Open Stockpiles and the Scale of Dust Suppression Shed. *Applied Sciences*. 12(22):11568. DOI: 10.3390/app122211568.

Meyer, C., Du Plessis, J. & Oberholzer, J. 1996. Available: https://researchspace.csir.co.za/server/api/core/bitstreams/362d17bd-e824-4ad1-a809-5b10a58572e3/content [2024, October 21].

Michigan Department of Environmental Quality. 2016. Available: https://www.michigan.gov/-/media/Project/Websites/egle/Documents/Regulatory-Assistance/Guidebooks/Fug-Dust-Man.pdf?rev=1bffa8aa79524fdabe234a7c6bdcc82e [2024, October 21].

Minerals Education Coalition. 2022. *Quartz*. Available: https://mineralseducationcoalition.org/minerals-database/quartz/ [2022, November 07].

Mossman, B.T. & Churg, A. 1998. Mechanisms in the Pathogenesis of Asbestosis and Silicosis. *American Journal of Respiratory and Critical Care Medicine*. 157(5):1666–1680. DOI: 10.1164/ajrccm.157.5.9707141.

Moumakwa, O. 2007. *An Overview of South Africa's Zircon Industry and the Role of BEE*. Available: https://www.dmr.gov.za/LinkClick.aspx?fileticket=jrKbWTc1Y1A%3D&portalid=0#:~:text=Smaller%20deposits%20are%20located%20along,Natal%20Sands%20and%20Namakwa%20Sands. [2023, August 16].

MRC Mineral Commodities. n.d. *Tormin Mineral Sands*. Available: https://www.mineralcommodities.com/operations-projects/south-africa/tormin-mineral-sands-operation/ [2023, August 04].

Mueller, D., Uibel, S., Takemura, M., Klingelhoefer, D. & Groneberg, D.A. 2011. Ships, ports and particulate air pollution - an analysis of recent studies. *Occupational Medicine and Toxicology*. 6. Available: https://occup-med.biomedcentral.com/articles/10.1186/1745-6673-6-31 [2023, January 03].

National Cancer Institute. 2022. *Thorium*. Available: https://www.cancer.gov/about-cancer/causes-prevention/risk/substances/thorium#:~:text=And%20there%20is%20research%20evidence,may%20be%20stored%20in%20bone. [2023, September 05].

National Institute for Occupational Safety and Health. 2019. *Manganese*. Available: https://www.cdc.gov/niosh/topics/manganese/default.html#print [2023, September 05].

National Portland Cement Saldanha. 2020. Available: https://www.afrisam.co.za/wp-content/uploads/2022/09/National-Portland-Cement-SLP-2021-2025-Final.pdf [2023, August 16].

New Jersey Department of Health and Senior Services. 2007. *Vanadium*.

Nidzgorska-Lencewicz, J. & Czarnecka, M. 2020. Thermal Inversion and Particulate Matter Concentration in Wrocław in Winter Season. *Atmosphere*. 11(12):1351. DOI: 10.3390/atmos11121351.

Niedźwiedź, T., Łupikasza, E.B., Małarzewski, Ł. & Budzik, T. 2021. Surface-based nocturnal air temperature inversions in southern Poland and their influence on PM10 and PM2.5 concentrations in Upper Silesia. *Theoretical and Applied Climatology*. 146(3–4):897–919. DOI: 10.1007/s00704-021-03752-4.

Norman White, G. & Dixon, J.B. 2003. *Soil Mineralogy, Laboratory Manual, Agronomy 626*.

Northeastern Regional Association of Coastal Ocean Observing Systems. n.d. *Beaufort Wind Scale*. Available: http://gyre.umeoce.maine.edu/data/gomoos/buoy/php/variable_description.php?variable=wind_2_speed [2023, September 04].

Oliveira, A., Cacodcar, J. & Motghare, D. 2014. Morbidity among iron ore mine workers in Goa. *Indian Journal of Public Health*. 58(1):57. DOI: 10.4103/0019-557X.128171.

Organiscak, J.A. & Randolph Reed, W.M. 2004. Characteristics of Fugitive Dust Generated from Unpaved Mine Haulage Roads.

Ostro, B. & Chestnut, L. 1998. Assessing the Health Benefits of Reducing Particulate Matter Air Pollution in the United States. *Environmental Research*. 76(2):94–106. DOI: 10.1006/enrs.1997.3799.

Ostro, B., Malig, B., Broadwin, R., Basu, R., Gold, E.B., Bromberger, J.T., Derby, C., Feinstein, S., et al. 2014. Chronic PM2.5 exposure and inflammation: Determining sensitive subgroups in mid-life women. *Environmental Research*. 132:168–175. DOI: 10.1016/j.envres.2014.03.042.

Palero-Fernández, F.J. & Martín-Izard, A. 2005. Trace element contents in galena and sphalerite from ore deposits of the Alcudia Valley mineral field (Eastern Sierra Morena, Spain). *Journal of Geochemical Exploration*. 86(1):1–25. DOI: 10.1016/j.gexplo.2005.03.001.

Parliamentary Monitoring Group. 2014. *Status of Air Quality in South Africa: briefing by Department and Civil Society, with Minister present*.

PD Naidoo & Associates & SRK Consulting Engineers and Scientists. n.d. *Environmental Impact Assessment Process: Proposed Phase 2 Expansion of the Transnet Iron Ore Handling Facility, Saldanha*. Available: https://www.transnet.net/BusinessWithUs/TNInfrastructurePlan/Final_BID.pdf [2024, October 21].

Pérez, I.A., García, M.Á., Sánchez, M.L., Pardo, N. & Fernández-Duque, B. 2020. Key Points in Air Pollution Meteorology. *International Journal of Environmental Research and Public Health*. 17(22):8349. DOI: 10.3390/ijerph17228349.

Petavratzi, E., Kingman, S. & Lowndes, I. 2005. Particulates from mining operations: A review of sources, effects and regulations. *Minerals Engineering*. 18(12):1183–1199. DOI: 10.1016/j.mineng.2005.06.017.

Pilling, M.J., ApSimon, H., Carruthers, D., Carslaw, D., Derwent, D., Dorling, S., Fisher, B., Harrison, R., et al. 2005. *Particulate Matter in the United Kingdom*. Available: https://uk-air.defra.gov.uk/library/assets/documents/reports/aqeg/Particulate_Matter_in_The_UK_2005_Summary.pdf [2024, October 21].

Pope, C.A., Ezzati, M. & Dockery, D.W. 2009. Fine-Particulate Air Pollution and Life Expectancy in the United States. *New England Journal of Medicine*. 360(4):376–386. DOI: 10.1056/NEJMsa0805646.

PurpleAir. n.d. *PurpleAir Classic Air Quality Monitor*. Available: https://www2.purpleair.com/.

Ratner, B. 2009. The correlation coefficient: Its values range between +1/−1, or do they? *Journal of Targeting, Measurement and Analysis for Marketing*. 17(2):139–142. DOI: 10.1057/jt.2009.5.

Le Roux, R.R., Bezuidenhout, J. & Smit, H.A.P. 2019. The influence of different types of granite on indoor radon concentrations of dwellings in the South African West Coast Peninsula. *Journal of Radiation Research and Applied Sciences*. 12(1):375–382. DOI: 10.1080/16878507.2019.1680043.

Saldanha Bay Municipality. n.d. *Environmental*.

Seidal, K., Jorgensen, N., Elinder, C.-G., Sjogren, B. & Vahter, M. 1993. Fatal cadmium-induced pneumonitis. *Scandinavian Journal of Work, Environment & Health*. 19(6). Available: https://www.jstor.org/stable/pdf/40966173.pdf?refreqid=excelsior%3A65b2947b87eaf6bd85cbe8012f87ac80&ab_segments=&origin=&initiator=&acceptTC=1 [2023, August 18].

Sekuła, P., Bokwa, A., Bartyzel, J., Bochenek, B., Chmura, Ł., Gałkowski, M. & Zimnoch, M. 2021. Measurement report: Effect of wind shear on

PM₁₀ concentration vertical structure in the urban boundary layer in a complex terrain. *Atmospheric Chemistry and Physics*. 21(15):12113–12139. DOI: 10.5194/acp-21-12113-2021.

Sensidyne. n.d. *GilAir-3 Air Sampling Pump*.

Senthil Kumar, R. & Rajkumar, P. 2014. Characterization of minerals in air dust particles in the state of Tamilnadu, India through FTIR, XRD and SEM analyses. *Infrared Physics & Technology*. 67:30–41. DOI: 10.1016/j.infrared.2014.06.002.

Sharratt, B. & Pi, H. 2018. Field and laboratory comparison of PM10 instruments in high winds. *Aeolian Research*. 32:42–52. DOI: 10.1016/j.aeolia.2018.01.006.

Sibanda, I. 2009. Characterization and Comparison of Aeolian Dust Collected by Horizontal Flux Gauges and Vertical Deposit Gauges. University of Witwaterstrand. Available: https://wiredspace.wits.ac.za/server/api/core/bitstreams/b50c13f3-7a7d-44d9-88c4-9b7c2f6779eb/content [2024, October 19].

Singh, V., Singh, S. & Biswal, A. 2021. Exceedances and trends of particulate matter (PM2.5) in five Indian megacities. *Science of The Total Environment*. 750:141461. DOI: 10.1016/j.scitotenv.2020.141461.

SLR Consulting. 2018. Strategic Environmental Assessment (SEA) of the Port of Saldanha: 2017 Revision.

Snyder, E.G., Watkins, T.H., Solomon, P.A., Thoma, E.D., Williams, R.W., Hagler, G.S.W., Shelow, D., Hindin, D.A., et al. 2013. The Changing Paradigm of Air Pollution Monitoring. *Environmental Science & Technology*. 47(20):11369–11377. DOI: 10.1021/es4022602.

South African Government. n.d. *National Infrastructure Plan*. Available: https://www.gov.za/issues/national-infrastructure-plan [2023, September 01].

South African History Online. n.d. *Saldanha*. Available: https://www.sahistory.org.za/place/saldanha [2022, April 10].

Stavroulas, I., Grivas, G., Michalopoulos, P., Liakakou, E., Bougiatioti, A., Kalkavouras, P., Fameli, K., Hatzianastassiou, N., et al. 2020. Field Evaluation of Low-Cost PM Sensors (Purple Air PA-II) Under Variable Urban Air Quality Conditions, in Greece. *Atmosphere*. 11(9):926. DOI: 10.3390/atmos11090926.

Syers, J.K., Williams, J.D.H., Campbell, A.S. & Walker, T.W. 1967. The Significance of Apatite Inclusions in Soil Phosphorus Studies.

Taylor, S.R. & McLennan, S.M. 1995. The geochemical evolution of the continental crust. *Reviews of Geophysics*. 33(2):241–265. DOI: 10.1029/95RG00262.

Thornton, I. 1996. Impacts of mining on the environment; some local, regional and global issues. *Applied Geochemistry*. 11(1–2):355–361. DOI: 10.1016/0883-2927(95)00064-X.

Tian, S., Liang, T. & Li, K. 2019. Fine road dust contamination in a mining area presents a likely air pollution hotspot and threat to human health. *Environment International*. 128:201–209. DOI: 10.1016/j.envint.2019.04.050.

Transnet. 2013. *Saldanha Terminal*. Available: https://www.transnetportterminals.net/Ports/Pages/Saldanha_Multi.aspx [2021, September 22].

Transnet. 2021. *Transnet Port Terminals Overview*. Available: https://www.transnet.net/InvestorRelations/AR2021/Port%20Terminals%202021.pdf [2024, October 21].

Tronox. 2020. *Namakwa Sands, South Africa*. Available: https://www.tronox.com/products/mineral-sands/operations/namakwa-sands-south-africa/ [2020, April 24].

United Nations Conference on Trade and Development. 2013. Available: https://unctad.org/system/files/official-document/cid30_en.pdf [2023, September 16].

United States Department of Health and Human Services. 2022a. *Toxicological Profile for Barium and Barium Compounds*.

United States Department of Health and Human Services. 2022b. *Toxicological Profile for Copper*. Available: https://www.atsdr.cdc.gov/ToxProfiles/tp132.pdf [2023, July 01].

United States Environmental Protection Agency. 2022a. *Particulate Matter (PM) Basic*. Available: https://www.epa.gov/pm-pollution/particulate-matter-pm-basics [2023, January 07].

United States Environmental Protection Agency. 2022b. *Fugitive Dust Control Measures and Best Practices*.

United States Environmental Protection Agency. 2022c. *Agriculture Nutrient Management and Fertilizer*. Available: https://www.epa.gov/agriculture/agriculture-nutrient-management-and-fertilizer#:~:text=Most%20fertilizers%20that%20are%20commonly,are%20necessary%20for%20plant%20growth. [2023, June 30].

United States Environmental Protection Agency. 2023a. *National Ambient Air Quality Standards (NAAQS) for PM*. Available: https://www.epa.gov/pm-pollution/national-ambient-air-quality-standards-naaqs-pm#:~:text=Rule%20Summary,-On%20February%207&text=%E2%80%8B%20EPA%20is%20setting%20the,with%20the%20available%20health%20science. [2024, October 21].

United States Environmental Protection Agency. 2023b. *EPA scientists develop and evaluate Federal Reference & Equivalent Methods for measuring key air pollutants*. Available: https://www.epa.gov/air-research/epa-scientists-develop-and-evaluate-federal-reference-equivalent-methods-measuring-key [2024, October 21].

United States Environmental Protection Agency. n.d. *Vocabulary Catalog*. Available: https://sor.epa.gov/sor_internet/registry/termreg/searchandretrieve/glossariesandkeywordlists/search.do [2024a, October 21].

United States Environmental Protection Agency. n.d. Available: https://www3.epa.gov/ttnamti1/files/ambient/pm25/qa/balance.pdf [2024b, October 21].

Vassilakos, Ch., Saraga, D., Maggos, Th., Michopoulos, J., Pateraki, S. & Helmis, C.G. 2005. Temporal variations of PM2.5 in the ambient air of a suburban site in Athens, Greece. *Science of The Total Environment*. 349(1–3):223–231. DOI: 10.1016/j.scitotenv.2005.01.012.

Vedanta. n.d. *Vedanta Zinc International*. Available: https://vedanta-zincinternational.com/ [2024, October 21].

Virgianto, R.H., Kinanti, N.P., Ferdiansyah, E. & Kartika, Q.A. 2021. The Effect of Precipitation on Scavenging of PM2.5 in Jakarta Based on Distributed Lag Non-Linear Models. *IPTEK The Journal for Technology and Science*. 32(2):115. DOI: 10.12962/j20882033.v32i2.7735.

Visser, S.M. & Cornelis, W. 2004. Wind and Rain Interaction in Erosion. *Tropical Resource Management Papers = Documents sur la Gestion des Ressources Tropicales*. Available: https://edepot.wur.nl/116402 [2023, September 21].

Voutsa, D. & Samara, C. 2002. Labile and bioaccessible fractions of heavy metals in the airborne particulate matter from urban and industrial areas. *Atmospheric Environment*. 36(22):3583–3590. DOI: 10.1016/S1352-2310(02)00282-0.

Wan, C., Zhao, Y., Zhang, D. & Yip, T.L. 2021. Identifying important ports in maritime container shipping networks along the Maritime Silk Road. *Ocean & Coastal Management*. 211:105738. DOI: 10.1016/j.ocecoaman.2021.105738.

Waza, A., Schneiders, K., May, J., Rodríguez, S., Epple, B. & Kandler, K. 2019. Field comparison of dry deposition samplers for collection of atmospheric mineral dust: results from single-particle characterization. *Atmospheric Measurement Techniques*. 12(12):6647–6665. DOI: 10.5194/amt-12-6647-2019.

Welman, L. & Ferreira, S. LA. 2016. The co-evolution of Saldanha Bay (town and hinterland) and its Port. *Local Economy: The Journal of the Local Economy Policy Unit*. 31(1–2):219–233. DOI: 10.1177/0269094215623849.

Wippich, C., Rissler, J., Koppisch, D. & Breuer, D. 2020. Estimating Respirable Dust Exposure from Inhalable Dust Exposure. *Annals of Work Exposures and Health*. 64(4):430–444. DOI: 10.1093/annweh/wxaa016.

World Health Organisation. 1999.

World Health Organisation. 2019. *Lead Poisoning and Health*. Available: http://www.who.int/news-room/fact-sheets/detail/lead-poisoning-and-health [2020, April 01].

World Health Organisation. 2021. *WHO global air quality guidelines*.

World Health Organisation. 2022. *Ambient (outdoor) air pollution*. Available: https://www.who.int/news-room/fact-sheets/detail/ambient-(outdoor)-air-quality-and-health [2023, January 24].

WSP. 2018. *Saldanha Bay Multipurpose Terminal AQIA Comments & Responses*.

Wu, J., Li, T., Zhang, C., Cheng, Q. & Shen, H. 2021. Hourly PM2.5 Concentration Monitoring With Spatiotemporal Continuity by the Fusion of Satellite and Station Observations. *IEEE Journal of Selected Topics in Applied Earth Observations and Remote Sensing*. 14:8019–8032. DOI: 10.1109/JSTARS.2021.3103020.

Yang, C.-T., Chen, H.-W., Chang, E.-J., Kristiani, E., Nguyen, K.L.P. & Chang, J.-S. 2021. Current advances and future challenges of AIoT applications in particulate matters (PM) monitoring and control. *Journal of Hazardous Materials*. 419:126442. DOI: 10.1016/j.jhazmat.2021.126442.

Yu, B., Ding, B.M., Fan, C.H., Liu, Q.D., Ding, L., Wang, B.S., Wang, J., Zhang, H.D., et al. 2016. Health Status of dust-exposed workers in a precision casting enterprise. 34(7):517–519. Available: https://pubmed.ncbi.nlm.nih.gov/27682487/ [2023, September 09].

Yuwono, A.S., Mulyanto, B., Fauzan, M., Mulyani, F. & Munthe, C.R. 2016. Generation of Total Suspended Particulate (TSP) in Ambient Air from Four Soil Types in Indonesia. *International Journal of Applied Environmental Sciences*. 11(4):995–1006. Available: https://d1wqtxts1xzle7.cloudfront.net/84670212/ijaesv11n4_13-libre.pdf?1650621415=&response-content-disposition=inline%3B+filename%3DGeneration_of_Total_Suspended_Particulat.pdf&Expires=1729622876&Signature=GgKq~O4ibaP~dilEwUmX94ipLUVKbhEAkAZtZ2Ncf1i5cKO8tnf6pdx9hL6zEcGN9B9Tv3FRZZ-3-Ards85Hd4JNwwy2Q2701LcbgbflVRf68ScfGoHs41DdSMPhUrUQqGLEZwEdMU3a~N6DZxnpcYOVyIM0qPg6jpF0d2AOyH1TXUmQTacLpz1Uu5oL34g-zMfwdeg79vJOI9Vfj2VSFCfNyfY40OkzaTAhDw7ujMuDuBRiHPZCaIbOE-Z1GmpzKshIb9REm3uE5PfxeW0LJuk0ivcR-HcpyfcRiJLqS~~2WudEIJXEl4xBrKMbvdZBpZb6wbtBF9a4I2bxdt-OUw__&Key-Pair-Id=APKAJLOHF5GGSLRBV4ZA [2024, October 19].

Zhou, Y., Zhang, Y., Ma, D., Lu, J., Luo, W., Fu, Y., Li, S., Feng, J., et al. 2020. Port-Related Emissions, Environmental Impacts and Their Implication on Green Traffic Policy in Shanghai. *Sustainability*. 12(10):4162. DOI: 10.3390/su12104162.

Appendices

Appendix A – PurpleAir Particulate Sensors Information

Location	Sampling Period
Blue Bay Lodge	28/01/2021 – 24/02/2022
Saldanha AQM Station	05/02/2021 – 22/10/2021
Louwville Private Home	23/02/2021 – 14/05/2021
St. Helena Bay Private Home	03/03/2021 – 04/08/2021
West Coast Mall	28/01/2021 – 03/04/2021
Langebaan Private Home	23/02/2021 – 08/07/2021
Vredenburg AQM Station	26/02/2021 – 30/06/2021

Appendix B – Physical Sample Information

Table 44: Dust Fallout Bucket Sample Information

	ID	Location	Sampling Period	Sampler	Analysis
Dust Sample	X	Blue Bay Lodge	25/02 – 05/08	Dust Fallout Bucket	XRD
Salt Sample	Y	Blue Bay Lodge			

Table 45: BSNE Sample Information

ID	Location	Sampling Period	Sampler	Analysis
Z	Blue Bay Lodge	25/02 – 05/08	BSNE	QEMSCAN
	Saldanha AQM Station			

Appendix C – PM_{10} Pollution Roses and Polar Plots for all Seven Study Sites

Blue Bay Lodge

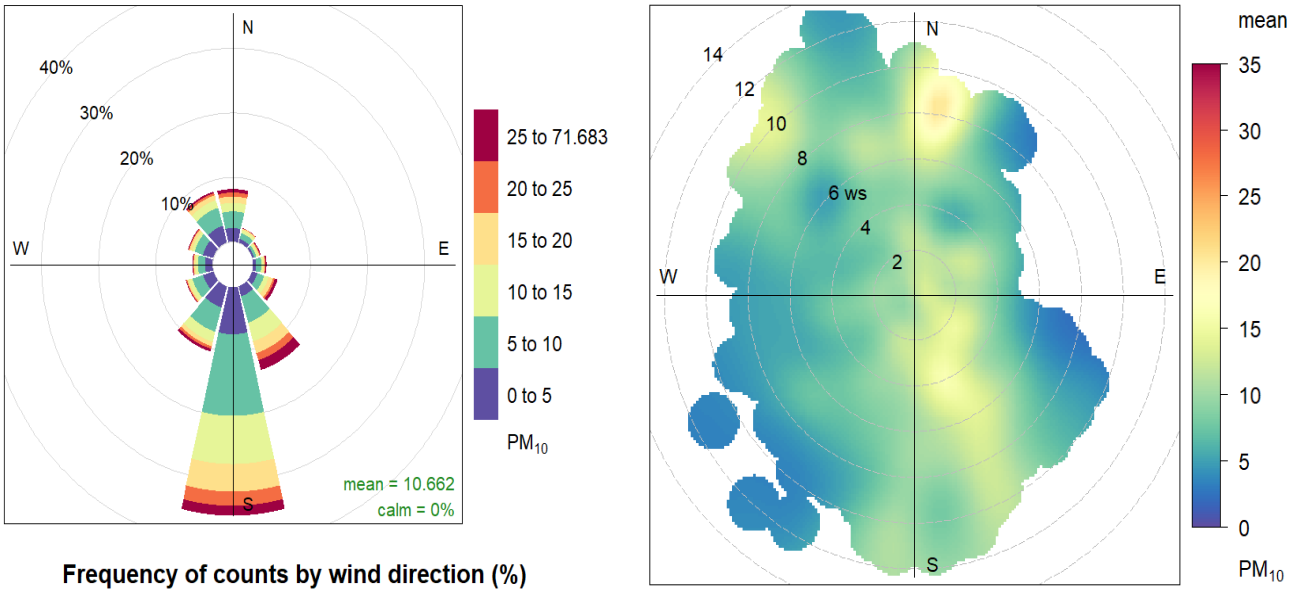

(a) (b)

Figure 80: The effect of wind direction and speed on PM_{10} Concentrations captured at Blue Bay Lodge using (a) a pollution rose and (b) a polar plot

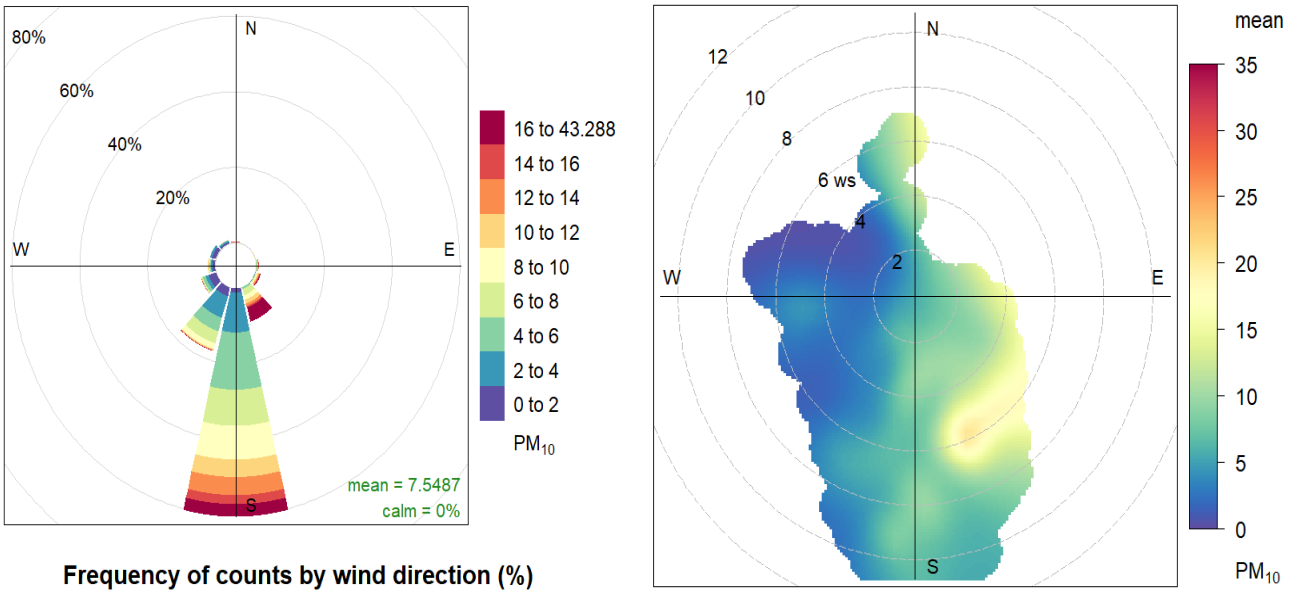

(a) (b)

Figure 81: Summer 2021 (January-February) at Blue Bay Lodge (a) PM_{10} Pollution Rose and (b) PM_{10} Polar Plot

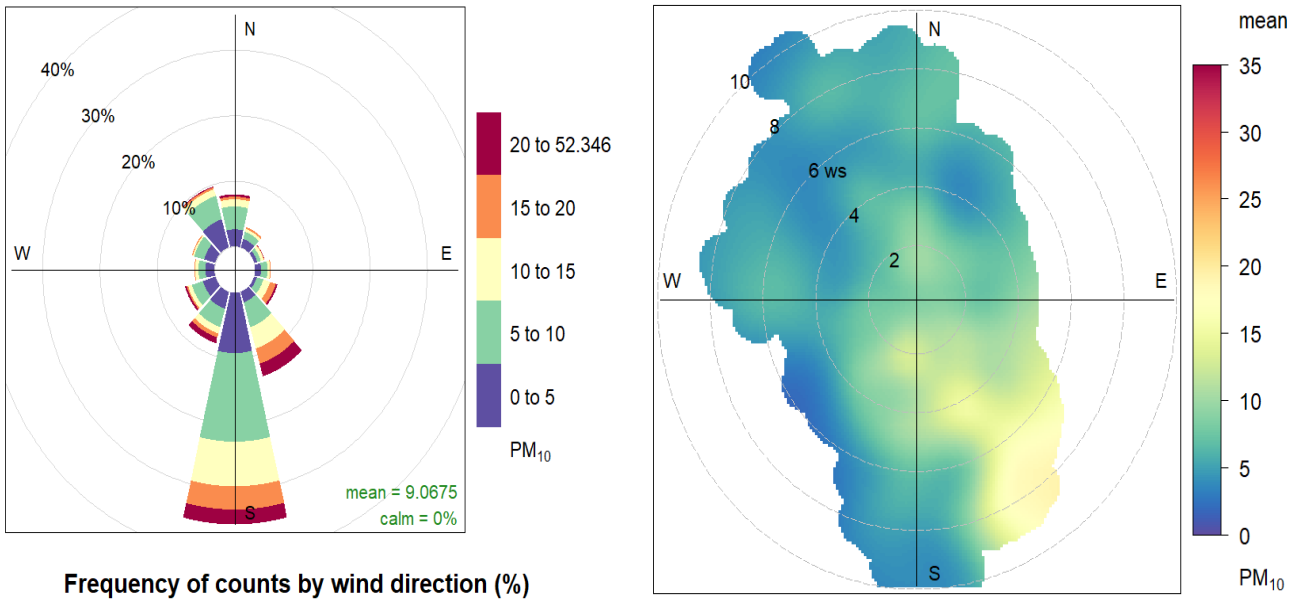

(a) (b)

Figure 82: Autumn 2021 (March-May) at Blue Bay Lodge (a) PM_{10} Pollution Rose and (b) PM_{10} Polar Plot

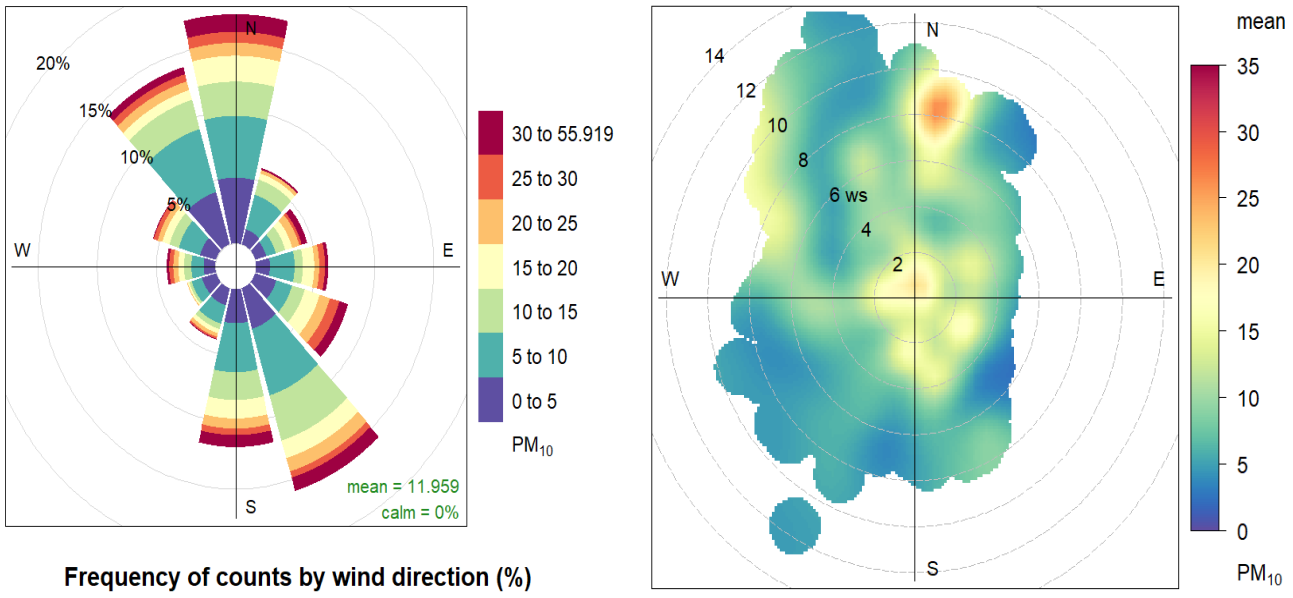

(a) (b)

Figure 83: Winter 2021 (June-August) at Blue Bay Lodge (a) PM_{10} Pollution Rose and (b) PM_{10} Polar Plot

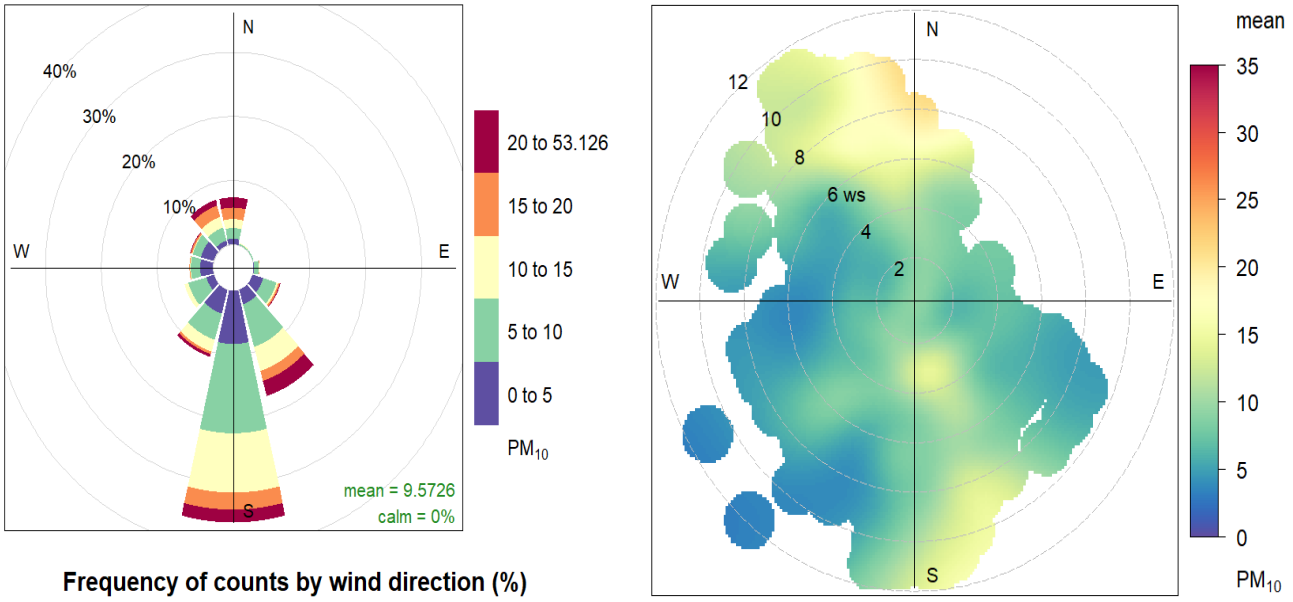

(a) (b)

Figure 84: Spring 2021 (September-November) at Blue Bay Lodge (a) PM_{10} Pollution Rose and (b) PM_{10} Polar Plot

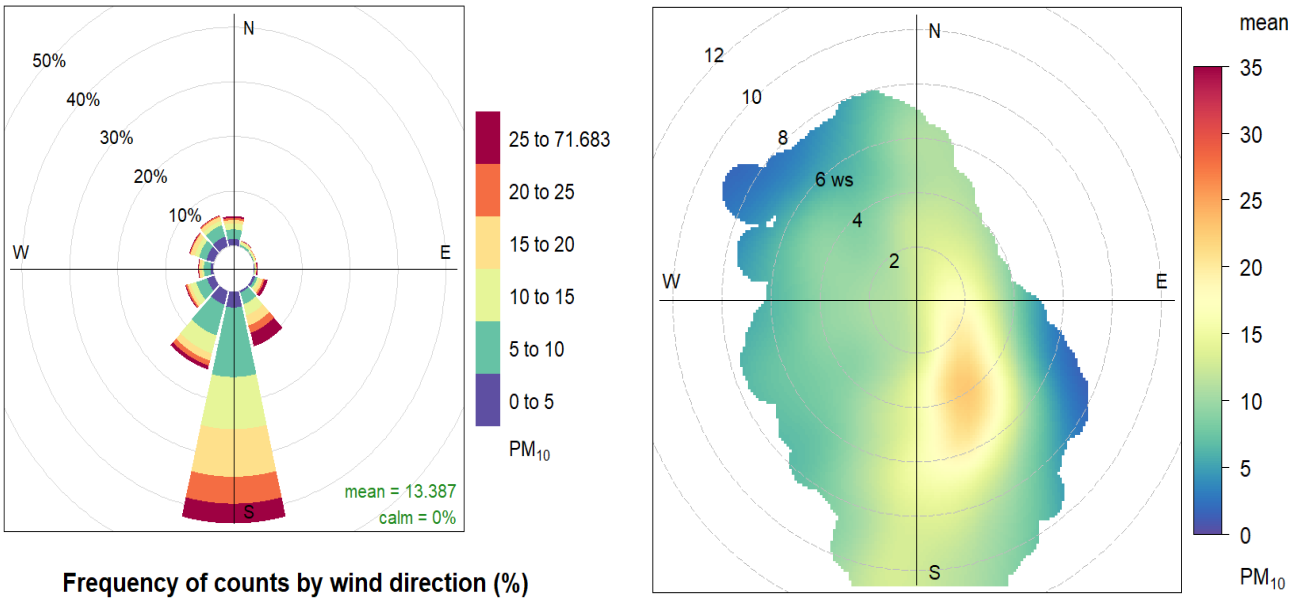

(a) (b)

Figure 85: Summer 2021/2022 (December-January) at Blue Bay Lodge (a) PM_{10} Pollution Rose and (b) PM_{10} Polar Plot

Saldanha AQM Station

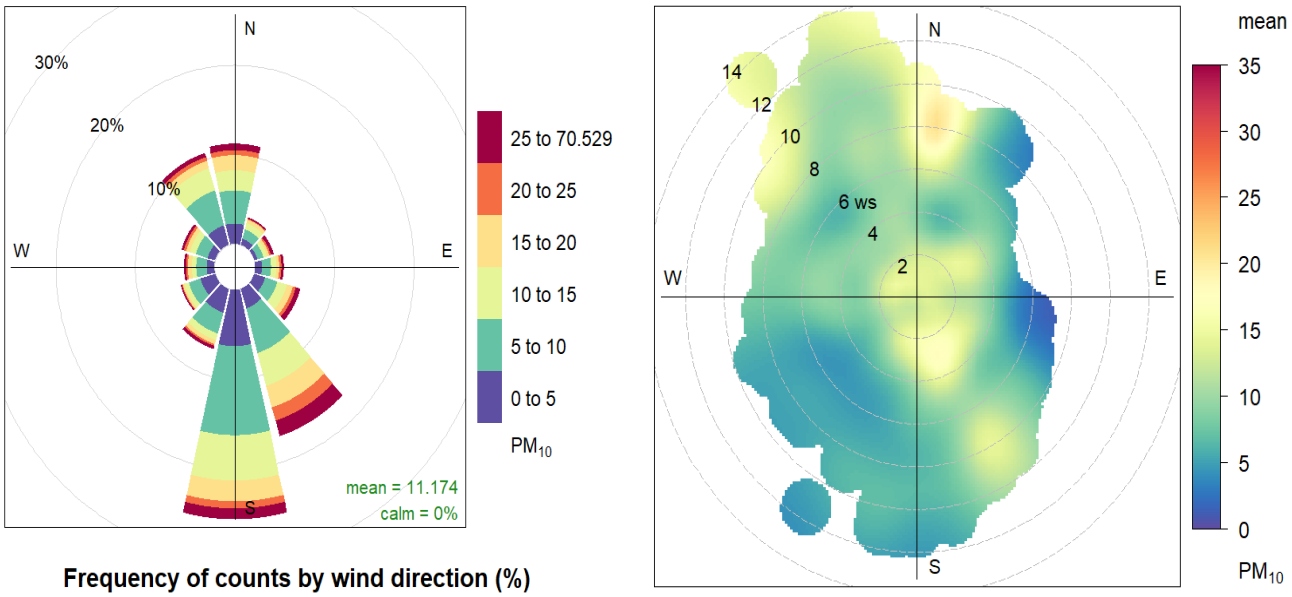

(a) (b)

Figure 86: The effect of wind direction and speed on PM_{10} Concentrations captured at the Saldanha AQM Station using (a) a pollution rose and (b) a polar plot

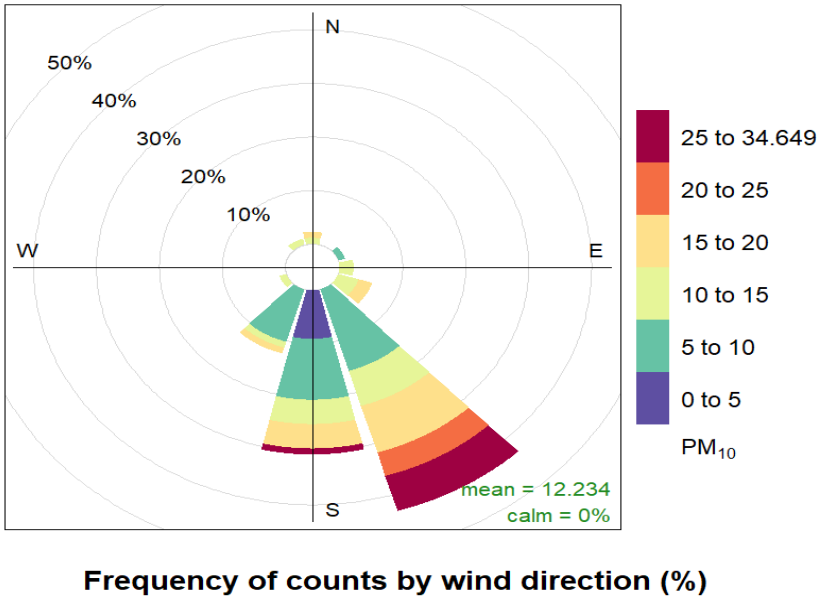

Figure 87: Summer 2021 (January-February) at the Saldanha AQM Station PM_{10} Pollution Rose

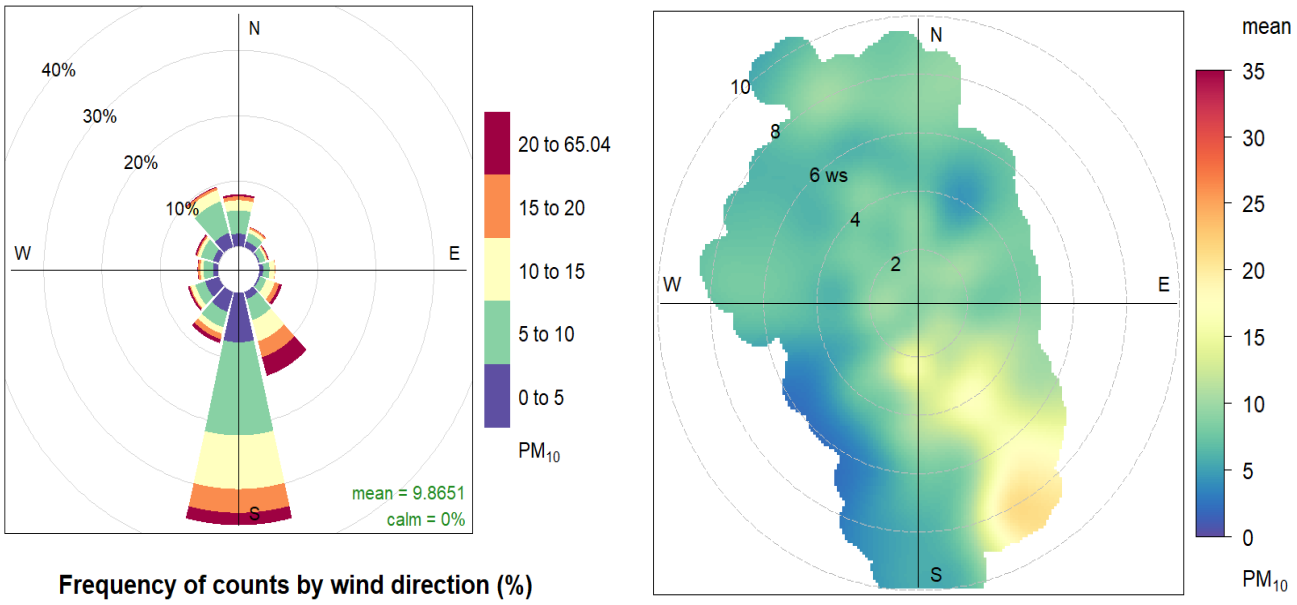

(a) (b)

Figure 88: Autumn 2021 (March-May) at Blue Bay Lodge (a) PM_{10} Pollution Rose and (b) PM_{10} Polar Plot

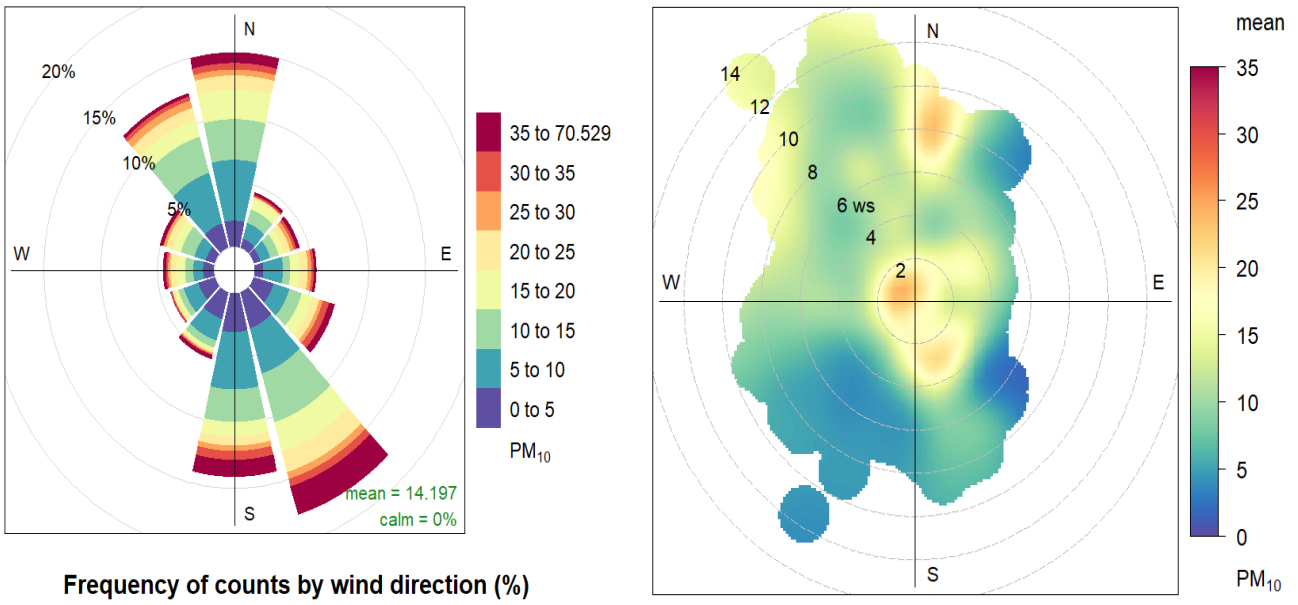

(a) (b)

Figure 89: Winter 2021 (June-August) at Blue Bay Lodge (a) PM_{10} Pollution Rose and (b) PM_{10} Polar Plot

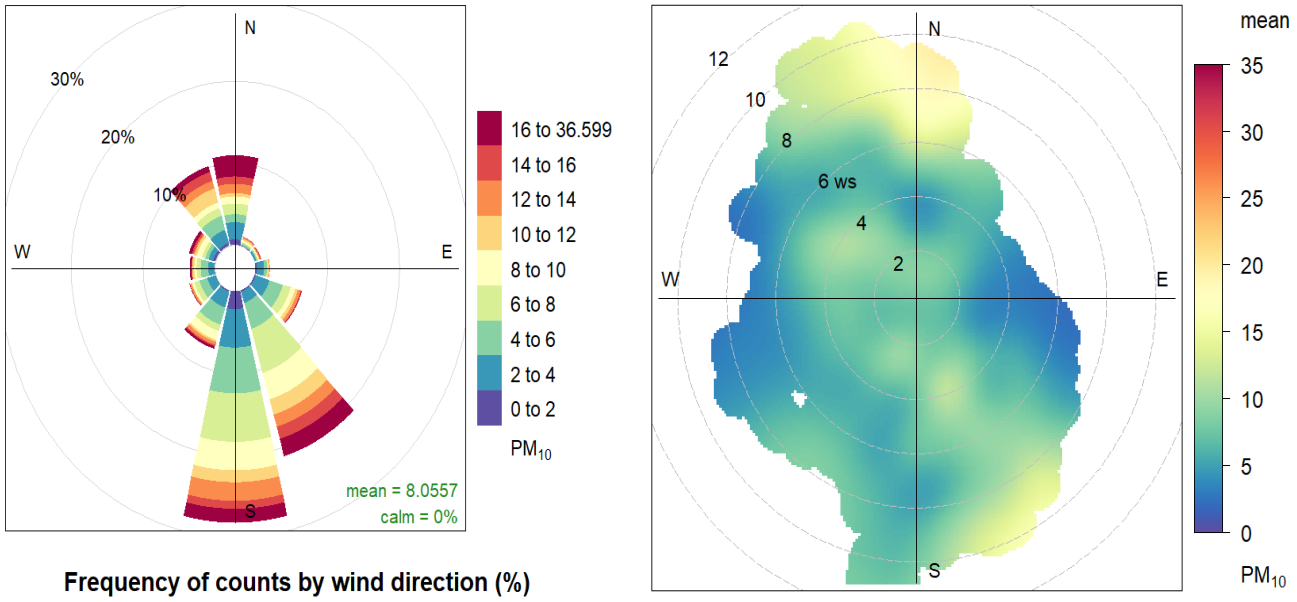

(a) (b)

Figure 90: Spring 2021 (September-October) at Blue Bay Lodge (a) PM_{10} Pollution Rose and (b) PM_{10} Polar Plot

Louwville Private Home

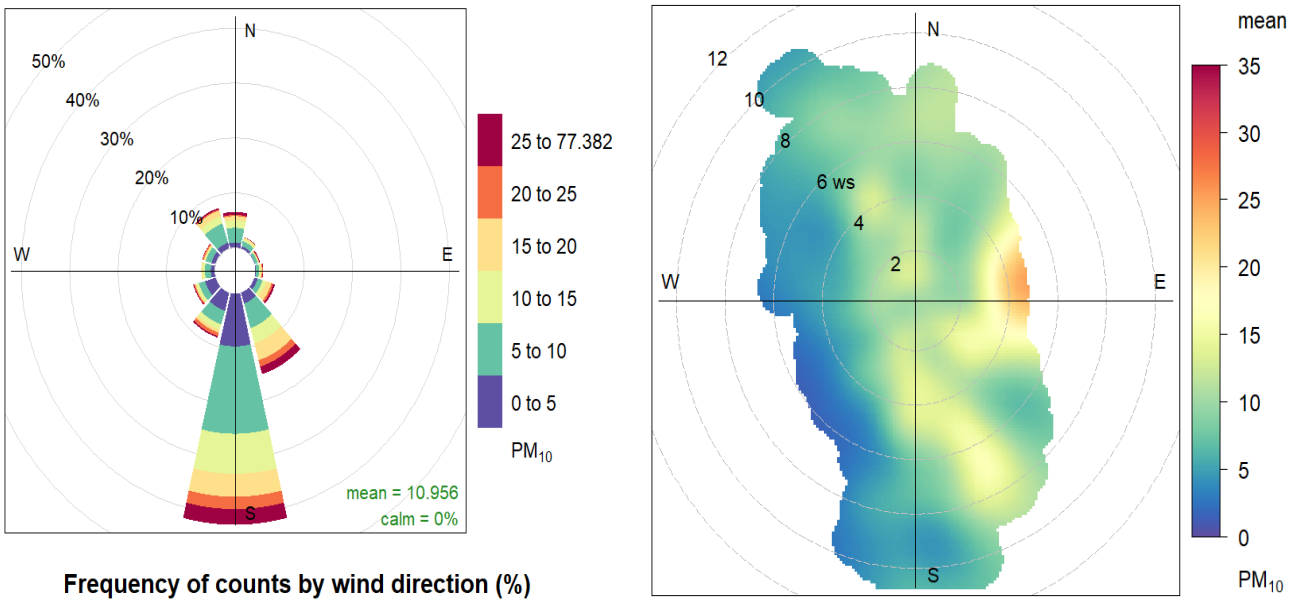

(a) (b)

Figure 91: The effect of wind direction and speed on PM_{10} Concentrations captured at the Louwville Private Home using (a) a pollution rose and (b) a polar plot

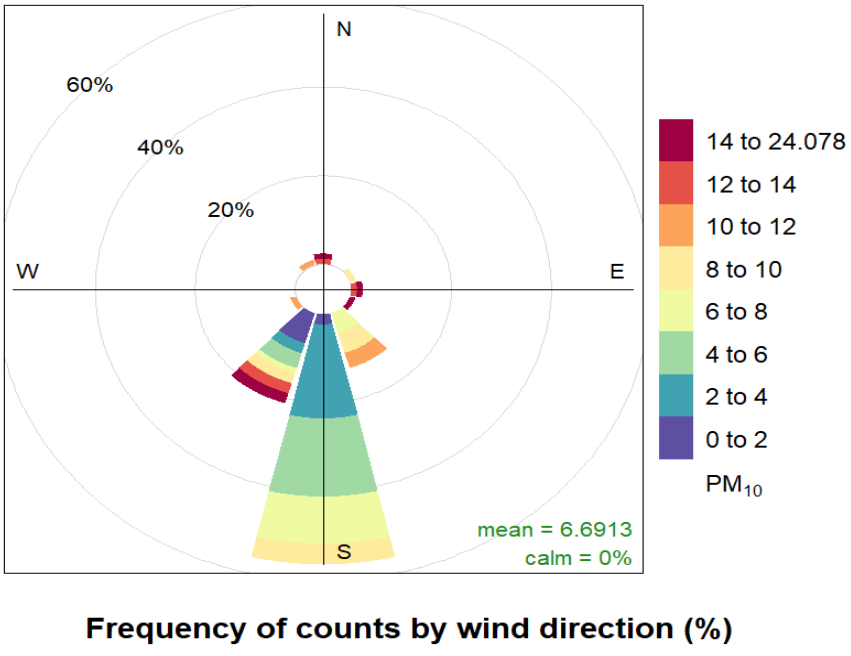

Figure 92: Summer 2021 (February) at Louwville Private Home PM_{10} Pollution Rose

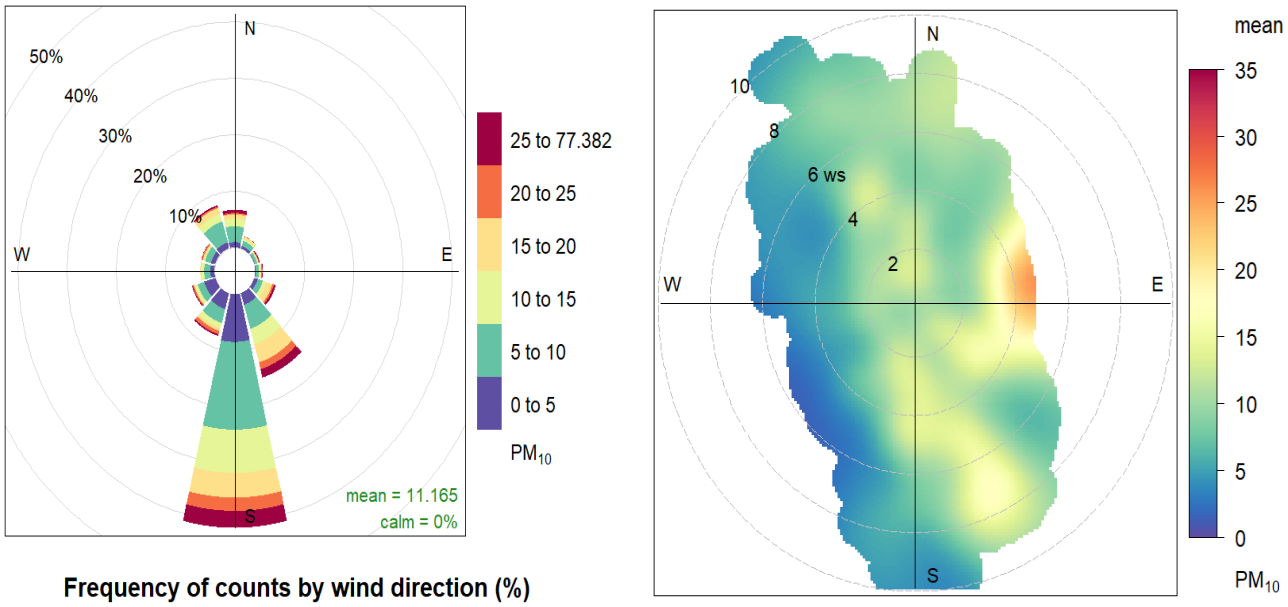

(a) (b)

Figure 93: Autumn 2021 (March-May) at Louwville Private Home (a) PM_{10} Pollution Rose and (b) PM_{10} Polar Plot

St. Helena Bay Private Home

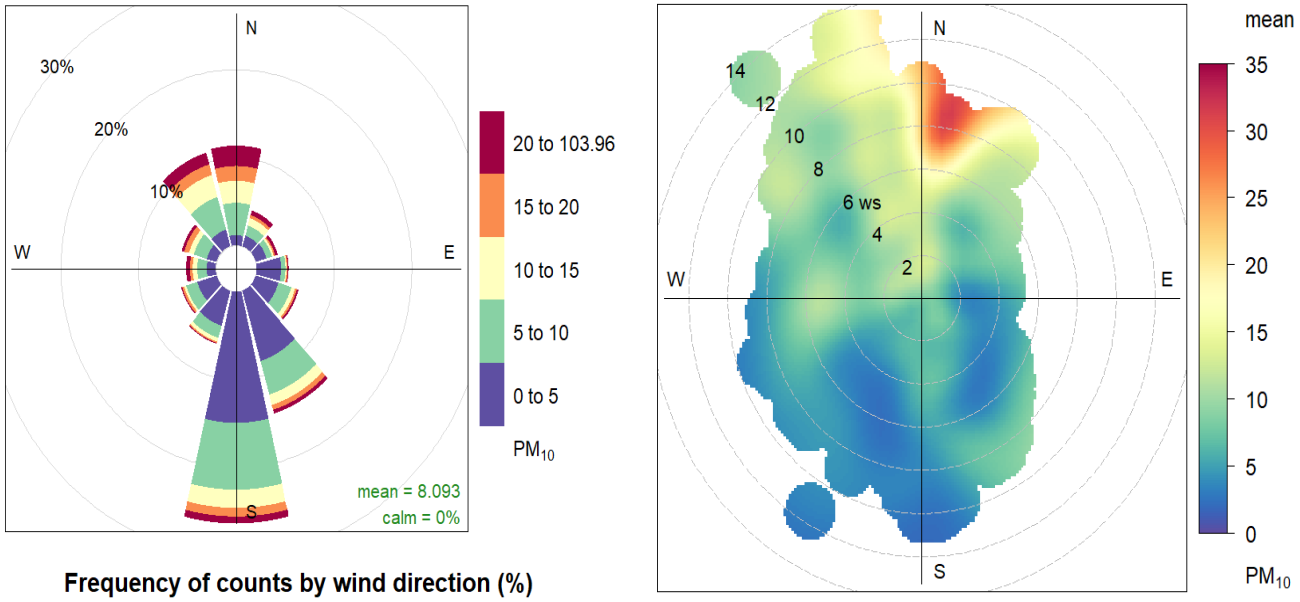

(a) (b)

Figure 94: The effect of wind direction and speed on PM_{10} Concentrations captured at the St. Helena Bay Private Home using (a) a pollution rose and (b) a polar plot

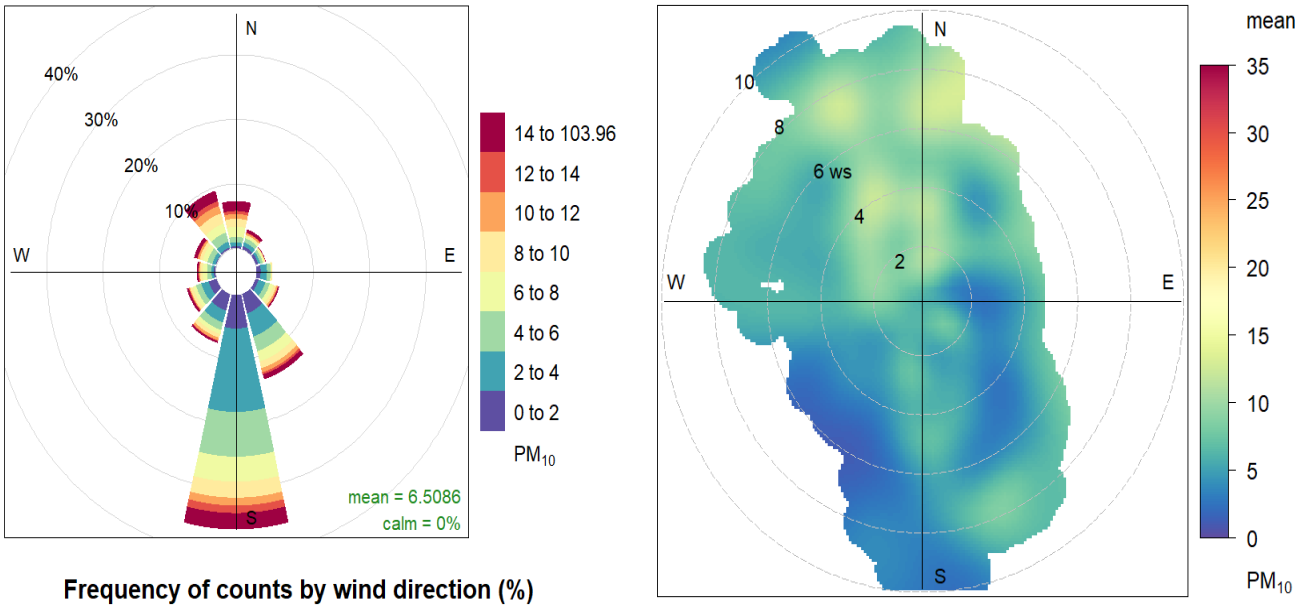

(a) (b)

Figure 95: Autumn 2021 (March-May) at St. Helena Bay Private Home (a) PM_{10} Pollution Rose and (b) PM_{10} Polar Plot

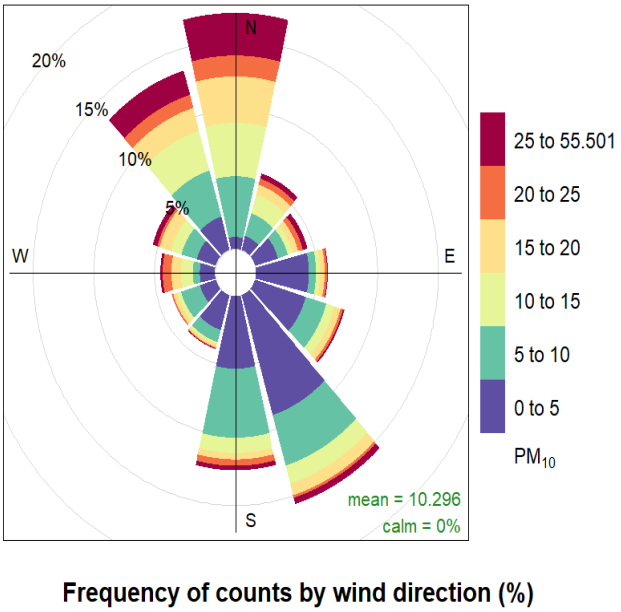

(a)

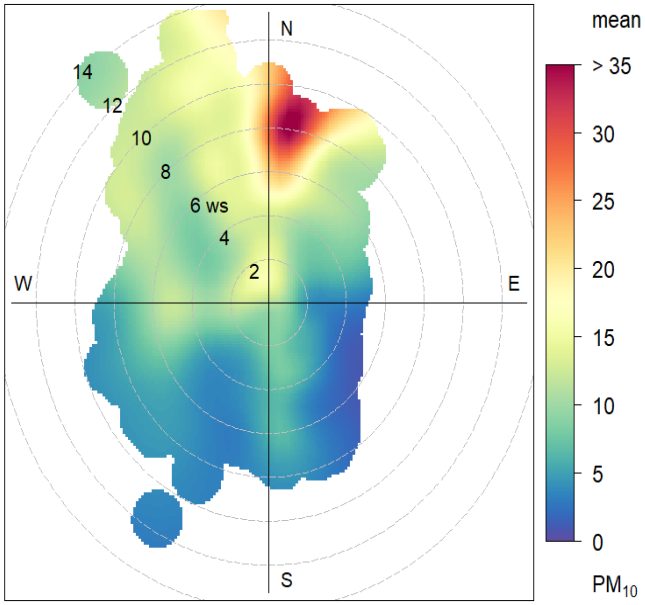

(b)

Figure 96: Winter 2021 (June-August) at St. Helena Bay Private Home (a) PM_{10} Pollution Rose and (b) PM_{10} Polar Plot

West Coast Mall

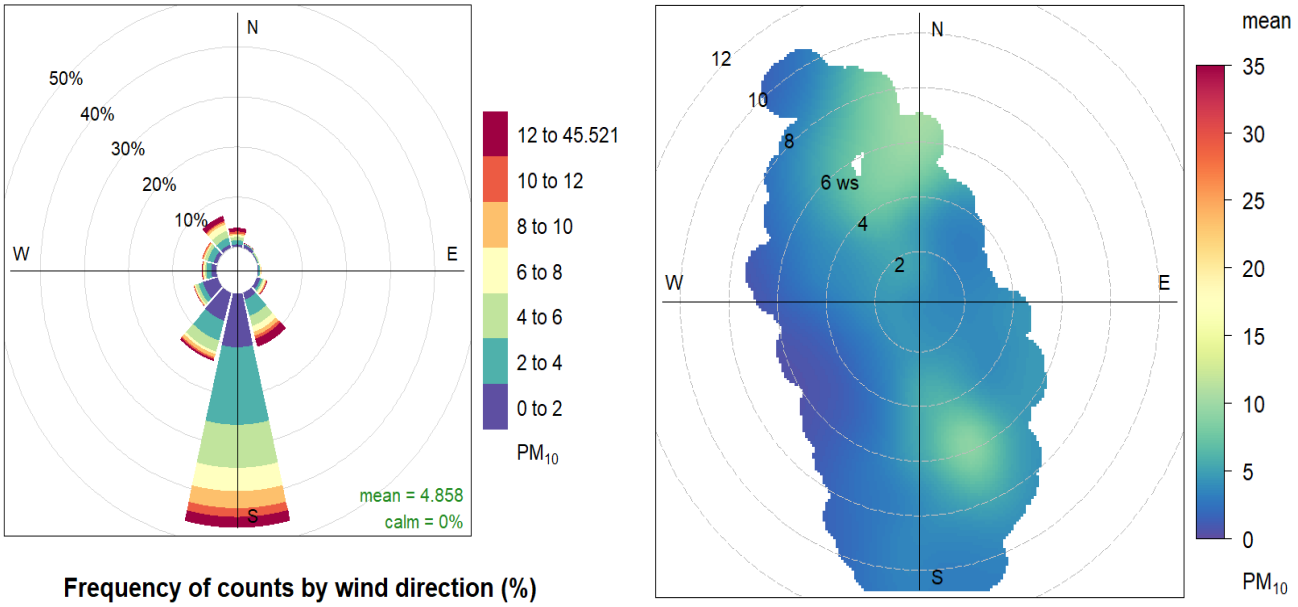

(a) (b)

Figure 97: The effect of wind direction and speed on PM_{10} Concentrations captured at the West Coast Mall using (a) a pollution rose and (b) a polar plot

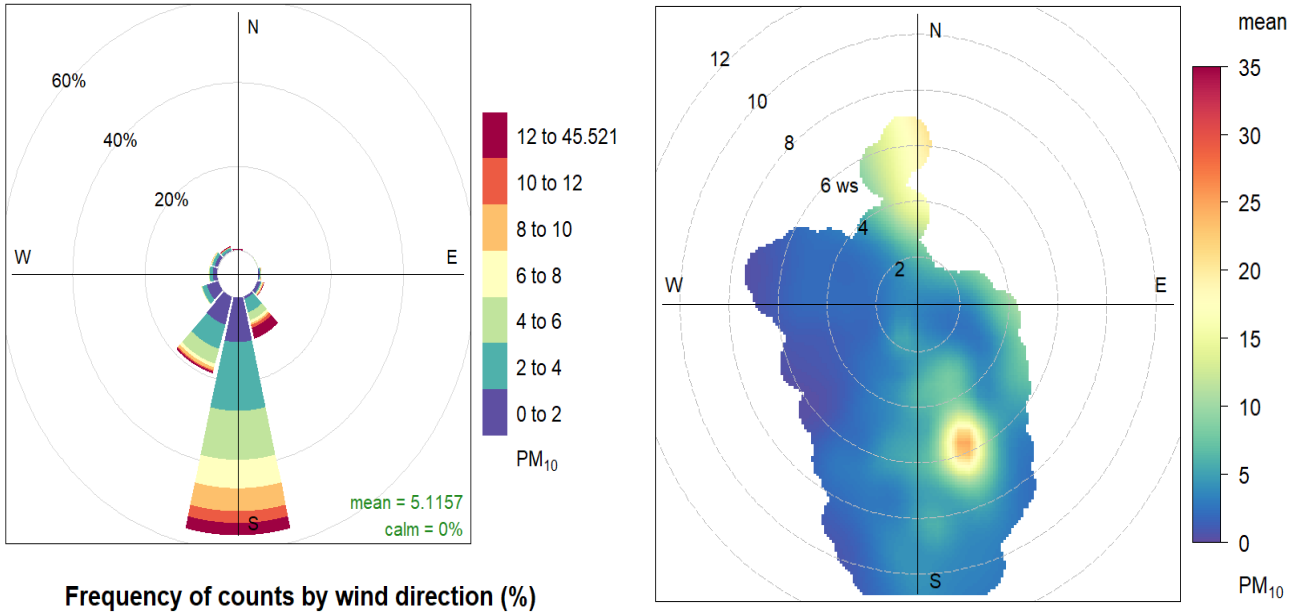

(a) (b)

Figure 98: Summer 2021 (January-February) at the West Coast Mall (a) PM_{10} Pollution Rose and (b) PM_{10} Polar Plot

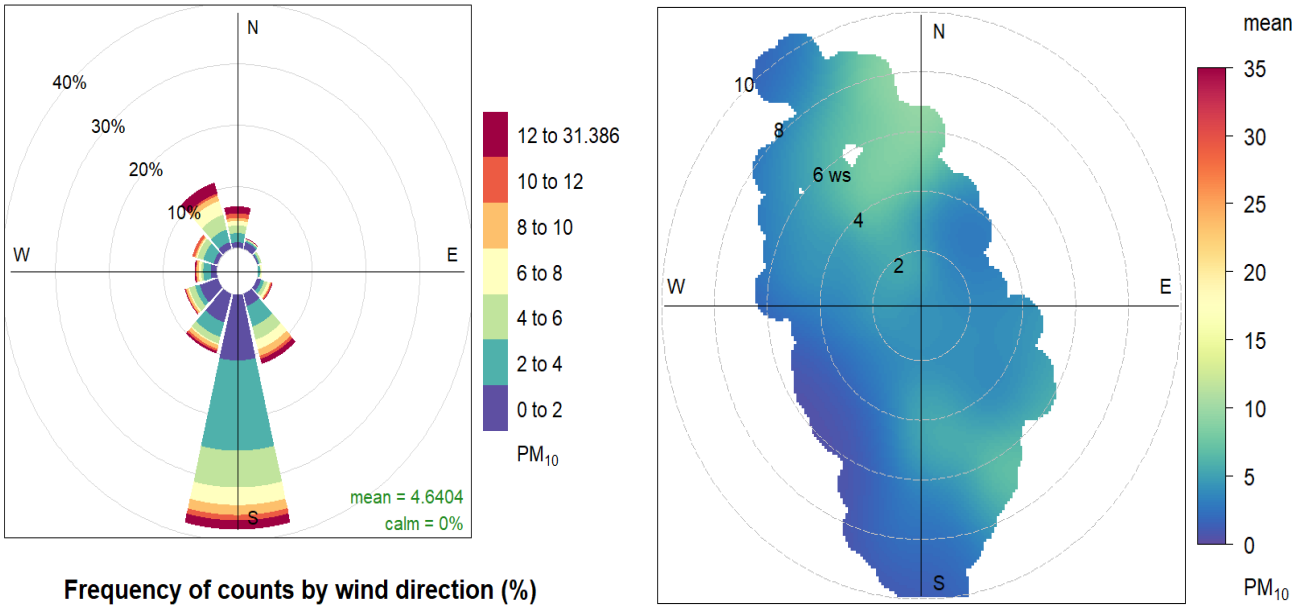

(a) (b)

Figure 99: Autumn 2021 (March-April) at the West Coast Mall (a) PM_{10} Pollution Rose and (b) PM_{10} Polar Plot

N

Langebaan Private Home

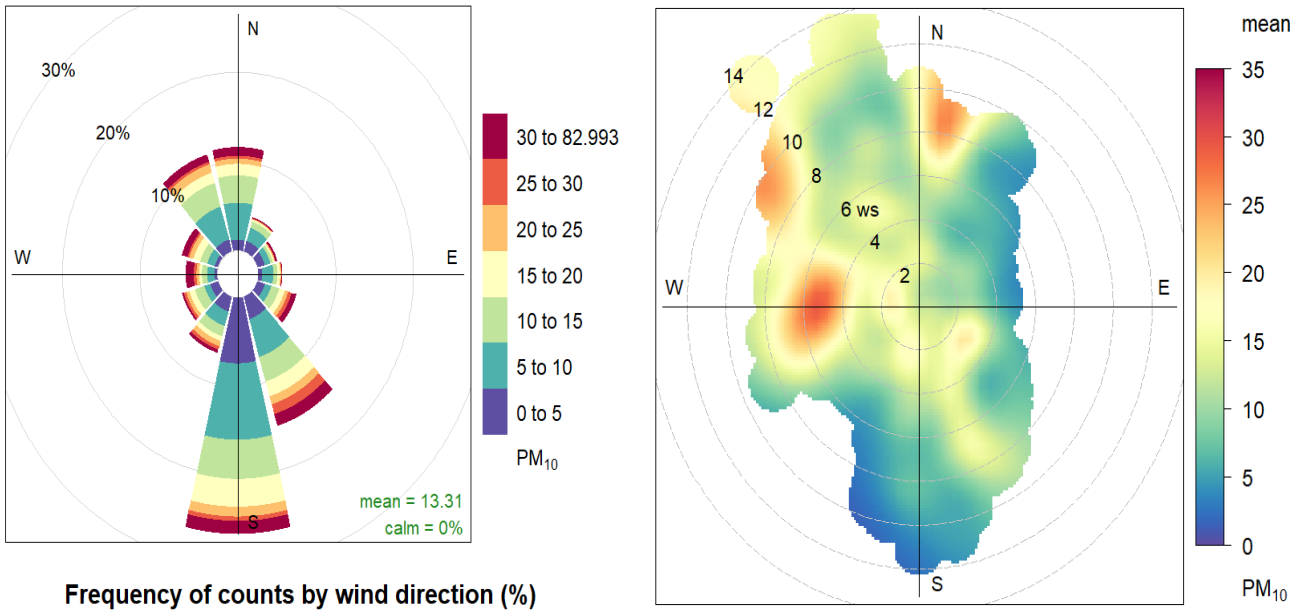

(a) (b)

Figure 100: The effect of wind direction and speed on PM_{10} Concentrations captured at the Langebaan Private Home using (a) a pollution rose and (b) a polar plot

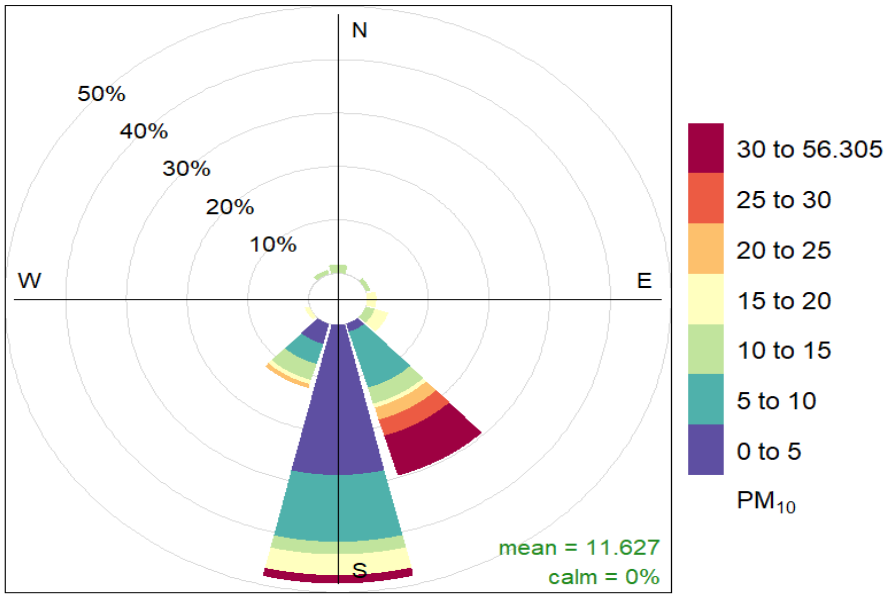

Figure 101: Summer 2021 (February) at the Langebaan Private Home PM_{10} Pollution Rose

O

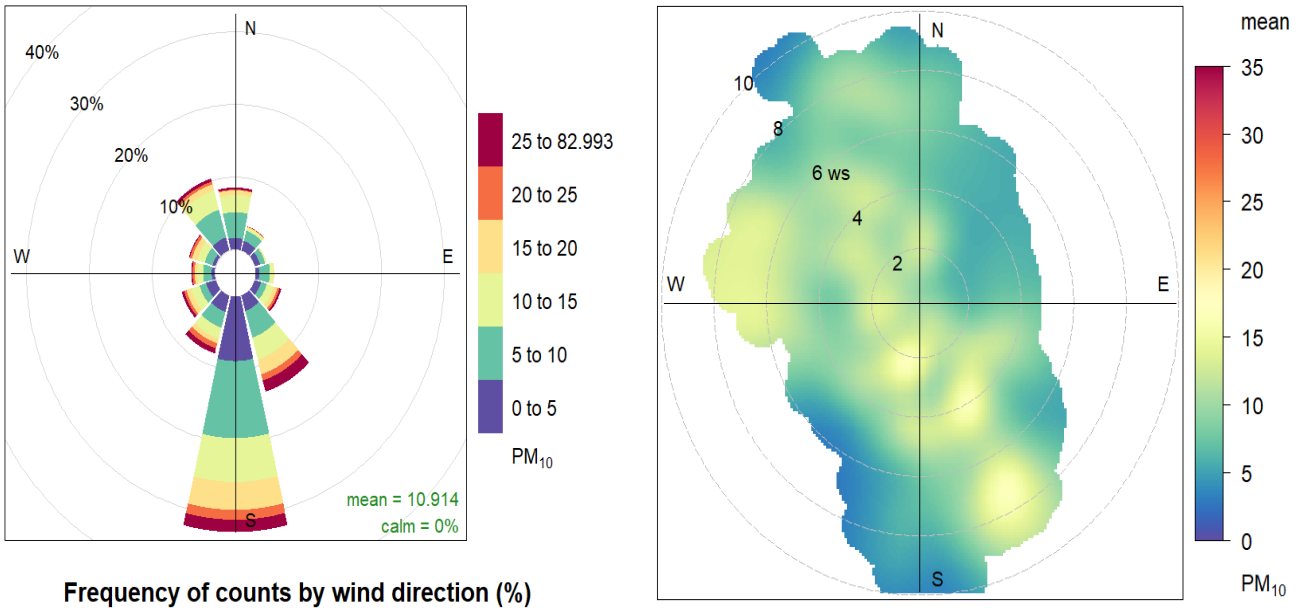

(a) (b)

Figure 102: Autumn 2021 (March-May) at the Langebaan Private Home (a) PM_{10} Pollution Rose and (b) PM_{10} Polar Plot

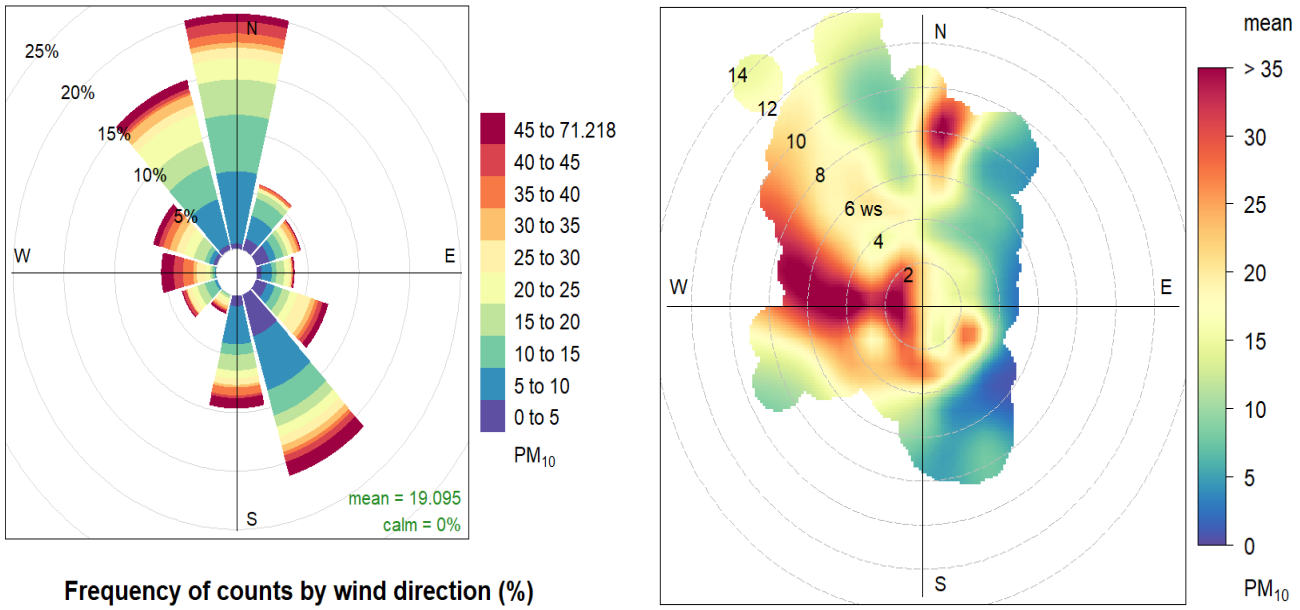

(a) (b)

Figure 103: Winter 2021 (June-July) at the Langebaan Private Home (a) PM_{10} Pollution Rose and (b) PM_{10} Polar Plot

Vredenburg AQM Station

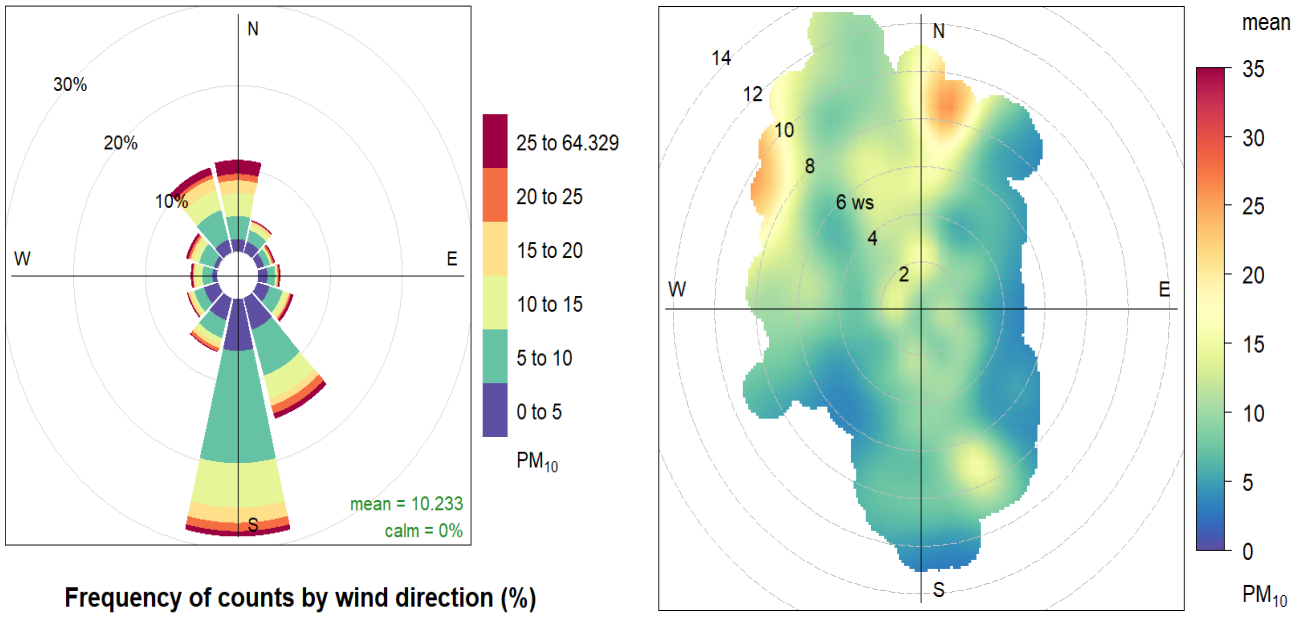

(a) (b)

Figure 104: The effect of wind direction and speed on PM_{10} Concentrations captured at the Vredenburg AQM Station using (a) a pollution rose and (b) a polar plot

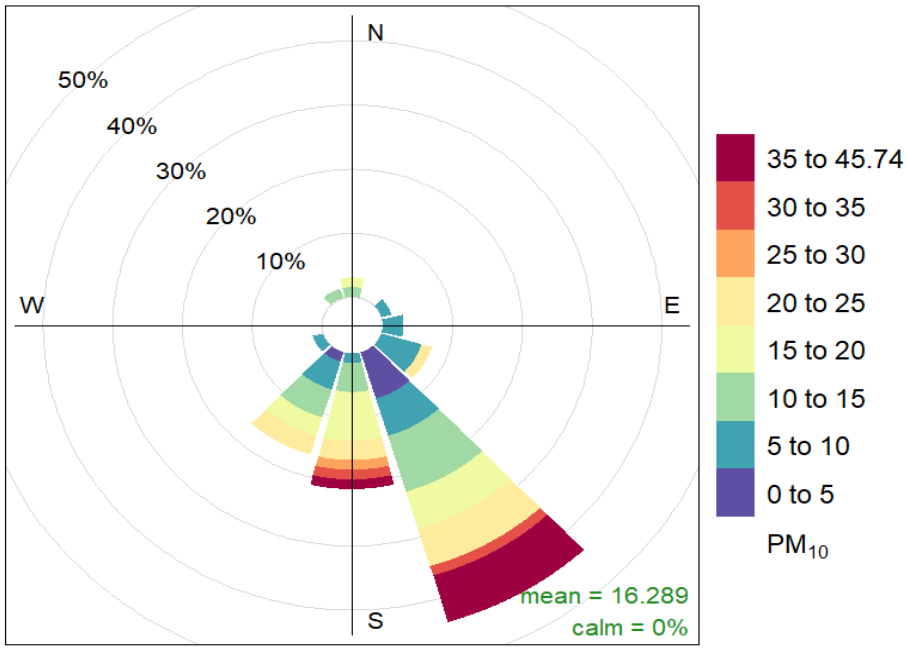

Figure 105: Summer 2021 (February) at the Vredenburg AQM Station PM_{10} Pollution Rose

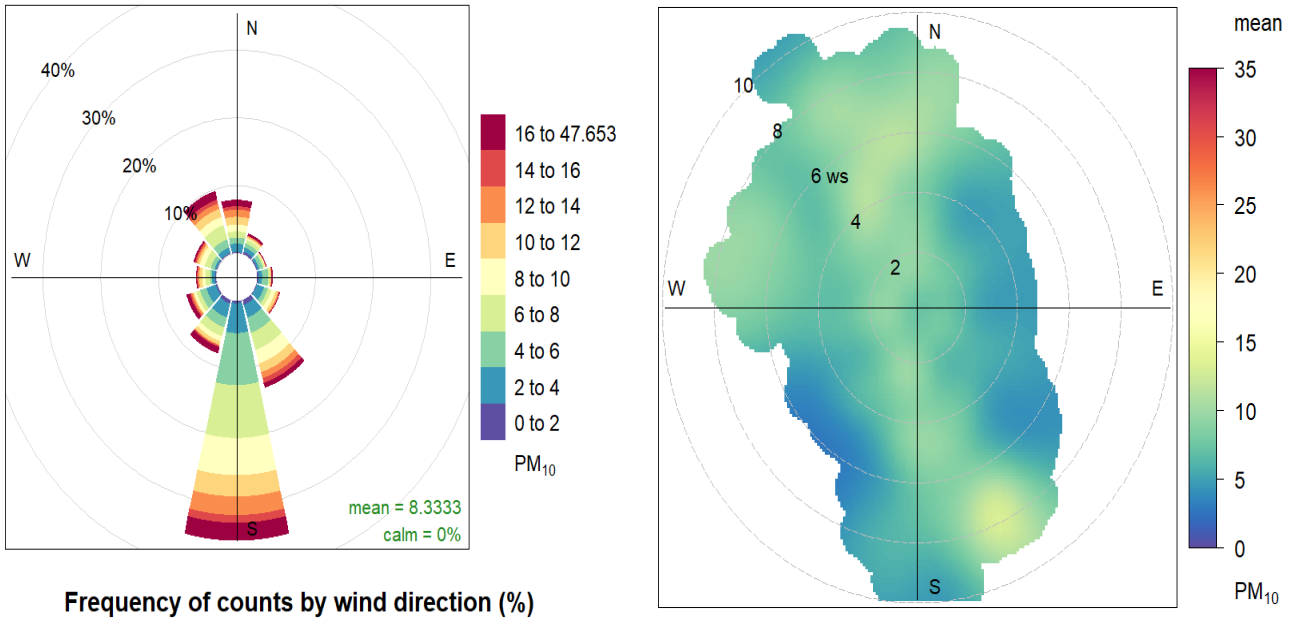

(a) (b)

Figure 106: Autumn 2021 (March-May) at the Vredenburg AQM Station (a) PM_{10} Pollution Rose and (b) PM_{10} Polar Plot

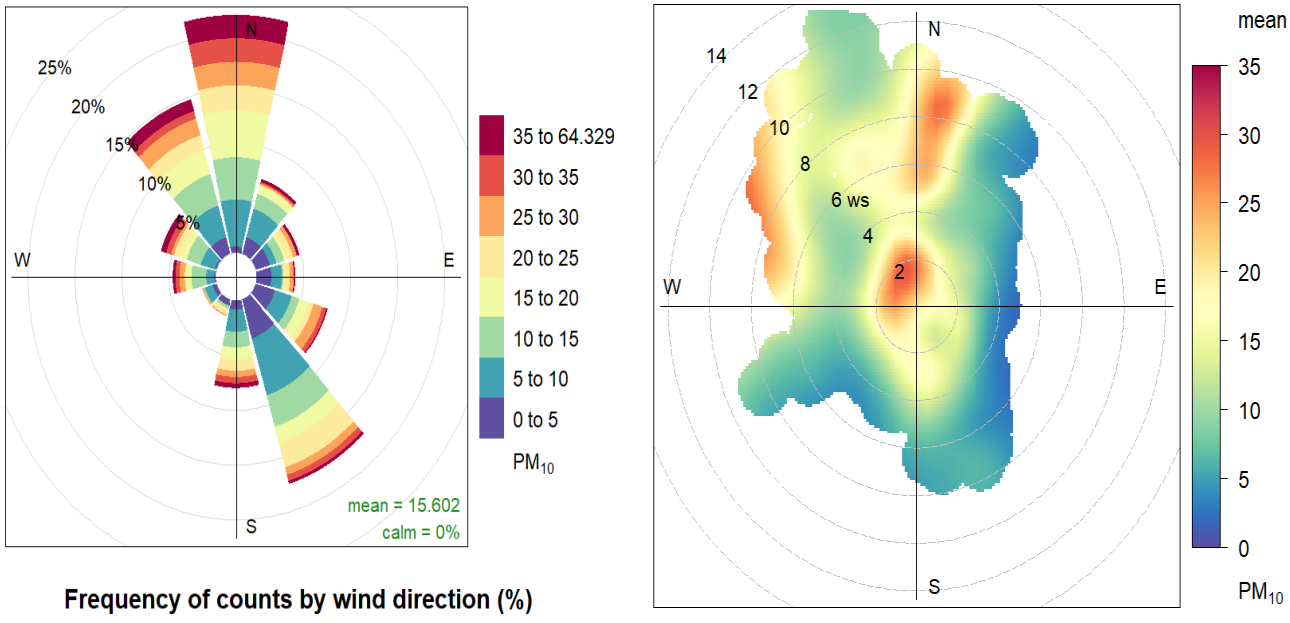

(a) (b)

Figure 107: Winter 2021 (June) at the Vredenburg AQM Station (a) PM_{10} Pollution Rose and (b) PM_{10} Polar Plot

Appendix D – Summary PM_{10} Plots including all Seven Study Sites

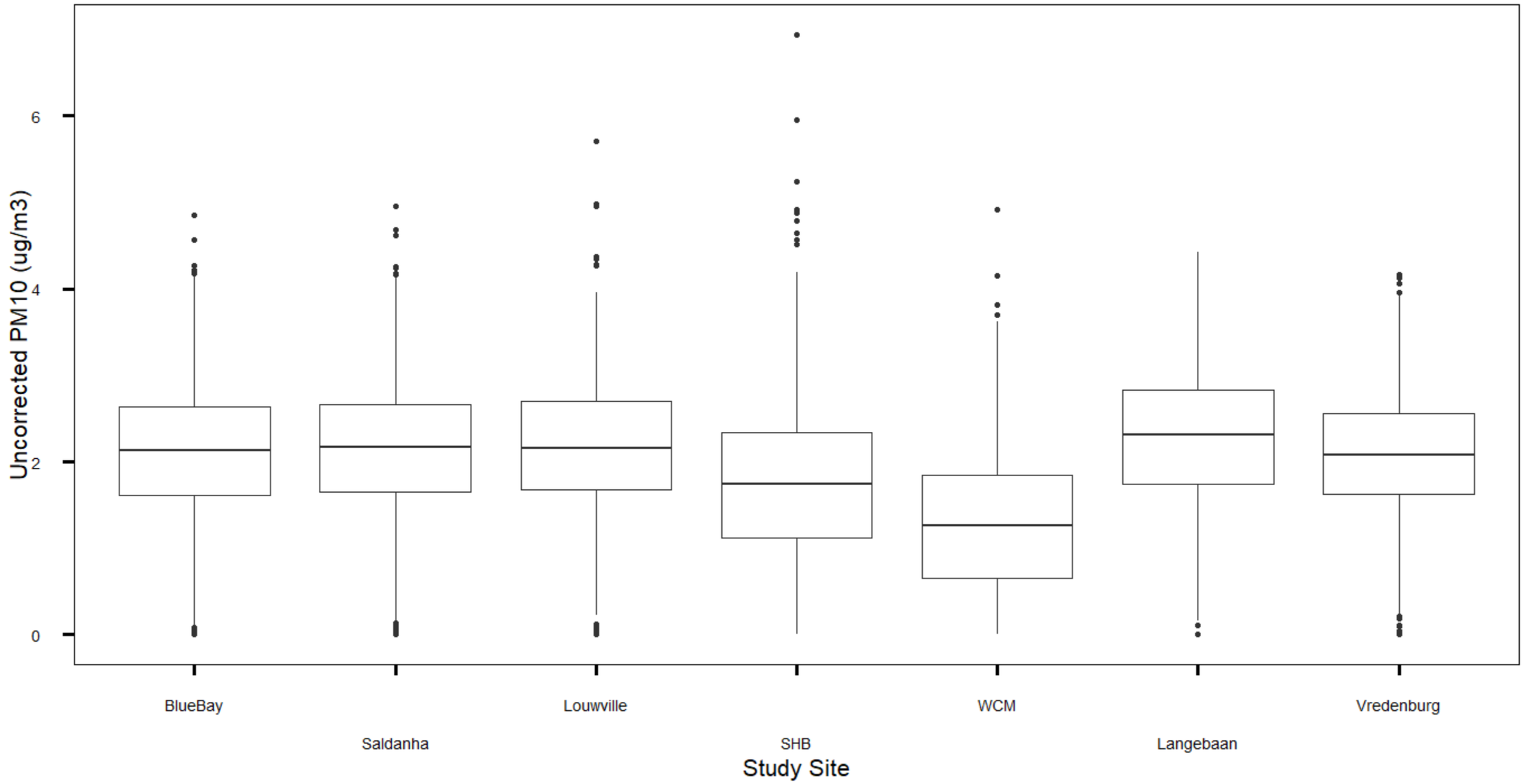

Figure 108: Summary of the Hourly Uncorrected PM_{10} Concentrations at all Seven Study Sites

*BlueBay = Blue Bay Lodge, Saldanha = Saldanha AQM Station, Louwville = Louwville Private Home, SHB = St. Helena Bay Private Home, WCM = West Coast Mall, Langebaan = Langebaan Private Home, Vredenburg = Vredenburg AQM Station

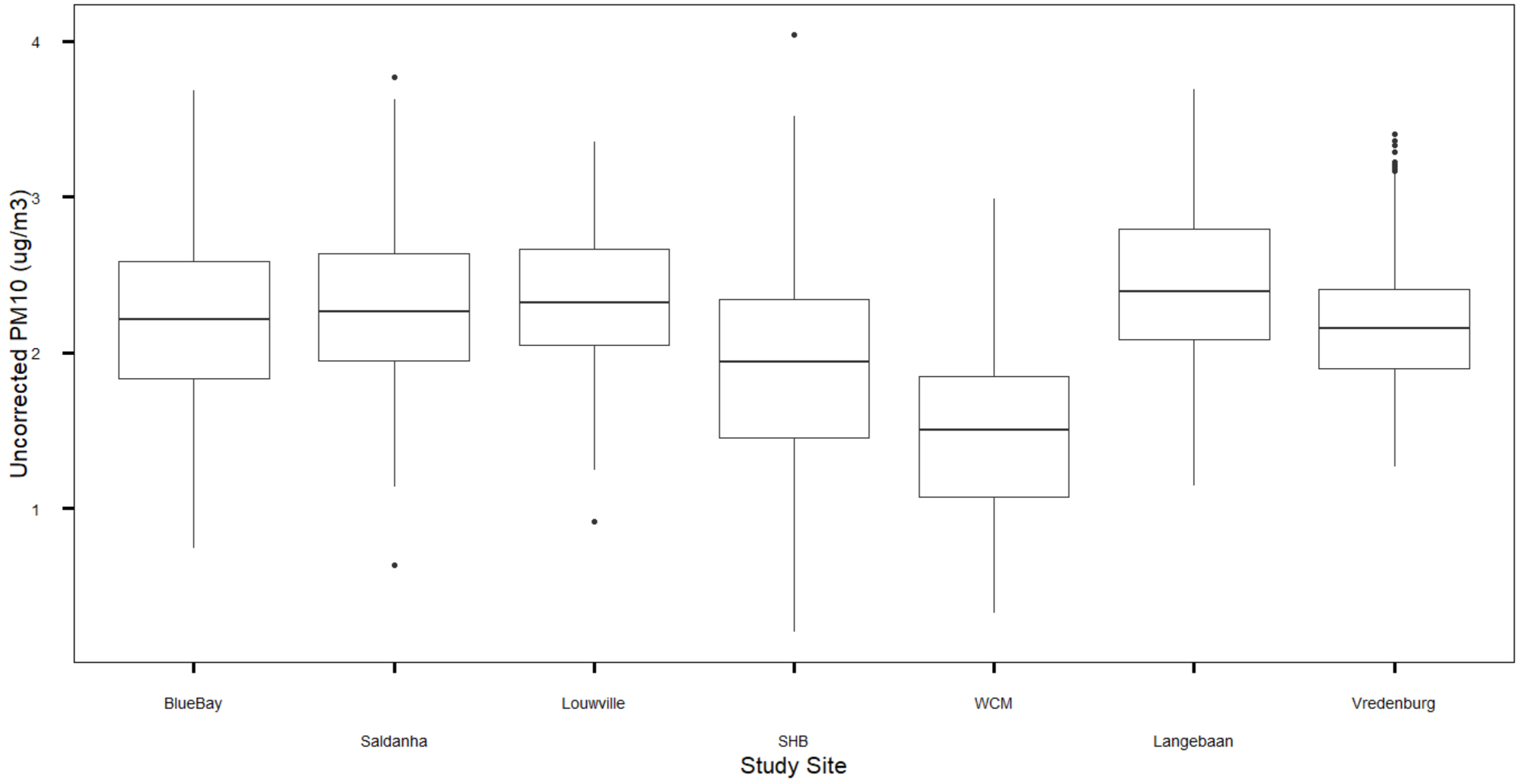

Figure 109: Summary of the 24-hour Uncorrected PM_{10} Concentrations at all Seven Study Sites

*BlueBay = Blue Bay Lodge, Saldanha = Saldanha AQM Station, Louwville = Louwville Private Home, SHB = St. Helena Bay Private Home, WCM = West Coast Mall, Langebaan = Langebaan Private Home, Vredenburg = Vredenburg AQM Station

T

Appendix E – $PM_{2.5}$ and PM_{10} Boxplot Interpretations

Table 46: Hourly $PM_{2.5}$ Box Plot Interpretations – Original Scale

	Blue Bay Lodge	Blue Bay Lodge Corrected	Saldanha AQM Station	Saldanha AQM Station Corrected	Louwville Private Home	Louwville Private Home Corrected	St. Helena Bay Private Home	St. Helena Bay Private Home Corrected	West Coast Mall	West Coast Mall Corrected	Langebaan Private Home	Langebaan Private Home Corrected	Vredenburg AQM Station	Vredenburg AQM Station Corrected
Minimum	0.015	0.00	0.077	0.00	0.025	0.00	0.01	0.00	0.026	0.00	0.044	0.00	0.45	0.00
Q1	3.14	1.93	3.57	2.94	2.68	2.28	1.37	1.69	1.28	0.00	3.46	2.29	3.35	0.00
Q2	5.50	3.39	6.38	4.55	5.08	3.63	3.20	3.07	2.57	1.11	6.59	4.08	5.48	1.40
Q3	9.29	5.26	11.01	6.90	9.37	5.94	6.60	4.97	5.06	2.75	11.62	6.72	9.32	4.19
Maximum	115.54	86.82	130.60	104.96	211.46	165.04	234.78	186.43	122.89	95.77	60.93	45.64	50.76	35.01
Mean	7.23	4.16	8.65	5.76	7.01	4.69	5.28	4.06	3.91	1.88	9.13	5.45	7.55	2.75
Upper Limit	18.51	10.24	22.19	12.84	19.40	11.42	14.45	9.89	10.73	6.86	23.86	13.36	18.27	10.48

Table 47: Hourly $PM_{2.5}$ Box Plot Interpretations - Logarithmic Scale

	Blue Bay Lodge	Blue Bay Lodge Corrected	Saldanha AQM Station	Saldanha AQM Station Corrected	Louwville Private Home	Louwville Private Home Corrected	St. Helena Bay Private Home	St. Helena Bay Private Home Corrected	West Coast Mall	West Coast Mall Corrected	Langebaan Private Home	Langebaan Private Home Corrected	Vredenburg AQM Station	Vredenburg AQM Station Corrected
Minimum	0.00	0.00	0.00	0.00	0.00	0.00	0.00	0.00	0.00	0.00	0.00	0.00	0.00	0.00
Q1	1.15	0.66	0.00	0.00	0.99	0.82	0.32	0.52	0.25	0.00	1.24	0.83	1.21	0.00
Q2	1.70	1.22	1.40	1.18	1.62	1.29	1.16	1.12	0.94	0.11	1.89	1.41	1.70	0.34
Q3	2.23	1.66	2.17	1.76	2.24	1.78	1.89	1.60	1.62	1.01	2.45	1.91	2.23	1.43
Maximum	4.75	4.46	4.87	4.65	5.35	5.11	5.46	5.23	4.81	4.56	4.11	3.82	3.93	3.56
Mean	1.67	1.17	1.30	1.07	1.59	1.29	1.19	1.10	1.01	0.52	1.85	1.39	1.72	0.74
Upper Limit	3.86	3.16	5.42	4.39	4.11	3.22	4.24	3.22	3.68	2.52	4.27	3.52	3.77	3.58

Table 48: 24-hour $PM_{2.5}$ Box Plot Interpretations – Original Scale

	Blue Bay Lodge	Blue Bay Lodge Corrected	Saldanha AQM Station	Saldanha AQM Station Corrected	Louwville Private Home	Louwville Private Home Corrected	St. Helena Bay Private Home	St. Helena Bay Private Home Corrected	West Coast Mall	West Coast Mall Corrected	Langebaan Private Home	Langebaan Private Home Corrected	Vredenburg AQM Station	Vredenburg AQM Station Corrected
Minimum	1.25	0.00	1.10	0.31	1.29	0.70	0.45	0.67	0.87	0.00	1.67	1.42	2.22	0.00
Q1	4.11	2.37	5.12	3.44	4.23	2.92	2.06	2.18	2.20	0.00	5.01	2.77	4.58	0.24
Q2	5.92	3.56	7.21	4.95	6.53	3.99	4.29	3.14	3.45	1.20	7.31	4.42	6.14	1.57
Q3	8.68	5.15	10.26	7.13	8.50	6.04	6.42	4.95	4.81	2.55	11.99	7.08	8.08	2.53
Maximum	29.70	17.96	34.45	22.71	19.58	13.65	38.52	32.07	17.53	11.25	29.28	18.45	26.06	16.20
Mean	7.26	4.13	8.66	5.76	6.96	4.64	5.46	4.19	4.02	1.81	9.09	5.41	7.46	2.53
Upper Limit	15.54	9.31	17.97	12.67	14.92	10.72	12.96	9.10	8.72	6.37	22.45	13.55	13.33	5.96

U

Table 49: 24-hour $PM_{2.5}$ Box Plot Interpretations – Logarithmic Scale

	Blue Bay Lodge	Blue Bay Lodge Corrected	Saldanha AQM Station	Saldanha AQM Station Corrected	Louwville Private Home	Louwville Private Home Corrected	St. Helena Bay Private Home	St. Helena Bay Private Home Corrected	West Coast Mall	West Coast Mall Corrected	Langebaan Private Home	Langebaan Private Home Corrected	Vredenburg AQM Station	Vredenburg AQM Station Corrected
Minimum	0.22	0.00	0.094	0.00	0.26	0.00	0.00	0.00	0.00	0.00	0.51	0.34	0.80	0.00
Q1	1.41	0.86	1.63	1.24	1.44	1.07	0.72	0.78	0.79	0.00	1.61	1.02	1.52	0.00
Q2	1.78	1.27	1.98	1.60	1.88	1.38	1.46	1.14	1.24	0.18	1.99	1.49	1.81	0.45
Q3	2.16	1.64	2.33	1.96	2.14	1.80	1.86	1.60	1.57	0.93	2.48	1.96	2.09	1.28
Maximum	3.39	2.89	3.54	3.12	2.97	2.61	3.65	3.47	2.86	2.42	3.38	2.91	3.26	2.79
Mean	1.80	1.24	2.00	1.59	1.78	1.39	1.37	1.22	1.21	0.52	2.02	1.51	1.86	0.70
Upper Limit	3.28	2.80	3.37	3.06	3.19	2.89	3.56	2.83	2.74	2.34	3.79	3.37	2.94	3.20

Table 50: Hourly PM_{10} Box Plot Interpretations – Original Scale

	Blue Bay Lodge	Saldanha AQM Station	Louwville Private Home	St. Helena Bay Private Home	West Coast Mall	Langebaan Private Home	Vredenburg AQM Station
Minimum	0.029	0.00	0.18	0.068	0.10	0.20	0.57
Q1	5.04	5.23	5.34	3.05	1.92	5.73	5.06
Q2	8.37	8.70	8.60	5.68	3.54	10.03	8.00
Q3	13.99	14.24	14.83	10.41	6.31	16.88	12.82
Maximum	126.90	141.00	299.57	1032.56	136.33	82.99	64.33
Mean	10.65	11.25	11.33	8.65	4.99	13.31	10.28
Upper Limit	27.42	27.76	29.07	21.46	12.91	33.60	24.47

Table 51: Hourly PM_{10} Box Plot Interpretations – Logarithmic Scale

	Blue Bay Lodge	Saldanha AQM Station	Louwville Private Home	St. Helena Bay Private Home	West Coast Mall	Langebaan Private Home	Vredenburg AQM Station
Minimum	0.00	0.00	0.00	0.00	0.00	0.00	0.00
Q1	1.62	1.65	1.68	1.11	0.65	1.74	1.62
Q2	2.12	2.16	2.15	1.74	1.27	2.31	2.08
Q3	2.64	2.66	2.70	2.34	1.84	2.83	2.55
Maximum	4.84	4.95	5.70	6.94	4.92	4.42	4.16
Mean	2.10	2.14	2.15	1.73	1.26	2.29	2.08
Upper Limit	4.17	4.16	4.23	4.19	3.63	4.45	3.94

Table 52: 24-hour PM_{10} Box Plot Interpretations – Original Scale

	Blue Bay Lodge	Saldanha AQM Station	Louwville Private Home	St. Helena Bay Private Home	West Coast Mall	Langebaan Private Home	Vredenburg AQM Station
Minimum	2.10	0.00	2.50	1.23	1.40	3.15	3.55
Q1	6.27	6.97	7.74	4.27	2.93	8.06	6.70
Q2	9.18	9.54	10.21	6.96	4.51	10.99	8.62
Q3	13.33	13.93	14.41	10.39	6.37	16.42	11.12
Maximum	39.89	43.37	28.57	57.11	19.87	40.13	30.15
Mean	10.65	11.21	11.29	8.641	5.15	13.23	10.28
Upper Limit	23.91	24.38	24.40	19.57	11.52	28.96	17.76

Table 53: 24-hour PM_{10} Box Plot Interpretations – Logarithmic Scale

	Blue Bay Lodge	Saldanha AQM Station	Louwville Private Home	St. Helena Bay Private Home	West Coast Mall	Langebaan Private Home	Vredenburg AQM Station
Minimum	0.74	0.00	0.91	0.20	0.33	1.15	1.27
Q1	1.84	1.94	2.05	1.45	1.07	2.09	1.90
Q2	2.22	2.26	2.32	1.94	1.51	2.40	2.15
Q3	2.59	2.63	2.67	2.34	1.85	2.80	2.41
Maximum	3.69	3.77	3.35	4.04	2.99	3.69	3.41
Mean	2.22	2.28	2.32	1.91	1.49	2.44	2.21
Upper Limit	3.72	3.67	3.60	3.68	3.02	3.87	3.17

Appendix F – XRD Graph

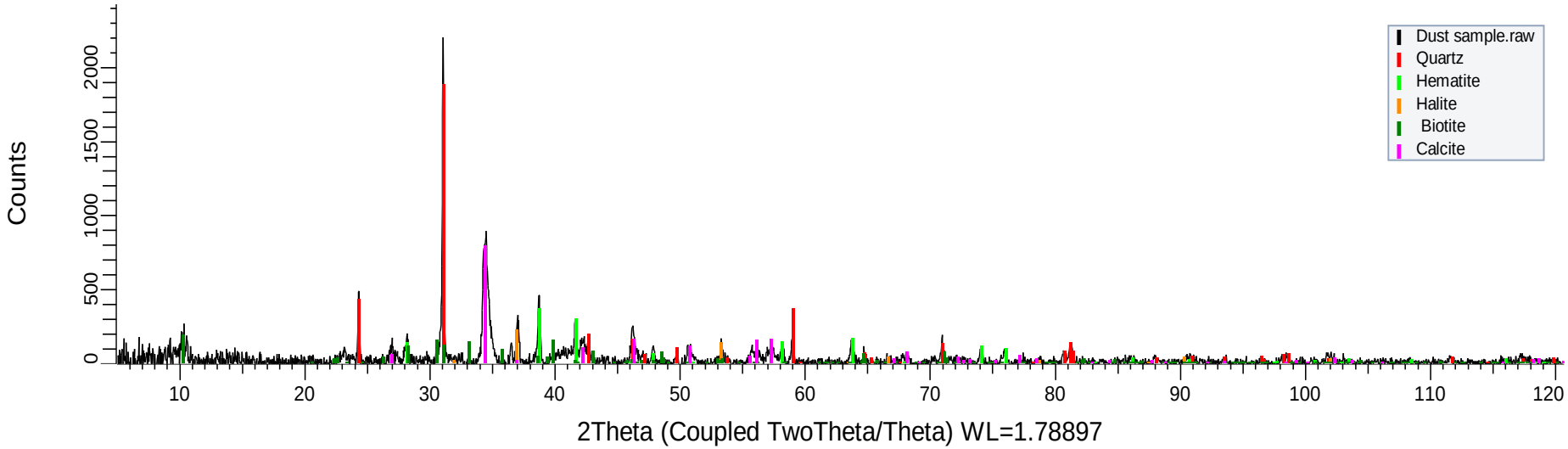

Figure 110: XRD of Dust Sub-Sample Graph

Appendix G – Sample Calculations for Dust Fall Rate and ICP Results

Dust Fall Rate

$$\text{Dust Fall Rate} = \frac{Mass\ of\ Sample}{Cross\ Sectional\ Area\ of\ Dust\ Bucket\ x\ Number\ of\ sampling\ days}$$

$$= \frac{1635.9\ mg}{\left[\frac{22}{7}\ x\ (0.075\ m^2)\right][27\ days]}$$

= 3 427 mg/m^2/day

ICP Element Concentration calculation

Two sample calculations are provided, one for lead which was presented in µg/kg.

$$[\text{Lead}] = \frac{40\ 092\ \mu g}{kg}\ x\ \frac{0.0323\ g}{1}\ x\ \frac{kg}{1000\ g}\ x\ \frac{min}{16.7\ L}\ x\ \frac{1000\ L}{m^3}\ x\ \frac{1}{28\ days}\ x\ \frac{day}{24\ hour}\ x\ \frac{hour}{60\ min}$$

= 0.0019 µg/m^3

Where:

Concentration of lead found on filter paper = 40 092 µg/kg

Mass of sample on filter paper = 0.0323 g

Flowrate of air = 16.7 L/min

Number of days = 28 days

Appendix H – $PM_{2.5}$ and PM_{10} Uncertainty Polar Plots at all Seven Study Sites

Blue Bay Lodge

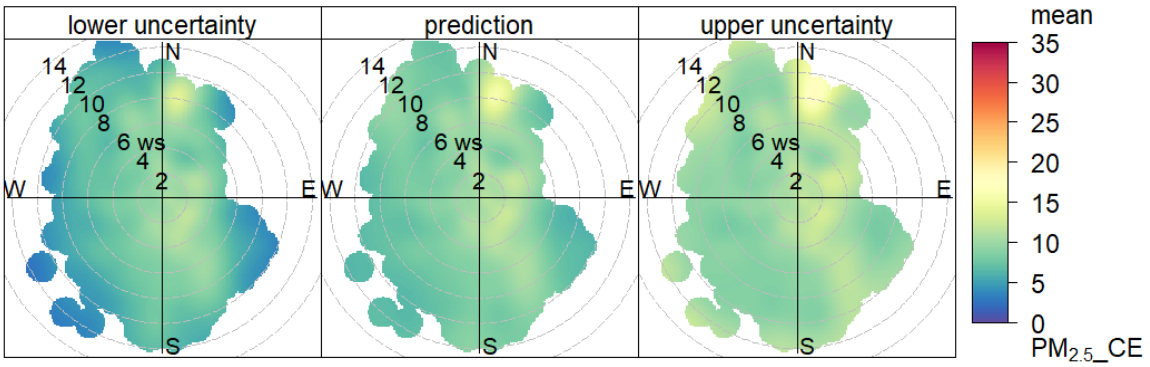

Figure 111: $PM_{2.5}$ Uncertainty Polar Plot for Blue Bay Lodge

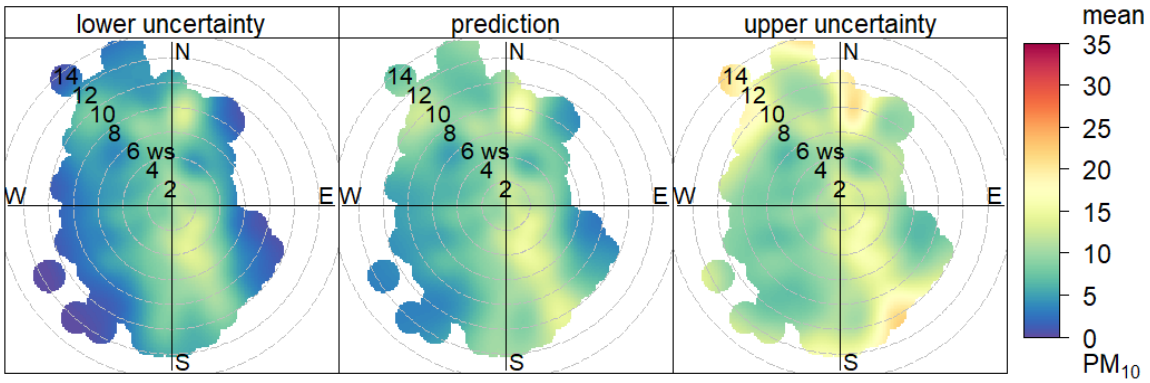

Figure 112: PM_{10} Uncertainty Polar Plot for Blue Bay Lodge

Saldanha AQM Station

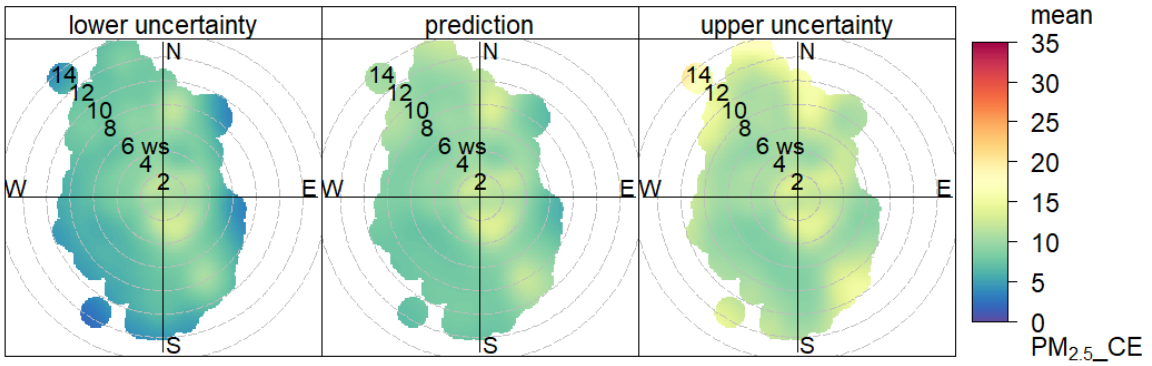

Figure 113: $PM_{2.5}$ Uncertainty Polar Plot for Saldanha AQM Station

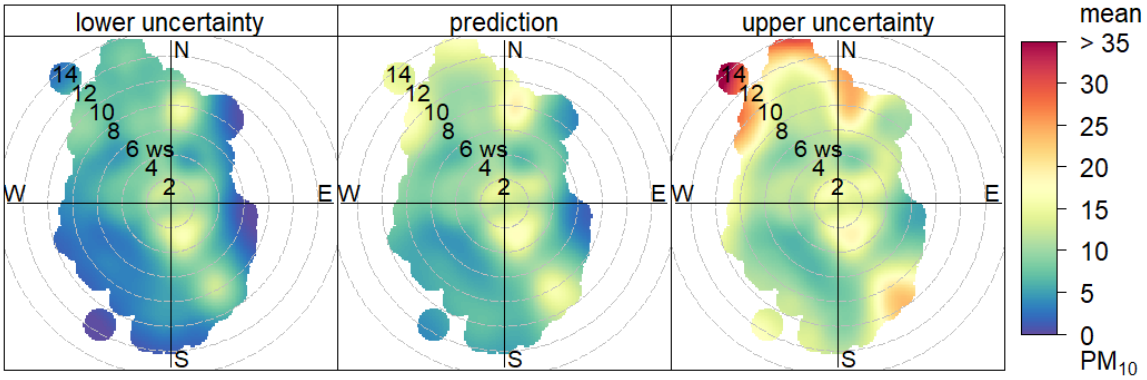

Figure 114: PM_{10} Uncertainty Polar Plot for Saldanha AQM Station

Louwville Private Home

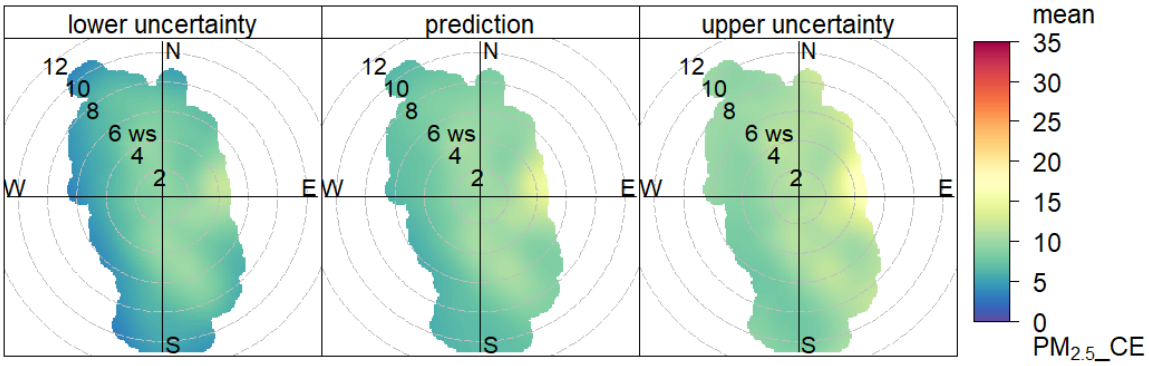

Figure 115: $PM_{2.5}$ Uncertainty Polar Plot for Louwville Private Home

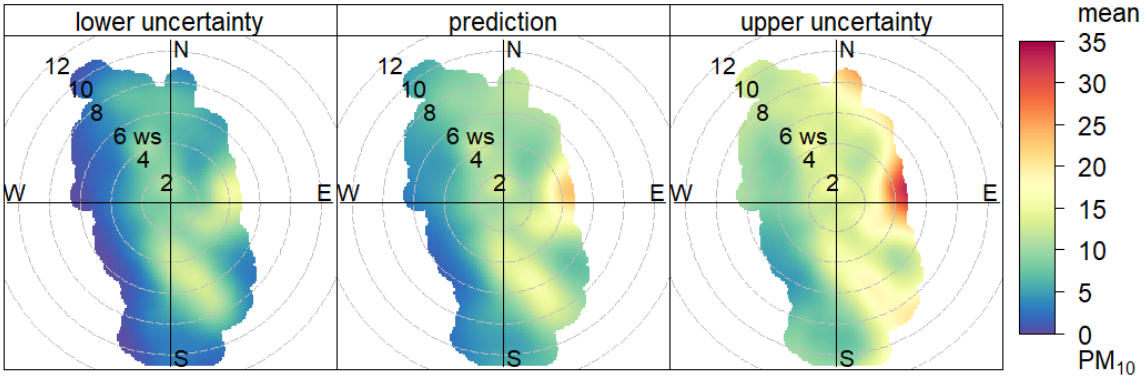

Figure 116: PM_{10} Uncertainty Polar Plot for Louwville Private Home

St. Helena Bay Private Home

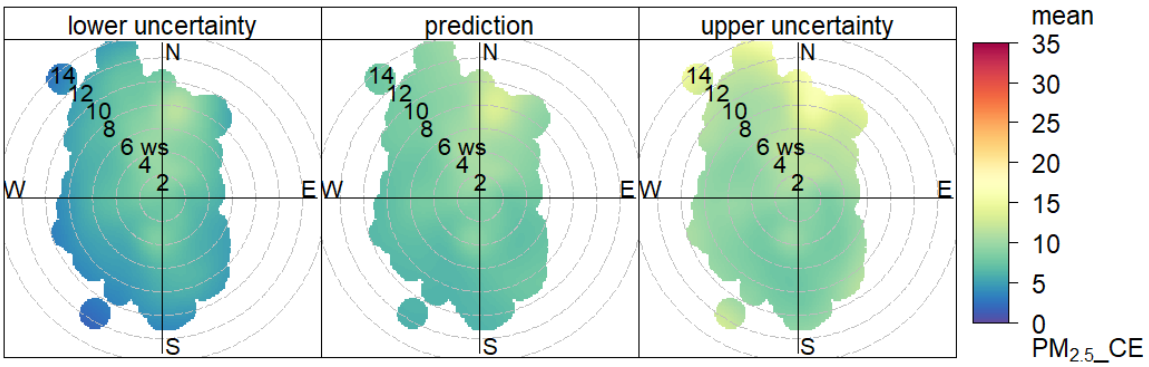

Figure 117: $PM_{2.5}$ Uncertainty Polar Plot for St. Helena Bay Private Home

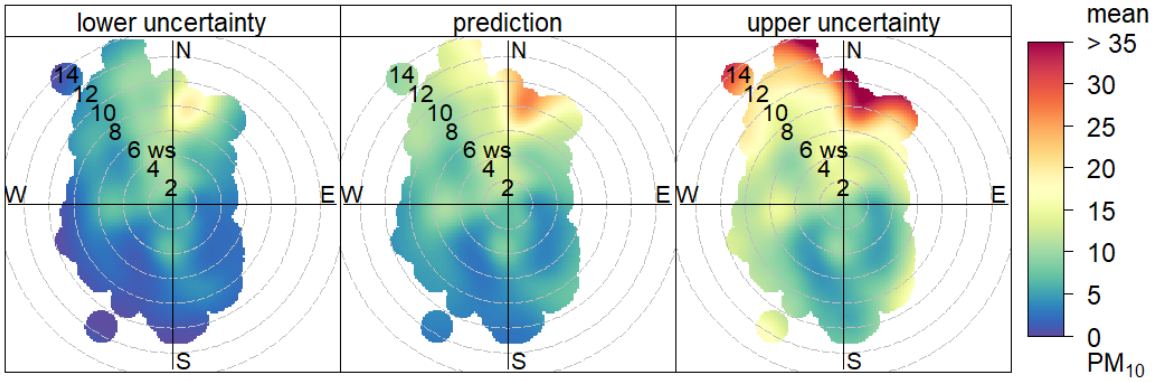

Figure 118: PM_{10} Uncertainty Polar Plot for St. Helena Bay Private Home

West Coast Mall

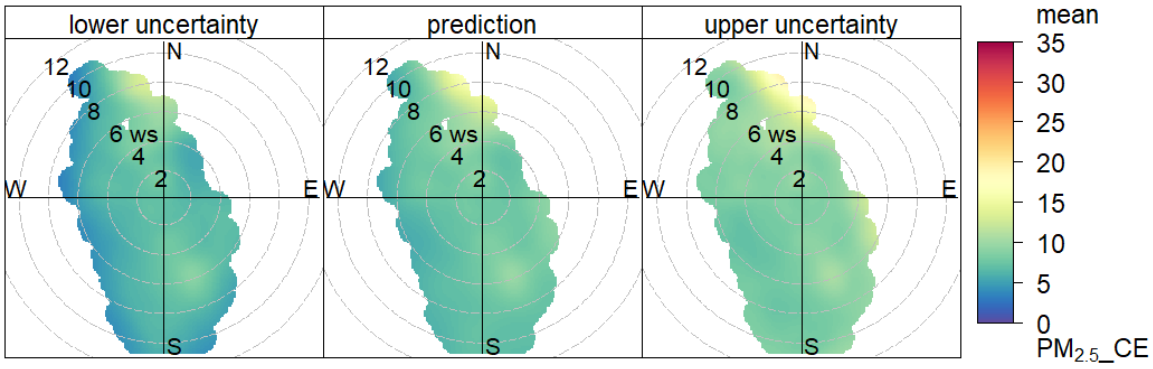

Figure 119: $PM_{2.5}$ Uncertainty Polar Plot for West Coast Mall

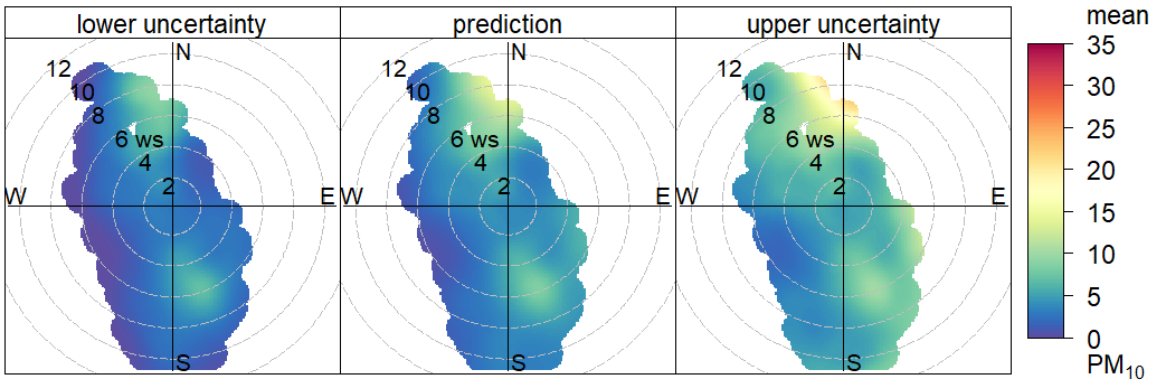

Figure 120: PM_{10} Uncertainty Polar Plot for West Coast Mall

Langebaan Private Home

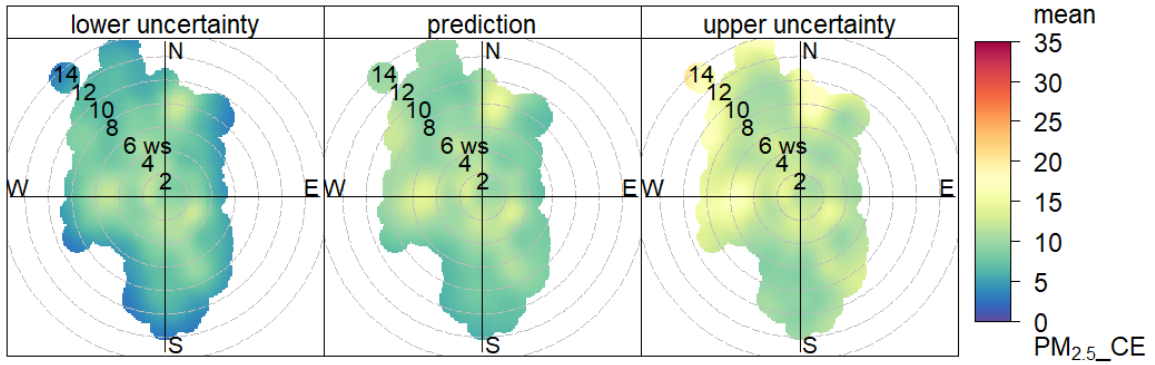

Figure 121: $PM_{2.5}$ Uncertainty Polar Plot for Langebaan Private Home

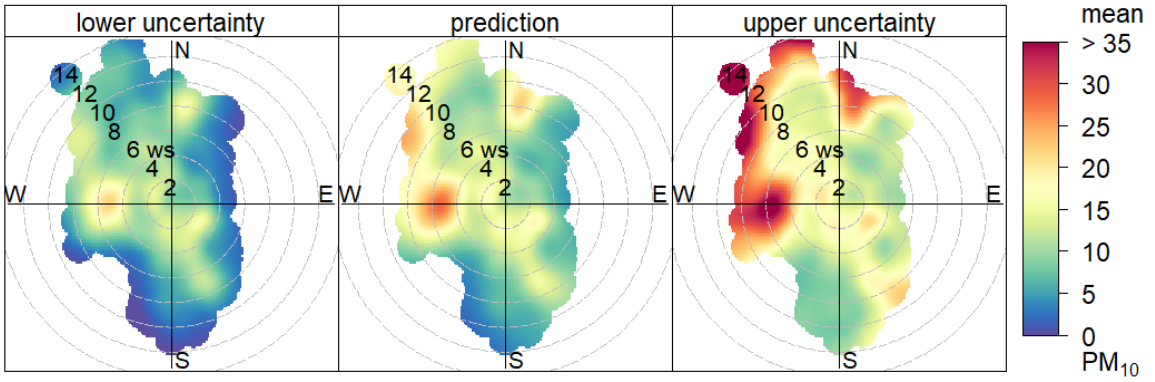

Figure 122: PM_{10} Uncertainty Polar Plot for Langebaan Private Home

Vredenburg AQM Station

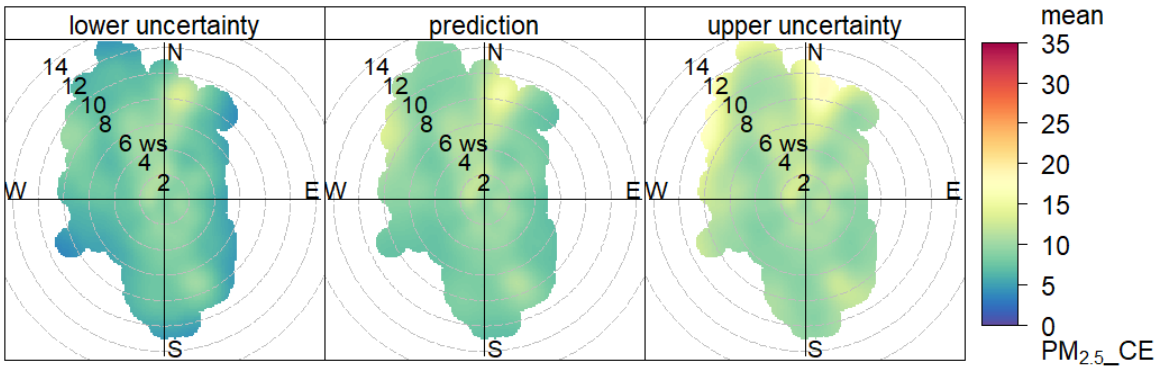

Figure 123: $PM_{2.5}$ Uncertainty Polar Plot for Vredenburg AQM Station

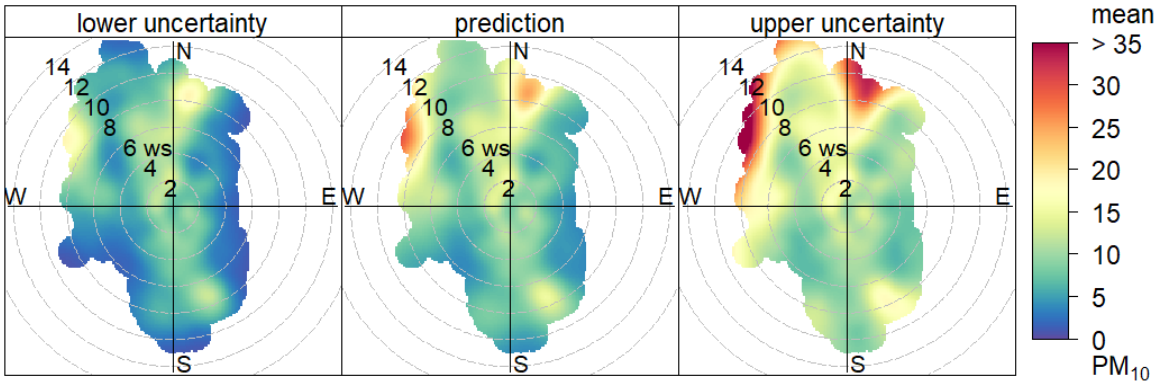

Figure 124: PM_{10} Uncertainty Polar Plot for Vredenburg AQM Station

Appendix I – The Distribution of Minerals across the Different Size Fractions in the BSNE Sample

Table 54: The distribution of quartz, hematite, mica and feldspar across the different size fractions

Size bins (µm)	Total mass% in size bin	Quartz			Hematite			Mica			Feldspar		
		Mass%	g	% of total	Mass%	g	% of total	Mass%	g	% of total	Mass%	g	% of total
<5	6.8	9.7	0.7	1.5	10.6	0.7	5.6	19.3	1.3	15.6	19.3	1.3	8.2
5-10	8.6	15.7	1.4	3.0	12.3	1.1	8.2	20.1	1.7	20.6	18.9	1.6	10.1
10-20	13.1	25.4	3.3	7.4	12.3	1.6	12.5	16.7	2.2	26.0	19.6	2.6	16.0
20-63	33.0	45.6	15.0	33.3	7.9	2.6	20.3	7.7	2.5	30.3	21.3	7.0	43.9
63-100	19.6	70.9	13.9	30.7	6.2	1.2	9.5	2.2	0.4	5.1	11.9	2.3	14.6
100-125	10.4	79.4	8.3	18.3	4.2	0.4	3.4	1.6	0.2	2.0	7.7	0.8	5.0
125-150	2.6	43.4	1.1	2.5	12.2	1.1	8.5	0.8	0.02	0.2	5.9	0.2	1.0
150-200	3.4	6.7	0.2	0.5	86.8	3.0	23.0	0.0	0.00	0.0	6.1	0.2	1.3
200-250	2.5	53.8	1.3	3.0	45.7	1.1	8.9	0.4	0.01	0.1	0.0	0.0	0.0
250-350	0.0	0.0	0.0	0.0	0.0	0.0	0.0	0.0	0.0	0.0	0.0	0.0	0.0
>350	0.0	0.0	0.0	0.0	0.0	0.0	0.0	0.0	0.0	0.0	0.0	0.0	0.0
Total	100		45.2	100.0		12.8	100.0		8.4	100.0		16.0	100

Table 55: The distribution of chlorite, kaolinite, amphibole and epidote across the different size fractions

Size bins (µm)	Chlorite			Kaolinite			Amphibole			Epidote		
	Mass%	g	% of total	Mass%	g	% of total	Mass%	g	% of total	Mass%	g	% of total
<5	1.9	0.1	21.3	8.5	0.6	21.7	9.7	0.7	35.4	0.4	0.03	14.4
5-10	1.5	0.1	21.3	8.1	0.7	26.1	6.3	0.5	29.1	0.5	0.04	22.8
10-20	1.4	0.2	30.2	5.7	0.7	28.0	2.8	0.4	19.7	0.4	0.05	27.8
20-63	0.5	0.2	27.2	1.5	0.5	18.6	0.8	0.3	14.2	0.2	0.07	35.0
63-100	0.0	0.0	0.0	0.7	0.1	5.2	0.1	0.02	1.1			
100-125	0.0	0.0	0.0	0.1	0.01	0.4	0.1	0.01	0.6			
125-150	0.0	0.0	0.0	0.0	0.0	0.0	0.0	0.0	0.0			
150-200	0.0	0.0	0.0	0.0	0.0	0.0	0.0	0.0	0.0			
200-250	0.0	0.0	0.0	0.0	0.0	0.0	0.0	0.0	0.0			
250-350	0.0	0.0	0.0	0.0	0.0	0.0	0.0	0.0	0.0			
>350	0.0	0.0	0.0	0.0	0.0	0.0	0.0	0.0	0.0			
Total		0.6	100.0		2.7	100.0		1.9	100.0		0.2	

Table 56: The distribution of sulphides, rutile/anatase, ilmenite and carbonates across the different size fractions

Size bins (µm)	Sulphides			Rutile/Anatase			Ilmenite			Carbonates		
	Mass%	g	% of total	Mass%	g	% of total	Mass%	g	% of total	Mass%	g	% of total
<5	4.0	0.3	24.2	0.3	0.02	11.6	0.1	0.007	6.3	8.8	0.6	8.5
5-10	2.4	0.2	18.4	0.2	0.02	9.8	0.1	0.009	8.0	9.1	0.8	11.1
10-20	1.8	0.2	21.0	0.3	0.04	22.3	0.2	0.03	24.3	9.5	1.2	17.7
20-63	1.0	0.3	29.4	0.3	0.10	56.3	0.2	0.07	61.3	8.0	2.6	37.5
63-100	0.4	0.1	7.0	0.0	0.0	0.0	0.0	0.0	0.0	4.6	0.9	12.8
100-125	0.0	0.0	0.0	0.0	0.0	0.0	0.0	0.0	0.0	6.4	0.7	9.5
125-150	0.0	0.0	0.0	0.0	0.0	0.0	0.0	0.0	0.0	7.8	0.2	2.9
150-200	0.0	0.0	0.0	0.0	0.0	0.0	0.0	0.0	0.0	0.0	0.0	0.0
200-250	0.0	0.0	0.0	0.0	0.0	0.0	0.0	0.0	0.0	0.0	0.0	0.0
250-350	0.0	0.0	0.0	0.0	0.0	0.0	0.0	0.0	0.0	0.0	0.0	0.0
>350	0.0	0.0	0.0	0.0	0.0	0.0	0.0	0.0	0.0	0.0	0.0	0.0
Total		1.1	100.0		0.2	100.0		0.1	100.0		7.0	100.0

Table 57: The distribution of apatite and "other" across the different size fractions

Size bins (µm)	Apatite			"Other"		
	Mass%	g	% of total	Mass%	g	% of total
<5	3.5	0.2	29.3	3.7	0.3	8.8
5-10	1.7	0.2	18.0	3.0	0.3	9.1
10-20	1.1	0.1	17.8	2.9	0.4	13.3
20-63	0.5	0.2	20.3	4.4	1.5	50.9
63-100	0.4	0.08	9.6	2.6	0.5	17.9
100-125	0.4	0.04	5.1	0.0	0.0	
125-150	0.0	0.0	0.0	0.0	0.0	
150-200	0.0	0.0	0.0	0.0	0.0	
200-250	0.0	0.0	0.0	0.0	0.0	
250-350	0.0	0.0	0.0	0.0	0.0	
>350	0.0	0.0	0.0	0.0	0.0	
Total		0.8	100		2.9	